SET INTERNATIONAL JOURNAL OF BROADCAST ENGINEERING

SET IJBE V. 5, 2019

ISSN print: 2446-9246
ISSN online: 2446-9432

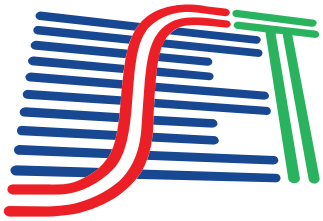

SET INTERNATIONAL JOURNAL OF BROADCAST ENGINEERING

SET IJBE V. 5, 2019

ISSN print: 2446-9246
ISSN online: 2446-9432

SET INTERNATIONAL JOURNAL OF BROADCAST ENGINEERING

ISSN PRINT: 2446-9246 | ISSN ONLINE: 2446-9432

INDEXED IN:

Google's system that offers tools for search of academic literature.

International Cataloging Data in the Publication - CIP - Librarian Zoraide Gasparini CRB/9 1529

S517 SET International Journal of Broadcast Engineering —— vol. 5, (Dec. 2019). – São Paulo: Brazilian Society of Television Engineering —— SET, 2019

Annual frequency
ISSN Print 2446- 9246
ISSN online 2446- 9432
Available at: http://www.set.org.br/ijbe

Broadcasting – Periodic. 2. Transmission Engineering. 3. Digital TV. I. SET. II. Title.

CDD: 384.54

ANNUAL | CIRCULATION : 500 EXEMPLARY | COMMUNICATION MANAGER: CARLA DÓREA BARTZ | GRAPHIC DESIGN AND DIAGRAM: SOLANGE LORENZO

EDITORIAL BOARD

CORPORATE AUTHOR AND EDITOR

SET – Brazilian Society of Television Engineering, or, in Portuguese, SET – Sociedade Brasileira de Engenharia de Televisão.
Address: Av. Auro Soares de Moura Andrade, 252, suites 31 and 32 - Barra Funda District - São Paulo - SP - Brazil - Postal Code: 01156-001

SET BOARD OF DIRECTORS

Deliberative Council

2019 - 2020

President: Carlos Fini

Vice-President: Claudio Eduardo Younis

OFFICE HOLDER	**SUBSTITUTE**
Carlos Fini	Ivan Miranda
Luiz Bellarmino Polak Padilha	David Estevam de Britto
Claudio Eduardo Younis	José Carlos Aronchi de Souza
Claudio Alberto Borgo	Luis Otavio Marchezetti
Mauro Alves Garcia	Almir Antonio Rosa
Daniela Helena Machado e Souza	José Salustiano Fagundes de Souza
Luis Alberto Menoni Popienia	Vinicius Augusto da Silva Vasconcellos
Raymundo Costa Pinto Barros	Marcelo Santos Wance de Souza
Roberto Dias Lima Franco	Valderez de Almeida Donzelli
José Antonio de Souza Garcia	Paulo Henrique Corona Viveiros de Castro
Sergio Eduardo di Santoro Bruzetti	José Chaves Felippe de Oliveira
José Eduardo Marti Cappia	Marco Tulio Nascimento
José Raimundo Lima da Cunha	Esdras Miranda de Araujo
Marcio Rogério Herman	Israel de Moraes Guratti
Cristiano Akamine	Carla Liberal Pagliari

Fiscal Council

Cintia Leite Nascimento	Rafael Silviera Leal
João Braz Borges	Sandra Regina Rogenfisch
Alexandre Aparecido Barrocal	Eduardo de Oliveira S. Bicudo

Council of Former Presidents

Adilson Pontes Malta	Liliana Nakonechnyj
Carlos Eduardo Oliveira Capelão	Olímpio José Franco
Fernando Mattoso Bittencourt Filho	Roberto Dias Lima Franco
José Munhoz	

ABOUT THE JOURNAL

SET INTERNATIONAL JOURNAL OF BROADCAST ENGINEERING

The SET IJBE, (SET International Journal of Broadcast Engineering) is an open access, peer-reviewed article--at-a-time international scientific journal whose objective is to cover knowledge about communications engineering in the field of broadcasting. The SET IJBE seeks the latest and most compelling research articles and state-of-the-art technologies.

Publishing schedule and schema

On-line version – Once an article is accepted and its final version approved by the Editorial Board, it will be published immediately on-line on a one article-at-a-time basis

Printed version – Once a year, all articles accepted and published on-line over the previous twelve months will be compiled for publication in a printed version.

Types of papers

Regular (Full) Papers: Traditional and original research [from 6 to 20 pages]

Tutorial Papers: Brand new OTT (Over-The-Top) detailed implementation and fully set up state-of-the art systems [4 – 6 pages]

Letters: Short notes and consideration about current and relevant techniques, technologies and implementations involving engineering solutions [1-3 pages]

Open Access Policy

Editorial Office:

If you require any additional information, please contact the SET IBJE (SET International Journal of Broadcast Engineering) administration staff:

Address: Av. Auro Soares de Moura Andrade, 252, suites 31/32, Postal Code:01156-001, São Paulo – SP – Brazil; E-mail: IJBE@set.org.br

Aims and Scope include, but are not limited to:

Advanced audio technology and processing
Advanced display technologies
Advanced RF Modulation Technologies
Advanced technologies and systems for emerging broadcasting applications
Applying IT Networks in Broadcast Facilities
Broadcast spectrum issues – re-packing, sharing
Cable & Satellite interconnection with terrestrial broadcasters
Cellular broadcast technologies
Communication, Networking & Broadcasting
Content Delivery Networks – CDN
Digital radio and television systems: Terrestrial, Cable, Satellite, Internet, Wireless.
Electromagnetic compatibility issues between collocated services (e.g. broadcast and LTE)
General Topics for Engineers (Math, Science & Engineering)
Hybrid receiver technology
Interactive Technology for broadcast
IP Networks management and configuration
Metadata systems and management
Mobile DTV systems (all aspects, both transmission and reception)
Mobile/dashboard technology
Next-gen broadcast platforms and standards development
Non-real time (NRT) broadcast services
Ratings technology, second screen technology and services
Secondary service system design; mitigation of interference in primary services
Securing Broadcast IT Networks
Signal Processing & Analysis
Software Defined Radio – SDR Technologies
Streaming delivery of broadcast content
Transmission, propagation, reception, re-distribution of broadcast signals AM, FM, and TV transmitter and antenna systems
Transport stream issues – ancillary services
Unlicensed device operation in TV white spaces

We wish to inform you that the activities, events and publications of the Brazilian Society of Television Engineering – SET, including this one, enjoy international support, under formal agreements, from the following international organizations. We also take this opportunity to thank them and reiterate how proud we are that they support our work.

SUMMARY

SET IJBE v. 5, 2019, 114 pages, 14 articles.

EDITORIAL

Dear reader,

In the IJBE 2019 edition, we are presenting several papers dealing with the thematic of broadcasting, including its technological innovations in audio signal processing, video, and images, digital television systems.

Communication is fundamental for the development of societies, and perhaps what distinguishes humanity from the other animal species of this planet is indeed its efficiency and plurality. Communication allows man to break down barriers and innovate, since all this human communication potential is amplified by creative activity, and is as much as the technology developed is most incredible, yet it is manking who invents and creates, in other words, there in lies all the creative potential. And in this way, by communicating we interact primarily in an audiovisual way, even though we have been given five senses, all of them capable of allowing the exchange of information and perceptions of the world.

Math has developed an Information Theory showing the limits of this ability to exchange content and identifying the importance of the message through information. Thus, communication is required, in the sense that it is through it that information, concepts, and representations are conveyed between people, and while the digital channels and systems make the necessary adaptations to convey these messages and there by enabling the media.

Thus, the development of long-range communication involving content production in a format easily understandable format to the human senses, with the greatest possible similarity to local and direct perception, while observing economic issues, challenges, and natural limits.

The pursuit of quality in the development of technologies that make digital communication systems more efficient is the focus of researchers to whom the IJBE provides an opportunity to publish their studies, experiments, and research in the scientific and technological areas of production and distribution of information content.

We hope you enjoy and take advantage of these papers and feel motivated to submit one of your own to us in the future.

Best wishes,

SET IJBE Editors

Implementation of an 8K-DTV broadcast system using SDR

Ricardo Seriacopi Rabaça
George Henrique Maranhão Garcia de Oliveira
Fadi Jerji
Cristiano Akamine

CITE THIS ARTICLE

Rabaça, Ricardo Seriacopi; de Oliveira, George Henrique Maranhão Garcia ; Jerji, Fadi; Akamine, Cristiano; 2019. Implementation of an 8K-DTV broadcast system using SDR. SET INTERNATIONAL JOURNAL OF BROADCAST ENGINEERING. ISSN Print: 2446-9246 ISSN Online: 2446-9432. doi: 10.18580/setijbe.2019.1. Web Link: http://dx.doi.org/10.18580/setijbe.2019.1

Implementation of an 8K-DTV broadcast system using SDR

Ricardo Seriacopi Rabaça, George Henrique Maranhão Garcia de Oliveira, Fadi Jerji, and Cristiano Akamine, *Member, SET*

Electrical Engineering and Computing Program
Mackenzie Presbyterian University
São Paulo, Brazil

ricardo_sr2@hotmail.com, george.oliveira@mackenzie.br, fadi.jerji@gmail.com, cristiano.akamine@mackenzie.br

***Abstract*—This paper presents an implementation of an 8K-DTV transmitter and receiver in Software Defined Radio/GNU Radio Companion. The main idea of this work is to provide a modified digital TV broadcast system, based on the Brazilian system (ISDB-T$_B$), using two adjacent channels of 6 MHz, channel bonding technique, soft-decision demapper, powerful channel coding and high order modulations, to achieve high bit rates and allow the transmission and reception of content in Ultra High Definition (8K) using indoor antennas. The implementation is done using the GNU Radio Companion software along with a Software Defined Radio platform to transmit and receive the Radio Frequency signal.**

***Keywords*—Integrated Services Digital Broadcasting Terrestrial - Version B (ISDB-T$_B$), Ultra High Definition Television (UHDTV), Channel Bonding (CB), Low-Density Parity-Check (LDPC), Software Defined Radio (SDR), GNU Radio Companion (GRC).**

I. Introduction

Due to increasing demand for higher resolution from content consumers, broadcast systems need to support higher bit rates. To achieve these goals, it is necessary to change some of broadcast system's characteristics such as the maximum modulation order, video compression method, physical layer technique and even the bandwidth.

In Brazil, the commercial transmission of Integrated Services Digital Broadcasting Terrestrial - Version B (ISDB-T$_B$) started in 2007 [1]. This system is based on the Japanese digital TV standard, but with some modifications in order to fit the Brazilian scenario [2]. Also, there is the fact that the Brazilian Analogue switch-off (ASO) process will be completed in 2023 [3]. Thus, it is necessary to develop a new standard or an evolution of the existent ISDB-T$_B$ standard that allows content transmission in Ultra High Definition (UHD), such as 4K and 8K resolutions.

In recent years, the consumer market has come to have a higher demand for UHD services, however, several papers regarding the developments on using Ultra High Definition Television (UHDTV) signals where presented at the Japan Broadcasting Corporation (NHK) in 1995 [4]. In 2002, the first public demonstration of an 8K signal transmission was done at the NHK science and technology research laboratory. In 2005, another public exhibition was held at Expo 2005 in Japanese province of Aichi. In 2006, the first 8K demo was done at the National Association of Broadcasters (NAB) Show. In 2012, "Rec. 2020" or "BT.2020" was regulated by the International Telecommunication Union-Radio-communications Sector (ITU-R) and a demonstration was held at the Olympic games in London. In 2016, satellite transmission tests were performed, a presentation during the Olympic games at Rio de Janeiro was realized and 8K compatible equipment was produced [4]–[6]. In 2017, an interface capable of transmitting 100 Gbps and compatible with 8k/50p-60p/4:4:4/12bit or 8k/100p120p/4:2:2/10bit image formats was developed. DC level balancing and clock signal recovery were done using 8 to 10 bit encoding [7].

The new standard developed by the Advanced Television Systems Committee (ATSC) the "ATSC 3.0", already in use in countries such as the United States and South Korea, allows the transmission of content in 4K deploying several improvements such as modern modulation and multiplexing techniques and powerful coders [8]–[10].

To allow content transmission in 4K and 8K, high bit rates are required. To achieve this goal, it becomes necessary to analyze new techniques that can be applied in an already existing system. The ISDB-T$_B$ allows for bit rates up to 23.234 Mbps using a bandwidth of 6 MHz and its highest modulation order (64-QAM) [11]. To reach the main objective of this work, which is the transmission of 8K content, a bit rate between 70 and 100 Mbps is required, depending on the used video configuration [12].

There are some studies such as [13]–[15], which demonstrate the use of modern modulation techniques, coding and multiplexing, so that it could reach a higher bit rates (to allow the transmission of 4K content in the enhanced layer) and still allow transmission of the traditional ISDB-T$_B$ in the core layer using the Layer Division Multiplexing (LDM) technique. The

This work was supported in part by the Coordination for the Improvement of Higher Education Personnel (CAPES), National Council for Scientific and Technological Development (CNPq) and MackPesquisa.

http://www.set.org.br/ijbe/ doi: 10.18580/setijbe.2019.1 Web Link: http://dx.doi.org/10.18580/setijbe.2019.1

main advantages of this method are the efficient spectrum use and the increase in the amount of data transmitted [16].

In this work the main idea is different, since it is desired to achieve even higher bit rates, which allow the transmission of content in 8K. Thus, a system that is based on the Brazilian standard was implemented, but using a higher bandwidth channel (6 + 6 MHz), Channel Bonding (CB) technique, soft decision demapper, Low-Density Parity-Check (LDPC) code and higher order modulations (256-QAM). In addition, some adjustments had to be made at some stages of the transmission and reception process, such as the development of an LDPC encoder and decoder and an uniform mapper and a soft decision demodulator, to be compatible with the modified system. The steps of interleaving (time and frequency), framing, Orthogonal Frequency Division Multiplexing (OFDM) modulation and Guard Interval (GI) insertion of the traditional ISDB-T_B were used [17].

The proposed broadcast system was implemented in Software Defined Radio (SDR) by using GNU Radio Companion (GRC) software. The GRC is a free and open-source software development toolkit that provides signal processing blocks to achieve SDR. It can be used with readily-available low-cost external Radio Frequency (RF) hardware or without hardware in a simulation-like environment. The software allows the creation of blocks using programming languages such as C, C++ and Python [18].

This paper is organized into three sections. In Section II, the most relevant information about the implementation of the proposed system are presented. And finally, Section III, contains the conclusion of this work.

II. 8K-DTV BROADCAST SYSTEM IMPLEMENTATION

A. *Transmitter*

At the transmission stage, a modified version of ISDB-T_B was implemented using some characteristics of ATSC 3.0, but with a modified message size to guarantee synchronism. The proposed transmitter uses a tailored irregular LDPC code, with a frame size of 19968 (4×4992) instead of the traditional sizes used in ATSC 3.0 standard (Short frame: 16200 and Normal frame: 64800) [8]. After that, a mapper is implemented with a uniform 256-QAM constellation.

The Fig. 1 shows the custom irregular LDPC code of the frame size 19968 and code rate 13/15.

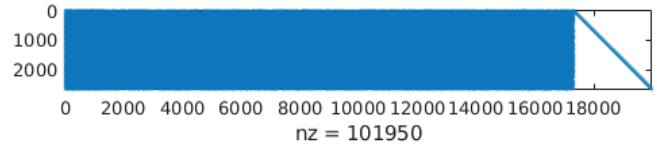

Fig. 1. Custom irregular LDPC code of the frame size 19968 and code rate 13/15.

Fig. 2 shows one of the transmitted 256-QAM constellation using 13 segments (Layer 1 - Left side Radio Frequency (RF) channel). Another 256-QAM constellation is transmitted in the right adjacent RF channel (Layer 2). For both 8K-DTV signals, Mode 3 (8K) was used and the Time Interleaver (TI) was set to 0.

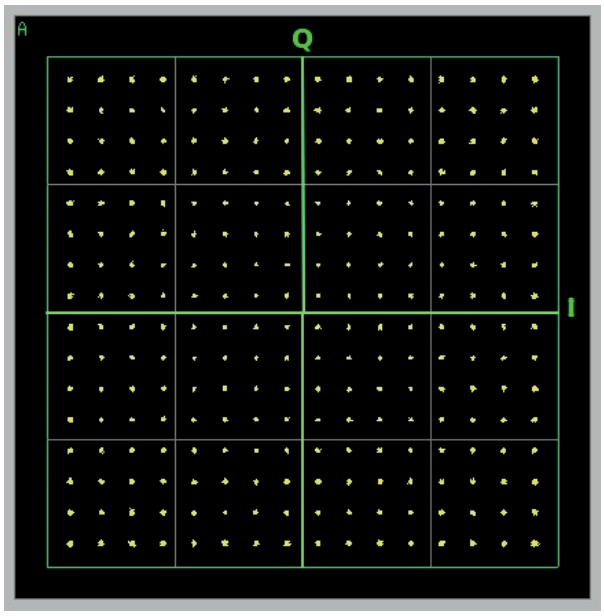

Fig. 2. 8K-DTV 256-QAM constellation (displayed on the spectrum analyzer).

To transmit a signal with a total bandwidth of 12 MHz, the proposed system used the Channel Bonding (CB) technique (an overall 12 MHz signal is realized by two neighbored 6 MHz RF channels). This technology allows scalable expansion of effective bandwidth provided to the receiver through simultaneous deployment of radio resources across multiple carriers. With multiple RF channel bonding, the total bandwidth can be any sum of the default single RF channel bandwidths (6 MHz for ISDB-T_B). [19].

The 8K-DTV spectrum using two channels with bandwidth of 6 MHz is shown in Fig. 3.

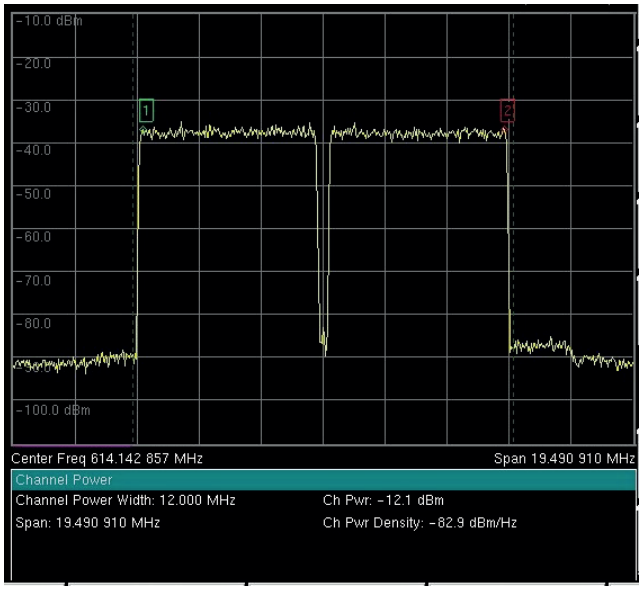

Fig. 3. 8K-DTV spectrum (6 + 6 MHz).

The 8K-DTV transmitter using two channels with each having a bandwidth of 6 MHz is shown in Fig. 4.

http://www.set.org.br/ijbe/ doi: 10.18580/setijbe.2019.1 Web Link: http://dx.doi.org/10.18580/setijbe.2019.1

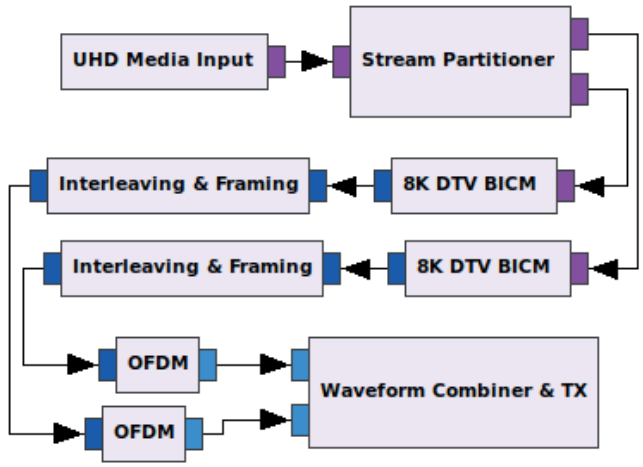

Fig. 4. 8K-DTV Transmitter using Channel Bonding.

In the diagram shown in the Fig. 4 the signal is separated in two streams before encoding and mapping stages. Both encoded and mapped streams are interleaved in time and frequency and passed through the stages of Framing, OFDM modulation and GI insertion separately [20]. After that, the modulated streams are transmitted on different Radio Frequency (RF) channels or spectrum parts from the TV transmitter [19].

For the correct functionality of this technique, it is necessary that the branches are synchronized similarly to the Single Frequency Networks (SFNs). In a SFN, a set of transmitters is synchronized in time and frequency to transmit the same signal. This means that all the transmitters of the network should transmit the same OFDM symbol at the same time and frequency [21]. Similarly, using CB technology, it is necessary for the transmitter branches to be synchronized, so that signals are transmitted at the same time [19].

One of the advantages of using the CB technique is that it is possible to transmit one 4K resolution channel and a second channel used as a complement (complementary bits) to reach the 8K resolution. In this work, one 8K stream is separated in two streams in order to be transmitted and then these streams are added together (at the reception stage) to recover the original 8K resolution Transport Stream (TS) file.

B. Receiver

The proposed receiver has 12 MHz bandwidth to receive two adjacent channels. After that, the synchronization of time, sampling, frequency and frame is performed. Then, the steps of OFDM demodulation, channel estimation and equalization and time and frequency de-interleaving are performed. Finally, the implementation of the reception stage is done using a Soft Decision demodulator that uses Log-Likelihood Ratio (LLR), which statistically defines whether a bit is "0" or "1" and the Sum-Product Algorithm LDPC decoder (SPA) is selected due to its high error correction performance.

The 8K-DTV receiver using two adjacent channels with bandwidth of 6 MHz is shown in Fig. 5 [15], [22].

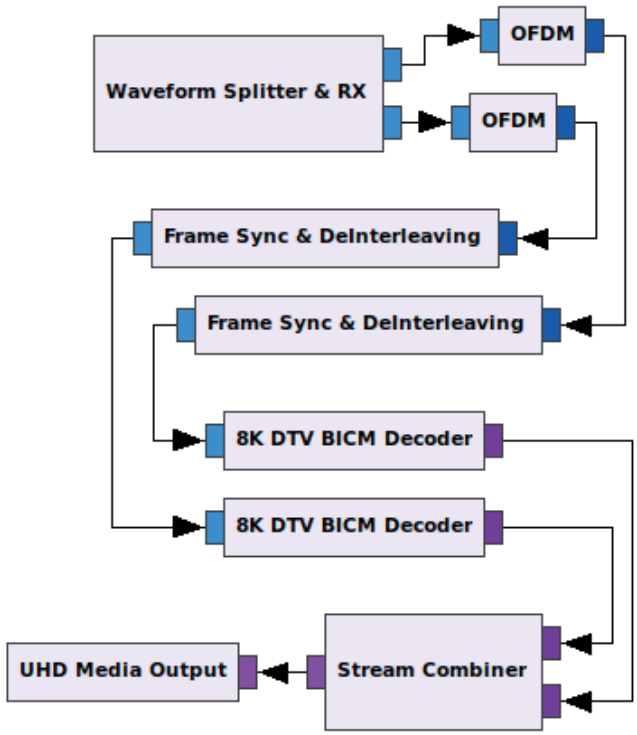

Fig. 5. 8K-DTV Receiver using Channel Bonding [15], [22].

In the diagram shown in the Fig. 5 [15], [22] the two signals are received (using multiple tuners that receive the modulated streams) and sent to the synchronization of time, sampling, frequency and frame stage. After that, the OFDM demodulation, channel estimation and equalization and time and frequency de-interleaving are performed. Both signals go through their respective demodulation and decoding steps (separately). Finally, they are combined in an unique stream [19].

C. Simulation with LDPC Sum-Product Algorithm

In order to verify the robustness of the 8K-DTV broadcast system, some simulations were done using the transmitter and receiver with CB. The simulation with the optimal LDPC decoder SPA was done to confirm that the system can be improved in the future, using better techniques and configurations [23].

A computer simulation was performed in order to find the minimum Signal to Noise ratio (SNR) for the proposed system. During the simulation, the values of Bit Error Rate (BER) and Frame Error Rate (FER) were measured.

During the tests, an additive white Gaussian noise (AWGN) was injected in order to measure the SNR (dB) value that corresponds to the BER threshold value of 3×10^{-6} and FER of 1×10^{-4} after applying the LDPC decoder. These thresholds are used considering a reception with less than one uncorrected error event per hour. This reception quality limit is defined as Quasi Error Free (QEF) and these values guarantee the QEF after the decoder [24].

http://www.set.org.br/ijbe/ doi: 10.18580/setijbe.2019.1 Web Link: http://dx.doi.org/10.18580/setijbe.2019.1

The binary data source Pseudo-Random Binary Sequence 23 (PRBS 23) was used in all of the tests. The maximum number of iterations for the LDPC decoder was set to 40.

For the first simulation configuration, a 16-QAM constellation, a Code Rate (CR) of 10/15 and 13/15, a frame size of 19968, a GI of 1/32 and an Inverse Fast Fourier Transform (IFFT) size of 8K were used. This configuration (with CR = 13/15) allows the transmission of content in 4K resolution. The second configuration used a 256-QAM with the same CR, frame size, GI and IFFT size, to achieve the 8K resolution. The results are presented in Table I.

TABLE I
SNR THRESHOLDS WITH CB TECHNIQUE.

LDPC SPA Simulation	Bit rate (Mbps)	Video Quality	SNR threshold (dB)
16-QAM CR = 10/15	27.58	4K	9.0
16-QAM CR = 13/15	35.86	4K	13.0
256-QAM CR = 10/15	55.16	4K	19.0
256-QAM CR = 13/15	71.71	8K	24.0

In the results shown in Table I the video quality information for all configurations were selected considering the use of High Efficiency Video Coding (HEVC).

III. CONCLUSION

The main objective of this work is reached, since the software transmission and reception with CB technology were achieved and a 8K resolution content could be transmitted and recovered using higher order constellation, soft decision demodulation, using two adjacent channels of 6 MHz and an optimal LDPC decoder (SPA).

The proposed 8K-DTV system was developed as a proof of concept, aiming to provide new ideas and possibilities for the development of a new digital TV standard for Brazil.

This work demonstrates the possibility of a software implementation of 8K broadcast system. The system performance can be enhanced by adding other channel encoders such as the Bose-Chaudhuri-Hocquenghem (BCH) and Cyclic Redundancy Check (CRC), for example. In addition, Non-Uniform Constellations (NUCs), bit and byte interleavers, more efficient ways to modulate and demodulate the signals, to realize the synchronization stages, among other techniques that could be used.

In addition to above factors, modern technologies applied to digital TV were also presented, such as the use of CB, which allows high bit rates to be achieved and permits the use of a channel with complementary information.

ACKNOWLEDGMENT

The authors would like to thank PPGEEC and their colleagues at Mackenzie's Digital TV Research Laboratory.

REFERENCES

[1] Digital Broadcasting Experts Group. (2018) Introduction of "ISDB-T". [Online]. Available: https://www.dibeg.org

[2] *Resolution number 640*, National Telecommunications Agency, July 2014, available in Portuguese. [Online]. Available: http://www.anatel.gov.br/legislacao/resolucoes/2014/785-resolucao-640#art4

[3] *MCTIC Regulation number 2992, of May 26, 2017*, Ministry of Science, Technology, Innovation and Communications, 2017, available in Portuguese. [Online]. Available: https://www.mctic.gov.br/mctic/opencms/legislacao/portarias/Portaria_MCTIC_n_2992_de_26052017.html

[4] M. Sugawara, "The world's first 8k/4k "regular" broadcasting," in *Hollywood Professional Association 2017*, feb. 2017.

[5] *Parameter values for ultra-high definition television systems for production and international programme exchange*, International Telecommunication Union - Radiocommunication Sector (ITU-R), 2015.

[6] T. Sakiyama, K. Ichikawa, M. Abe, S. Mitsuhashi, T. Yamashita, and M. Miyazaki, "8k-uhdtv production equipment and workflow which realize an unprecedented video experience," in *SMPTE 2016 Annual Technical Conference and Exhibition*, Oct 2016, pp. 1–11.

[7] S. Yamashita and K. Takahashi, "A 100gbps interface for 4k/8k uhdtv signals," in *SMPTE 2016 Annual Technical Conference and Exhibition*, Oct 2016, pp. 1–14.

[8] *ATSC Standard: Physical Layer Protocol (A/322)*, Advanced Television Systems Committee, Washington, D.C, September 2016.

[9] S. Jeon, J. Lee, S. Kwon, B. Lim, S. Ahn, Y. Shin, J. Lee, and S. Park, "Field trial results for atsc 3.0 txid transmission and detection in single frequency network of seoul," in *2018 IEEE International Symposium on Broadband Multimedia Systems and Broadcasting (BMSB)*, June 2018, pp. 1–4.

[10] S. Park, J. Lee, S. Kwon, B. Lim, S. Ahn, H. M. Kim, S. Jeon, J. Lee, M. Simon, M. Aitken, K. Gage, Y. Wu, L. Zhang, W. Li, and J. Kim, "Performance analysis of all modulation and code combinations in atsc 3.0 physical layer protocol," *IEEE Transactions on Broadcasting*, vol. 65, no. 2, pp. 197–210, June 2019.

[11] *NBR 15601: Digital terrestrial television - Transmission system*, Brazilian Association of Technical Standards, Rio de Janeiro, 2008, available in Portuguese.

[12] Y. Sugito, S. Iwasaki, K. Chida, K. Iguchi, K. Kanda, X. Lei, H. Miyoshi, and K. Kazui, "A study on the required video bit-rate for 8k 120-hz hevc/h.265 temporal scalable coding," in *2018 Picture Coding Symposium (PCS)*, June 2018, pp. 106–110.

[13] G. H. M. G. de Oliveira, C. Akamine, and Y. P. Maciel, "Implementation of isdb-t ldm broadcast system using ldpc codes," in *2016 IEEE International Symposium on Broadband Multimedia Systems and Broadcasting (BMSB)*, June 2016, pp. 1–4.

[14] R. S. Rabaca, G. H. M. garcia de oliveira, G. R. Ganzaroli, F. Jerji, and C. Akamine, "Implementation of an isdb-tbldm broadcast system using the bicm stage of atsc 3.0 on enhanced layer and diversity at reception," in *2018 IEEE International Symposium on Broadband Multimedia Systems and Broadcasting (BMSB)*, June 2018, pp. 1–6.

[15] R. S. Rabaça, G. H. M. G. de Oliveira, F. Jerji, and C. Akamine, "Implementation of a real-time isdb-tb ldm receiver using sdr," in *2019 IEEE International Symposium on Broadband Multimedia Systems and Broadcasting (BMSB)*, June 2019, pp. 1–6.

[16] S. I. Park, H. M. Kim, and P. Angueira, "Hardware implementation and complexity analysis of layered division multiplexing (ldm) system for atsc 3.0," in *NAB Broadcast Engineering Conference*, 2015, pp. 77–81.

[17] *Transmission System for Digital Terrestrial Broadcasting - STD-B31 - V1.6 E2*, Association of Radio Industries and Businesses, 2015.

[18] GNU Radio. (2018) GNU Radio Companion. [Online]. Available: https://wiki.gnuradio.org/index.php/Main_Page

[19] L. Stadelmeier, D. Schneider, J. Zöllner, and J. J. Gimenez, "Channel bonding for atsc3.0," *IEEE Transactions on Broadcasting*, vol. 62, no. 1, pp. 289–297, March 2016.

[20] R. S. Rabaça, C. Akamine, G. H. M. G. de Oliveira, and Y. P. Maciel, "Implementation of ldm/isdb-t broadcast system using diversity at reception," in *2017 IEEE International Symposium on Broadband Multimedia Systems and Broadcasting (BMSB)*, June 2017, pp. 1–4.

[21] C. Akamine, Y. Iano, G. de Melo Valeira, and G. Bedicks, "Remultiplexing isdb-t bts into dvb ts for sfn," *IEEE Transactions on Broadcasting*, vol. 55, no. 4, pp. 802–809, Dec 2009.

[22] F. Larroca, P. Flores-Guridi, G. Gómez, V. González Barbone, and P. Belzarena, "An open and free isdb-t full seg receiver implemented in gnu radio," in *Wireless Innovation Forum Conference on Wireless Communications Technologies and Software Defined Radio (WInnComm*

16), Reston, Virginia, USA, 15-17 mar, 2016, pp. 1–10. [Online]. Available: https://iie.fing.edu.uy/publicaciones/2016/LFGGB16

[23] F. R. Kschischang, B. J. Frey, and H. Loeliger, "Factor graphs and the sum-product algorithm," *IEEE Transactions on Information Theory*, vol. 47, no. 2, pp. 498–519, Feb 2001.

[24] *NorDig Unified Test Plan for Integrated Receiver Decoders for use in cable, satellite, terrestrial and IP-based networks*, December 2017. [Online]. Available: https://nordig.org/wp-content/uploads/2017/12/NorDig-Unified_Test_Plan_ver_2.6.0.pdf

Received in 2019-07-10 | Approved in 2019-11-25

http://www.set.org.br/ijbe/ doi: 10.18580/setijbe.2019.1 Web Link: http://dx.doi.org/10.18580/setijbe.2019.1

Wireless Production Tools - PMSE - Radio Spectrum Scanning at the Brazilian 2018 FIA Formula OneWorld Championship

Matthias Fehr
Mario Minami
Felipe Filgueiras
Pia Seeger
André F. Ponchet
Georg Fischer

CITE THIS ARTICLE:
Fehr, Matthias, Minami, Mario, Filgueiras, Felipe, Seeger, Pia, Ponchet, Andre Fontoura, Fischer, Georg; 2019. Wireless Production Tools - PMSE Radio - Spectrum Scanning at the Brazilian 2018 FIA Formula One World Championship. SET INTERNATIONAL JOURNAL OF BROADCAST ENGINEERING. ISSN Print: 2446-9246 ISSN Online: 2446-9432. doi: 10.18580/setijbe.2019.2. Web Link: http://dx.doi.org/10.18580/setijbe.2019.2

Wireless Production Tools - PMSE - Radio Spectrum Scanning at the Brazilian 2018 FIA Formula One World Championship

Radio Spectrum Sharing and Regulation point of view

Matthias Fehr[*], Mario Minami[†], Felipe Filgueiras[‡], Pia Seeger[‡†], Andre Fontoura Ponchet[†], Georg Fischer[⁂]

[*]APWPT - *Association of Professional Wireless Production Technologies,* Postal Box 68, Baiersdorf, Germany
[†]CECS - *Information Engineering, UFABC - Federal University of ABC,* Santo Andre, SP, 09210-580, Brazil
[‡]DTPD - *Globo TV Group,* Jardim Botanico, RJ, 22460-901, Brazil
[‡]Beuth University of Applied Science - Berlin, Germany
[⁂]FAU - *Friedrich-Alexander University Erlangen* - 91058 Erlangen, Nuremberg, Germany

e-mail: matthias.fehr@apwpt.org, mario.minami@ufabc.edu.br, felipe.costa@tvglobo.com.br, pia.seeger@gmx.de, andre.ponchet@ufabc.edu.br, georg.fischer@fau.de

***Abstract* - Major international sporting competitions such as Formula 1 GP Championship offer a great opportunity to assess the use of the radio spectrum in many respects, such as operation, regulation, equipment, demands and conflicts between all involved professionals, content producers, technical support and local regulatory agencies. In this piece of work, spectral scanning measurements were performed in the range of 410 to 870 MHz, covering audio PMSE, e.g. wireless microphones, at the 2018 F1 GP Brazil from November 9th to 11th, 2018. The spectral scanning equipment was installed at two different locations, the international technical area for the TV stations (compound) with the UFABC semi-portable 6 GHz R&S spectrum analyzer and in the TV Globo booth with APWPT's semi-portable R&S spectrum analyzer in the middle of the pit line. There was a distance of about 2 km between the two locations and both sets of equipment were controlled by specialized software. The radio spectrum was in use by the race technical teams and the TV content production teams. Aside of the production, transmission and communication of data and content between the various teams and their car drivers, there was also a film crew in a helicopter, equipped with video cameras. At the three official days of the event, from November 9th Friday to 11th Sunday, during the initial numerous practice laps of the Interlagos racetrack, the official classification laps and the F1 GP Race itself, many links of audio PMSE were continuously monitored. Finally, the spectrum recordings were compared with TV Globo's coordination information (initial plan for assigning frequencies to wireless devices, the 'coordination table') to reduce errors in the evaluation of the spectrum recording. Using previous reports, produced since 2014, we can compare the number of microphone links used in the Brazilian F1 GP and contrast with similar recording procedures at the Italian F1 GP during the same period.**

***Index Terms* – PMSE, Spectrum Scanning, Spectrum Occupancy, F1 Race, Spectrum Regulation, Spectrum Sharing, 4G/5G IMT, link density.**

I. Introduction

The use of wireless production tools is constantly changing. A sustainable trend is that more and more wireless applications are seeking access to spectrum. The focus of APWPT is the interference-free production of content and events in Art, Culture, Broadcast and the Creative Industry. Today, wireless production tools must combine ever higher production quality with the necessary flexibility, at a low cost. Most visitors to events and productions cannot see these tools. In addition, APWPT is actively involved in many working groups and supports them with carefully researched information. Part of this work is the close cooperation with many experienced teams in content and event production. The methodology for spectrum recording in the context of event production and the subsequent evaluation of the recorded data is a considerable challenge. This requires a scientifically consistent approach in combination with quality assurance methods - APWPT has learned this over many years. Therefore, APWPT is very grateful that universities from Brazil and Germany are supporting the work on foundations for consistent results.

This paper is organized as follows: section I – Introduction, with contextualize spectrum scanning and the measurements in Formula One with a quick explanation of the methodology; section II - Recording of Radio Spectrum in Sao Paulo, describes the measurements made at the 2018 Brazilian Formula 1 Grand Prix; section III - Evaluation of the observed Radio Spectrum use by PMSE, the analysis of recorded data and at the end, section IV finals Discussions and Conclusions.

Previous work

The initial ideas for spectrum recording and occupancy detection were sketched out in 2007 and initial spectrum recordings were carried out afterwards. Very quickly it became clear that the comparison of spectrum recordings of different events at different locations is a complex task. In addition, access to event production and the installation of antennas and scanner technology is challenging. Here the practical access

http://www.set.org.br/ijbe/ doi: 10.18580/setijbe.2019.2 Web Link: http://dx.doi.org/10.18580/setijbe.2019.2

conditions very often deviate from technically reasonable schemes. Together with our supporting organizations, APWPT has presented and discussed to the public the slowly developing methodology. The experience gained was transferred into an ever-improved methodology and programmed into free software: the "PMSE Occupation Recorder".

Spectrum recordings in the context of Formula One

RAI's production team in Italy has been performing spectrum recording for several years despite limited resources. Representative results could be presented in the context of the European Microwave Week [1]. PMSE Workshops at EuMW conferences have been held annually at various locations since 1998 and is a special scientific highlight of public relations work).

A particularly interesting question was whether the spectrum occupancy by wireless production tools in Brazil differs considerably from that in Europe. With the support of European contacts to the Formula 1 team, the necessary preparations were started. One necessary action was the comparison of the frequency coordination information of Formula 1 productions. What is frequency coordination information? Is the initial plan for assigning frequencies to wireless devices turned into reality? How much tweaking and deviation from initial plans happens during an event? Every commercial event production optimizes, partly over months or years, the access to radio frequencies by wireless production tools. In the process, locally available frequencies and the needs of event production are compared and optimized. During International Broadcasting Convention - IBC2018 [2] , September 2018 in Amsterdam, multi-year coordination information from Brazil and Italy was presented [3]. Figure 1 shows an update of the presented coordination information of Audio PMSE [4] where we can note an interesting trend difference. The number of coordinated audio links is increasing in Italy and in Brazil. The following look into the spectrum recordings shows the probable cause.

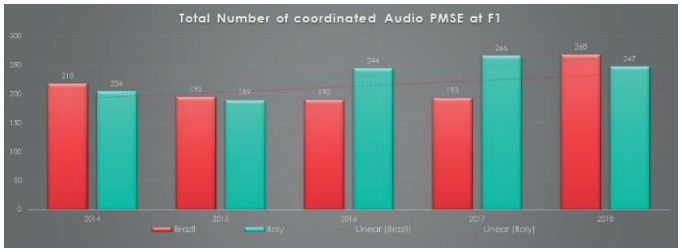

Figure 1: comparison of frequency coordination data over several years (data source: Globo TV and RAI)

Brief intro to spectrum recording methodology

Automatic level correction

The signal strength of the reception level at the scanner input frequently exceeds the scanner dynamic range. The scanner-input attenuation is therefore automatically adjusted to the local situation by the spectrum scanning software operated on an external computer. The scanning data contains information on the setting of variable input attenuator, but the recorded level is not modified. During the data analysis, the recorded dynamic range will be recreated as close to reality as possible. On the bottom of the output graphic this is noted with '*True recorded signal*' or '*Chart re-calculated at the bottom area by up to L_{max} dB*' (where L_{max} represents the maximum value of the level correction).

Recording of scanned spectrum data

It is of special concern during spectrum recordings to store the recorded data as transparently as possible. Therefore, a special method of data storage has been chosen. Each scan cycle is stored in a new ASCII file – indicated as log files in tables 2 and 4 - and, in addition to the scan data, contains important metadata for subsequent data evaluation.

Summary of some advantages of the methodology:

- Each data set can be imported into Excel or similar tools and evaluated separately.
- Each record contains important data project identification.
- Each record contains information for comprehensive analysis, such as the measurement bandwidth.
- Each record contains information that the scan has been completed or that the input attenuator was changed.
- If available, record will contain the location coordinates.
- If available, each data set contains information on antenna cable attenuation, filter attenuation, or gain from external components inserted before the scanner input.
- Each record contains the number of scan stations and its own scanner number.
- Multiple scanners' data can be combined by data fusion.

Previously known disadvantages:

- Speed of data storage and loading is reduced compared to binary single file recording.
- The maximum number of scans is limited to the Windows operating system or the hard disk file system.
- In practice, however, scans with more than 400,000 individual files were evaluated on computers with Windows 7 or Windows 10 (both in 64-bit version).

How is each single spectrum scan performed?

Depending on the examined frequency range, the necessary scanner bandwidth and scanner detectors are selected at the beginning of spectrum recording.

Example for the UHF TV range:

- For the frequency range 470 to 862 MHz, the main scan is performed with a resolution bandwidth of 100 kHz and an RMS detector. In addition, a reduced bandwidth of 30 kHz can also be used on request. This reduction allows the detection of relatively narrowband reception signals but requires significantly more time for the scan. The frequency step size of these scans is 20 kHz.
- A different scan bandwidth is used for the frequency range 410 to 470 MHz. Since in the frequency range 410 to 470 MHz mostly narrow-band links are operated, a bandwidth

http://www.set.org.br/ijbe/ doi: 10.18580/setijbe.2019.2 Web Link: http://dx.doi.org/10.18580/setijbe.2019.2

of 30 kHz is used here. The range 470-870 MHz is again recorded with 100 kHz bandwidth. The frequency step size of these scans is 10 kHz.

- Additional scan with large bandwidth. After each single scan with 30 or 100 kHz bandwidth, an additional scan with a bandwidth of 10 MHz is performed (not supported by every scanner). In each single scan, the power levels of all recorded signals are added together. This sum power is the criterion for controlling the input attenuator of the scanner. After many test series it was possible to find a compromise between the avoidance of a level overdrive of the scanner receiver and its possibly reduced sensitivity.

II. Recording of Radio Spectrum in Sao Paulo

The spectrum recording took place over a period of three days. On the first day, the frequency range from 410 to 870 MHz was recorded. On the second and third day only the frequency range 470 to 862 MHz was recorded. This allowed for frequency scans to be performed with shorter time intervals. In addition, we had to use a different measuring antenna at the 1st scan station from the second day on. The new antenna only supported 470 to 862 MHz.

The spectrum scans were conducted jointly with the Federal University of ABC (UFABC). The regional broadcaster Globo TV (DTPD) provided access to two different locations at the Autodromo José Carlos Pace [5], marked by yellow pins at figure 2.

Figure 2: locations of the spectrum recordings during F1 - Sao Paulo (source: Google Maps)

Locations of the scan stations

According figure 2, the two recording stations were located at:

- 1st Station: GPS latitude = -23.701117°/GPS longitude = -46.695833°
- 2nd Station: GPS latitude = -23.705283°/GPS longitude = -46.699717°.

The figure 3 shows the race track altitude profile.

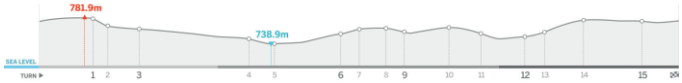

Figure 3: elevation changes at Autodromo José Carlos Pace. Source: [6].

Measuring instruments used for spectrum recording

- 1st Station, Responsible: Federal University of ABC (UFABC)
  Equipment: Rohde&Schwarz, FSL-6, 100691/016, 1.91
  Antenna: A2003, Omnidirectional antenna, vertically polarized
- 2nd Station, Responsible: Association of Professional Wireless Production Technologies e. V.
  Equipment: Rohde&Schwarz, FSL-3, 101308/003, 1.90
  Antenna: SD3000, Wide-band antenna, vertically polarized.

Pictures of the scanner's installation

Figure 4: second scan station

Figure 5: indoor antenna of 1st scan station

Figure 6: spectrum plot of a hand-held scanner

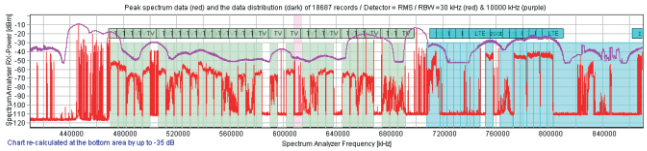

Figure 7: recorded spectrum allocation 410-870 MHz - frequency domain (18686 data records)

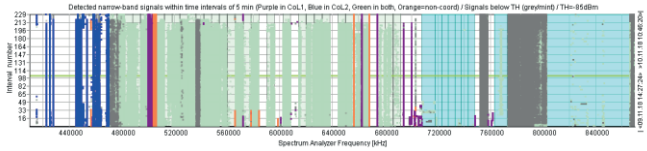

Figure 8: recorded spectrum allocation 410-870 MHz - time domain (18686 data records)

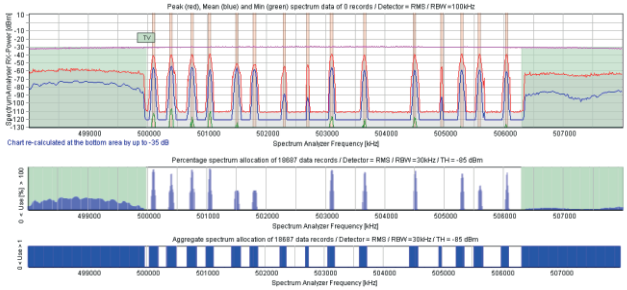

Figure 9-11: 15 detected links in 498-508 MHz and their level variance (18686 data records)

From the second day of the spectrum scans onwards a high pass filter was inserted at the antenna input connector of the second scanner station. This reduced the level of strong signals below 470 MHz and allowed the scanner above to support a better use of the limited receiver dynamic range.

Figure 7 illustrates the aggregated spectrum recording in frequency domain from both scanners, performed on first day while figure 8 illustrates the time domain.

On the first day, a spectrum scan was performed in the enlarged frequency range from 410 MHz to 862 MHz. Thus, two important topics could be addressed, i.e. Checking the functionality of both scan stations and generating an overview of frequency usage below 470 MHz.

Figures 9-12 show parts of the frequency recordings that represent the signals recorded by them.

http://www.set.org.br/ijbe/ doi: 10.18580/setijbe.2019.2 Web Link: http://dx.doi.org/10.18580/setijbe.2019.2

These pictures show exemplarily the substantial signal dynamics, which can occur in the event production. Tables 1 and 2 summarize the recorded spectrum information measured on the first day and tables 3 and 4 summarize the spectrum information captured on second and third day.

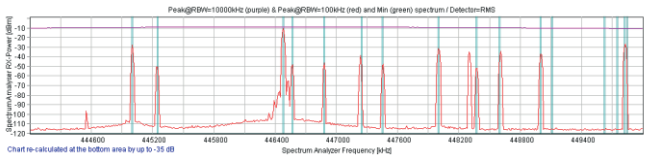

Figure 12: 13 detected links in 444-450 MHz and their level variance > 100 dB (18686 data records)

Table 1 - Brief summary of the recorded spectrum information[e], 1st day

Description	Spec Information
Scanned frequency band	410 to 870 MHz
Range of scanned frequency band	460 MHz
TV channels in use by Broadcast	31
Radio spectrum in use by Broadcast	186 MHz
LTE channels in use by IMT[f]	12
Radio spectrum in use by IMT	60 MHz
Radio spectrum in use by non-PMSE WB sys	83 MHz
Radio spectrum in use by WB PMSE systems	10 MHz
Radio spectrum remaining NB and WB PMSE	141 MHz
Radio spectrum below 470 MHz (TalkBack)	60 MHz
NB PMSE detected in 410-870 MHz	97
NB PMSE detected in 410-470 MHz	54
NB PMSE detected in 470-870 MHz	43
NB PMSE manually marked outside TV ch	56
NB PMSE manually marked in 410-470 MHz	43
NB PMSE manually marked in TV channels	4
Spectrum for detected PMSE in 410-470 MHz [a][b]	4.9 MHz/97 Links
Spectrum for detected PMSE in 470-870 MHz [c][d]	30.5 MHz/60 links
Required spectrum for NB and WB PMSE [b]	45.4 MHz
Spec density of all detected PMSE in 410-870 MHz [b]	1.135 Links/MHz
Spec density of detected NB PMSE in 410-870 MHz [b]	1.113 Links/MHz
Spec density of detected NB PMSE in 410-470 MHz [b]	1.617 Links/MHz
Spec density of detected NB PMSE in 470-870 MHz [b]	0.741 Links/MHz
Coordinated PMSE in the scanned freq band	269
Coordinated NB PMSE in the scanned band	266
Coordinated audio PMSE in WB systems	2
Coordinated video PMSE in WB systems	1
Coordinated NB PMSE in 410-470 MHz	88
Coordinated NB PMSE in 470-870 MHz	178
Spec density of all coordinated PMSE in 410-870 MHz	0.585 Links/MHz
Spec density of coordinated NB PMSE in 410-470 MHz	1.467 Links/MHz
Spec density of all coordinated PMSE in 470-870 MHz	0.453 Links/MHz
Spec density of coordinated NB PMSE in 470-870 MHz	0.445 Links/MHz

(a) Calculation bases on a 50 kHz grid and two additional 25 kHz guard bands

(b) Calculation considers manually marked links

(c) Calculation bases on a 500 kHz grid and two additional 250 kHz guard bands and considers manually marked links

(d) This calculation does not consider required guard bands to TV or IMT channels

(e) Stat software version: PMSE Occupation Recorder R6.3.15a

Some environment pictures are presented in figures 13 to 15. Figure 16 illustrates the aggregated spectrum recording in frequency domain obtained from both scanners, performed on second and third day while figure 17 illustrates the time domain.

On the second and third day the frequency range 470-862 MHz was recorded. The aggregated signal spectrum shows a rarely occurring dense frequency usage. Figures 18 to 20 show a selected frequency range and the signals recorded in it are shown again.

Table 2 – Minimum and Maximum receiver input level[a], 1st day

Information on receiver input level	Freq. Level@ RBW	level	Log file
Max scanning	30 kHz	-10.21 dBm	Scan1110180932371970.txt at 446480 kHz
	10 MHz	-9.06 dBm	Scan1110180927486873.txt at 446130 kHz
Min scanning	30 kHz	-123.92 dBm	Scan1109182020217319.txt at 439530 kHz
Max on 1st scanner	100 kHz	-10.21 dBm	Scan1110180932371970.txt at 446480 kHz
Min on 1st scanner	100 kHz	-112.69 dBm	Scan1110180524505408.txt at 491980 kHz
Max on 2nd scanner	100 kHz	-13.72 dBm	Scan1109181657425772.txt at 700100 kHz
Min on 2nd scanner	100 kHz	-123.92 dBm	Scan1109182020217319.txt at 439530 kHz
Maximum scanner input attenuator position: 20 dB			

(a) Stat software version: PMSE Occupation Recorder R6.3.15a

Figure 13: the car race from the visitors' point of view

Figure 14: typical antenna installation

Figure 15: view into one of several visitor areas

The figure 21 shows the combined frequency usage by LTE (IMT), an ENG/OB system and narrow band PMSE links.

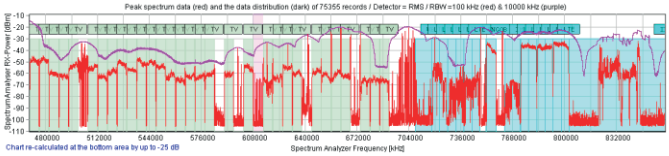

Figure 16: recorded spectrum allocation 410-870 MHz - frequency domain (75354 data records)

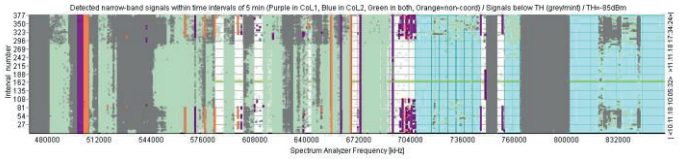

Figure 17: recorded spectrum allocation 410-870 MHz - frequency domain (75354 data records)

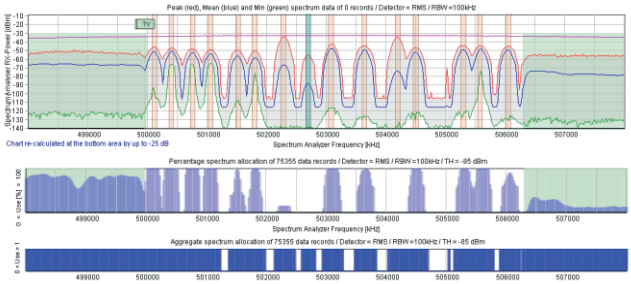

Figures 18-20: example of 14 detected and 1 manually marked links in 498-508 MHz and their level variance (75354 data records)

http://www.set.org.br/ijbe/ doi: 10.18580/setijbe.2019.2 Web Link: http://dx.doi.org/10.18580/setijbe.2019.2

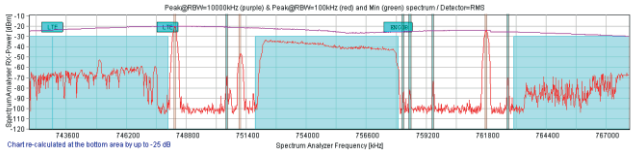

Figure 21: example of 3 detected, 5 manually marked narrow-band links and 1 wide-band ENG/OB in the 700 MHz duplex gap

Table 3 - Brief summary of the recorded spectrum information[(c)], 2nd and 3rd day

Description	Spec Information
Scanned frequency band	470 to 862 MHz
Range of scanned frequency band	392 MHz
TV channels in use by Broadcast	31
Radio spectrum in use by Broadcast	186 MHz
LTE channels in use by IMT	12
Radio spectrum in use by IMT	60 MHz
Radio spectrum in use by non-PMSE WB sys	75 MHz
Radio spectrum in use by WB PMSE systems	10 MHz
Radio spec remaining for NB and WB PMSE	81 MHz
Radio spectrum below 470 MHz (TalkBack)	60 MHz
NB PMSE detected outside of TV channels	51
NB PMSE manually marked outside TV ch	23
NB PMSE manually marked in TV channels	3
Required spectrum for detected NB PMSE [(a)]	39.00 MHz/ 77 Links
Required spectrum for NB and WB PMSE [(b)]	49.00 MHz
Spectrum density of detected NB PMSE [(b)]	0.951 Links/MHz
Coordinated PMSE in the scanned freq band	162
Coordinated NB PMSE in the scanned band	159
Coordinated audio PMSE in WB systems	2
Coordinated video PMSE in WB systems	1
Spec density of all coordinated PMSE	2.000 Links/MHz

(a) Calculation bases on a 500 kHz grid and two additional 250 kHz guard bands and manually marked links. This calculation does not consider required guard bands to TV or IMT channels
(b) Calculation considers manually marked links
(c) Stat software version: PMSE Occupation Recorder R6.3.15a

Table 4 – Minimum and Maximum receiver input level[(a)], 2nd and 3rd day

Information on receiver input level	Freq Level@ RBW	level	Log file
Maximum scanning	100 kHz	-20.21 dBm	Scan111018170459l002.txt at 748300 kHz
	10 MHz	-14.2 dBm	Scan111118113243762 4.txt at 468360 kHz
Minimum scanning	100 kHz	-120.14 dBm	Scan111181024319771.txt at 706540 kHz
Max on 1st scanner	100 kHz	-20.21 dBm	Scan111018170459l002.txt at 748300 kHz
Min on 1st scanner	100 kHz	-120.14 dBm	Scan111181024319771.txt at 706540 kHz
Max on 2nd scanner	100 kHz	-25.85 dBm	Scan111018120248829 4.txt at 641720 kHz
Min on 2nd scanner	100 kHz	-118.35 dBm	Scan111181041047556.txt at 805480 kHz
Maximum scanner input attenuator position: 10 dB			

III. EVALUATION OF THE OBSERVED RADIO SPECTRUM USE BY PMSE

In addition to the comprehensive data recorded in Sao Paulo or available as coordination information, additional data were available from the Formula One productions in Monza [3] in 2017 and 2018. Table 5 compares the available information (Please pays attention to technical notes below the table.)

Use of PMSE in the gaps between TV channels

A special usage scenario was observed in Sao Paulo - the operation of Audio PMSE between occupied TV channels.

Figures 22 and 23 show a typical situation, PMSEs operated in the gaps between digital TV channels. This operation of PMSE in the gaps between television channels is assessed as a critical scenario.

The scan antenna of the first scan station was in a large fabric tent. The fabric surface of this tent was coated with a thin layer of metal. Therefore, an additional path attenuation of about 6 dB is estimated.

Table 5: Comparison of coordination information and detected PMSE links

Category	Brazil 2018	Italy 2017	Italy 2018
Number of coordinated PMSE links in 410-870 MHz	269	269	247
Number of coordinated PMSE links in 410-470 MHz	88	45	N/A [(2)]
Number of coordinated PMSE links in 470-870 MHz	178 + 3 in WB links	224	N/A [(2)]
Radio spectrum in use by Broadcast	186 MHz	48 MHz	88
Radio spectrum in use by IMT and non-PMSE wb. systems	143 MHz	60 MHz	60
Radio spectrum remaining for PMSE in 410-870 MHz [(1)]	141 MHz	352 MHz	318
Spectrum density of all coordinated PMSE in 410-870 MHz [(1)]	1.135 Links/ MHz	0.585 Links/ MHz	N/A [(2)]
Spectrum density of all coordinated PMSE in 410-470 MHz [(1)]	1.617 Links/ MHz	0.750 Links/ MHz	N/A [(2)]
Spec density of all coordinated PMSE in 470-870 MHz [(1)]	0.741 Links/ MHz	0.560 Links/ MHz	N/A [(2)]
Spectrum density of all detected PMSE in 410-870 MHz [(1)]	0.585 Links/ MHz [(4)]	N/A [(3)]	0.390 Links/ MHz [(5)]
Spectrum density of detected NB PMSE in 410-870 MHz [(1)]	0.453 Links/ MHz [(4)]	0.455 Links/ MHz [(5)]	0.390 Links/ MHz [(5)]
Spectrum density of detected NB PMSE in 410-470 MHz [(1)]	1.467 Links/ MHz [(4)]	1.183 Links/ MHz [(5)]	0.717 Links/ MHz [(5)]
Spectrum density of detected NB PMSE in 470-870 MHz [(1)]	0.445 Links/ MHz [(4)]	0.305 Links/ MHz [(5)]	0.302 Links/ MHz [(5)]
Spectrum density of detected NB PMSE in 470-870 MHz [(1)]	0.951 Links/ MHz [(6)]	0.305 Links/ MHz [(5)]	0.302 Links/ MHz [(5)]

[(1)] This calculation does not consider required guard bands from PMSE to TV or IMT channels.
[(2)] No detailed coordination information available.
[(3)] No wide-band PMSE inks detected.
[(4)] Considers only links that were detected on 1st day.
[(5)] Relatively small number of spectrum scans allows only a limited comparison of the results.
[(6)] Considers only links that were detected on 2nd to 3rd day.

The zoomed scans in figures 24 and 25 show the spectrum use in an unoccupied TV channel between two occupied TV channels.

Comparison of the recorded signals: location 1 and location 2

The spectral scanning equipment was installed at two different locations, at location 1 - the international technical area for the TV stations (compound) with the UFABC semi-portable 6 GHz R&S spectrum analyser shown in figure 26 and at location 2 - the TV Globo booth with APWPT's semi-portable 3 GHz R&S spectrum analyser in the middle of the pit line, shown in figure 27.

The scan antenna of the first scan station was in a large fabric tent. The fabric surface of this tent was coated with a thin layer of metal. Therefore, an additional path attenuation of about 6 dB is estimated.

Figure 28 shows the final output of the aggregation of all scans from all locations.

The possible effect of high network density of TV transmitters for the production quality of Audio PMSE

In Sao Paulo, the signals from 31 TV stations were recorded. In this section, we try to specify the signal level of the TV transmitters at the receiver input of the audio PMSE.

http://www.set.org.br/ijbe/ doi: 10.18580/setijbe.2019.1 Web Link: http://dx.doi.org/10.18580/setijbe.2019.1

The red line in figure 29 shows the signal level measured in a bandwidth of 100 kHz and the purple line refers to a bandwidth of 10 MHz - both measured with RMS detector - a level up to -38 dBm. Considering the crest factor of the TV signal, the maximum peak interferer level is expected to be significantly above -30 dBm.

Effect of the antenna polarization

As Globo DTPD staff noted, the polarization in Brazil by regulation is horizontal for the reception, so all broadcasters use horizontal transmission or elliptical polarization. Because the scan antennas had a vertical polarization, a higher reception level of the TV stations must be expected for PMSE antennas that deviate from vertical polarization.

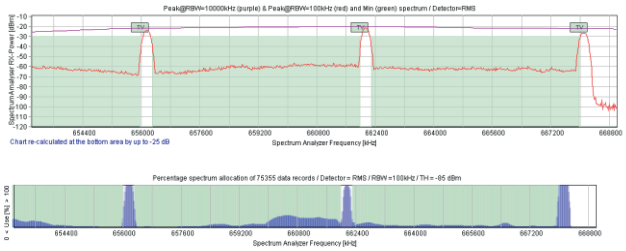

Figure 22-23: aggregated spectrum from 653-669 MHz (2nd day, 75354 data records)

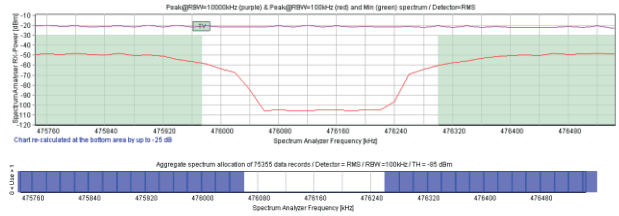

Figure 24-25: aggregated spectrum from 475.744- 476.544 MHz (2nd day, 75354 data records)

Location 1 - TV Globo booth

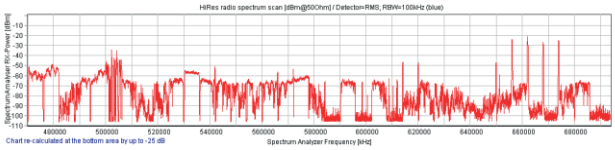

Figure 26: 1st scanner, aggregated spectrum from 470-694 MHz (2nd day, 45154 data records)

Location 2 - international technical area

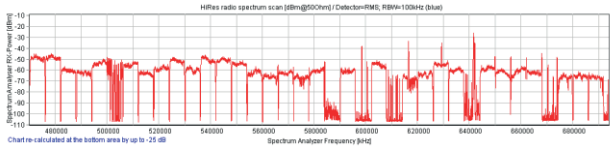

Figure 27: 2nd scanner, aggregated spectrum from 470-694 MHz (2nd day, 30200 data records)

Location 1 and 2

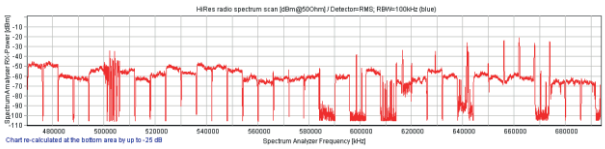

Figure 28: aggregated spectrum of both locations from 470-694 MHz (2nd day, 75354 data records)

Maximum recorded receive level at Location 1 and 2

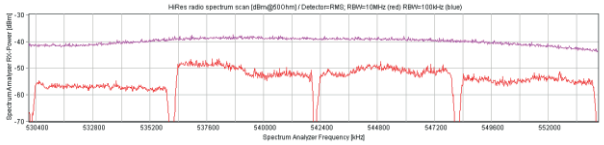

Figure 29: spectrum recording in a resolution bandwidth of 200 kHz (red) and 10 MHz, both with RMS detector

Bandwidth to be taken into account for the calculation of intermodulation

Audio PMSE receivers known to us have a frontend bandwidth of probably more than 24 MHz. However, several receivers are often connected to a common antenna via an active splitter. This non-linear transmission block must also be taken into account.

The users and frequency coordinators of Audio PMSE must carefully consider this scenario.

Aggregated scan from November 2018

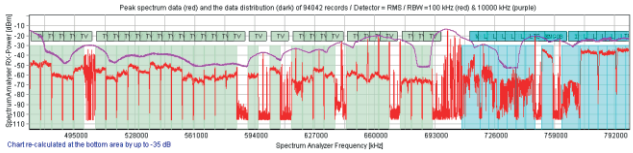

Figure 30: spectrum recording in frequency domain

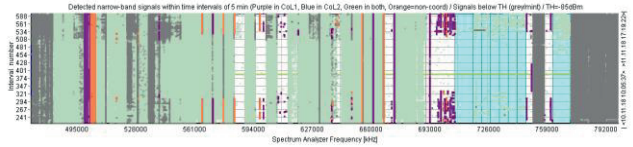

Figure 31: spectrum recording in frequency and time domain

Aggregated scan from August 8th, 2019

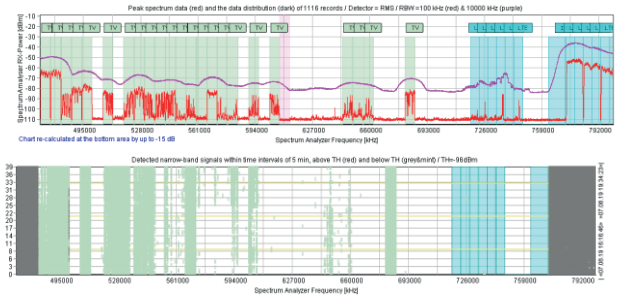

Figure 32-33: spectrum recording in frequency and time domain

Comparison of frequency use by TV and IMT (application of the land mobile service) and possible changes

Interesting is the use of the spectrum outside the production of events. Therefore, in this section we will compare the frequency use in the band 470 to 800 MHz during F1 production in October 2018 with an additional scan from August 2019. Below in the figures 30 to 33 one can see the actual spectrum access of broadcast and mobile communications and possible changes in their operation.

Restriction of this evaluation

Both spectrum recordings took place at different locations and with different antenna heights. It is therefore possible that the spectrum recording in August may show an incomplete TV and IMT coverage. Another indicator for a worse antenna position of the second scan is the level of most signals reduced by more than 10 dB.

http://www.set.org.br/ijbe/ doi: 10.18580/setijbe.2019.2 Web Link: http://dx.doi.org/10.18580/setijbe.2019.2

Table 6 - Spectrum recordings

Date	Number of TV sections	TV MHz]	Number of IMT sections	IMT [MHz]	Scan time
November 2018	31	186	12	60	~3 days
August 2019	25	150	12	60	~3 hours

Both sets of scans show that the UHF TV band is intensively in use by digital TV and IMT. During the event and content production the 'white spaces' are in temporarily use by PMSE.

To illustrate a little the complexity of content production teams working at the event, figure 34 shows the equipment installed on the ground, figure 35 the helicopter video recording, figures 36 and 38 show different teams working, figure 37 the flying helicopter and a crane boom behind the pit lane. Figures 39-40 shows some satellite antenna (at compound) and other antenna arrays (next to the pit lane).

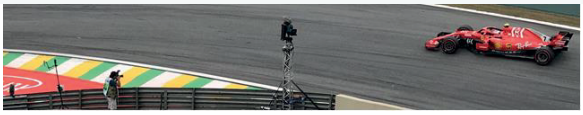

Figure 34: equipment of the event production installed on the ground, a photographer and the racing car

Figure 35: view of the helicopter that was used for the flying video recording

Figure 36: New Gathering Team in operation

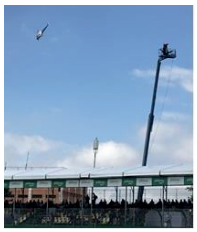

Figure 37: Helicopter and camera on a crane boom

Figure 38: view into an on-site content production vehicle

Figure 39: typical arrangement of antennas for team and satellite communication

Figure 40: typical arrangement of antennas for further radio systems of the event

IV – Discussions and Conclusions

In this RF Scanning, we show that the number of wireless PMSE microphones use increased in the Formula One GP Brazil from 2014 to 2018, like in the Italian GP. This last measurement procedure was the most detailed scan to date in the wireless PMSE microphones band at Brazilian F1 GP. The figure 41 shows a re-draw of figure A.2 of ETSI TR system document for PMSE microphones [7] and the convergence to 0.34 links/MHz density in large spectrum consistent with our recorded data to this event.

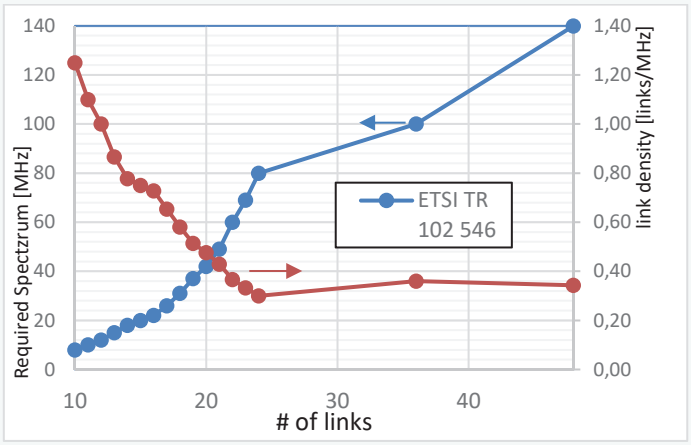

Figure 41: Required Spectrum and link density vs. Number of links

During the Brazilian Formula One event the operation of PMSE in the gaps between television channels was observed and is assessed as a critical scenario. Considering the high density of registered TV channels, non-linear transmission blocks must also be taken into account and users and frequency coordinators of Audio PMSE must carefully consider this scenario too.

Only a summary of all available information in relation to this work is presented in this work. Those who require further, more detailed information should please contact APWPT via office@apwpt.org.

V. Acknowledgments

Comparable to many previous spectrum recordings, this activity was only possible with intensive technical and logistical support. Among many others we extend warm thanks to the following teams and people: Formula One, professors Ivan Roberto de Santana Casella and Stilante Koch Manfrin of Federal University of ABC, RAI Italy and Sennheiser.
The authors gratefully acknowledge the Globo TV and the collaboration of the involved staff to use their services and facilities for conduction of this research.

VI. References

[1] EuMW, "European Microwave Week," 10 August 2019. [Online]. Available: https://www.eumweek.com/.

[2] International Broadcasting Event, "IBC Show," 13 September 2018. [Online]. Available: https://show.ibc.org/.

http://www.set.org.br/ijbe/ doi: 10.18580/setijbe.2019.2 Web Link: http://dx.doi.org/10.18580/setijbe.2019.2

[3] P. Seeger, "IBC SHOW 2018 - 10 years of APWPT", 10 August 2019. [Online]. Available: https://www.apwpt.org/downloads/ibc2018_frequencies-f1-gp.pdf.

[4] ETSI, "Programme making & special events (PMSE)," 11 August 2019. [Online]. Available: https://www.etsi.org/technologies/pmse.

[5] Wikipedia, "Autódromo José Carlos Pace," 08 August 2019. [Online]. Available: https://de.wikipedia.org/wiki/Autódromo_José_Carlos_Pace.

[6] FIA, "Highs and lows - which F1 track has the most elevation changes?" 10 August 2019. [Online]. Available: https://www.formula1.com/en/latest/features/2016/10/highs-and-lows---which-f1-track-has-the-most-elevation-changes-.html.

[7] ETSI TR 102 546, Electromagnetic compatibility and Radio spectrum Matters (ERM); Technical characteristics for Professional Wireless Microphone Systems (PWMS); System Reference Document, V1.1.1 (2007-02), Sophia Antipolis, 2007.

[8] ETSI, "4th Generation (LTE)," ETSI, 20 August 2019. [Online]. Available: [Accessed 20 Aug 2019]. https://www.etsi.org/technologies/mobile/4g.

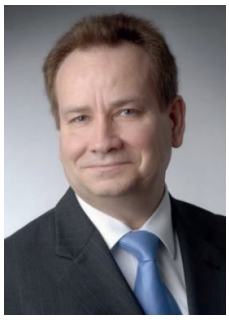

Matthias Fehr is a graduated engineer in Industrial Electronics, Dipl.-Ing. (FH), 1985, Microprocessor Systems, Dipl.-Ing. (FH), 1989 and Biomedical Technology and Bio-Cybernetics, Dipl.-Ing. (TH), 1990. From 1984 to 1990 he was the head of the Department for Electronic Tool Building and Prototypes in the Institute "FOE" of University Ilmenau. From 1990 to 2001 he was the head of the Aeronautical Radio Development Department at Walter Dittel GmbH.
From 2001 to 2008 he worked as a technical coordinator for radio frequency projects in the Research Division of Sennheiser Electronic GmbH. Since 2008 he is President / Chairman of Executive Board of APWPT, the world-wide working Association of PMSE users and PMSE manufacturers.

Mario Minami received BSc degree in Physics (1990) from IFUSP, Institute of Physics of the University of São Paulo, BSc degree in Pedagogy (2009) from Nove de Julho University, MSc (1993) and PhD (1998) in Electrical Engineering from the Polytechnic School of the University of São Paulo, EPUSP. Since 1993 at now, he is an associated researcher at the Signal Processing Laboratory (LPS) at EPUSP.
Since 2010 he is Associate Professor of Information Engineering at UFABC, CECS, in the Multimedia Communications Group. Member of Signals and Systems Laboratory (2012) and the Cybernetic Pedagogic Robotic group (2016) at UFABC. Member of IEEE Signal Processing Society and Acoustical Society of America. His research interests are in Speech Signal Recognition and Synthesis, Speech Analysis and Coding, Digital Audio Modeling, Image Processing in Digital Games and Robotics in Education.

Felipe Filgueiras is a Telecommunications Technician (2012) and Telecommunication engineering student. He has been working in the RF area for 8 years and since 2013 at TV Globo where he is the coordinator of DTPD division.
His division is responsible by coordination of all frequencies used for each sporting events of the Globo Group and regularizing them with the competent regulatory agencies.

Pia Seeger received BE degree (2016) at Beuth Hochschule für Technik Berlin, Germany, MSc in Information Engineering (2017) at University Federal of ABC (UFABC), Brazil, and Master of Engineering (2018) at Beuth Hochschule für Technik Berlin, Germany. She worked in Bene Lux event technology (2012), Steffens and Hecht Stahlbau GmbH (2013), satis&fy AG (2015) all in Hamburg, Germany.

André F. Ponchet obtained the titles of Electrical Engineer from the Federal University of Ceará (2002), Master in Telecommunications
Engineering (2006) and PhD in Electrical Engineering (2016) from the State University of Campinas. He have been working on RF IC design since 2009. In 2017 started to work as an assistant professor at the Center for Engineering, Modeling and Applied Social Sciences at the Federal University of ABC.
Dr. Ponchet interests include: analog and RF Integrated circuits design, broadband amplifiers for millimeter wave applications, RF transceiver architectures, optoelectronics and silicon integrated photonics.

Georg Fischer (M'01–SM'08) received the Diploma degree in electrical engineering from RWTH Aachen University (1992), and the Dr.-Ing. degree in electrical engineering from the University of Paderborn, (1997) both in Germany. From 1993 to 1996, he was a Research Assistant with the University of Paderborn, working with adaptive antenna array systems. From 1996 to 2008, he performed research with Bell Labs, Lucent (later Alcatel-Lucent, now NOKIA) in GSM, UMTS systems.
Since April 2008, he has been a Professor for electronics engineering with the University of Erlangen–Nuremberg FAU. He holds over 50 patents concerning microwave and communications technology. His research interests are in transceiver design, analog/digital partitioning, converters, enhanced amplifier architectures, duplex filters, metamaterial structures, GaN transistor technology and circuit design, and RF microelectromechanical systems (MEMS) with specific emphasis on frequency agile, tunable, and reconfigurable RF systems for software-define radio (SDR) and cognitive radio (CR) applications. His new research interests concentrate on wireless multimedia transmission like PMSE (Program Making and Special Events). He is a Senior Member of the IEEE Microwave Theory and Techniques Society (MTT-S)/Antennas and Propagation Society (AP-S)/Communications Society (COMSOC)/ Vehicular Technology Society (VTC)/ IEEE Engineering in Medicine and Biology Society (EMBS) and member of VDE-ITG and European Microwave Association (EUMA).

Received in 2019-07-10 | Approved in 2019-10-21

http://www.set.org.br/ijbe/ doi: 10.18580/setijbe.2019.2 Web Link: http://dx.doi.org/10.18580/setijbe.2019.2

How Artificial Intelligence impacts the programs broadcast by Globo TV: Case studies

Alvaro Antelo
Edmundo Hoyle

CITE THIS ARTICLE:
Antelo, Alvaro and Hoyle, Edmundo; 2019. How Artificial Intelligence impacts the programs broadcast by Globo TV: Case studies. SET INTERNATIONAL JOURNAL OF BROADCAST ENGINEERING. ISSN Print: 2446-9246 ISSN Online: 2446-9432. doi: 10.18580/setijbe.2019.3. Web Link: http://dx.doi.org/10.18580/setijbe.2019.3

How Artificial Intelligence impacts the programs broadcast by Globo TV: Case studies

Alvaro Antelo, Edmundo Hoyle

***Abstract*—In this article we show how Artificial Intelligence (AI) are impacting multimedia content creation, processing and delivery in the programs broadcasted by Globo TV. AI is mostly perceived as a new tool capable of optimizing and enhancing processes through automation in ways that were unthinkable in the recent past. Three broadcast programs were chosed as targets for AI algorithms deployment in our current workflow aiming at increased productivity, cost reduction and novel ways to generate content.**

***Index Terms*—Artificial Intelligence Deep Learning Image Processing Broadcast TV.**

I. Introduction

ADVANCES in AI have enabled manufacturers and broadcasters to develop and implement smarter tools and applications to boost the entire content lifecycle.

Deep learning is an aspect of AI that is concerned with emulating the learning approach that human beings use to gain certain types of knowledge. The phrase “deep learning” probably conjures up images of sentient robots staging a hostile takeover. But in reality, deep learning is just another way to describe large neural networks, a technology you encounter every day when you browse the Internet or use your mobile phone. A basic neural network might have one or two hidden layers, while a deep learning network might have dozens or even hundreds.

Today many AI applications exists around us, and we use them normally without perceiving it. For example when somebody is looking for images that included an object of interest. A short list with the main applications could be similar to this:

- Automatic Machine Translation.
- Object Classification in Photographs.
- Automatic Handwriting Generation.
- Character Text Generation.
- Self-driving vehicles
- Image Caption Generation.
- Automatic object segmentation.
- Colorization of Black and White Images.

In this article we explain how Globo TV utilize common AI techniques to increase it’s productivity, reduce costs and create novel ways to generate content. The organization of this article is as follows: The first section shows a brief summary about the three techniques of deep learning used by Globo TV in each of their programs broadcasted. In the second section we’ll talk about how each broadcast program was impacted by the techniques of deep learning described in the previous section. The workflow used in the process to exploit the AI algorithms will be showed in the four section. The last section contains the conclusions about our experiences.

A. Antelo and E. Hoyle are with Department of Research and Development of TV Globo.
E-mail: alvinho, edmundo.hoyle @tvglobo.com.br

II. State-of-Art

In this section we describe briefly the three techniques of deep learning that were used in three programs broadcasted by Globo TV. Starting with neural style transfer which was used in The Voice kids, followed by automatic colorization used in *Cidade Proibida* and ending with semantic segmentation employed in segmentation the ”secret reporter” in the program *Fantástico*.

A. Neural Style transfer

In 2015, Gatys et al. [1] showed a seminal work that demonstrated how convolutional neural networks (CNN) could be used to generate stylized images from a texture example. This process of using a CNN to render a content image in different styles is referred to as Neural Style Transfer. Their experimental results demonstrated that the content and style in a photo were separable, which indicates the probability of changing a photo’s style while preserving desired semantic content as showed in Figure 1.

Fig. 1: A simple sample using Neural Style Transfer. Upper left: Input image, lower left: style, right side: output image

A wide range of implementations have been made freely available in [2] [3] [4], based varyingly on different neural network frameworks such as Caffe [5] and Tensorflow [6] and wrappers such as Torch and PyCaffe [7]. Joshi et al. in [8] shows a high-level case study about what its like to apply style transfer techniques to cinema, they used the technique to redraw key scenes in the short movie Come Swim in the style of the impressionistic painting that inspired the film. Figure 2 shows a sample from the movie .

http://www.set.org.br/ijbe/ doi: 10.18580/setijbe.2019.3 Web Link: http://dx.doi.org/10.18580/setijbe.2019.3

Fig. 2: Usage of Neural Style Transfer in Come Swim; top: content image, top right : style image, bottom: upsampled result. Images taken from [8]

B. Automatic Colorization

The power of convolutional neural networks for image processing is mostly demonstrated on the seemingly impossible task such as colorizing a black and white picture. Anyone familiar with color conversion math will readily attest that once color information is lost there is no way to restore it. Deep learning proved that it is possible to colorize a black and white picture because as Zhang *et al.* said [9] "in many cases, the semantics of the scene and its surface texture provide ample cues for many regions in each image: the grass is typically green, the sky is typically blue, and the ladybug is most definitely red"; also citing Larsson [10] "Automatic colorization serves as a proxy measure for visual understanding", implying a close relation between colorization and semantic segmentation; in other words the network must be able to detect and segment visual objects prior to assigning a probable color to its region. In fact, most convolutional networks trained for colorization begin with networks trained for object detection and classification and are further tuned for colorization with a large dataset of color images. Computerized colorization techniques existed prior to machine learning but they relied on human artists to scribble color on image regions and a computer assisted the colorization process by completing the color fill throughout similar regions. The first fully automated colorization pipeline goes back to Cheng *et al.* [11] in which various features are extracted from the images and the different patches of the image are colorized using a small neural network. Automatic colorization using deep

Fig. 3: Black and white images colorized using automatic colorization. Images taken from [12]

learning predicts plausible colors to image regions without any human intervention. To accomplish this, a neural network has to be trained with millions of reference color images, exposed to only the luminance channel and as it tries to estimate the colors, any deviations from ground truth on the pixel level at the output gets backpropagated inside the network in the form of error information and the whole process iterates as it converges during several thousands iterations throughout all training images. We found that the most common colorspace used in research is CIE LAB because it is designed to be a perceptually linear space but it is converted to YUV or RGB as needed on the output. During the experiments, we found that the presence of significant amounts of noise and also low contrast images on the black and white pictures reduced the colorization performance of all networks, so we introduced a pre-processing stage which does noise reduction and contrast normalization prior to the colorization.

C. Semantic segmentation

Semantic segmentation is the task of clustering parts of images together which belong to the same object class. For this to happen it is necessary to identify the classes of objects in images and also to localize them inside the images with reasonable accuracy. The segmentation of objects is one of the key problems in the field of computer vision, the Figure 4 explains the evolution of object segmentation. Garcia-Garcia *et al.* said in [13] "Looking at the big picture, semantic segmentation is one of the high-level task that paves the way towards complete scene understanding". Many applications depend on accurate semantic segmentation such as autonomous driving, human-machine interaction, image search engines and augmented reality. It is important to distinguish semantic segmentation from object detection which only has to distinguish different instances of the same object in the image; for example the image of a car behind a tree is split into two objects using object detection but only one car with semantic segmentation. There exists a wide range of segmentation algorithms, mainly

http://www.set.org.br/ijbe/ doi: 10.18580/setijbe.2019.3 Web Link: http://dx.doi.org/10.18580/setijbe.2019.3

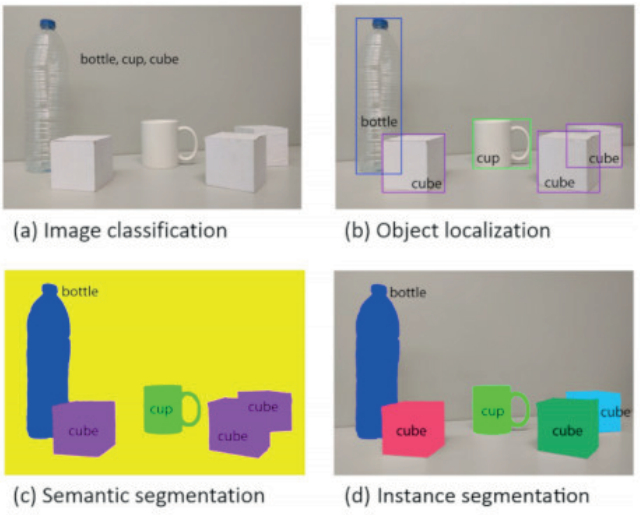

Fig. 4: Evolution of object recognition or scene understanding from coarse-grained to fine-grained inference: classification, detection or localization, semantic segmentation, and instance segmentation. Image taken from [13]

variating on the number of classes of objects it's able to process, for example an autonomous car system has a semantic segmentation based on binary classes such as street versus non-street or more classes as road signs, people, vehicles, etc. Deep neural networks, usually convolutional neural networks dominate this field nowadays and their accuracy far surpasses any other methods of segmentation. In order to train a neural network for this task, one has to start with a dataset of images previously annotated, in other words the images must be labeled with masks identifying all classes that will have to be learned, for example the image of a car has to have all pixels containing the car marked as a single region, if there is a person in that image too it has to be labeled as a different class. Google provided the Tensorflow Object Detection API [14], this API made the segmentation objects such as persons, cars and many others as shown in Figure 5.

III. Case Studies

This section describe how the techniques showed in the previous section were used in the GLOBO TV programs.

A. The Voice Kids

The Voice Kids is a version of The Voice tv series franchise in which kids participate. The Brazilian version went on air on 2016, and in this program, singers perform on a stage with big screens on the background. The technique was used to create the videos that go on the big screens behind the participants of The Voice Kids. The neural style transfer was our first initiative to produce content using Artificial Intelligence methods on Globo TV. In this program the participant Juan Carlos Poca was going to sing the song " o amor" (Zezé Di Camargo and Luciano) and the team needed soft videos that could keep pace with the music. They had already thought of using landscapes and adding some kind of effect on them. Various

Fig. 5: Segmentation and recognition sample using the Tensorflow Object Detection API

styles and paintings of artists were trained and applied directly over videos select by the producers, and the paintings of impressionist artist Claude Monet were selected as the style that produce the best results. Figure 6 shows two image samples extracted from the videos showed in The Voice Kids Brasil, and in [15] it is possible to view the performance. This is a novel way to generate content with relative low cost.

Fig. 6: Images from the Voice Kids Brasil with the screens showing images created with neural style transfer

http://www.set.org.br/ijbe/ doi: 10.18580/setijbe.2019.3 Web Link: http://dx.doi.org/10.18580/setijbe.2019.3

B. Cidade Proibida

Cidade Proibida "Forbidden city" is a twelve episodes Globo TV series aired weekly beginning on September 2017. It's a detective story set on 1950 Rio de Janeiro and uses many old black and white film footage. The clips were used in the context of flashbacks of the main character and as short sonorized clips exhibited whenever the main character moves around the city. It was decided that these clips would be colorized in order to appeal more to the audiences. Image colorization bureaus such as Dynamichrome [16] company do this on a manual basis with superb color rendition but costs can go up to US$ 100,00 per image and time spent depending on the image can take from a day to an entire month. Total duration of footage per episode was around fifteen seconds which at 24 frames per second gives 360 frames per episode, or 4320 frames for the whole series. This amount of frames makes it impossible to tackle with colorization on a manual basis, because of the high cost and time needed to colorize all frames. In order to decrease the costs we looked at automatic colorization using deep learning as a valid option. In our tests the processing time to colorize was two seconds per frame, therefore the process to colorize all frames was 144 minutes. We used custom linux images on g3.4xlarge virtual instances in Amazon EC2 to provide us with the necessary computing power to achieve the result in a reasonable amount of time. The machine cost is $ 1,14 per hour, totaling approximately $ 200,00 to colorize all videos. Figure 7 show two sample frames with theirs respective images colorized that were used in the series *Cidade Proibida*

Fig. 7: Original Black and white frames and their respective colorization used in *Cidade Proibida*

C. Fantástico

Fantástico is a Brazilian weekly television news magazine broadcast on Sunday nights on Globo TV since August 5, 1973. It is an open-ended newscast with hosts introducing and reporting stories. One of the segments, named "Secret Reporter" is hosted by Eduardo Faustini, a brazilian journalist, being one of the most important investigative reporters of Globo TV. To preserve his physical integrity, he never revealed his identity in these investigations, so there is a need to obfuscate his image in post production. For each story, the time spent in hiding the reporter was taking about 3 days. This required the team to meet a week in advance, each time a new story will be produced to determine an upper limit on the amount of material that could be used. It is a painstaking process that takes days to create only a few seconds of video. The main objective of this project was to reduce the time spent by the art team in hiding the reporter in the video scenes aired in *Fantástico*. Deep learning semantic segmentation was employed to identify, localize and masquerade Faustini's image in an automated fashion. Semantic segmentation is implemented in a deep learning network that was trained with thousands of images segmented and manually annotated, in these images there are people, cars, chairs, dogs etc. With the trained network this algorithm returns the masks of the objects found in the image, be it people, cars or any other object found. In our case we only used the segmentation marked as a person. After the processing, the algorithm returns a video containing the masking area to be refined by the Arts team. The whole process takes about 1 minute for each second of video, and due to the fact that it can be run in parallel, now it makes no difference if 1 or 20 videos arrive at the same time. With the reduction in processing time, it is now possible to receive a greater amount of material and it opens the possibility of

http://www.set.org.br/ijbe/ doi: 10.18580/setijbe.2019.3 Web Link: http://dx.doi.org/10.18580/setijbe.2019.3

Fig. 8: The Secret Reporter hidden behind the blue mask

including new material received at the last-minute. In addition to the gains in productivity, the new process allows the artist to be more focused on his main work (doing art) and not on a painstaking manual process of creating masks. The cost to keep the system running on Amazon is around 50 dollars per month, a very low cost for the huge benefits brought to the production of the program. Figure 8 show a few images showing the Secret Reporter hidden behind the blue mask. There is also a link for a video showing some footage from the program [17]

IV. Workflow

All cases described in this paper use their own deep learning technique but the process life cycle is very similar between them. The infrastructure for this process was built on Amazon Web Services (AWS) in order to decouple them from our internal workflow and also to leverage elastic scaling, in other words the infrastructure would be deployed on demand as

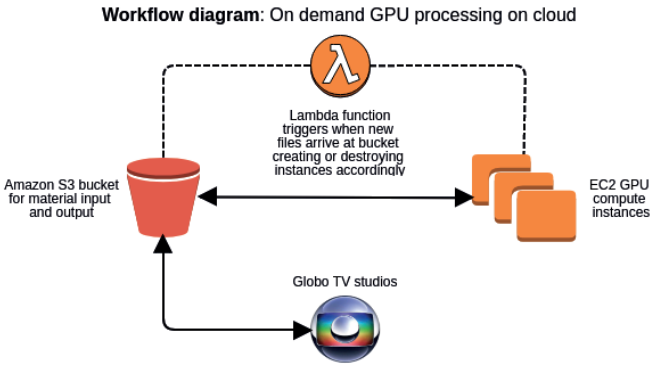

Fig. 9: AWS Workflow process

new videos got uploaded and destroyed as soon as it is not necessary anymore. In order to store the video files before and after processing we used Amazon S3 simple storage service which is an object storage accessed by web services interfaces; in practice an editor would open a web interface and upload video clips to be processed. As soon as the files got uploaded, AWS lambda which is an event driven serverless computing platform would trigger the instantiation of GPU machines containing the AI algorithms, ready to begin consuming the newly received video files. For each video file a new machine spun up so processing occurred on a parallel fashion. At the end of processing, the resulting video files got written on the S3 bucket and the machine which finishes the job got destroyed. The editor can therefore look at the output bucket on S3 and start downloading the processed video files. Figure 9 shows the workflow process in AWS.

V. Conclusion and Future Explorations

In this paper we presented three applications of deep learning algorithms applied on the production of three broadcast programs. In all cases we saw benefits be it on the productivity aspect or in novel ways to generate content. Using cloud deployment makes it easy to just plug the algorithms in our current workflow minimizing eventual integration problems. Artificial intelligence opens up new opportunities for productivity enhancement in the broadcast environment.

Looking from the sole perspective of automation, we see many avenues for innovation in video related workflows, especially in human related tasks closedly tied to visual understanding, for example tagging images, searching for images, archiving material, in quality control and error detection on video, switching video based on content, etc. Those tasks are currently assigned to humans but can be significantly offloaded to AI algorithms providing massive improvements in throughput and possibly error reduction.

References

[1] Leon A. Gatys, Alexander S. Ecker, and Matthias Bethge. A neural algorithm of artistic style. *CoRR*, abs/1508.06576, 2015.
[2] Frank Liu. style-transfer. https://github.com/fzliu/style-transfer. Accessed: 2018-06-30.
[3] Justin Johnson. neural-style. https://github.com/jcjohnson/neural-style. Accessed: 2018-06-30.

http://www.set.org.br/ijbe/ doi: 10.18580/setijbe.2019.3 Web Link: http://dx.doi.org/10.18580/setijbe.2019.3

[4] Anish Athalye. neural-style. https://github.com/anishathalye/neural-style. Accessed: 2018-06-30.
[5] Yangqing Jia, Evan Shelhamer, Jeff Donahue, Sergey Karayev, Jonathan Long, Ross B. Girshick, Sergio Guadarrama, and Trevor Darrell. Caffe: Convolutional architecture for fast feature embedding. *CoRR*, abs/1408.5093, 2014.
[6] Martín Abadi, Ashish Agarwal, Paul Barham, Eugene Brevdo, Zhifeng Chen, Craig Citro, Gregory S. Corrado, Andy Davis, Jeffrey Dean, Matthieu Devin, Sanjay Ghemawat, Ian J. Goodfellow, Andrew Harp, Geoffrey Irving, Michael Isard, Yangqing Jia, Rafal Józefowicz, Lukasz Kaiser, Manjunath Kudlur, Josh Levenberg, Dan Mané, Rajat Monga, Sherry Moore, Derek Gordon Murray, Chris Olah, Mike Schuster, Jonathon Shlens, Benoit Steiner, Ilya Sutskever, Kunal Talwar, Paul A. Tucker, Vincent Vanhoucke, Vijay Vasudevan, Fernanda B. Viégas, Oriol Vinyals, Pete Warden, Martin Wattenberg, Martin Wicke, Yuan Yu, and Xiaoqiang Zheng. Tensorflow: Large-scale machine learning on heterogeneous distributed systems. *CoRR*, abs/1603.04467, 2016.
[7] Soheil Bahrampour, Naveen Ramakrishnan, Lukas Schott, and Mohak Shah. Comparative study of caffe, neon, theano, and torch for deep learning. *CoRR*, abs/1511.06435, 2015.
[8] Bhautik Joshi, Kristen Stewart, and David Shapiro. Bringing impressionism to life with neural style transfer in come swim. In *Proceedings of the ACM SIGGRAPH Digital Production Symposium*, DigiPro '17, pages 5:1–5:5, New York, NY, USA, 2017. ACM.
[9] Richard Zhang, Phillip Isola, and Alexei A. Efros. Colorful image colorization. *CoRR*, abs/1603.08511, 2016.
[10] Gustav Larsson, Michael Maire, and Gregory Shakhnarovich. Learning representations for automatic colorization. *CoRR*, abs/1603.06668, 2016.
[11] Zezhou Cheng, Qingxiong Yang, and Bin Sheng. Deep colorization. *CoRR*, abs/1605.00075, 2016.
[12] Satoshi Iizuka, Edgar Simo-Serra, and Hiroshi Ishikawa. Let there be Color!: Joint End-to-end Learning of Global and Local Image Priors for Automatic Image Colorization with Simultaneous Classification. *ACM Transactions on Graphics (Proc. of SIGGRAPH 2016)*, 35(4):110:1–110:11, 2016.
[13] Alberto Garcia-Garcia, Sergio Orts-Escolano, Sergiu Oprea, Victor Villena-Martinez, and José García Rodríguez. A review on deep learning techniques applied to semantic segmentation. *CoRR*, abs/1704.06857, 2017.
[14] Jonathan Huang, Vivek Rathod, Chen Sun, Menglong Zhu, Anoop Korattikara, Alireza Fathi, Ian Fischer, Zbigniew Wojna, Yang Song, Sergio Guadarrama, and Kevin Murphy. Speed/accuracy trade-offs for modern convolutional object detectors. *CoRR*, abs/1611.10012, 2016.
[15] The Voice Kids Brazil. Juan carlos poca performance. https://www.youtube.com/watch?v=6w_FM47iRp0. Accessed: 2018-06-30.
[16] Dynamichrome. http://dynamichrome.com/.
[17] Fantantisco. Reportersecreto. https://globoplay.globo.com/v/6716012/programa/?s=3m31s. Accessed: 2018-06-30.

Alvaro Antelo received his BSc at the University Veiga de Almeida of Rio de Janeiro (Brasil) in 2001. Actually he works as researcher at TV Globo and his main research interests include deep learning, video over IP and networking.

Edmundo Hoyle received his Bsc in Physics at National University of Trujillo (Peru) in 2004 and his DSc at the Federal University of Rio de Janeiro (Brasil) with specialization in Image Processing in 2013. Actually he works as researcher at TV Globo and his main research interests are image processing, computer vision and deep learning.

Received in 2018-06-30 | Approved in 2019-07-10

http://www.set.org.br/ijbe/ doi: 10.18580/setijbe.2019.3 Web Link: http://dx.doi.org/10.18580/setijbe.2019.3

An index to measure the engagement of Globoplay users – Globo's OTT Platform

Felipe Parpinelli Constâncio
Gabriel Sodré Belém
Karla Klahold de Souza Biscaro

CITE THIS ARTICLE

Constâncio, Felipe Parpinelli; Belém, Gabriel Sodré and Biscaro, Karla Klahold de Souza;2019. An index to measure the engagement of Globoplay users – Globo's OTT Platform. SET INTERNATIONAL JOURNAL OF BROADCAST ENGINEERING. ISSN Print: 2446-9246 ISSN Online: 2446-9432. doi: 10.18580/setijbe.2019.4. Web Link: http://dx.doi.or-g/10.18580/setijbe.2019.4

An index to measure the engagement of Globoplay users – Globo's OTT Platform

Felipe Parpinelli Constâncio, Gabriel Sodré Belém and Karla Klahold de Souza Biscaro

Abstract — **Engagement is a very abstract and very important metric to measure the evolution of the product and understand the users. In this study, we will show how, through data science techniques our team has created an index of engagement, what we call IEN, for our users base crossing data and providing different weights for playtime, diversity of watched programs and frequency of use. And from this index, we generate segments of users. We will also show how we create interventions for these user segments, allowing you to use more complex business rules in the product.**

Index Terms **— Globoplay, VOD, OTT, Engagement index**

I. INTRODUCTION

GLOBO is the largest media group in Brazil and the largest Latin America content producer. We reach 100 million people daily on our properties.

Globoplay is the group's OTT platform, with a wide variety of AVOD, SVOD and Live Streaming content, including international tv series, movies, reality shows, telenovelas, local news and so on.

Understanding and measuring the relationship between the engagement of our users with their advertising and subscription lifetime value including their propensity to churn is a rather complex task due to this wide variety of content, seasonality, forms of payment and consumption, such as VOD and catch-up.

We had a number of challenges in this task of understanding and pursuing a single user engagement metric, the first one was knowing which variables to choose and which best define user engagement. The advantage of dealing with a single index to accurately describe engagement is that we avoid dealing with different metrics at the same time to do this kind of assessment, as well as makes easier to rank or categorize the users.

Globoplay has three types of users: subscribers, free and anonymous. We understand that for this work, the ideal would be to split and create a specific index for each of the types of users. In this study, we focus on subscribers and free users.

After some testing with possible variables, we came up with three product metrics for the subscriber: playtime in hours, user frequency on the platform (user sessions), and diversity of watched titles. And for the free user, we use the combination of three other variables: number of videos watched, playtime in hours and frequency (distinct days watching videos). To understand the importance and define the weights of each of these variables, we use the PCA technique, Principal Component Analysis.

II. METHODOLOGY

Principal component analysis (PCA) is a multivariate technique which objective is to reduce dimensionality, each component is a linear combination of the features of interest. In our case, we want to develop an index that translates the engagement of the users, meaning we want to reduce a set of information about video consumption into one metric.

The first principal component is a linear combination of the features with maximal variance, so considering the first principal component as the engagement index is very interesting because maximize information content considering the variance of the features as well as the correlation among them. Consider the first principal component, **Y**, as a weighted average of p features ($\boldsymbol{X_1, X_2, \ldots, X_p}$) that has the largest variance, in this case the variance of Y is:

$$Var(\boldsymbol{Y}) = \boldsymbol{a'Sa}$$

Where a is the vector of optimal weights and **S** is the variance-covariance matrix of **X** (the set of p features).

The first principal component maximizes the Var(**Y**) subject to the normalization constraint **a'a** = 1. Notice that features with larger variance are given larger weights, the same occurs to correlated variables [2].

III. ENGAGEMENT INDEX FOR SUBSCRIBER USERS

As previously mentioned, for the subscriber user case, we consider the following variables: Playtime in hours, frequency in the platform and variety of titles. For each user, we calculate weekly the sum of each of these variables. Using the PCA technique, we had 80% of the variability explained by the first principal component. From the first main component, we can obtain the weights of each of the variables used: weight frequency ($\boldsymbol{w_f}$), weight playtime ($\boldsymbol{w_p}$) and weight title diversity ($\boldsymbol{w_t}$).

Through the PCA, the following weights were determined for each variable, obtained from our development sample:

a) $\boldsymbol{w_f} = 0.88$

b) $\boldsymbol{w_p} = 0.45$

c) $\boldsymbol{w_t} = 0.11$

http://www.set.org.br/ijbe/ doi: 10.18580/setijbe.2019.4 Web Link: http://dx.doi.org/10.18580/setijbe.2019.4

Therefore, the Engagement Index (IEN) is calculated from the multiplication between the weights obtained by the sum of the weekly consumption of these variables by the user, from the following formula:

$$IEN = \sum_{d=1}^{7} \boldsymbol{F_d} \times \boldsymbol{w_f} + \sum_{d=1}^{7} \boldsymbol{P_d} \times \boldsymbol{w_p} + \sum_{d=1}^{7} \boldsymbol{T_d} \times \boldsymbol{w_t}$$

Where:
$\boldsymbol{P_d}$ = user playtime in hours;
$\boldsymbol{F_d}$ = user frequency;
$\boldsymbol{T_d}$ = variety of user title;
d = day;
$\boldsymbol{w_f}$ = weight frequency;
$\boldsymbol{w_p}$ = weight playtime;
$\boldsymbol{w_t}$ = weight title diversity

This generates a continuous value that expresses the engagement of each user on the platform. We then get the engagement rates corresponding to the 20th, 40th, 60th and 80th percentiles, which allows us to classify our users into 5 engagement groups as shown in table I:

Table I
Relationship between the defined classes and the engagement index

Engagement class	Engagement index
marathoner	$IEN \geq 9.84$
assiduous	$5.13 \leq IEN < 9.84$
regular	$2.76 \leq IEN < 5.13$
eventual	$1.31 \leq IEN < 2.76$
accidental	$IEN < 1.31$

In the table II, we show a lift analysis of each user segment:

Table II
Lift analysis between engagement classes and their consumption

Engagement class	Hours Playtime (%)	Video views (%)	Distinct Days (%)
marathoner	0.00	0.00	0.00
assiduous	-65.83	-59.29	-30.56
regular	-83.33	-78.57	-44.44
eventual	-92.67	-89.29	-61.11
accidental	-98.47	-92.86	-72.22

With the classes defined from the engagement index, we focus on identifying in this sample the percentage of unsubscriptions in each of these groups and seek to understand the relationship of engagement with churn, we show this correlation in the table III:

Table III
Relationship between the defined classes and Churn

Engagement class	Churners (%)	Lift (%)
marathoner	16	0
assiduous	14	-12.50
regular	19	18.75
eventual	22	37.50
accidental	29	81.25

Notice that 51% of churns in this sample were concentrated in the two lowest engagement profiles.

IV. Engagement Index for Free users

After getting a numerical index that explained subscriber engagement, the next challenge was to study the "free" user behavior. This is further subdivided into two groups, the "free logged in" and the "anonymous" ones. The first subgroup is formed by those who have registration and, consequently, have a unique identification. The second is a more complex case to study since it is not possible to observe the same individual in different accesses. Therefore, anonymous users will be a challenge for future discussions.

Although the "Free logged User Engagement Index" used a methodology similar to the "Subscriber Engagement Index", it's important to realize that they are two distinct behavior groups. While subscribing users have access to all product content, logged in free is limited to watching only excerpts and a few full contents, not having access to the main international content, for example.

In addition, both groups present their value to the product differently. While the subscriber generates revenue by paying monthly for unlimited access, the free user watches more publicity. Given the business need of this group of users, three attributes have been determined for index composition. The first of these is the amount of watching videos ($\boldsymbol{w_v}$), which is directly related to advertising consumption since on Globoplay an advertisement is displayed at the beginning of each video. Another parameter is the video playtime ($\boldsymbol{w_p}$). Also present in the subscriber's index, representing the volume of hours consumed by users. Finally, the distinct days that users consumed video on platform ($\boldsymbol{w_f}$). This time is represented by the number of different days on which the user had video consumption. Once again, the attributes are consolidated weekly, with values weighted by the PCA algorithm, implying the following weights:

a) $\boldsymbol{w_v} = 0.89$

b) $\boldsymbol{w_p} = 0.39$

c) $\boldsymbol{w_f} = 0.23$

http://www.set.org.br/ijbe/ doi: 10.18580/setijbe.2019.4 Web Link: http://dx.doi.org/10.18580/setijbe.2019.4

Therefore, the engagement index (IEN) for free users is formed by the sum of weight products by the sum of weekly consumption of each variable, resulting in the following formula:

$$IEN = \sum_{d=1}^{7} V_d \times w_v + \sum_{d=1}^{7} P_d \times w_p + \sum_{d=1}^{7} F_d \times w_f$$

Where:

V_d = Total amount of videos watched by user;
P_d = user playtime in hours;
F_d = user frequency;
d = day;
w_v = weight of amount videos watched;
w_p = weight user playtime;
w_f = weight user frequency

The principal component analysis method was reliable when it reached 79.25% of explanatory variability. The boxplot shown in Figure 1 illustrates the variability of the attributes.

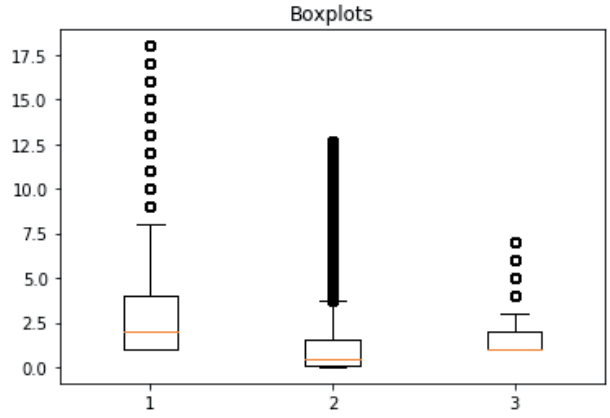

Figure 1 - Boxplot with the used variables

For the development of this index, was considered the period of May 2019, a period that is less impacted by anomalies of consumption and seasonality. And in order to use values that most closely match the actual behavior of the user group, the percentile method [4] was used to remove data with values above the 95th percentile for the "number of videos" and "video playtime" attribute, since that these data have low representativeness in the sample. As the frequency has low variability in relation to the other parameters, it was not necessary to apply any method to remove outliers.

The percentile method was also applied to define the engagement profiles, where the first quintile determined the upper limit value for the least engaged group and the fourth quintile the lower limit for the most engaged users. The profiles were defined as shown in Table IV, from the most engaged to the least engaged users:

Table IV
Relationship between the defined classes and the engagement index for free users

Engagement class	Engagement index
marathoner	IEN ≥ 5.74
assiduous	2.96 ≤ IEN > 5.74
regular	1.74 ≤ IEN > 2.96
eventual	1.16 ≤ IEN > 1.74
accidental	IEN < 1.16

The first analysis considered the consumption behavior of each profile. Calculating the average value of each attribute for the five groups, we bring in table V a lift analysis of each user segment:

Table V
Lift analysis between engagement classes and their consumption

Engagement class	Video Playtime (%)	Video views (%)	Frequency (%)
marathoner	0.00	0.00	0.00
assiduous	-60.74	-59.79	-43.40
regular	-80.37	-77.76	-60.69
eventual	-87.80	-88.48	-68.55
accidental	-99.20	-88.48	-68.55

Notice that accidental and eventual users differ only in the amount of "video playtime".

The marathoner group has a subscription propensity that is 54% higher than the accidental group as illustrates Table V. It noticed that 47% of sales are concentrated in the two most engaged profiles. The following table illustrates how free user engagement correlates directly with the propensity to subscribe.
The Table VI illustrates how free user engagement correlates directly with the propensity to subscribe.

Table VI
Lift analysis between engagement classes and their consumption

Engagement class	Lift of the propensity to subscribe (%)
accidental	0
eventual	+ 5.6
regular	+ 14.8
assiduous	+ 31.5
marathoner	+ 57.4

V. USE CASE

Due to the high seasonality and success of some TV shows we sometimes face a high churn rate after the end of this content.

Recently the telenovela “A Dona do Pedaço” is very popular among the Globoplay subscribers and it is responsible for a representative amount of video playtime in the platform. In order to avoid churn after the end of this content, we clustered the subscribers into groups of higher and lower risk of churn and described them in terms of consumption and demographic information, for example what are they favorite content and etc.

The audience selected for this case study were consumers of “A Dona Do Pedaço” from August 26, 2019, to October 31, 2019. We used a clustering technique called K-means [1], a simple and very popular unsupervised algorithm. To do that we used 4 variables: engagement index (IEN), engagement index (IEN) disregarding the consumption of “A Dona do Pedaço”, subscription time and distinct days of consumption of video. Through the elbow method [3], we identified that

http://www.set.org.br/ijbe/ doi: 10.18580/setijbe.2019.4 Web Link: http://dx.doi.org/10.18580/setijbe.2019.4

we can discriminate our sample into 4 groups, as shown in the figure 2:

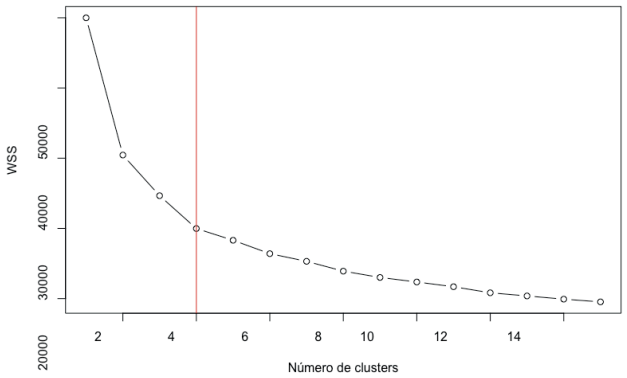

Figure 2 - The elbow method

The groups were named as: A, B, C and D and are presented in Table VII:

Table VII
Distribution of users by clusters

Cluster	**A**	**B**	**C**	**D**
Usuários (%)	14,47%	31,94%	38,85%	14,74%

To facilitate the understanding of segmentation analysis we use the PCA, this time for the purpose of reducing dimensionality. The graph in the Figure 3, shows the groups by principal components 1 and 2, which together add up to 79% of data variability. Principal component 1 (Dim1) describes user engagement and principal component 2 (Dim2) is represented by the subscription time:

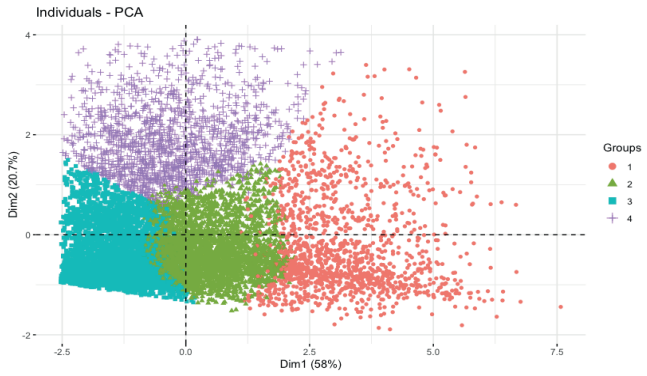

Figure 3 - dimensionality reduction

$$Dim1 = 0.54 \times \boldsymbol{e_1} + 0.53 \times \boldsymbol{e_2} + \boldsymbol{d} \times 0.47 + \boldsymbol{s} \times 0.02$$

$$Dim2 = -0.08 \times \boldsymbol{e_1} + (-0.12) \times \boldsymbol{e_2} + \boldsymbol{d} \times 0.21 + \boldsymbol{s} \times 0.97$$

Where:

$\mathbf{e_1}$ = IEN;
$\mathbf{e_2}$ = IEN disregarding "A dona do pedaço";
d = distinct days of video consuption;
s = subscription time;

From the four clusters generated, we observe the following behaviors:

1. Cluster **C** presents the highest risk group, because has a lower IEN and a shorter subscription time if compared to the others.

2.Cluster **B** has a high IEN, but not so old subscribers.

3. Clusters **A** and **D** were considered lower risk groups, where in cluster **A** there is a high IEN and in **D** not having such a high engagement, they are old subscribers, which greatly reduces the likelihood of churn

Table VIII
Relation of variables means with clusters

Cluster	**A**	**B**	**C**	**D**
Mean of iEN	56.4	25.3	9.8	17.3
Mean of iEN without "A dona do pedaço"	48.4	19.7	7.3	12.6
Mean of Subscribe Days	254.3	148.1	143.0	772.8
Mean of Distinct Days	25.7	21.0	8.5	17.1

As a result of this work, different types of A / B testing were created, enabling the Globoplay business team to create push notifications, email marketing and various product-specific approaches within these user groups.

VI. Conclusion

The engagement index seems to be a reliable metric to describe the engagement of Globoplay users, as was shown is this paper we could validate the abstract concept we wanted to measure with this index.

The engagement index (IEN) increases as the video playtime, diversity of titles, quantity of videos and frequency increases. Furthermore, the engagement index is correlated to the inclination of being a subscriber and to canceling the subscription as well. And it is an efficient method to rank and categorize our users, which is very useful in many ways.

http://www.set.org.br/ijbe/ doi: 10.18580/setijbe.2019.4 Web Link: http://dx.doi.org/10.18580/setijbe.2019.4

REFERENCES

[1] HASTIE, TREVOR, TREVOR HASTIE, ROBERT TIBSHIRANI, AND J. H. FRIEDMAN. 2001. *The elements of statistical learning: data mining, inference, and prediction*. New York: Springer.

[2] BISWAS, BASUDEB & CALIENDO, FRANK. (2004). A Multivariate Analysis and Extension of the Human Development Index. Utah State University, Department of Economics, Working Papers.

[3] GARETH JAMES, DANIELA WITTEN, TREVOR HASTIE, ROBERT TIBSHIRANI. An Introduction to Statistical Learning: with Applications in R. New York: Springer, 2013.

[4] BELÉM, GABRIEL; SILVA, RAYSSA; PERES, RODRIGO (Coord.). Utilização De Kernel E Percentis Para Identificar Outliers E Observações Pouco Representativas. Rio de Janeiro, 2018. 58 p. Trabalho de Conclusão de Curso (Engenharia Eletrônica) - Centro Federal de Educação Tecnológica Celso Suckow da Fonseca (cefet/rj) , 2018.

Felipe Parpinelli Constâncio was born in Rio de Janeiro, Brazil, in 1989. Senior Software Developer working in Globoplay at Globo.com. Received the B.S. in Information Systems from Pontifical Catholic University of Rio de Janeiro (PUC-Rio), in 2013. Currently is MSc. degree candidate in Computer Science with emphasis in Data Science at the same university.

Gabriel Sodré Belém was born in Rio de Janeiro, Brazil, in 1994. He received the B.S. degree in Electronic Engineering from Federal Center for Technological Education Celso Suckow da Fonseca (CEFET), Rio de Janeiro, in 2019. He joined Globo.com in 2018, as an intern, and currently works as a Data Engineer at Globoplay.

Karla Klahold de Souza Biscaro graduated in Statistics by the Federal University of São Carlos (UFSCar), São Carlos – SP. She works as a Data Scientist at Globo.com

Received in 2019-11-12 | Approved in 2019-11-28

http://www.set.org.br/ijbe/ doi: 10.18580/setijbe.2019.4 Web Link: http://dx.doi.org/10.18580/setijbe.2019.4

Coverage Estimation for Advanced Terrestrial Television ATSC 3.0

Fernanda Marinho Magalhães
Arismar Cerqueira Sodré Junior

CITE THIS ARTICLE

Magalhães, Fernanda Marinho Magalhães and Sodré Junior, Arismar Cerqueira; 2019. Coverage Estimation for Advanced Terrestrial Television ATSC 3.0. SET INTERNATIONAL JOURNAL OF BROADCAST ENGINEERING. ISSN Print: 2446-9246 ISSN Online: 2446-9432. doi: 10.18580/setijbe.2019.5. Web Link: http://dx.doi.org/10.18580/setijbe.2019.5

Coverage Estimation for Advanced Terrestrial Television – ATSC 3.0

Fernanda Marinho Magalhães [1] & Arismar Cerqueira Sodré Junior[2]

Summary - The ATSC 3.0 standard allows for the provision of new high data rate services, so it has been considered as a benchmark in television broadcasting technology worldwide. This paper presents a numerical study of coverage prediction using Progira software. Coverage is evaluated using ISDB-Tb and ATSC 3.0 digital terrestrial television standards in the cities of Santa Rita do Sapucaí-MG and São Paulo-SP.

Keywords — ATSC 3.0, ISDB-TB, Propagation, and TV

I. INTRODUCTION

The growing development of wireless technologies makes it necessary to ensure sufficient transmission capacity to provide various high-quality services. The improvement of multimedia content with the emergence of cutting-edge technologies such as 4K UHDTV or the new HEVC video encoding standard is pushing the limits of network capacity.

In the case of Digital Terrestrial Television (DTTV), the importance of improving spectral efficiency is critical to maintaining it as an attractive and competitive platform against cable or wireless solutions. The launch of television broadcast spectrum for the fourth generation of mobile broadband (4G) services in the 700 MHz band has limited the spectrum dedicated to terrestrial broadcasting. Therefore, TDT enhancement involves an improvement in spectral efficiency.

As such, recent digital television standards are focused on improving these two aspects of broadcasting, such as ATSC 3.0. This standard was developed by the Advanced Television Systems Committee and considers rates of 50 Mb/s, in order to receive the best definition content available today and have great flexibility depending on the desired service.

Additionally new transmission techniques have been developed, in particular different multiplexing modes for digital television networks. Layered Division Multiplexing (LDM) allows the allocation of fixed and mobile services divided into energy. Channel Bonding enables the use of two independent RF channels for a single data stream. ATSC 3.0 provides for the use of 2x2 Multiple Input Multiple Output (MIMO) with cross-polarization antennas [1]. This paper reports simulations performed on Progira software, which runs on the ArcGis geoprocessing platform [2], to assess the coverage of the new ATSC 3.0 digital television system.

II. ATSC 3.0

ATSC 3.0 is the new Terrestrial Digital Television standard developed by the Advanced Television Systems Committee (ATSC). This standard is based on Orthogonal Frequency Division Multiplexing (OFDM) and the use of Low Density Parity Check (LDPC) for low density parity checking. The physical layer implemented is aimed at greater robustness, flexibility and efficiency than previous standards due to the use of non-uniform constellations, LDPC codes and LDM.

The main parameters of an ATSC 3.0 transmission mode are:

- Bandwidth 6 to 8 MHz;
- FFT 8, 16 and 32K;
- Guard interval from 27.78 µsec to 703.70 µsec in twelve patterns;
- Scattered pilot frequency spacing: Normal or Dense are the values used;
- Scattered pilot time spacing - The values available are 2 or 4;
- Constellation size - The orders 4, 16, 64, 256, 1024 and 4096-QAM are defined;
- LDPC with 16200 or 64800 bit FEC internal code;
- LDPC code rate between 2/15 and 13/15;
- BCH: Bose,Ray-Chaudhuri and Hocquenghem FEC outer code used in the BICM module. ON y OFF are the options;
- Frame length of 100, 150, 200 or 250 ms.
- Typical LD injection level of -4dB [1].

ATSC 3.0 standardization features Order Two MIMO (MIMO 2x2) with cross-polarized technology. In other words, it is a technology in which two antennas are used, one vertically polarized and one horizontally polarized, both on the transmitter side and the receiver side. In addition, on the receiver side, two tuners are required to receive and decode the MIMO signal. In particular, this standard applies MIMO to make use of spatial diversity to minimize the effects of small and large scale fading, shading and path loss. Systems with spatial diversity can be splitted into four classes: SISO (Single Input Single Output); SIMO (Single Input Multiple Output); MISO (Multiple Input Single Output); MIMO (Multiply Input Multiply Output) [3].

ISDB-Tb was developed from the evolution of the Japanese ISDB-T (Integrated Services Digital Broadcasting Terrestrial) standard and was officially launched in Brazil in 2007. This

http://www.set.org.br/ijbe/ doi: 10.18580/setijbe.2019.5 Web Link: http://dx.doi.org/10.18580/setijbe.2019.5

system is flexible and designed to deliver high quality audio and high definition image for fixed and mobile reception. The transmission of digital terrestrial television service is divided into source coding, channel coding, OFDM modulation and broadcasting [4]. Table I presents a comparison between ISDB-Tb and ATSC 3.0 systems.

TABLE I
COMPARISON OVERVIEW BETWEEN ISDB-Tb E ATSC 3.0 [1] [4].

PARAMETERS	SYSTEM	
	ISDB-Tb	ATSC 3.0
Transport Protocol	TS	IP
Guard Range	1/4; 1/8; 1/16 e 1/32	3/512, 3/256, 1/64, 3/128, 1/32, 3/64, 1/16, 19/256, 3/32, 57.512, 3/16, 1/8, 19/128, 1/4
Video Compression	H.264	H.265
Audio Compression	MPEG-4 HE AAC	MPEG-H
Diversity	SISO	SISO;MISO;MIMO
Band	6; 7 ; 8 MHz	6; 7; 8 MHz
Internal decoder	CC: 1/2; 2/3; 3/4; 4/5; 5/6; 7/8	LDPC: {2,3,4,5,6,7,8,9,10,11,12,13}/15
Modulation	DQPSK, QPSK, 16-QAM, 64-QAM	QPSK, 2D-16NUC, 2D- 64NUC, 2D-256NUC, 1D- 1024NUC, 1D-4096NUC
Frame size	1632 bits	16200 e 64800 bits
External Decoder	RS(204,188,8)	BCH, CRC OU NENHUM
Rotated Constellation	`---	não
IFFT Size	2K; 4K; 8K	8K; 16K; 32K

III. PROGIRA SOFTWARE

Coverage prediction software should have a land and construction map to calculate the field strength of each pixel of the area of interest, taking into account diffraction, tropospheric dispersion, reflection, refraction, and land and construction entry loss.

In this study, the Progira coverage prediction software was used, which works on the ArcGis geoprocessing platform [2]. Fig. 1 reports the ISDB-T standard parameters, which were considered in the numerical simulations, including 64-QAM modulation, FEC 3/4, 10m reception antenna height and 10dBd reception antenna gain [5]. Fig. 2 shows the ATSC 3.0 system parameters, such as FFT of 32K, 4096-QAM modulation, 13/15 code rate and 28ms guard interval, which result in a rate of 55.25 Mb/s.

Progira software provides the most important propagation models in the literature: CRC – Predict, ITUR P.1546-5, ITUR GE06, ITUR P.370-7, ITUR P.526-13, ITUR P.1812-3, Deygout- Assisi, Longley-Rice and Okumura-Hata. The propagation model used in the simulations was the CRC-Predic, which implements calculation of the diffraction attenuation on the terrain and part of the loss caused by terrain reflections. The loss due to reflection is estimated using a clutter, which is a set of polygons with the region classification, such as degree of urbanization and vegetation. There is an attenuation value associated with each polygon class [6].

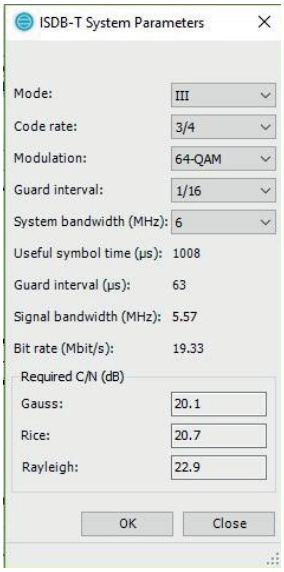

Fig. 1 - ISDB-TB Patterns used on simulation

The electric field intensity of television and retransmission stations using digital technology will be determined on the basis of Tables E (50,90), which correspond to field strength values exceeded in 50% of locations for 90% of the time, at distances from 1km to 1,000km from the irradiation center of a dipole antenna powered by 1kW of effective power [5]. The service area of a digital terrestrial television broadcast or retransmission station corresponds to the area bounded by the service contour, characterized by the values of electric field strength [5]. Finally, the software uses IBGE data to determine the population covered by the TV signal.

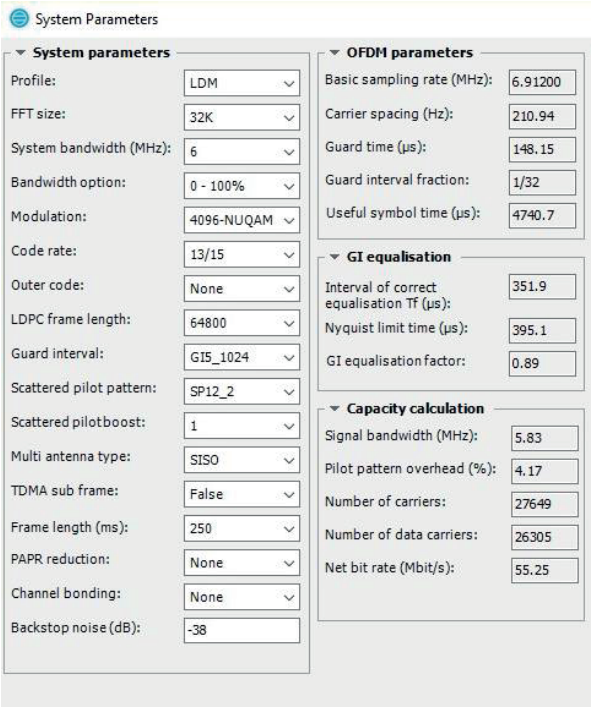

Fig. 2 - ATSC 3.0 Patterns used on simulation

http://www.set.org.br/ijbe/ doi: 10.18580/setijbe.2019.5 Web Link: http://dx.doi.org/10.18580/setijbe.2019.5

IV. RESULTS

The cities Santa Rita do Sapucaí-MG and São Paulo-SP were chosen for the study of Digital Terrestrial Television using ISDB-T and ATSC 3.0 standards, under the propagation conditions shown in Fig. 3 and Fig. 4, respectively. The specifications of each of the city broadcasting sites are described in Tab. II.

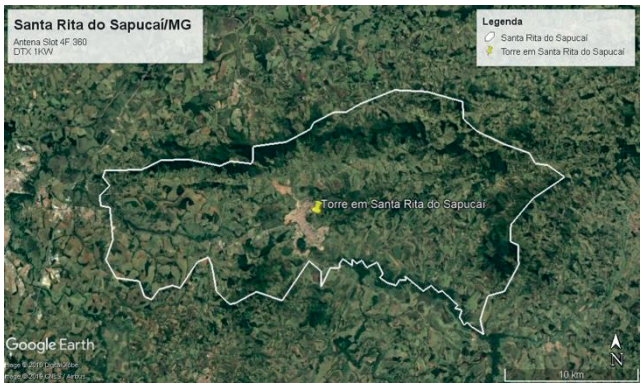

Fig. 3 – Map of Santa Rita do Sapucaí-MG, with the broadcast site identified with the yellow mark.

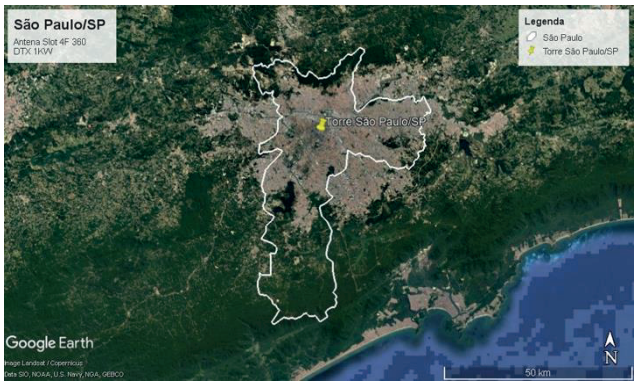

Fig. 4 – Map of São Paulo-SP, with the broadcast site identified with the yellow mark.

TABLE II
TECHNICAL SPECIFICATIONS OF SANTA RITA E SÃO PAULO SITES

LOCALIDADE / ESPECIFICAÇÕES		Sta Rita do Sapucaí/MG	São Paulo/SP
CANAL (UHF)		20	20
POTÊNCIA TRANSMISSOR DIGITAL		1KW	1KW
COORDENADAS DE INSTALAÇÃO	Latitude	22° 14' 36,74" S	23° 33' 43,43" S
	Longitude	45° 41' 53,26" W	46° 39' 13,94" W
SISTEMA IRRADIANTE	Tipo	Slot 4 Fendas omni	Slot 4 Fendas omni
	Polarização	Horizontal	Horizontal
	Ganho	7,6 dBd	7,6 dBd
	HCI	32 m	155 m
	Azimute	260° NV	140° NV
	Tilt	0°	0°
LINHA DE TRANSMISSÃO	Tipo	1 5/8"	1 5/8"
	Comprimento	37 m	80 m
	Atenuação	0,5701 dB/37m	1,2328 dB/80m
ERP (W)	Horizontal	4497,8	
	Vertical	---	

The ISDB-TB standard data used in the simulations are presented in Table III to provide a rate of 19.33 Mb/s for a signal-noise ratio (SNR) of 20.1 dB [7], as shown in the coverage map of Figure 5, considering fixed reception (10/0dBd) and a 51dBuV/m field. In this way, a population of about 167,566 inhabitants of the South of Minas Gerais, distributed in cities near Santa Rita Station, can be served, as reported in Table V. The results for the city of São Paulo are presented in Figure 6 and Table VI, which identifies a population served of 13,825,116 inhabitants.

TABLE III
PARAMETERS OF THE TRANSMISSION MODE USED
ISDB-T FIXED SERVICE

BAND	6 MHz
FEC	3/4
MODULATION	64-QAM
GUARD INTERVAL	1/16

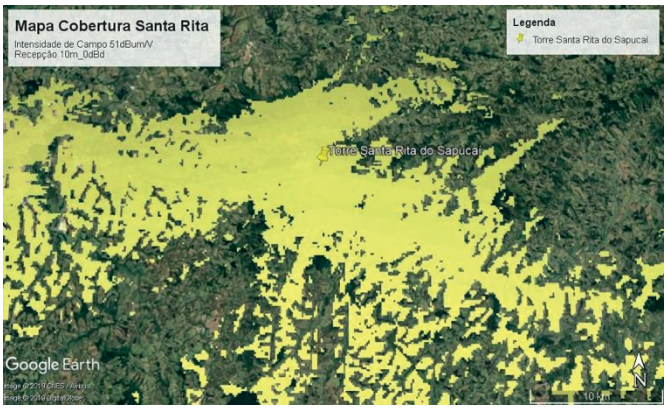

Fig. 5- Coverage Map on Santa Rita do Sapucaí-MG site considering fixed reception (10m / 0dBd) and field of 51dBuV / m.

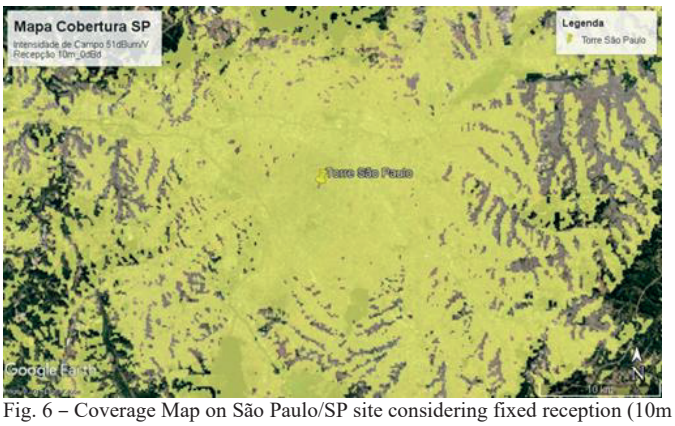

Fig. 6 – Coverage Map on São Paulo/SP site considering fixed reception (10m / 0dBd) and field of 51dBuV / m.

ATSC 3.0 coverage prediction simulations were also performed, according to the parameters of Table IV, using SISO.

TABLE IV

http://www.set.org.br/ijbe/ doi: 10.18580/setijbe.2019.5 Web Link: http://dx.doi.org/10.18580/setijbe.2019.5

PARAMETERS OF THE TRANSMISSION MODE USED IN ATSC FIXED SERVICE 3.0

BW	6 MHz	QAM	1024
FFT	32K	LDPC	64800 bits
GI	148.148 µs	LDPC (Code Rate)	13/15
DX	Normal	BCH	ON
DY	2	Frame	200 ms

Thus, a rate of 45.64 Mb/s was obtained for SNR = 30.18 dB. Figure 7 and Table VII report the results for ATSC 3.0 with SISO, where a large coverage area with population served of 15,086,762 in habitants is observed.

TABLE V
POPULATION COVERED BY ISDB-Tb STANDARD IN SOUTH MINAS GERAIS

City	Total pop	Served Pop	Served Pop %
Santa Rita do Sapucaí	37.436	35.497	94,8
Pouso Alegre	129.581	108.784	84
São José do Alegre	3.989	2.959	74,2
Brasópolis	14.517	4.041	27,8
Piranguinho	7.976	2.095	26,3
Paraisópolis	19.262	3.472	18
Conceição dos Ouros	10.340	1.800	17,4
Cachoeira de Minas	10.970	1.153	10,5
Senador José Bento	1.865	135	7,2
Tocos do Moji	3.948	251	6,4
Itajubá	90.019	4.713	5,2
Wenceslau Braz	2.547	130	5,1
Gonçalves	4.194	176	4,2
Piranguçu	5.179	203	3,9
São Sebastião da Bela Vista	4.912	157	3,2
Borda da Mata	17.020	514	3
Pedralva	11.402	342	3
Córrego Do Bom Jesus	3.725	101	2,7
Delfim Moreira	7.943	172	2,2
Estiva	10.826	215	2
Bom Repouso	10.427	173	1,7
Maria Da Fé	14.156	151	1,1
Careaçu	6.254	57	0,9
Congonhal	10.361	85	0,8
Consolação	1.719	6	0,3
Inconfidentes	6.905	18	0,3
Natércia	4.611	14	0,3
Heliodora	6.094	10	0,2
Ipuiúna	9.444	19	0,2
Ouro Fino	31.370	61	0,2
Camanducaia	20.839	25	0,1
Cristina	10.146	14	0,1
Santa Rita De Caldas	8.975	10	0,1
Sapucaí-Mirim	6.227	7	0,1
Silvianópolis	5.985	6	0,1
TOTAL POPULATION COVERAGE		167.566	---

TABLE VI

SÃO PAULO SERVED POPULATION WITH THE ISDB-TB STANDARD.

City	Total pop	Served Pop	Served Pop %
São Paulo	11.206.957	8.855.507	79
Guarulhos	1.214.007	900.934	74,2
São Bernardo Do Campo	761.735	613.777	80,6
Santo André	673.645	555.901	82,5
Osasco	665.402	480.177	72,2
Diadema	385.513	291.872	75,7
Mauá	415.103	275.618	66,4
Carapicuíba	369.020	247.955	67,2
Taboão Da Serra	244.149	221.159	90,6
Embu	239.994	193.005	80,4
Itaquaquecetuba	321.384	176.120	54,8
Barueri	240.595	163.416	67,9
São Caetano do Sul	148.474	137.599	92,7
Mogi das Cruzes	386.517	119.933	31
Cotia	200.042	109.731	54,9
Itapecerica da Serra	149.039	83.229	55,8
Ferraz De Vasconcelos	168.016	73.524	43,8
Suzano	261.487	64.019	24,5
Itapevi	200.626	56.262	28
Jandira	108.283	50.623	46,8
Arujá	74.669	35.703	47,8
Ribeirão Pires	112.752	26.677	23,7
Embu-Guaçu	62.446	26.015	41,7
Santana De Parnaíba	108.747	25.084	23,1
Poá	105.779	22.045	20,8
Vargem Grande Paulista	42.806	8.622	20,1
Rio Grande Da Serra	43.776	3.148	7,2
São Roque	78.642	2.514	3,2
Mairiporã	80.615	1.634	2
Caieiras	86.352	1.534	1,8
Pirapora Do Bom Jesus	15.691	883	5,6
Cajamar	64.044	505	0,8
Nazaré Paulista	16.390	122	0,7
Franco Da Rocha	123.467	102	0,1
São Lourenço Da Serra	13.885	92	0,7
Araçariguama	16.920	40	0,2
Cabreúva	41.518	35	0,1
TOTAL POPULATION COVERAGE		13.825.116	---

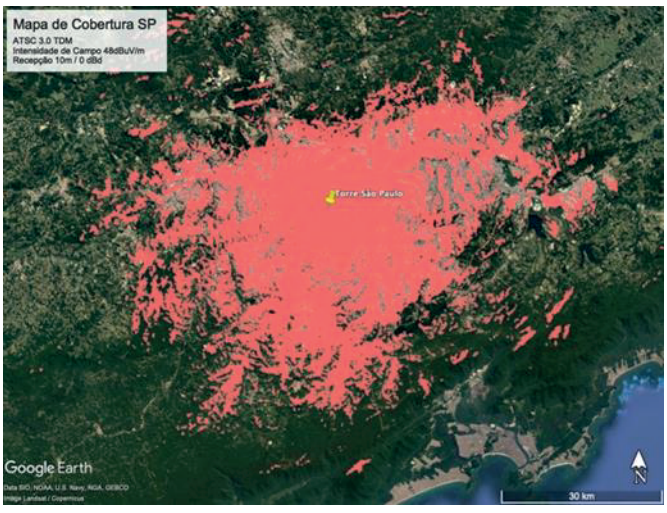

http://www.set.org.br/ijbe/ doi: 10.18580/setijbe.2019.5 Web Link: http://dx.doi.org/10.18580/setijbe.2019.5

Fig. 7 - Coverage Map on São Paulo/SP site using ATSC 3.0 standard, TDM and SISO antenna.

TABLE VII
SÃO PAULO / SP SERVED POPULATION FOR ATSC 3.0

City	Total pop	Served Pop	Served Pop %
São Paulo	11.206.957	9.514.798	84,9
Guarulhos	1.214.007	997.592	82,2
São Bernardo Do Campo	761.735	656.091	86,1
Santo André	673.645	597.024	88,6
Osasco	665.402	530.961	79,8
Diadema	385.513	325.191	84,4
Mauá	415.103	304.855	73,4
Carapicuíba	369.020	277.651	75,2
Taboão Da Serra	244.149	231.842	95
Embu	239.994	207.728	86,6
Itaquaquecetuba	321.384	203.201	63,2
Barueri	240.595	184.884	76,8
Mogi Das Cruzes	386.517	166.551	43,1
São Caetano Do Sul	148.474	142.883	96,2
Cotia	200.042	123.987	62
Itapecerica Da Serra	149.039	98.126	65,8
Ferraz De Vasconcelos	168.016	90.152	53,7
Suzano	261.487	89.446	34,2
Itapevi	200.626	79.844	39,8
Jandira	108.283	63.517	58,7
Arujá	74.669	41.997	56,2
Ribeirão Pires	112.752	38.256	33,9
Embu-Guaçu	62.446	31.525	50,5
Santana De Parnaíba	108.747	30.595	28,1
Poá	105.779	28.954	27,4
Vargem Grande Paulista	42.806	10.792	25,2
Rio Grande Da Serra	43.776	7.695	17,6
São Roque	78.642	3.301	4,2
Mairiporã	80.615	2.348	2,9
Caieiras	86.352	2.048	2,4
Pirapora Do Bom Jesus	15.691	1.215	7,7
Cajamar	64.044	713	1,1
Jundiaí	368.998	241	0,1
Franco Da Rocha	123.467	219	0,2
Nazaré Paulista	16.390	164	1
São Lourenço Da Serra	13.885	158	1,1
Araçariguama	16.920	55	0,3
Biritiba-Mirim	28.541	55	0,2
Cabreúva	41.518	49	0,1
Salesópolis	15.580	27	0,2
Campos Do Jordão	47.289	25	0,1
Igaratá	8.799	6	0,1
TOTAL POPULATION COVERAGE		15.086.762	---

After numerous simulations, it was found that the coverage map and population served for MIMO mode was identical to SISO mode. We contacted Progira and they confirmed to us that the MIMO function is available in the software but is still in the implementation phase.

V. CONCLUSIONS

This work reported numerical coverage prediction simulations performed with the Progira software in the context of the cities of Santa Rita do Sapucaí-MG and São Paulo-SP. The simulations showed that the ATSC 3.0 system, compared to the ISDB-T, can deliver twice the usable rate for a 6MHz band, as well as greater coverage for both the city of Santa Rita do Sapucaí and São Paulo. Specifically, the ISDB-T standard obtained a rate of 19.33 Mb/s for SNR=20.1 dB, while for the ATSC 3.0 standard a rate of 45.64 Mb/s for SNR=30.18 dB.

For the ISDB-T standard, a population of about 167,566 inhabitants of Southern Minas Gerais, distributed in cities near Santa Rita do Sapucaí-MG station and 13.825,116 inhabitants distributed in cities near São Paulo-SP Station, can be served. For the ATSC 3.0 standard, in addition to the useful rate gain, a significant coverage gain was observed in cities near the São Paulo-SP Station that resulted in a population of 15.086,762 inhabitants.

VI. REFERENCES.

[1] Advanced Television Systems Committee. "ATSC Standard: Physical Layer Protocol (A/322). Doc. A/322:2106." Washington, D.C, USA, September 2016.

[2] ARCGIS. Online. Disponível em https://www.esri.com/en-us/arcgis/about-arcgis/overview, acesso em 28 de abril de 2019.

[3] G. Lorenzo Cifuentes “Coverage estimation for the next-generation digital terrestrial television standard atsc 3.0: ldm, channel bonding and mimo”, Universidade Politécnica de Valência.2016. unplushed.

[4] P. G. Esperante, C. Akamine, G. Bedicks Jr “Comparison of Terrestrial DTV Systems: isdb-tb and dvb-t2 in 6 mhz”, IEEE latin america transactions, volume 14, páginas 45 à 56, 2016.

[5] Ministério das Comunicações Gabinete do Ministro “Portaria nº 925, de 22 de agosto de 2014”, DOU de 27/08/2014 (nº 164, Seção 1, pág. 93).

[6] F. S. Silva, L. J. Matos, F. A. C. Peres, G. L Siqueira, “Coverage prediction models fitted to the signal measurements of digital TV in Brazilian cities”, 2013 SBMO/IEEE MTT-S International Microwave & Optoelectronics Conference (IMOC), 2013.

[7] ARIB STD-B31, Versão 1.6, traduzida para o inglês, 2005. Online. Disponível em: https://www.arib.or.jp/english/index.html, acesso em 28 de fevereiro de 2019.

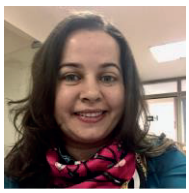

Fernanda Marinho Magalhães is attending postgraduate course in Network and Telecommunications Engineering from INATEL. Graduated in Electrical Engineering from Nove de Julho University, graduated in Economics from UESC and Electronic Technician from CEFET / BA. Has been working in the area of television broadcasting for over 15 years, closely following the birth and implementation of the digital terrestrial TV standard in Brazil. Her topics of interest are broadband multimedia communications, digital broadcasting and communication systems engineering.

Arismar Cerqueira Sodré Junior has a Scholarship of CNPq 1D Research Productivity , holds a degree in Electrical Engineering from

the Federal University of Bahia (2001), a Master's degree in Electrical Engineering from the State University of Campinas (2002), a Ph.D. in Telecommunications Engineering from Scuola Superiore Sant´ Anna - Italy and University of Bath - England (2006) and Post-Doctorate in Electrical Engineering from UNICAMP (2009). Currently works as Assistant Professor IV of Inatel. Arismar has 10 patents, 19 products transferred to industry and 223 articles published in international and national journals and congresses.

Received in 2019-07-15 | Approved in 2019-09-21

http://www.set.org.br/ijbe/ doi: 10.18580/setijbe.2019.5 Web Link: http://dx.doi.org/10.18580/setijbe.2019.5

Proposal for Improvement of Information Transmission in OFDM Systems Using the CBEDE Methodology

Reinaldo Padilha
Yuzo Iano
Ana Carolina Borges Monteiro
Rangel Arthur

CITE THIS ARTICLE

Padilha, Reinaldo, Iano, Yuzo, Monteiro, Ana Carolina Borges and Arthur, Rangel; 2019. Proposal for Improvement of Information Transmission in OFDM Systems Using the CBEDE Methodology. SET INTERNATIONAL JOURNAL OF BROADCAST ENGINEERING. ISSN Print: 2446-9246 ISSN Online: 2446-9432. doi: 10.18580/setijbe.2019.6. Web Link: http://dx.doi.org/10.18580/setijbe.2019.6

Proposal for Improvement of Information Transmission in OFDM Systems Using the CBEDE Methodology

Reinaldo Padilha, Yuzo Iano, Ana Carolina Borges Monteiro and Rangel Arthur

***Abstract* — In a world where people are increasingly connected, one of the key challenges is better quality data transmission, just as the increase in demand increases the need for attention to choose the best technology according to each transmission need, mainly by voice and video. The Orthogonal Frequency Division Multiplexing (OFDM) modulation technique has emerged as technological evolution, wherein a conventional transmission system, the symbols are sent in sequence through a single carrier, whose spectrum occupies the entire available frequency range, however OFDM consists in the parallel transmission of data in several subcarriers, with PSK modulation and with sub-carrier transmission rates as low as the number of them. Based on that, the present study implements a model based on discrete events applied to a broadcasting system, using the Simulink of the MATLAB software, aiming to improve the transmission of content, through the pre-coding process of bits applying discrete events in the signal before the modulation process. This proposal brings a different approach, in which the signal transmission on the channel is realized in the discrete domain with the implementation of discrete entities in the process of bit generation. The results show better computational performance related to memory utilization relative to the compression of the information, showing improvement of more than 22%.**

Index Terms* — *discrete events, OFDM, DPQSK, memory, simulation, bits.

I. INTRODUCTION

In the area of telecommunications, new applications are coming up with a lot of speed, which requires a big compromise between the transmitted bit rate and the bandwidth, which can be seen in the current multimedia systems, bit rates vary from a few kbps (for voice), up to 20 Mbps, to HDTV (High Definition Television), the high definition television. Thus, when facing such challenges, the first point to consider is how to transmit a large number of bits/s, guaranteeing the quality of the service, that is, what modulation, as well as the best and most appropriate system, can meet, in the best way, the contradictory commitments (bit rate and bandwidth) [1].

A solution horizon that could be the use of equalization techniques in the receiver; however, there are practical difficulties with the way this real-time equalization operates at rates of the order of Mbps, and the use of compact and low-cost hardware. Therefore, a very promising technology that eliminates the need for complex equalizers is OFDM (Orthogonal Frequency Division Multiplexing), being a modulation technique that uses multiple carriers [2].

Nowadays the demand for bandwidth is increasing, especially for mobile devices, in that way OFDM is introduced as one of the solutions to enable bandwidth efficiency and robustness, because this technology is a basic building block for many of the current modulation schemes including 802.11 WLAN, 802.16 WiMAX, and 3GPP LTE, as well as others [2] [3].

The principle of OFDM technology is to divide the high data rate stream into parallel low rate data streams using Fast Fourier Transform (FFT), this

R. Padilha is currently studying for a Ph.D.'s degree in Electrical Engineering, acting Laboratory of Visual Communications at the State University of Campinas (padilha@decom.fee.unicamp.br).
Y. Iano is teacher and coordinator of the Laboratory of Visual Communications at the State University of Campinas (yuzo@decom.fee.unicamp.br)
A. C. B. Monteiro is currently studying for a Ph.D.'s degree in Electrical Engineering, acting Laboratory of Visual Communications at the State University of Campinas (monteiro@decom.fee.unicamp.br).
R. Arthur is a teacher of Faculty of Technology (FT) of Unicamp, lecturer, and advisor to the Innovation Agency (Inova) of Unicamp (rangel@ft.unicamp.br).

http://www.set.org.br/ijbe/ doi: 10.18580/setijbe.2019.6 Web Link: http://dx.doi.org/10.18580/setijbe.2019.6

scheme is widely used in wireless communication system, such as IEEE 802.11 standard, cellular communication (eg, WiMAX and LTE Advanced) and digital broadcasting standard (e.g., DVB-T), and considering that OFDM technology is combined by modulation with more bits per symbol, thus increasing data transmission throughput [2] [4].

OFDM is a digital multi-carrier modulation scheme that extends the concept of single subcarrier modulation by using multiple subcarriers within the same single channel, i.e., is a multichannel modulation-based transmission system, also called a parallel or multiplexed transmission system, which then appears as an alternative to alleviate the problems of the serial system, which uses simple carrier modulation [5].

Rather than transmit a high-rate stream of data with a single subcarrier, OFDM makes use of a large number of closely spaced orthogonal subcarriers that are transmitted in parallel. Each subcarrier is modulated with a conventional digital modulation scheme (such as QPSK, 16QAM, DQPSK, as well as any others) at the low symbol rate. Generating a technological advantage of parallel or multi-carrier transmission, on the serial transmission, reducing the sensitivity of the system to channel delay spread, and therefore, interference between symbols [6] [7].

The technique of Discrete Event is focused on its use in the representation of a given system, which analyzes this as a sequence of operations performed through entities of certain types such as data packets, in this case for a telecommunications system. These entities are discrete items of interest in modeling and simulation with the discrete event technique, being their respective meaning depending on what is modeled and the type of system, in the same way, can have attributes that affect the way they are handled or changing the entity flows through the process [8] [9].

Discrete events are the results of actions occurring through the system, an event has the property of changing the system state, being these intentional actions, spontaneously controlled or with the verification of a condition. The technique has been used a lot in the modeling of concepts with a high level of abstraction, that is to say, patients in a hospital in context of a healthcare system, people in a queue, transaction systems for databases, communication protocols in telecommunication's systems, people in call centers, vehicles in intelligent transport systems, process control in control engineering, military equipment in defense systems, emails on a server, data packets being transmitted in communication system , among others [8] [9] [10].

Thus, in this research, the authors developed an OFDM transmission model for broadcasting using an AWGN (Additive White Gaussian Noise) channel with advanced modulation format DQPSK (Differential Quadrature Phase Shift Keying) in simulation environment [42], with the objective of to increase the transmission capacity of information content through the channel related to the lower memory consumption.

The proposal comes from the bit treatment with discrete events methodology, named CBEDE (Coded of Bits for Entities by means of Discrete Events), modeled in the step of bit generation, with the added differential of the use of discrete events applied in the physical layer of a transmission channel, being this a low-level of abstraction, reaching the second objective this research.

The present paper is organized as follows: Section 2 discusses traditional OFDM modeling, showing the modeling of AWGN transmission channel. Section 3 presents and presents the proposed framework of this paper, presenting the CBEDE methodology. Section 4 presents the results and, finally, in Section 5, the conclusions and the potential of the research are presented.

II. TRADITIONAL MODEL

The basic concept of OFDM is the property of multiple narrow-band channels, with the ability to send samples concurrently using multiples orthogonal sub-channels whereas in other techniques they are only wide-band channel sending the only sample using the entire band, OFDM is better due to the characteristic of multiple sub-channels (sub-carriers) carry samples sent at a lower rate, being almost same bandwidth with wide-band channel, and only some of the sub-channels are affected by interferers, and with the additional do not need guard bands [11].

OFDM is, therefore, a multiplexing scheme which divides the data stream from the narrowband data channel, sharing the bandwidth available, OFDM has subcarrier that orthogonality, unlike its predecessor Frequency Division Multiplexing (FDM) [11] [12].

This method is then based on the well-known FDM technique, wherein it different streams of information are mapped onto separate parallel channels, each of these channels being separated

http://www.set.org.br/ijbe/ doi: 10.18580/setijbe.2019.6 Web Link: http://dx.doi.org/10.18580/setijbe.2019.6

from the others by a frequency guard band thus reducing interference between adjacent channels. Since the OFDM scheme differs from traditional FDM in interrelated ways like multiple carriers (called subcarriers) carry the information stream, its subcarriers are orthogonal to each other, and a guard interval is added to each symbol to minimize the channel delay spread and intersymbol interference [13].

OFDM is a relatively new spectrally efficient digital modulation scheme employing multiple carriers that are mutually orthogonal to one another over a given time interval, which each carrier, consisting of a pair of sine wave and a cosine wave, is referred to as a subcarrier ', and the available transmission bandwidth is equally divided among the N sub-carriers. Each of them, upon data modulation, may be categorized as a narrowband modulated signal but the overall OFDM signal is a wideband signal for a moderate or large value of 'N'. As the modulation operation is carried out at its baseband level, and consequently the baseband modulated signal is translated in the frequency domain by frequency up-conversion to the required radio frequency band, as well as another desired type [5] [14].

In this way, the data bits are converted from serial to parallel and each subcarrier is modulated using phase or amplitude modulation, in which the frequency domain, multiple adjacent tones or subcarriers are independently modulated with complex data, this is called the symbol mapping, where each subcarrier is independently modulated. An interesting and particular practical feature of the OFDM modulation scheme consists of that shaping pulse is not necessary for the modulating signals due to a group of orthogonal carriers, when modulated by random pulse sequences, have sketched spectral characteristics [15].

Then, all the modulated signals are carried by OFDM carrier where they use IFFT module (performed on the frequency-domain subcarriers to produce the OFDM symbol in the time-domain) to create complex signal containing all subcarrier. The data parallel stream is converted to serial stream and real and image signal respectively are processed on Digital to Analog Converter. Then, they are quantized by Analog to Digital Converter ADC and the signal is calculated by a Fast Fourier Transform (FFT) module. The data symbols are then demodulated by symbol mapping block according to the modulation used, and the parallel data stream is converted into data serial to obtain the desired data [7] [15].

The importance of orthogonally of the OFDM signal is described as a set of closely spaced FDM subcarriers, wherein the frequency domain, each transmitted subcarrier results in a sync function with side lobes producing overlapping spectral between subcarriers, which has reducing properties of interference between a subcarrier and increase spectrum efficiency utilization [5] [16].

Resulting in subcarrier interference with the exception of orthogonally spaced frequencies, where the individual peaks of subcarriers all line up with the nulls of the other subcarriers, not interfering so with the system's ability to recover the original signal (the receiver correlates the incoming signal recovering the original set of bits sent) [5] [15] [16].

This modulation has another important issue with regard to the effect of the transmission channel, having high spectral efficiency, favored data transfer at high rates (typically beyond 1Mbps) in wireless networks. In this way, the use of orthogonal subcarriers allows more subcarriers per bandwidth, which results in an increase in spectral efficiency, and prevents interference between overlapping carriers [5] [17].

OFDM has a wide range of applications in modern wireless digital transmission systems asynchronous digital subscriber line (ADSL), high-speed DSL, very high-speed DSL use OFDM for high-speed data transfer transmission, as well as Digital Audio Broadcasting (DAB) and Digital Video Broadcasting (DVB), still considering IEEE 802.11a, IEEE 802.11g and HYPERLAN2 wireless Local Area Network (WLAN) standards include OFDM for supporting higher bit rates and IEEE 802.16 Wireless Metropolitan Area Network (MAN) standard [18].

The AWGN channel is a practical and efficient model of communication system widely used related to its simplicity and mathematical treatment, implying in a large set of physical channels, which introduces in the transmitted signals a noise modeled statistically as a white Gaussian additive process [19].

In the context of wireless communications, the main source of thermal noise is the addition of random signals arising from the vibration of atoms in the receiver electronics, where the AWGN has properties of statistically characterizing these random radio noise present in the signal. Still taking into consideration that systems operating in AWGN conditions can be exemplified as space communications with highly directional antennas and some point-to-point microwave links [20] [21] [22].

http://www.set.org.br/ijbe/ doi: 10.18580/setijbe.2019.6 Web Link: http://dx.doi.org/10.18580/setijbe.2019.6

The modulation format DQPSK (Differential Quadrature Phase Shift Keying) is widely used in satellite broadcasting, for Digital Video and Radio Broadcasting, having a wide scope of performance in various cellular wireless standards like GSM, CDMA, LTE, 802.11 WLAN, 802.16 fixed and mobile WiMAX, as well as CABLE TV applications. In the same way, it has properties for higher bit rates of HD video and a high satellite bandwidth [23] [24].

In DQPSK, each set of bits is represented by a symbol, causing a determined phase variation in the carrier signal, the bits for the data symbols are determined by the phase change of the previous symbol, there were four possible states 0, π, +π/4, -π/4, where each symbol represents two bits of information. The division of the binary pattern is equal to QPSK (Quadrature Phase Shift Keying), except that a bit string is shifted in phase with respect to π / 4 or π / 2 depending on the system being implemented. That is, there are 8 ideal state positions in the DQPSK constellation, being ideal state positions for symbols alternating between the four states of 45 degrees and four states on the axis, due to this alternation, the ideal trajectory between symbols never crosses zero [23] [24].

This session is presented to broadcasting OFDM system modeled with an AWGN channel with DQPSK modulation. Thus, was used the Simulink simulation environment of the MATLAB® software in its version 8.3 of 64 bits (2014a).

In a digitally implemented OFDM system, the input bits are generated frame-based, 16-ary random integers with 960 samples/frame, grouped and mapped to source data symbols that are a complex number, after are modulated with DQPSK modulation, then shaping of OFDM symbols, before 960 samples/frame and are now converted into a 48×20 array, creating an efficient FFT size, and thus appends zeroes to increase the column size to 64, which modifies the indices of the array for input to the Inverse Fast Fourier transform (IFFT). With the column size set at 64, the OFDM modulation is implemented using a 64-point IFFT, and a gain is applied which applies a normalization of $1/\sqrt{64} = 1/8$ [5] [25].

And then the Cyclic Prefix, whose parameters are basically added to appends 16 symbols for the cyclic prefix and expands the output array to 80×20 are added. Passing through a digital-to-analog conversion, which modifies the 80×20 array to a single dimension for input to the Saleh model, which characterizes the power amplifier [26] [27] [28].

This model is operated with AM/AM = [1 0] and AM/PM = [0 0], thereby forcing the OFDM signal to remain within the linear region of the power amplifier, causing the OFDM signal to remain in the nonlinear region of the power amplifier [26] [27] [28].

The setting of the AWGN channel follows a signal-to-noise ratio of 15 dB, initial seed of 67, power input signal of 1 watt and sample time of 1 second. And then the signal again is converted into a single dimensional vector back to an 80×20 array, analog to digital conversion, removing the Cyclic Prefix, following the gain normalization at $1/\sqrt{64} = 1/8$, and a 64-point FFT is performed, making the way back to the original state of the signal, again producing the frame-based signal, removing the inserted zeros, producing the 48×20 array [26] [27] [29].

Performing a conversion again on the signal to which this signal with 48×20 array back to the 960-sample frame for insertion into the DQPSK demodulator [30].

What this complex process described above accomplishes is that the generated bits, as well as the OFDM symbols, are treated by the transmitter as though they are in the frequency domain and are the inputs to an IFFT that transforms the data into the time-domain [5] [31].

The IFFT takes in N source symbols at a time where N is the number of subcarriers in the system. Each of these N input symbols has a symbol of T seconds. Recall that the output of the IFFT is N orthogonal sinusoids. These orthogonal sinusoids each have a different frequency and the lowest frequency is DC [5] [31].

The IFFT output is the summation of all N sinusoids. Thus, the IFFT provides a simple way to modulate data onto N orthogonal subcarriers. The N output samples from the IFFT make up a single OFDM symbol. After some additional processing, the time-domain signal that results from the IFFT is transmitted across the AWGN channel. At the receiver, an FFT is used to process the received signal and bring it into the frequency domain which is used to recover the original data bits, as shown in Figure 01 [5] [32].

http://www.set.org.br/ijbe/ doi: 10.18580/setijbe.2019.6 Web Link: http://dx.doi.org/10.18580/setijbe.2019.6

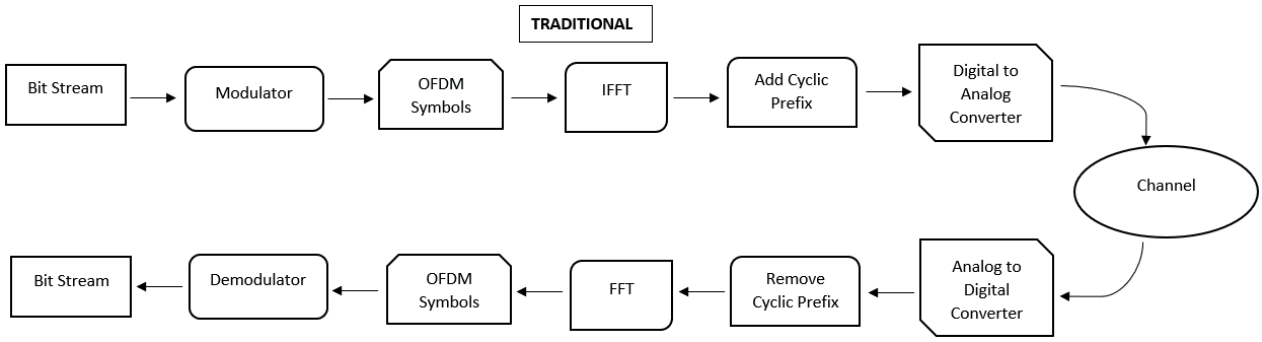

Figure 01 – Traditional Model

III. PROPOSAL

The modeling of the pre-coding process according to the discrete events is similar to that shown in the previous section. Differentiating that in this model, was added the discrete events of pre-coding with discrete events.

In this way, discrete entities were generated in the bit generation process, corresponding to bits 0 and 1, then a conversion of an event-based data signal to a time-based data signal is performed, where these bits are maintained in accordance with the discrete domain of interest, the value of the signal before the conversion being identical to that of the converted signal.

Both time-based signals and event-based signals will be in the time domain.

A Zero-Order Hold (ZOH) is responsible for defining the sampling in a practical sense, being used for discrete samples at regular intervals, affecting the final effect of the conversion of the signal to the time domain, causing its reconstruction and maintaining each sample value for a specific time interval and identical to the original.

The differential of this research is in the use of discrete events applied in such low-level of abstraction, being the bit generation.

And after applying the technique in the step of generating bits as discrete entities, the signal flow is identical to that shown in the previous section, passing through the respective OFDM steps, being modulated in DQPSK, passing through the AWGN channel, and then the signal is demodulated.

The model presented in Figure 02, incorporates the traditional modeling with the proposed methodology, as well as highlights the part modeled according to the approach of discrete events, in blue, as previously described.

In Figure 03, in the simulation environment 10000 seconds were used, where for the comparative criterion the flows of transmission of the modulated signal in DQPSK signal related to OFDM with the proposal (below) and OFDM traditional model (top) were placed, noting that both methodologies generated the same result.

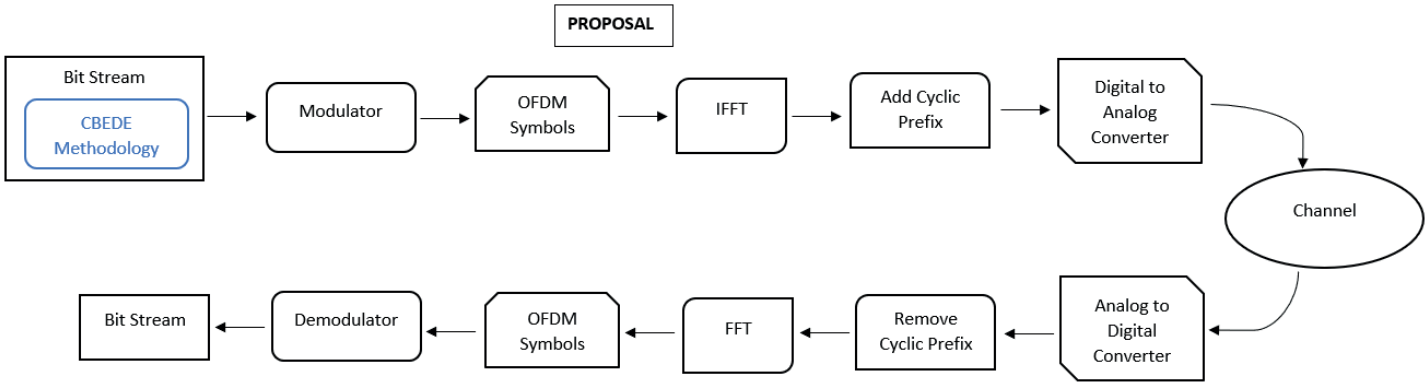

Figure 02 – Model with the proposal

http://www.set.org.br/ijbe/ doi: 10.18580/setijbe.2019.6 Web Link: http://dx.doi.org/10.18580/setijbe.2019.6

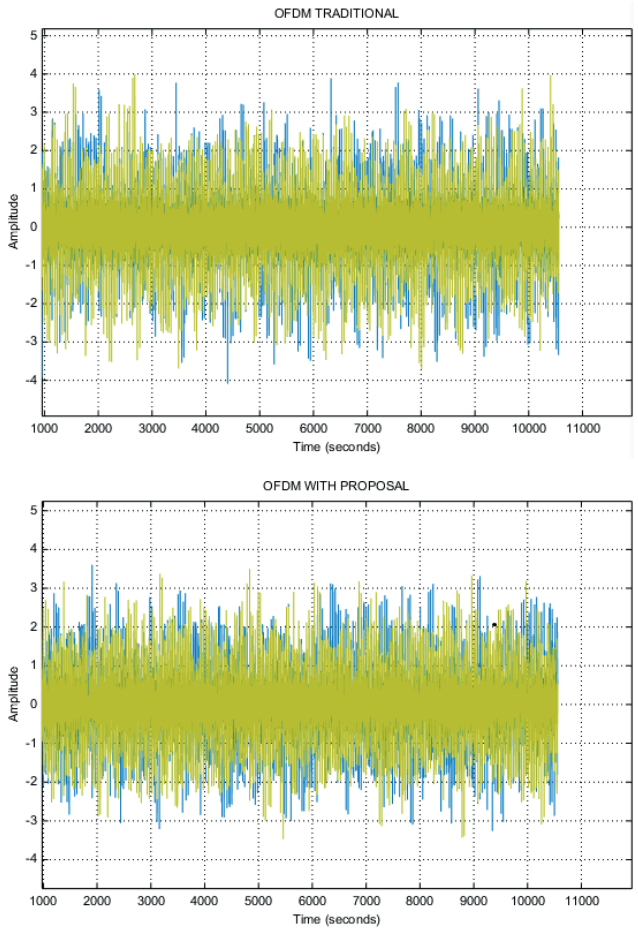

Figure 03 –Transmission Flow DQPSK OFDM

For the same comparative purpose, the Constellation Diagram was used to view the constellation of the modulated digital signal OFDM also being useful for comparing the performance of one system with another.

In Figure 04 is shown the results for visualization of the constellations with 15 dB, according to signal related to OFDM with the proposal (right) and OFDM traditional model (left).

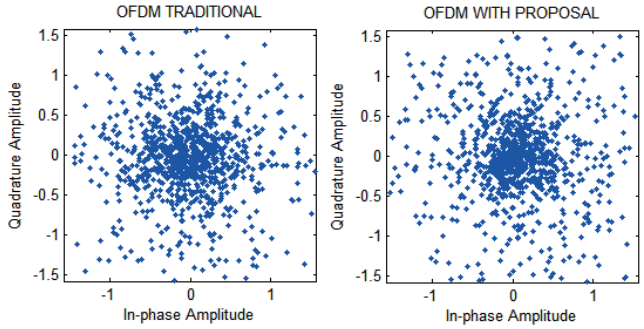

Figure 04 – DQPSK OFDM Constellations

IV. RESULTS

In this section, the results will be presented in relation to the evaluations of memory consumption of the models according to the studied techniques, modeled and presented in the previous session. Also, it is presented the performance comparison between them, simulated on a physical machine with hardware configuration, being an Intel Core i3 processor and 4GB RAM.

The "sldiagnostics" function displays information about the modeling system in Simulink, being responsible for calculating the sum of all the memory consumption processes used in the model in simulation, by the ProcessMemUsage parameter, which counts the amount of memory utilized in each phase of the model, during the entire simulation, displaying the total amount in MB [33].

In the same way, it was analyzed the first simulation of both models, being observed the first simulation regarding their memory consumption [33], having the comparative of better performance as shown in TABLE I and related with the Figure 05, with respect to them and that it is important to be in the first simulation that the variables are allocated, and the memory reserved for the execution of the model

TABLE I. COMPUTATIONAL IMPROVEMENT

Memory Consumption		
	traditional	***proposal***
Broadcasting DQPSK OFDM	60,3672	49,3359

In this way, it can be understood that in a transmission channel including the proposal and in another one only traditional methodology, where it is transmitted the same information content (quantity of bits), without any loss (signal and constellation). The results related to the memory consumption of the proposal are relative to the compression of the information [33], as shown in TABLE I and related with Figure 05.

http://www.set.org.br/ijbe/ doi: 10.18580/setijbe.2019.6 Web Link: http://dx.doi.org/10.18580/setijbe.2019.6

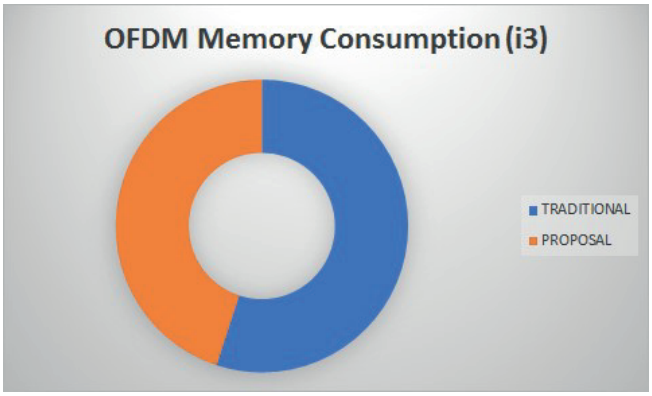

Figure 05 – OFDM First Memory Consumption

V. CONCLUSIONS

OFDM is a modulation and data transmission technique that uses its bandwidth divided into multiple orthogonal carriers, called subcarriers, for modulation, using the frequency spectrum with advanced techniques, in which it allows high data rate transmissions without problems with the ISI, by the use of orthogonality between the carriers, unlike the single carrier system, when frequency selective fading occurs only the symbols transmitted on the carriers affected by fading are lost. These subcarriers are called orthogonal because they do not have frequency overlap, thus not interfering with each other. It has a basic principle the conversion of a serial data stream of high transmission rate into multiple parallel sub-streams of the low transmission rate. Its main advantage over single carrier techniques is that it can achieve the same transfer rate due to the parallelism of low rate subcarriers with greater resistance to poor conditions of the medium such as high frequency attenuation, inter- symbol, interference caused by multiple paths (common in wireless networks, due to reflection).

Thus, the use of discrete events applied in a low-level of abstraction such as the bit, in generation phase in a broadcasting system which uses OFDM, was the differential of this research since it does not apply discrete events in this way. Where evaluating the results, it is shown that the simulation models of broadcasting systems take a different approach from what is normally done, a proposal containing a concept of a technique naturally applied at higher levels, in a lower abstraction level, in bits in the transmission of a channel, provides positive results with a 22.36% improvement to a naturally powerful technique (OFDM), which strengthens it even more.

Although taking into account that an extension of the results of this research, the compression of the information, strongly affects similar methods performed in higher layers, for example, format types such as HEVC, MPEG-4, AVC/H.264, as well the others, can improve them even more since this proposal acts on the bits.

REFERENCES

[1] Dunlop, John. Telecommunications engineering. Routledge, 2017.
[2] Abdoli, Javad, Ming Jia, and Jianglei Ma. "Filtered OFDM: A new waveform for future wireless systems." 2015 IEEE 16th International Workshop on Signal Processing Advances in Wireless Communications (SPAWC). IEEE, 2015.
[3] Rahman, MuhibUr, et al. "Bandwidth enhancement and frequency scanning array antenna using novel UWB filter integration technique for OFDM UWB radar applications in wireless vital signs monitoring." Sensors 18.9 (2018): 3155.
[4] Wang, Yanyan, et al. "An enhanced OFDM for broadcasting systems using uniform subband division and multistage interpolator." 2017 IEEE International Symposium on Broadband Multimedia Systems and Broadcasting (BMSB). IEEE, 2017.
[5] Galande, N., and A. Shah. "Concepts and Brief Survey of Conventional and wavelet OFDM." International Journal of Science, Engineering and Technology Research 5.1 (2016): 149-152.
[6] Yeh, Chien-Hung, et al. "Utilization of multi-band OFDM modulation to increase traffic rate of phosphor-LED wireless VLC." Optics express 23.2 (2015): 1133-1138.
[7] Mao, Tianqi, et al. "Dual-mode index modulation aided OFDM." IEEE Access 5 (2016): 50-60.
[8] Brito, Thiago Barros, Edson Felipe Capovilla Trevisan, and Rui Carlos Botter. "A conceptual comparison between discrete and continuous simulation to motivate the hybrid simulation methodology." Proceedings of the Winter Simulation Conference. Winter Simulation Conference, 2011.
[9] Chahal, Kirandeep, and Tillal Eldabi. "A multi-perspective comparison for selection between system dynamics and discrete event simulation." International Journal of Business Information Systems 6.1 (2010): 4-17.
[10] Cassandras, C. G., & Lafortune, S. (2009). Introduction to discrete event systems. Springer Science & Business Media.
[11] Zeng, Yong, and Rui Zhang. "Millimeter wave MIMO with lens antenna array: A new path division multiplexing paradigm." IEEE Transactions on Communications 64.4 (2016): 1557-1571.
[12] Bandy, William R., Yuri Okunev, and Wayne E. Shanks. "Data Transmission via Wide Band Acoustic Channels." U.S. Patent Application No. 14/948,764.
[13] Bhattacharya, Ansuman, et al. "Multimedia channel allocation in cognitive radio networks using FDM-FDMA and OFDM-FDMA." arXiv preprint arXiv:1603.03938 (2016).
[14] Bodinier, Quentin, Faouzi Bader, and Jacques Palicot. "Modeling interference between OFDM/OQAM and CP-OFDM: Limitations of the PSD-based model." 2016 23rd International Conference on Telecommunications (ICT). IEEE, 2016.

http://www.set.org.br/ijbe/ doi: 10.18580/setijbe.2019.6 Web Link: http://dx.doi.org/10.18580/setijbe.2019.6

[15] Wen, Miaowen, et al. "On the achievable rate of OFDM with index modulation." IEEE Transactions on Signal Processing 64.8 (2015): 1919-1932.
[16] Saied, Osama, et al. "Single carrier optical FDM in visible light communication." 2016 10th International Symposium on Communication Systems, Networks and Digital Signal Processing (CSNDSP). IEEE, 2016.
[17] Muslimin, J., et al. "Experimental Studies on the Effect of Antenna Orientations to the Performance of OFDM-based System." International Journal of Electrical and Computer Engineering 8.4 (2018): 2588.
[18] Kumari, Shailly, and Rajesh Mehra. "Selective Mapping and Partial Transmit Sequence Based PAPR Reduction for OFDM Applications." IOSR Journal of VLSI and Signal Processing 6.6 (2016): 70-76.
[19] Rama Krishna, A., Chakravarthy, A. S. N. & Sastry, A. S. C. S. (2016). Variable Modulation Schemes for AWGN Channel based Device to Device Communication. Indian Journal of Science and Technology, Vol 9(20), DOI: 10.17485 / ijst / 2016 / v9i20 / 89973.
[20] Bossert, M. (1999). Channel coding for telecommunications. John Wiley & Sons, Inc..
[21] Lakshmanan, M. K., & Nikookar, H. (2006). A review of wavelets for digital wireless communication. Wireless Personal Communications, 37(3-4), 387-420.
[22] Barnela, M., & Kumar, D. S. (2014). Digital modulation schemes employed in wireless communication: A literature review. International Journal of Wired and Wireless Communications, 2(2), 15-21.
[23] Ling, S. O. A., Zen, H., Othman, A. K. B. H., Adnan, M., & Bello, O. (2017). A Review on Cooperative Diversity Techniques Bypassing Channel Estimation. arXiv preprint arXiv:1711.10643.
[24] Tozer, Edwin Paul J. Broadcast engineer's reference book. Focal Press, 2012
[25] Fukuda, Rafael Masashi, and Taufik Abrão. "OFDM System Implementation in DSP Platform TMS320C6678." Journal of Computer and Communications 4.11 (2016): 26.
[26] Xia, Xiang-Gen, Tianxian Zhang, and Lingjiang Kong. "MIMO OFDM radar IRCI free range reconstruction with sufficient cyclic prefix." IEEE Transactions on Aerospace and Electronic Systems 51.3 (2015): 2276-2293.
[27] Nagashima, T., et al. "Cyclic prefix insertion for all-optical fractional OFDM." 2015 International Conference on Photonics in Switching (PS). IEEE, 2015.
[28] Venkatesan, Sivarama, and Reinaldo A. Valenzuela. "OFDM for 5G: Cyclic prefix versus zero postfix, and filtering versus windowing." 2016 IEEE International Conference on Communications (ICC). IEEE, 2016.
[29] Zhao, Lu, Juan Montojo, and Christian Pietsch. "Hybrid waveform design combining OFDM and cyclic prefix based single carrier for millimeter-wave wireless communication." U.S. Patent No. 9,960,938. 1 May 2018.
[30] Abdoli, Javad, Ming Jia, and Jianglei Ma. "Filtered OFDM: A new waveform for future wireless systems." 2015 IEEE 16th International Workshop on Signal Processing Advances in Wireless Communications (SPAWC). IEEE, 2015.
[31] Galande, N., and A. Shah. "Concepts and Brief Survey of Conventional and wavelet OFDM." International Journal of Science, Engineering and Technology Research 5.1 (2016): 149-152.
[32] Heiskala, Juha, and John Terry Ph D. OFDM wireless LANs: A theoretical and practical guide. Sams, 2001.
[33] Padilha, Reinaldo França. "Proposta de um método complementar de compressão de dados por meio da metodologia de eventos discretos aplicada em um baixo nível de abstração= Proposal of a complementary method of data compression by discrete event methodology applied at a low level of abstraction." (2018).

Reinaldo Padilha. Graduated in Computer Engineering (University Regional Center of Espírito Santo de Pinhal - 2014). Currently is a Ph.D. Candidate by Department of Communications (DECOM), Faculty of Electrical and Computer Engineering (FEEC) at State University of Campinas (UNICAMP), and a researcher at the Laboratory of Visual Communications (LCV). He also is currently Proceedings Chair of the Brazilian Symposium on Technology (BTSym). Has interest and affinity in the area of technological and scientific research as well as knowledge in programming and development in C / C ++, Java and .NET languages. The main topics of interest are Simulation, Operating Systems, Software Engineering, Wireless and Network, Internet of Things, Broadcasting and Telecommunications Systems.

Profº Yuzo Iano. BS (1972), Master's degree (1974) and a Ph.D. degree (1986) in Electrical Engineering from the State University of Campinas, Brazil. Since then he has been working in the technological production field, with 1 patent granted, 8 patent applications filed, and 36 projects completed with research and development agencies. Successfully supervised 29 doctoral theses, 49 master's dissertations, 74 undergraduate and 48 scientific initiation works. He has participated in 100 master's examination boards, 50 doctoral degrees, author of 2 books and more than 250 published articles. He is currently Professor at the State University of Campinas, Brazil, Editor-in-Chief of the SET International Journal of Broadcast Engineering and General Chair of the Brazilian Symposium on Technology (BTSym). He has experience in Electrical Engineering, with knowledge in Telecommunications, Electronics and Information Technology, mainly in the field of audio-visual communications and data.

Ana Carolina Borges Monteiro. Graduated in Biomedicine from Centro Universitário Amparense - UNIFIA (2015). Currently is a Ph.D. Candidate by Department of Communications (DECOM), Faculty of Electrical and Computer Engineering (FEEC) at State University of Campinas (UNICAMP), and a researcher at the Laboratory of Visual Communications (LCV). She also is currently Registration Chair of the Brazilian Symposium on Technology (BTSym). Has expertise in the areas of Clinical Analysis

and digital image processing through MATLAB software. This knowledge was acquired through the realization of research projects and internship in municipal hospital, as also experience in the revision of scientific works by acting as a reviewer in congresses.

Rangel Arthur He holds a degree in Electrical Engineering from the Paulista State University Júlio de Mesquita Filho (1999), a Master's degree in Electrical Engineering (2002) and a PhD in Electrical Engineering (2007) from the State University of Campinas. Over the years from 2011 to 2014 he was Coordinator and Associate Coordinator of Technology Courses in Telecommunication Systems and Telecommunication Engineering of FT, which was created in its management. From 2015 to 2016 he was Associate Director of the Technology (FT) of Unicamp. He is currently lecturer and advisor to the Innovation Agency (Inova) of Unicamp. He has experience in the area of Electrical Engineering, with emphasis on Telecommunications Systems, working mainly on the following topics: computer vision, embedded systems and control systems.

Received in 2018-05-28 | Approved in 2019-11-25

http://www.set.org.br/ijbe/ doi: 10.18580/setijbe.2019.6 Web Link: http://dx.doi.org/10.18580/setijbe.2019.6

Analysis of digital TV signal reception: a case study for antennas transmitting in horizontal and elliptical polarization

Deisi Luiza Wosch Passarelli
Keiko Verônica Ono Fonseca
Alexandre de Almeida Prado Pohl

CITE THIS ARTICLE

Passarelli, Deise Luiza Wosh, Fonseca, Keiko Verônica Ono, Pohl, Alexandre de Almeida Prado; 2019. Analysis of digital TV signal reception: a case study for antennas transmitting in horizontal and elliptical polarization. SET INTERNATIONAL JOURNAL OF BROADCAST ENGINEERING. ISSN Print: 2446-9246 ISSN Online: 2446-9432. doi: 10.18580/setijbe.2019.7. Web Link: http://dx.doi.org/10.18580/setijbe.2019.7

Analysis of digital TV signal reception: a case study for antennas transmitting in horizontal and elliptical polarization

Deisi Luiza Wosch Passarelli, RPC, Keiko Verônica Ono Fonseca, UTFPR and Alexandre de Almeida Prado Pohl, UTFPR.

Abstract — This work presents results on the prediction and measurement of TV signal propagation in the Brazilian city of Maringá from antennas transmitting in the horizontal and elliptical polarization. Measurements were taken at forty -eight fixed locations and by the survey vehicle moving at constant speed along previously determined path ssumming approximately two thousand and seven hundred data points. A comparison of results obtained with chosen radiopropagation models and measured data is provided and discussed .

Key Words - Elliptical polarization a ntenna. Horizontal polarization antenna. Radiop ropagation models. UHF. Digital television.

I. Introduction

The Brazilian television broadcast system is an open, real time and free reception service present in 97.1% of the households [1]. In November 2003 the federal government signed the Decree 4.901 establishing the Brazilian Digital Television System – SBTVD [2], which was followed in 2006 by the Decree 5.820 that officialized its implementation [3]. The commercial broadcast of digital TV began in São Paulo on December 2, 2007. In 2016 the digital TV coverage reached more than 75% of the Brazilian population, about 152 million people. The analog TV broadcast switch off began in 2016 in Rio Verde, Goiás and by the end of 2018 1,378 Brazilian cities, corresponding to 128 million people, had their analog TV signals switched off [4].

The open TV market corresponds to around 60% of the entire national advertising market, with gross operating revenue of 29.55 billion reais in 2014 [5]. The open broadcast system in Brazilian households has been in existence for over sixty years and it sustains a successful and consolidated business model based on the transmission and reception of electromagnetic waves. Therefore, the study of the radiopropagation phenomena and the allocation of frequency bands used by television stations have always been a matter that needs to comply with current legislation and aims to maximize return of investment. At the same time, the demand of qualified engineers for developing digital television broadcasting projects has increased as they need to face different challenges, such as the requirements for establishing the reception threshold inside the intended coverage area.

A television broadcast project consists of the specification of the carrier frequency (channel), the transmission equipment, the transmission antenna, support structures (tower), cables, connectors, combiners and accessories.

The transmitting antenna is one of the main components of the television system. The role of the antenna is to transform the energy received from the transmitter into an electromagnetic field pattern that is sent out to the desired points of reception. Its main technical characteristics are the irradiation, gain and polarization diagram. The correct choice of the transmission antenna leads to the increase of signal penetration in the coverage area and contribute to the population adherence to the new technology. In addition to the conventional reception with an external antenna installed horizontally in the premises, the reception of digital TV signals can be also achieved using portable devices. This fact has motivated designers and antenna manufacturers to develop projects in which other types of polarization are employed in the transmission antenna.

In order to increase the TV signal penetration, the project designer needs to understand the impact of the transmission parameters (transmission power, radiant system, the type of antenna, its radiation diagram and polarization, among others) as well as of the environment issues on the signal propagation within the coverage area. In this way, studies are carried out based on radiopropagation models, either deterministic or empirical, that estimate the electromagnetic wave behavior over the propagation path. The comparison of results obtained by means of the propagation models with those obtained from field tests provides insights and technical references for the design improvement and/or refinement of the TV transmission system.

In this work we analyze the results of field tests carried out in the Brazilian city of Maringá, using two types of antennas, one transmitting in the horizontal and the other in the elliptical polarization mode. The results are compared with those predicted by radiopropagation models and discussed on the basis of their fitting into the models.

This paper is organized as follows: section II describes the radiopropagation models used to predict the signal strength within the coverage area; section III describes the characteristics of equipment and the field tests; section IV reports on the simulation and comparison with field results, followed by section V, which presents the conclusion and the final remarks about our contribution.

II. Propagation Models

The prediction of the electric signal strength along a path is fundamental in order to understand the wave propagation and the limits of the coverage area. In this study we employed the propagation models known as Okumura (Hata), ITU-R 370-70, ITU-R 1546 and CRC-Predict to perform an estimation and comparison with data obtained from the field tests. Such models have long proved their consistency and were chosen because they are large-scale models, are able to predict the average field strength over large distances (hundreds of meters to kilometers) between the transmitter and the receiver and because of their applicability to the UHF band (in order to cope with the frequency range of the field measurements), not to mention that they are easily available through software tools. Other models have also been

http://www.set.org.br/ijbe/ doi: 10.18580/setijbe.2019.7 Web Link: http://dx.doi.org/10.18580/setijbe.2019.7

employed in this study; whose results can be found in [6]. The models were applied to the same field cenario and are summarized in the following section.

A. Okumura (Hata) - Open, Suburban e Urban

The Okumura model [7] was developed using data from measurements obtained in urban and suburban areas of Tokyo. The model considers a distance from transmitter to receiver up to 30 km, a transmitting antenna height of up to 200m and receiver antenna height of less than 10m. The model is applied to the open, suburban and urban scenarios with appropriate correction factors, depending on the region.

$$Lu = 69.55 + 26.16 \log f - 13.82 \log h_b - a_{hm} + (44.9 - 6.55\ log\ h_b) \log d \quad (dB) \tag{1}$$

In this equation f is the operation frequency in MHz, h_b is the height of the transmitting antenna in meters, a_{hm} is the height correction factor of the mobile antenna (see below) and d is the distance from the transmitter to receiver in kilometers. For a medium or small city, in which a suburban scenario applies, a_{hm} is given as:

$$a_{hm} = (1.1 \log f - 0.7)h_m - (1.56\ log\ f - 0.8) \tag{2}$$

For a big city (Urban):

$$a_{hm} = 8.29\ (\log\ (1.54\ h_m))^2 - 1.1 \quad when\ f \leq 200\ MHz \tag{3}$$

$$a_{hm} = 3.20\ (log(11.75\ h_m))^2 - 4.97 \quad when\ f > 400\ MHz \tag{4}$$

in which h_m is the receiver antenna height (in meters). In suburban areas the equation is modified as:

$$Lsu = Lu - 2\ (\ log(\frac{f}{28}))^2 - 5.4\ (dB) \tag{5}$$

And in rural, open areas, the equation is given as:

$$Lro = Lu - 4.48\ (\log f)^2 + 18.33 \log f - 40.94\ (dB) \tag{6}$$

B. ITU-R 370

The ITU-R 370-7 describes the propagation model [8] for predicting the field strength of the broadcasting service in the frequency range of 30 to 1,000 MHz and for a distance of up to 1,000 km. The recommendation document presents attenuation curves for predicting the loss. The field strengths are adjusted to correspond to a power of 1 kW radiated from a half-wave dipole.

C. ITU-R 1546

The ITUR 1546 [9] describes the procedures to be followed for predicting the field strength of the broadcasting, land mobile, maritime mobile and certain fixed services, from 30 MHz to 3,000 MHz and for a distance from 1 km to 1.000 km. The Recommendation ITU-R P.1546, version 1, is used for the propagation estimation of broadcasting projects as defined in Attachment II of the Brazilian Telecom regulator (Anatel resolution 398, April 7, 2005) [10]. The model is an extension of the ITU-R.P370 model. Attenuation is derived from a family of curves, as in the ITU-R.P370, with a number of other correction factors added. The attenuation is obtained by the field strength interpolation as a function of distance, frequency, percentage time, and transmitting antenna.

D. CRC-Predict

CRC-PREDICT [11] is a propagation model developed by the Canadian government (Canadian Research Center, CRC) and it is based on physical optics and the Fresnel-Kirchhoff theory. The total loss is the sum of the diffraction losses on the ground and an estimation of the additional attenuation related to the clutter, which is defined as a set of polygons with the classification of the region according to the urbanization and vegetation. The intensity of urbanization and the type of vegetation are associated with an additional attenuation table due to the reflections originated in these scenarios. The norm also addresses reflections on the ground, tropospheric mirroring, variability of locations and temporal availability due to atmospheric effects.

III. FIELD TESTS

This section describes the field tests performed in the Brazilian city of Maringá. The digital transmitting station is located at Rua Santa Joaquina de Vedruna, 625, Zona 05, Maringá, State of Paraná, at the geographical coordinates of 23º 25' 29,3" S and 51º 57' 13,7" W. For the signal transmission, two slot type antennas were installed in the same tower at the height of approximately 54 meters, one transmitting in the horizontal polarization with a gain of 7.32 dBd (5.39 x) and the other transmitting in the elliptic polarization with a horizontal gain of 6.44 dBd (4.41 x) and vertical gain of 3.8 dBd. The antennas transmitted the signal with the same radiated power, but not simultaneously during the measurement campaign. As the employed antennas were from different manufacturers, some technical characteristics are different as, for instance, the gain. During the tests the transmitter power was set to ensure that the same radiated power was emitted by both antennas. This was accomplished by using the maximum effective radiated power, calculated according to:

$$ERPmax = Pt * GTmax * Ef \tag{7}$$

in which P_t is the transmitter output power in kW, GTmax is the maximum radiant system gain and Ef is the transmission line efficiency. The following data is used:

- Cable efficiency (the same for the two antennas): 0.93. It is calculated according to the recommendation given in [12];
- Horizontal polarization antenna: 7.32 dBd (5.39 x);
- Elliptical polarization antenna: 6.44 dBd (horizontal, 4.41 x).

First, given that 3.6 kW is set at the transmiter, the ERPmax for the elliptical polarization antenna is calculated as

$$ERPmax = 3.6 \text{ kW x } 4.41 \text{ times x } 0.93 = 14.76 \text{ kW}. \quad (8)$$

On the other hand, fixing the 14.76 KW as the ERPmax, the transmitter power for the horizontal polarization antenna is calculated as:

$$14.76 \text{ kW} = PT \text{ x } 5.39 \text{ times x } 0.93 \text{ or } = 2.94 \text{ kW} \quad (9)$$

In summary, the transmitter power for the horizontal polarized antenna was adjusted to 2.94 kW and for the elliptical polarization antenna the transmitter power was set to 3.6 kW, both having an ERPmax of 14.76 kW.

Table 1 summarizes the technical characteristics of the transmitting station.

TABLE 1
TECHNICAL CHARACTERISTICS - TRANSMISSION STATION

Technical characteristics Transmitting station	Description
Canal	Channel 41, (632 to 638 MHz) with a 6 MHz band
Encoder	Manufacturer NEC, Model: VC 7301 (HD) and VC7010 (LD)
Multiplexador	Manufacturer NEC, Model: MX-1500
Modulator	Linear manufacturer, Model: IS8001
Transmitter	Power: 3.6 KW (*elliptical polarization antenna*) Power: 2.94 KW (*horizontal polarization antenna*)
Transmission line	Type: Coaxial-50 Ohms
	Diameter: 1 5/8 "
	Length: 64 meters
	Manufacturer: RFS-*Radio Frequency Systems*
	Model: HCA-158-50J
	Attenuation: 1.69 dB every 100 meters
Horizontal polarization antenna	Type: Slot
	Polarization: Horizontal
	Gain: 7.32 dBd or 5.39 times
	Installation: 54.05 meters
Elliptical polarization antenna	Type: Slot
	Polarization: elliptical-70 \% H and 30 \% V
	Gain Horizontal : 6.44 dBd or 4.41 times
	Gain Vertical : 3,8 dBd or 2.4 times
	Installation: 54.00 meters

For monitoring the reception signal at both, fixed and mobile location points (henceforth denoted only as points unless stated otherwise), a field survey vehicle was used. The vehicle is composed of home antennas, field strength meters, GPS (Global Postioning System) receivers for geolocation, TV monitors, a digital signal reception converter, coaxial cables, dividers, a camera and a retractable 8-meter mast to which the antennas were fixed. Two identical antennas were used for the fixed reception of the digital TV signals: one installed in the horizontal and the other installed in the vertical position, as shown in Figure 1. Both were fixed on the mast and elevated to a height a viewer would usually install them in his residence. The objective was to measure the signal composition on both linear polarizations at each reception point. The antennas with 8 elements each and a gain of 11 dBi were manufactured by Proeletronic [13] and specified for operation in the range from 470 to 890 MHz, corresponding to channels 14 to 83. For the mobile reception a monopole omnidirectional antenna, model DTV-150, manufactured by Aquarium [14] was used and installed on the top of the survey vehicle. Table 2 presents a summary of the technical specifications of both antennas.

Fig. 1. Receiver antenna installed vertically and horizontally

TABLE 2
TECHNICAL CHARACTERISTICS – RECEPTION STATION

Technical characteristics of reception		Description
GPS		Manufacturer: Garmin - model: 3Plus
Monitor		Manufacturer: Sansung 20" model: T20C310LB
Converter		Manufacturer: Aiko model: HD-1018
Spectrum analyzer		Manufacturer: Agilent
Splitter		Model: Greatek 1:2 5-2400 MHz
Antenna Fixed Reception	Type	Periodic Log
	Manufacturer	Proeletronic
	Model	Total Band
	Frequency range	470 to 890 MHz
	Quant. Elements	8 elements
	Gain	11 dBi
Antenna Mobile Reception	Type	Monopole
	Manufacturer	Aquário
	Model	DTV-150
	Frequency range	30 to 890 MHz
	Quant. Elements	Omnidirectional
	Gain	3 dBi
Cabo (tipo)		Coaxial/Ethernet and power supply
Cabo (comprimento)		10 m (fixed antenna) and 2 m (monopole)

For the measurement with the horizontal-based and elliptical-based polarization 48 points were selected at fixed locations: 30 points within Maringá and 18 points selected in 10 other nearby municipalities (Marialva, Angulo, Paiçandu, Sarandi, Astorga, Mandaguaçu, Floresta, Itambé, Bom Sucesso and Mandaguari), as shown in Figure 2. The mobile reception was performed along highways and streets totalizing 2700 points: a) approximately 1270 points measured in the streets of downtown Maringá, near buildings and subject to greater incidence of multipath; b) 850 points along the Colombo Avenue in Maringá, as shown in Figure 3; c) 225 points along the highway connecting Maringá to Marialva and d) 240 points along the highway connecting Maringá to Mandaguaçu.

Fig. 2. Google Earth image - fixed points in Maringá

Fig. 3. Google Earth image: path taken (red) at Maringá - Marialva highway for the mobile reception measurements.

First the signal was transmitted using the horizontal polarization based antenna and measurements were taken at the fixed sites and along the mentioned path. The process was repeated along the same path using the elliptical polarization based antenna. The received power (dBm), the carrier-to-noise ratio (C/N, dB), the modulation error rate (MER) and the signal spectrum were measured and recorded. Measurement of the oneseg signal (low definition) was taken with the moving vehicle along the highways and streets using the monopole antenna, the GPS receiver, the spectrum analyzer and a notebook running a software developed by the Universidade Tecnológica Federal do Paraná. Measurements of the geographic coordinates, the received power and symbol error rate (MER) were taken every 6 seconds, corresponding to a separation of 10 to 15 meters within a region, depending on the speed of the vehicle, although attempst have been made to keep it as constant as possible.

IV. SIMULATION AND RESULTS

Two software tools, Signal EDX [15] and CRC-COVLAB [16] were employed. These packages contained the propagation models needed to predict the received power in the coverage area. The tools require may use digitized ground files and information on the type of obstacles at each point, known as clutters. The transmission and reception parameters are found in Table 1 and 2, respectively.

The antenna diagrams were also considered (input). By using the scale of the horizontal antenna diagram given by ratio E/Emax of antenna diagram in each of its plane and matching the various gains at the corresponding azimuths and elevations, it was possible to estimate the relative gain in each direction and angle. This information was used as input variables into the propagation models. Based on the measured and computed data a statistical analysis was perfomed and the mean error, the mean error in absolute values and the RMS error were obtained. A figure of merit, defined as the hit rate, was used to compare how close the measured results were from the data obtained using the propagation models. To facilitate the visualization and interpretation, the data was ranked according to a scale that varied from 0 to 5. For instance, when measured and calculated power levels presented a difference between 0 and 2 dB, such data was given a score 5. When the difference was between 2.01 and 4 dB, a score 4 was assigned, a difference between 4.01 to 6 dB was given a score 3, for differences between 6.01 to 8 a score 2 was used, differences between 8.01 dB to 10 dB were scored as 1 and when the difference was above 10 dB the score was 0. Thus, the higher the score, the more accurate is the used propagation model for that particular region.

A. Measuement at the fixed locations

In order to compare which models were most suited for characterizing the propagation loss, Figure 4 and Figure 5 show the RMS error (dB) and the hit rate, respectively, concerning calculation and measured data at the 48 fixed points, taking into account the type of antenna used in the transmission. The comparison shows that the minimum values of the RMS error were verified for the ITU-R370 model, which delivered an error of 8.5 dB for the elliptical, and 9.6 dB for the horizontal polarization antenna, respectively, as seen in Fig, 4. Considering the hit rate, the CRC-Predict model presented the highest score (1.9) among all models for both antenna types, as shown in Figure 5.

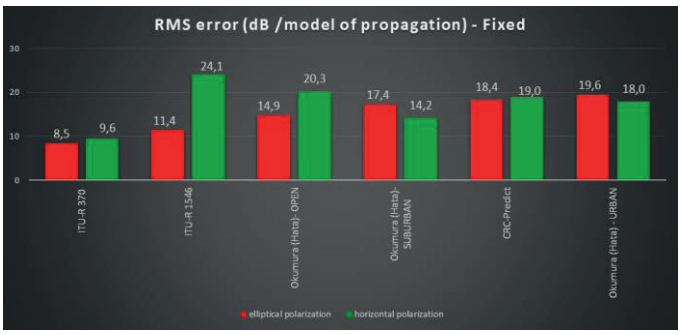

Fig. 4. RMS error in dB for each propagation model - fixed points

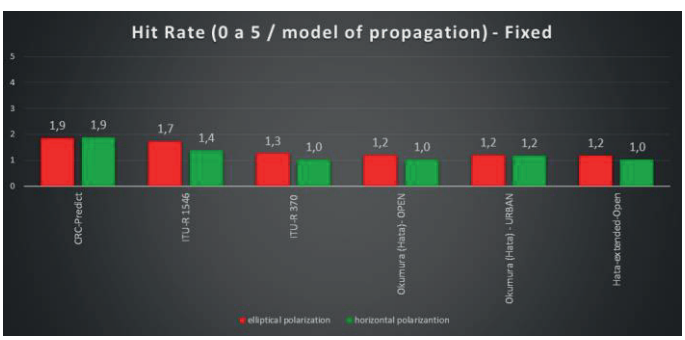

Fig. 5. Average hit rate (0 to 5) for each propagation model - fixed points

Figures 6 and 7 show the received power (dBm) versus distance (km) behavior for the transmission with the horizontal polarization, in which data points were plotted considering the increasing distance from the antenna. In Figura 6 the ITU-R REC. 370 model is used, while in Figure 7 the CRC – Predict model is employed for estimating the loss. Figures 8 and 9 show results of the received power versus distance behavior, but for the transmission with the elliptical polarization antenna. For all cases we observe that the measured data agrees well with estimated values delivered by the ITU-R Rec. 370 and CRC models, within the calculated error range.

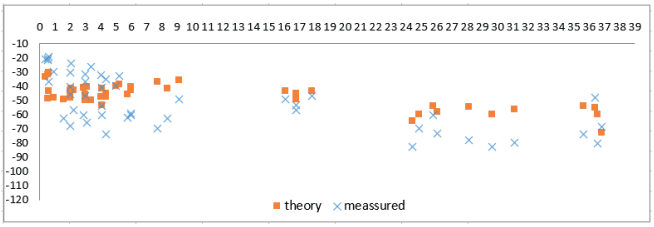

Fig. 6. Received power level (dBm) x distance from the point (km) - model: ITU-R REC. 370 - horizontal polarization – 48 fixed points

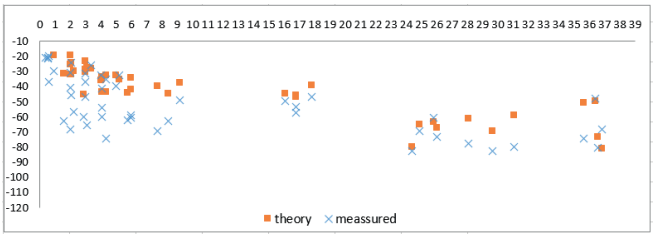

Fig. 7. Received power level (dBm) x point distance (km) - model: CRC Predict - horizontal polarization – 48 fixed points

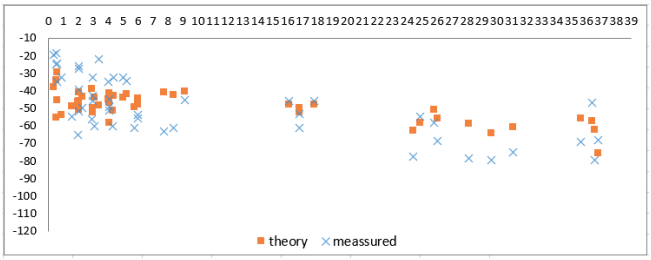

Fig. 8. Received power level (dBm) x point distance (km) - model: ITU-R REC. 370 - elliptical polarization – 48 fixed points

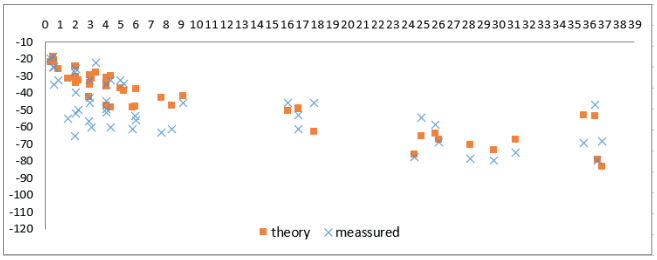

Fig. 9. Received power level (dBm) x point distance (km) - model: CRC Predict - elliptical polarization – 48 fixed points

B. *Measurement with the moving vehicle*

Figures 10 and 11 show results for the RMS error (dB) and the hit rate corresponding to 225 points of signal reception taken along the Maringá - Marialva highway. Figure 10 shows the RMS error for the transmission with the horizontal and eliptical polarization antennas. It is observed that the Okumura (Hata) Suburban presented the lowest RMS error for the transmission with the elliptical polarization antenna, followed by the ITU-R Rec. 370 and the Okumura (Hata) OPEN, with 5.8, 6.9 dB 7.7 dB, respectively. However, the calculated RMS error for the transmission with the horizontal polarization is higher (13.9 dB for the Okumura (Hata) Suburban and 10.8 dB for the ITUR-370, respectively).

Figure 11 shows the hit rate data. In this case, the ITU-R 1546, the ITU-R 370 and the Okumura model (Hata) Suburban with an average score of 2.8, 2.7 and 2.3, respectively, for the elliptical polarization antenna are considered the models that best describe the propagation along that path. The hit rate scores for the transmission with the horizontal antenna are, however, lower.

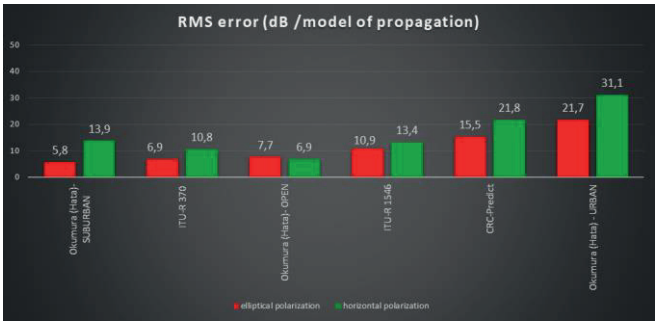

Fig. 10. RMS error in dB for each propagation model - moving points: Maringá to Marialva highway

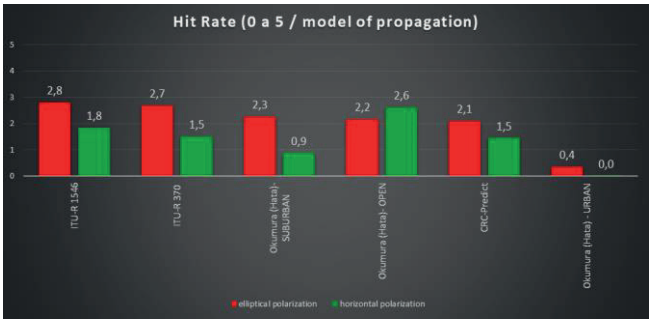

Fig. 11. Average hit rate (0 to 5) for each propagation model - moving points: Maringá to Marialva highway

Figure 12 and Figure 13 show the plot of the measured and calculated received power (dBm) versus distance (km) for signals transmitted with the horizontal and elliptical polarization antennas along the same highway. The Okumura (Hata) OPEN and the ITU-R 1546 propagation models were employed for the comparison based on the transmission with the horizontal and elliptical polarization antennas, respectively. The total distance covered along the path was 15,9 km. It is possible to observe that the compatibility with the calculated data is improved for distances longer than 6 km.

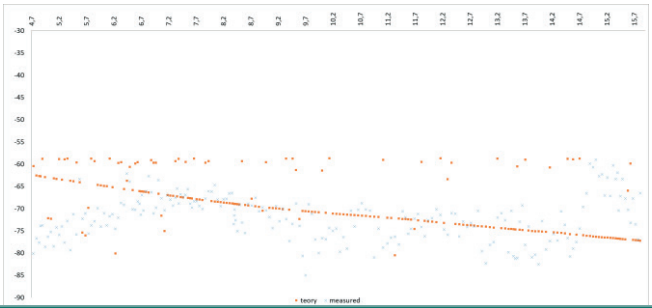

Fig.12 - Received power level (dBm) x distance from point (km) - model: Okumura (Hata) Open - Horizontal polarization - moving points: Maringá to Marialva highway

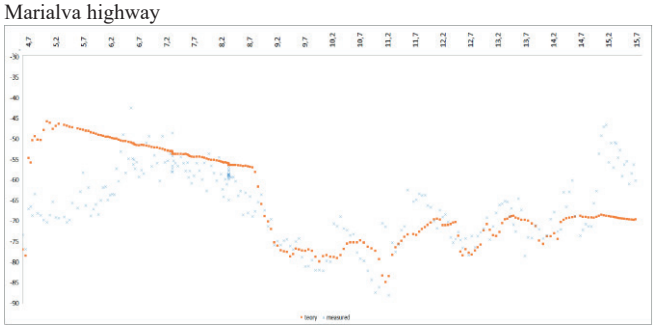

Fig.13- Received power level (dBm) x distance from point (km) - modelo: ITUR 1546 - elliptical polarization - moving points: Maringá to Marialva highway

Based on the results obtained through comparison from of figures of merit of RMS error and hit rate, Table 3 presents a summary listing the best models according to each measuring condition (fixed or moving) and region. The established criteria established for choosing the best results were the lowest values for the RMS error and the highest for the hit rate.

TABLE 3
BEST MODEL OF PROPAGATION BY REGION

Region	Number of points	Best model Horizontal polarization	Best model Elliptical polarization
Fixed	48	ITUR 370	ITUR 370
Fixed	48	CRC Predict	CRC Predict
Movement-Center	1270	Okumura (Hata) - Suburban	Okumura (Hata) - Suburban
Movement-Av. Colombo	850	Okumura (Hata) - Suburban	Okumura (Hata) - Suburban
Movement-Maringá Marialva Highway	225	Okumura (Hata) - Open	ITUR 1546
Movement-Maringá Mandaguaçu Highway	240	Okumura (Hata) - Open	Okumura (Hata) - Open

V. CONCLUSION

The estimation of propagation losses is a complex task due to the large number of variables involved, such as terrain conditions along the path of propagation, environmental conditions and man-made obstacles, such as houses and buildings. Even large concentrations of people close to the receiver may interfere with the propagation. Therefore, propagation models are important and relevant to the project designer, but their use requires a previous understanding of their application and limitations concerning a particular environment. In this way, the present work was first motivated by the proper application of the radiopropagation models and the analysis of their numerical results. The work was also motivated by the observation and understanding of the influence of the transmitting antenna, considering their polarization configuration and impact on the signal strength at the receiver site. The measurement campaign was perfomed in the city of Maringá, located in the State of Paraná, and surrounding region.

The results are compared with those predicted by radiopropagation models and discussed on the basis of their fitting into the models. The figures of merit of RMS error and hit rate were used to perform the comparison. For measurements taken at fixed points in the city of Maringá the analysis shows that the ITU-R 370 and CRC predictions are the propagation models that best fit the measured data. Figures 4 and 5 also show that results obtained for the transmission with the horizontal and elliptical polarization differ only slightly for such models and no evidence is shown that one polarization performs better than the other. For measurements taken with the moving vehicle, considering the data from Figures 10 and 11, the analysis shows that Okumura (Hata) Suburban and the ITU-R 1546 are the propagation models that delivered the best results. However, concerning the signal reception, results point out to a better better performance for the transmission with the elliptical polarization antenna along the Marialva to Maringa highway as compared to the results obtained with the horizontal polarization antenna. Other results concerning the measurement campaign in the region of Maringá and associated analysis can be seen in [6], which basically lead to the same conclusion for the cases presented in this work.

Future work could explore the application of propagation models taking into account a detailed environment database (such as, details of buildings and obstructions). Measurement campaigns performed in other regions and the application of the same analysis could provide system designers with more trustfull data for future projetcs. In this way, that the present work contributes to the establishment of good practices for the specification of broadcasting projects and helps broadcasting professionals to improve their understanding of the signal coverage in regions similar to the ones covered in this study.

REFERENCES

[1] IBGE. Pesquisa Nacional de Amostra por Domicílios-PNAD. [S.l.], 2015. Available in: <https://brasilemsintese.ibge.gov.br/habitacao/bens-duraveis.html>. Acessed on July 24, 2019.

[2] BRASIL. Institui o sistema brasileiro de televisão digital – sbtvd. In: Decreto no 4.901, de 26 de novembro de 2003. Diário Oficial da União, 2003. Seção 1, p. 7. Available in: <http://www.anatel.gov.br/legislacao/decretos/349-decreto-4901>. Acessed on July 24, 2019.

[3] BRASIL. Dispõe sobre a implantação do SBTVD, estabelece diretrizes para a transição do sistema de transmissão analógica para o sistema de transmissão digital do serviço de radiodifusão de sons e imagens e do serviço de retransmissão de televisão, e dá outras providências. In: Decreto no 5.820, de 29 de junho de 2006. Diário Oficial da União, 2006. Available in:< http://www.planalto.gov.br/ccivil_03/_Ato2004-2006/2006/Decreto/D5820.htm >. Acessed on July 24, 2019

[4] ANATEL. Mosaico - Canais de Radiodifusão. 2018. Available in: <http://sistemas.anatel.gov. br/se/public/view/b/srd.php>. Acessed on July 17, 2019.

[5] ABERT. Relatório enviado as emissoras de rádio e televisão, Raio X da Radiodifusão Brasileira. 2017. Acessed on July 12, 2019.

[6] Passarelli, D. L. W. Estudo de modelos de radiopropagação para a recepção de TV utilizando antena de transmissão na polarização horizontal e elíptica. Dissertação de Mestrado – Programa de Pós-Graduação em Engenharia Elétrica e Informática Industrial, Universidade Tecnológica Federal do Paraná - UTFPR, Curitiba, 2018. Available in: < http://repositorio.utfpr.edu.br/jspui/handle/1/3873>. Acessed on July 24, 2019.

[7] OKUMURA, Y. et al. Field strength and variability in UHF and UHF land-mobile radio service. [S.l.]: Rev.Elec.Commun.Lab, 1968. v. 16. P. 825-873. Acessed on July 01, 2018.

[8] ITU. Recommendation ITU-R p.370-7- VHF and UHF propagation curves for the frequency range from 30 MHz to 1 000 MHz. Broadcasting services. 1995. Available in: https://www.itu.int/rec/R-REC-P.370-7-199510-W/en<https://www.itu.int/rec/R-REC-P.370-7-199510-W/en>.

[9] ITU-R. Method for point-to-area predictions for terrestrial services in the frequency range 30 MHz to 3 000 MHz. In: ITU. Recommendation ITU-R P15461. 2003. Available in: <https://www.itu.int/rec/R-REC-P.1546-1-200304-S/en>. Acessed on July 24, 2019.

[10] ANATEL. Recomendação itu-r p.1546-1 método de previsões ponto-área para serviços terrestres na faixa de frequências de 30 MHz a 3000 MHz. In: ANATEL. Anexo II - Resolução 398 de 07 de abril de 2005. Diário Oficial da União 19 abr.2005, 2005. Available in: <http://www.anatel.gov.br/legislacao/resolucoes/2005/288-resolucao-398>. Accessed on June 30, 2019.

[11] ITU. Description of crc-predict a vhf and uhf propagation model. In: ITU. Contribuition ITUR R03-WP6E-C-0017. 2003. Available in: <https://www.itu.int/md/R03-WP6E-C-0017/ en>. Accessed on June 29, 2019

[12] ANATEL. Aprova o regulamento técnico para a prestação do serviço de radiodifusão de sons e imagens e do serviço de retransmissão de televisão. In: ANATEL. Resolução no 284, de 7 de dezembro de 2001. 2001. Available in: <http http://www.anatel.gov.br/legislacao/resolucoes/2001/270-resolucao-284>. Acessed on July 17, 2019.

[13] PROELETRONIC. Available in: <http:// https://proeletronic.com.br/ >. Acessed on July 07, 2019.

[14] AQUARIUM. Available in: <http:// www.aquario.com.br/produto/dtv-150/>. Acessed on July 23, 2019.

[15] EDX. EDX Signal. 2007. Available in: <http://edx.com/products/ edx-signalpro/>. Acessed on July 20, 2019.

[16] CRC. CRC - COVLAB software. 2010. Available in: <http:// https://crc-covlab.software.informer.com/2.2/ >. Acessed on July 20, 2019

Deisi Luiza Wosch Passarelli. She has more than 18 years of experience in the broadcasting industry: trainee, technical designer, coordinator of Telecommunication Projects. Institutional representative in government agencies, 10 years in representation and intermediation activities in the Ministry of Communications and National Telecommunications Agency. Ability in broadcasting projects in general, Telecommunications Projects Coordinator for more than 15 years, Master's Degree in Telecommunications by the Federal University of Technology- Paraná (UTFPR) (2015), UTFPR Telecommunication Systems Technologist (2013), Bachelor in Business Administration by Foundation for Social Studies of Paraná FESP (2005) and Technician in electronics by UTFPR (2001).

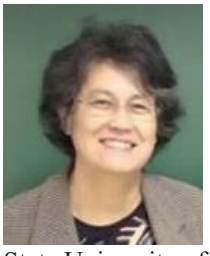

Keiko Verônica Ono Fonseca. Full professor at the Federal University of Technology - Paraná (UTFPR). Postdoctoral studies at TU Dresden (Faculty of Informatics, 2013), PhD in Electrical Engineering from the Federal University of Santa Catarina (1997), MSc in Electrical Engineering from the State University of Campinas (1988); graduated in Electrical Engineering from the Federal University of Paraná (1985). IEEE Member (ComSoc), Brazilian Computer Society (SBC) member, and IEICE (Japan) member. EU-BR H2020 SecureCloud project leader at UTFPR. Smart Cities project leader at UTFPR (Sweden-Curitiba project funded by Vinnova). Her research focus are real-time communication systems, data security and privacy, image processing. She acts as a volunteer for the development of the Badminton sport in Brazil.

Alexandre de Almeida Prado Pohl. He is graduated in Physics from the Universidade Estadual de Campinas (1982), where he also obtained the master's degree (Physics, 1987). He received his doctorate from the Technical University of Braunschweig, Germany, in Electrical Engineering (1994) and his postdoctoral degree from the University of Sydney, Australia (2007). He is currently a professor at the Federal University of Tecnhology - Paraná, where he teaches disciplines related to the areas of photonics and telecommunications and leads a research group focusing on telecommunications and optical communications. He has worked in technological development with companies, research institutes and universities, whose collaboration has resulted in the development of software, innovative prototypes and various articles refereed in periodicals and annals of national and international conferences. He is a member of the Brazilian Society of Microwaves and Optoelectronics (SBMO), a senior member of the Brazilian Telecommunications Society (SBrT), where he served as Vice President of Finance between 2012 and 2015, member of the Brazilian Society of Optics and Photonics (SBFoton) and senior member of The Optical Society (OSA). He was a member of the University Council (2010-2013), the Research and Postgraduate Council of UTFPR (2014-2017) and Director of Research and Postgraduate Course of the Curitiba University of UTFPR between 2014 and 2017. He holds a Development Productivity Technological and Innovative Extension Scholarship, level 1D, from CNPq.

Received in 2019-07-26 | Approved in 2019-11-25

http://www.set.org.br/ijbe/ doi: 10.18580/setijbe.2019.7 Web Link: http://dx.doi.org/10.18580/setijbe.2019.7

Comparison of Propagation Models Using Propagation Features

Alberto Leonardo Penteado Botelho

CITE THIS ARTICLE

Botelho, Alberto Leonardo Penteado; 2019. Comparison kb Onkl]c]pkj - k`alo 5oejc Propagation Featureo. SET INTERNATIONAL JOURNAL OF BROADCAST ENGINEERING. ISSN Print: 2446-9246 ISSN Online: 2446-9432. doi: 10.18580/setijbe.2019.8. Web Link: http://dx.doi.org/10.18580/setijbe.2019.8

Comparison of Propagation Models Using Propagation Features

Alberto Leonardo Penteado Botelho

***Abstract* — The propagation model is a critical point for predicting the coverage area. The complexity of the coverage prediction is enhanced by the possibility of SFN (Single Frequency Network) operation, which allows the installation of auxiliary relays in shadow areas. By knowing the techniques used by each propagation model, it was possible to use the literature as a reference to categorize the types of paths by the propagation situation. This paper presents a comparison study of the simulated propagation models in the Progira software with field measurements in a massive SFN of RecordTV Rio, in the city of Rio de Janeiro. The comparison considered the error mean in all the paths and each of types of paths, so it was possible to obtain an overview of which propagation model is best suited for each propagation situation. It presents details of the techniques used in propagation models, a brief review of the main propagation models and the mean of errors for each type of paths. The results presented contribute to a better interpretation of which propagation model or the propagation model technique can be more efficient in a micro-region, which can optimize the planning of an auxiliary transmission.**

***Index Terms* — Terrestrial Digital Television, Propagation Model, Single Frequency Network, Reflection, Refraction, Diffraction.**

I. Introduction

The SBTVD (Brazilian Digital Television System) is a digital terrestrial television standard adopted in Brazil, developed from the evolution of the Japanese standard ISDB-T (Integrated Services Digital Broadcasting Terrestrial) standard. The terrestrial television stations are composed of a network retransmitting stations that aim to expand the coverage area of the main generation station [1]. A trustworthy prediction coverage allows the planning of the transmission system so that the irradiations can maintain the desired levels.

SBTVD has an important frequency reuse feature, which is the operation in SFN (Single Frequency Network), as it allows a television generating station to operate with its transmitting stations on the same frequency [2].

SFN adds a greater complexity in the prediction of coverage, considering that the legislation allows the installation of auxiliary retransmitting stations in shadow areas without the need of acquisition of new conferment, as long as it does not increase the area of provision of the service, maximizing the necessity for a prediction of reliable coverage in micro-regions [3].

An important challenge of the coverage prediction is the choice of the best propagation model that best suits the conditions of propagation of the studied locality.

A comparison between models of propagation of a massive SFN in the locality of Rio de Janeiro, concluded that the propagation model ITUR P.1812-3 in the dense urban geographic region option, presented smaller average error when comparing with field measurements [4].

SBTVD allows the installation of auxiliary stations to cover small areas without coverage. These shadow areas may have a distinct propagation characteristic, where the lowest mean error propagation model may or may not predict the field strength with the highest fidelity. A propagation model with the smallest mean error in the specific micro region propagation characteristics can optimize signal intensity prediction with maximum fidelity.

This work intends to categorize the types of paths according to the propagation features. Each propagation model uses a distinct technique, but many techniques use the same concepts.

knowing the techniques used by propagation models, it is possible to categorize the paths, using the literature as a reference to distinguish propagation situations.

By categorizing the paths, it is possible to compile mean errors for each type of paths and provide the broadcaster with greater security by proposing a specific propagation model to study a micro-region.

The Progira coverage area prediction software was used and made available by LM Telecom [5] and the field measurement in the metropolitan area of Rio de Janeiro was made available by RecordTV Rio (Record Television of Rio de Janeiro Ltda).

This article is divided into seven sections, in addition to this introductory section. In Section II, a brief description of the effects of radio propagation on terrestrial television transmissions is presented. In Section III, the techniques used by the most important propagation models in the literature are presented. Section IV presents a brief summary of the propagation models presented in this study. In Section V, the best techniques of comparison of propagation models are demonstrated. In Section VI, the results of the average error for each type of path are presented. Finally, in Section VII, the main conclusions and final considerations of the work are presented.

II. Radiopropagation

The video, audio and data generated in the television studio are encoded, modulated and sent by RF to the transmission system which amplifies the power and radiates the signal through the transmission antenna. The antenna radiation patterns describes antenna gain in each horizontal and vertical azimuth direction [6].

A. L. P. Botelho is with the LM Telecomunicações, São Paulo / SP (email: abotelho@lmtelecom.com.br)

http://www.set.org.br/ijbe/ doi: 10.18580/setijbe.2019.8 Web Link: http://dx.doi.org/10.18580/setijbe.2019.8

In transmission, the electromagnetic wave travels from the transmitting station to the receiver at the opposite end, where the path traveled by the Fresnel zone can vary from a line of sight to a line that is severely obstructed by buildings, mountains or vegetation [7].

In free space, the electromagnetic waves disperse in all the radial ones and their energy is dissipated by the environment [8].

When the electromagnetic wave focus on a surface interface separating two environments, one part of the wave is reflected to the first environment, a second part of the wave is refracted to the second environment and a third part bypasses the environment and diffracts. The resulting reflection, refraction and diffraction phenomena depend on the electromagnetic characteristics of the environment and angle of incidence [9].

The best method to maximize the coverage area is to adjust the installation of the equipment by field measurement, but the high costs and the time involved make it deterrent. With knowledge of the topographic and environmental characteristics, it is possible to use a mathematical tool to predict field strength throughout the service area [6]. When making trustworthy predictions of coverage, the necessity for field measurements to adjust the coverage area is reduced, optimizing time and cost [10].

The path is the representation of the topographic survey along the route between transmission and reception. Through the profile of the link, it is possible to get an overview of the obstacles, the points of reflection and the influence of the land [3].

The Propagation Model is the mathematical tool that describes how the signal is radiated during the path between the transmitter and the receiver, which is intended to predict signal power throughout the service area. Several propagation models are available in the literature, where each model presents specific algorithm [7].

III. Propagation Models Techniques

The propagation models available in the literature use different techniques, however, many of the different techniques present the same concepts [11].

Scattering of electromagnetic energy in free space is characterized by the absence of a body capable of influencing the propagation between transmission and reception and should be considered the dispersion of energy in the atmosphere [12].

Troposphere Refraction occurs because the refractive index of the atmosphere changes with depth, which causes the slope of the wave path downwards and its index depends on pressure, temperature and humidity of the atmosphere [12].

Figure 1 shows the geometry of free space propagation and refraction propagation, where IR_{EL} represents the free space irradiation and IR_{RFR} represents the refractive irradiation in the troposphere.

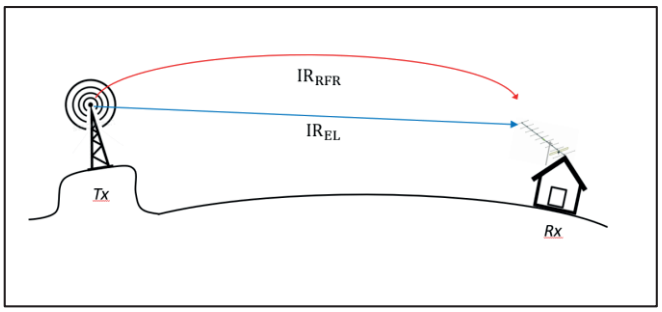

Figure 1: Geometry of propagation in free space and by refraction.

The refractive index in the atmosphere may vary in different climatic regions. Climatic correction curves can be applied [13].

Reflection occurs in line of sight, where the signal is transported by a direct line and by a line reflected in different phase. If the terrain is scratchy, there may be more than one reflection and its index depends on the electric characteristic of the terrain [13]. Figure 2 shows reflection propagation geometry, where IR_{EL} represents free space irradiation and IR_{RL1} and IR_{RL2} represent reflection irradiation.

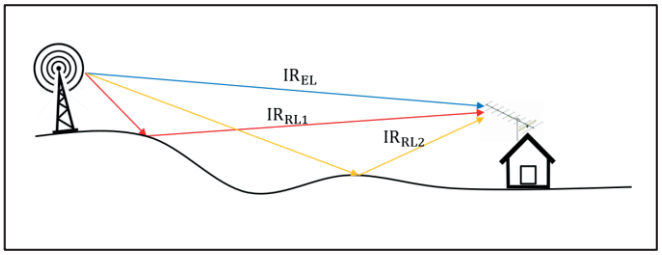

Figure 2: Geometry of propagation by reflection.

Diffraction in obstacle knife edge assumes that there is a knife-shaped obstacle. The diffraction index depends on the angle and the distances between the transmitter and the obstacle and between the obstacle and the receiver. In the existence of two or more obstacles, the equation must be systematically repeated [14]. Figure 3 shows the geometry of diffraction propagation in knife edge obstacle, where IR_{Dif1} represents the irradiance between the transmission and the Gf (ridge of the knife edge obstacle) and where IR_{Dif2} represents the irradiation between the Gf to the reception.

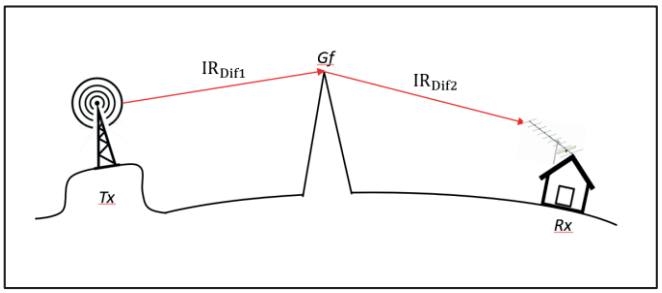

Figure 3: Geometry of propagation by diffraction in knife edge obstacle.

Diffraction in rounded obstacle assumes that the radius of curvature of the obstacle corresponds to the radius of curvature at the apex of a parabola adjusted to the profile of the obstacle in the vicinity of the top. The diffraction index depends on the angle and the distances between the transmitter and the tangent of the obstacle and between the tangent of the obstacle and the receiver [15]. Figure 4 shows

http://www.set.org.br/ijbe/ doi: 10.18580/setijbe.2019.8 Web Link: http://dx.doi.org/10.18580/setijbe.2019.8

the geometry of diffraction propagation in rounded obstacle, where IR_{Dif1} represents the irradiance between the transmission OAr (rounded obstacle tangency tip) and where IR_{Dif2} represents the irradiation between OAr and reception.

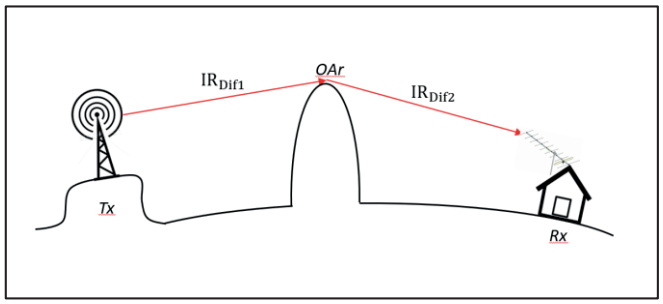

Figure 4: Geometry of propagation by diffraction in rounded obstacle.

Diffraction by the terrain assumes that the line of sight is obstructed by the terrain. The refractive index depends on the distance, the antenna height, the electromagnetic constant of the terrain, the frequency, the radius of the earth and the terrain characteristic that can be smooth, irregular rounded or knife-shaped [13]. Figure 5 shows the geometry of diffraction propagation by the ground, where IR_{DifT} represents the irradiance between the transmission to the reception by the terrain.

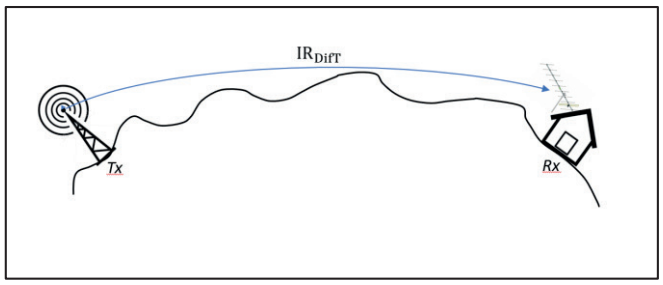

Figure 5: Geometry of propagation by diffraction of the terrain.

Delta Bullington Diffraction, considers a sequence of knife-edge obstacles and adds diffraction across the terrain with part of Bullington. The slopes are calculated in relation to the baseline uniting the height of the transmission to the reception and the line of sight. The diffraction index depends on the angle and the distances between the transmitter and the vertex and between the vertex and the receiver [16]. Figure 6 shows the geometry of the Delta Bullington propagation, where IR_{dB1} represents the irradiance between the transmission and v (vertex) and where IR_{dB2} represents the irradiance between v and receive.

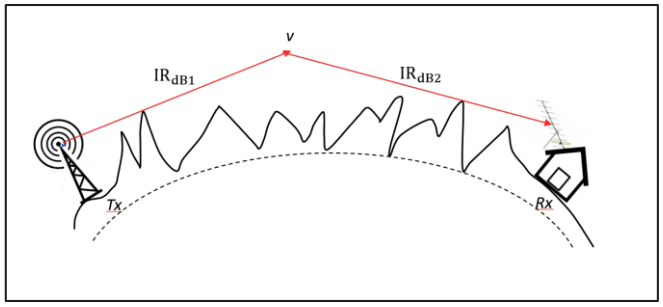

Figure 6: Geometry of propagation by Delta Bullington.

Propagation curves interpolate and extrapolate field strength curves derived empirically as a function of distance, antenna height, frequency, and percentage time. The height of the antenna relative to the ground simulates the effects of propagation [17]. Figure 7 shows propagation geometry by propagation curves, where IR_{El} represents the irradiance between transmission and reception, the NMT represents the average level of the terrain and the $HNMT$ represents the height of the antenna in relation to the average level of the terrain.

Models based on propagation curves can apply correction curve of variation of terrain heights between transmission and reception [18].

Loss in clutter uses map of buildings and vegetation. Each polygon of the clutter is characterized by parameters of height of buildings or trees, indication of their density, degree of absorption and clutter height that can be known or estimated. In the polygon, the effects of loss, reflection and diffraction are simulated [19]. Figure 8 shows the geometry of the propagation by losses in the clutter, where IR_{El} represents the irradiation between the transmission and reception, IR_{Clt} represents the irradiation in the clutter, IR_{Dif} represents the diffraction irradiation at the top of the clutter and IR_{Rl} represents reflection irradiation.

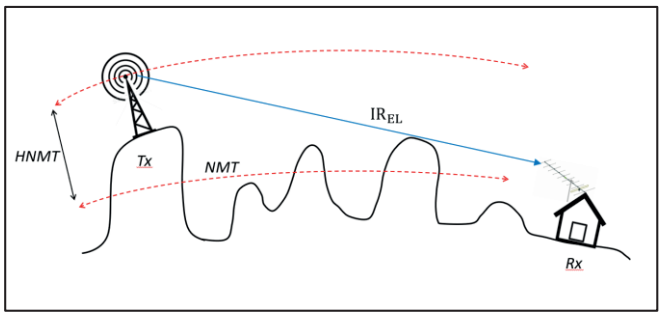

Figure 7: Geometry of propagation by propagation curves.

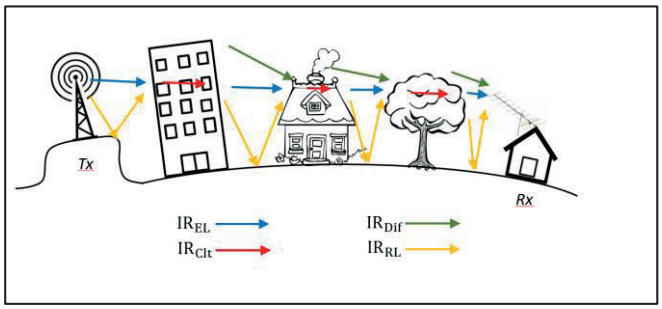

Figure 8: Geometry of propagation by clutter losses.

The clutter location variability refers to the height correction curve of the receiving antenna. The higher the receiving antenna is in relation to the clutter, the smaller the effects of the clutter [16].

IV. Propagation Models

Free space is a model that calculates the field strength, considers only the scattering of electromagnetic energy and neglects the effects of reflection, refraction and diffraction [9].

Longley-Rice is a propagation model based on calculations of losses in the path of the electromagnetic wave. In line of sight, the model considers refraction in the troposphere and reflection in smooth or irregular terrain. With obstructed line

of sight by a peaked formation, it considers diffraction in obstacle knife edge with or without reflection. With obstructed line of sight by convex formation, it considers diffraction in rounded obstacle with or without reflection. With an obstructed line of sight by a sequence of obstacles, it considers diffraction by the terrain. Longley-Rice also considers climate correction curves [13].

Okumura-Hata is a model of propagation curves developed by Okumura and synthesized in equation by Hata. It has propagation curves for different levels of urbanization [20].

Deygout-Assis is a propagation model based on calculations of losses in the path of the electromagnetic wave developed by Deygout. With line of sight, it considers calculation of scattering of electromagnetic energy. With a view obstructed by one or more peaked formations, it considers diffraction in knife edge obstacles [14]. Assis extended the Deygout model to a line of sight obstructed by convex obstacles and considered diffraction in a rounded obstacle [21].

ITUR P.370-7 is a model of propagation curves drawn from data obtained in the Mediterranean and North Sea regions for field strengths exceeded by 50% of locations for different percentages of time. It has correction curves of variation of terrain heights [18].

ITUR GE06 is a model of propagation curves for field strengths exceeded by 50% of locations for different percentages of time. It has propagation curves for different climatic regions [22].

ITUR P.526-11 is a propagation model based on calculations of losses in the path of the electromagnetic wave. With line of sight, it considers calculation of scattering of electromagnetic energy. With a line of sight obstructed by one or more convex formations, it considers diffraction in a rounded obstacle. With obstructed line of sight by a peaked formation, it considers diffraction in obstacle knife edge. With obstructed line of site by two peaked formations or obstruction in smooth terrain, it considers diffraction by the terrain. With a line of sight obstructed by a sequence of obstacles, it considers Delta Bullington [15].

ITUR P.1546-5 is a model of propagation curves for field strengths exceeded by 50% of locations for different percentages of time. It has correction curves for obstruction and curves for correction of wide differences between the transmission and reception antenna heights [17].

CRC-Predict is a model that calculates losses in the clutter. Each polygon results in losses by refraction, reflection and diffraction. It has curves of location variability of the receiving antenna in relation to the height of the clutter. For regions with clutter data with very small obstacles, consider the dispersion, refraction and climatic correction curves of the Longley-Rice propagation model and the localization variability of the Okumura-Hata propagation model [19].

ITUR P.1812-3 is a propagation model based on calculations of losses in the path of the electromagnetic wave and losses in the clutter. With line of sight it considers refraction in the troposphere. With obstructed line of sight by smooth formation, it considers diffraction by the terrain. With obstructed line of sight by irregular formation, it considers Delta Bullington. The calculations consider losses in the clutter. Each polygon results in losses by refraction, reflection and diffraction. It has curves of location variability of the receiving antenna in relation to the height of the clutter [16].

V. Propagation Models Comparison

The best method for comparing propagation models is to analyze the mean field measurement error with each of the available propagation models.

For the field measurement, RecordTV Rio was chosen in the metropolitan region of Rio de Janeiro. The metropolitan area of Rio de Janeiro has a very varied predominant terrain, with high cliffs, seas of hills, hills and valleys, representing the most complex situation of propagation and of great challenge for propagation models. The complexity of the propagation is enhanced by RecordTV Rio operating in massive SFN, in the most varied transmission situations, with Special Class main station, 2 Class A retransmitters stations and 11 auxiliary stations.

RecordTV Rio provided 41 field measurements for this work. 19 measurements from the main station transmission, 14 measurements from the retransmitter stations and 8 measurements from the auxiliary stations. The field measurement sites were distributed in the metropolitan region of Rio de Janeiro to represent the maximum diversity of propagation characteristics.

The field measurement used a measurement instrument with a resolution of 10 kHz and a measurement range of 130 dBμV. The antenna used has a gain of 14 dBi at the center frequency of 623 MHz, corresponding to the television channel 39, realized at 10 meters of height in relation to the ground and attenuation of cable and connectors of 2 dB.

The software used to predict the coverage area was Progira, [23]. Progira offers 10 propagation models. The propagation models have selectable options of climate, population density or terrain type, thus all models with all selectable options were considered, totaling 37 variations of propagation models.

There is no single criterion for deciding the best method for comparing propagation models, but the mean error should be as small as possible [24].

DMA (Absolute Mean Deviation) calculates the arithmetic mean of the absolute deviations of each measure, does not take into account whether it was overestimated or underestimated, and it is important to analyze which model of propagation that approximates the field measurement by simple mean, according to Equation 1.

σ (Standard Deviation) computes the square root of the ratio of the sum of the squares of the deviations and is important to analyze if the results obtained by the propagation models are scattered over a wide range of values, according to Equation 2.

RMS (Root Mean Square) is a statistical measure of the magnitude of a variable quantity of discrete values, where the mean error is low by canceling positive and negative errors when added and it is important to designate if the errors are addictive and tend to more or less, according to Equation 3 [25].

$$DMA = \frac{1}{N}\sum_{i=1}^{na}|VM - VP| \quad (1)$$

$$\sigma = \sqrt{\frac{1}{N-1}\sum_{i=1}^{na}(VM - VP)^2 - N \times \frac{1}{N}\sum_{i=1}^{na}(VM - VP)^2} \quad (2)$$

http://www.set.org.br/ijbe/ doi: 10.18580/setijbe.2019.8 Web Link: http://dx.doi.org/10.18580/setijbe.2019.8

$$RMS = \sqrt{\frac{1}{N}\sum_{i=1}^{na}(VM - VP)^2 + \sigma^2} \quad (3)$$

Where:
DMA = Absolute Mean Deviation;
σ = Standard Deviation;
N = Number of samples;
na = sample;
RMS = Root Mean Square;
VM = Measured value in field;
VP = Measured value in software.

VI. Results

When comparing the values measured in the field with the simulated values in the software, it was possible to calculate DMA, σ and RMS of each propagation model, according to Table I.

When analyzing each model in isolation, Table I concludes that the ITUR 1812-3 propagation model, in the dense urban geographic region option, presents the smallest mean error and is the most reliable to be used in the Rio de Janeiro study. In analyzing the techniques of propagation models, Table I concludes that the models that employ losses in the clutter, present better efficiency.

Table I - Average error of all paths compared to field measurement.

Average (dB)				
Propagation Model	Selectable Option	DMA	σ	RMS
ITUR 1812-3	Dense Urban	6,9	1,4	7,2
ITUR 526-13	General Method	7,6	1,5	7,9
ITUR 1812-3	Forest / Urban	8,1	1,6	8,5
CRC-Predict	Continntal / Great Lakes / Maritime Overland / Maritime Oversea	8,9	2,4	9,4
ITUR 1812-3	Suburban	9,1	1,7	9,5
ITUR1 812-3	Database	9,1	1,7	9,5
Deygout-Assis	Knife Edge	9,6	2,2	10,1
ITUR G06	Rural / Open / Suburban	9,6	2,2	10,1
Okumura - Hata	Quasi Open	10,3	2,1	10,8
ITUR 370-7	Rural	10,5	1,9	10,9
ITUR 370-7	Suburban / Urban	10,5	1,9	11,0
Deygout-Assis	Main Rounded	10,5	3,0	11,2
Okumura - Hata	Open	10,9	2,3	11,5
ITUR 1546-5	Rural / Open	11,0	2,8	11,6
ITUR 1546-5	Suburban	11,1	2,9	11,7
Longley-Rice	Equatorial	11,8	2,4	12,3
Longley-Rice	Maritime Temperate Oversea	11,8	2,4	12,3
Longley-Rice	Desert	11,8	2,4	12,3
Longley-Rice	Maritime Temperate Overland	11,8	2,4	12,3
Longley-Rice	Continental Subtropical	11,8	2,4	12,3
Longley-Rice	Maritime Tropical	11,9	2,4	12,4
Deygout-Assis	Rounded	12,3	4,0	13,3
Longley-Rice	Continental Temperate	12,6	2,7	13,1
ITUR 526-13	Rounded	12,9	3,4	13,6
Free Space	---	15,9	3,2	16,6
Okumura - Hata	Suburban	15,9	2,8	16,6
ITUR G06	Urban	16,6	3,2	17,3
ITUR 1546-5	Urban	18,8	3,9	19,7
ITUR G06	Dense Urban	21,5	3,9	22,4
ITUR 1546-5	Dense Urban	22,3	4,2	23,2
Okumura - Hata	Urban	22,7	3,9	23,6

When analyzing the terrain and environmental characteristics of each path, there is a heterogeneous distribution of propagation conditions. When comparing the terrain geometry of each path with the techniques described in Section III, it is possible to categorize the path by the propagation characteristic.

21 paths have a line of sight with very high transmission heights in relation to the terrain, in which the HNMT exceeds 400 meters. Under these conditions, the Fresnel zone travels a high distance from the ground and clutter, reducing the effects of propagation on the terrain. 6 paths have a line of sight with low transmission heights in relation to the terrain, in which the HNMT is lower than 150 meters. Under these conditions, the Fresnel zone travels very close to the ground and clutter, increasing the effects of propagation on the terrain.

9 paths are obstructed by a knife-shaped elevation. Under these conditions, propagation diffraction predominates in the knife edge obstacle.

3 paths are obstructed by two or more knife-edged elevations. Under these conditions, diffraction propagation predominates in knife edge obstacles, which can be calculated by systematically repeating a knife edge algorithm or Delta Bullington algorithm.

2 paths are totally obstructed in all their extension. Under these conditions, predominates propagation by diffraction of the terrain.

Table II compares the values measured in the field with the simulated values by software, only in the line of sight paths, with HNMT above 400 meters.

Table II - Medium error of line of sight and HNMT links above 400 meters compared to field measurement.

Average (dB)				
Propagation Model	Selectable Option	DMA	σ	RMS
ITUR 1546-5	Rural / Open	3,6	0,8	3,8
ITUR 1546-5	Suburban	3,6	0,8	3,8
ITUR G06	Rural / Open / Suburban	4,0	0,9	4,3
ITUR 1812-3	Clutter Dense Urban	5,3	1,5	5,8
Okumura -Hata	Open	5,8	1,4	6,3
ITUR 1812-3	Forest / Urban	6,2	1,8	6,8
Okumura - Hata	Quasi Open	6,8	1,9	7,4
CRC-Predict	Continntal / Great Lakes / Maritime Overland / Maritime Oversea	6,9	1,8	7,5
Deygout-Assis	Rounded	7,0	2,0	7,6
Deygout-Assis	Knife Edge	7,0	2,0	7,6
ITUR 526-13	General Method	7,4	2,1	8,1
ITUR1 812-3	Clutter Database	7,7	2,1	8,4
ITUR 1812-3	Clutter Suburban	7,8	2,1	8,4

http://www.set.org.br/ijbe/ doi: 10.18580/setijbe.2019.8 Web Link: http://dx.doi.org/10.18580/setijbe.2019.8

Longley-Rice	Equatorial	7,9	2,1	8,6
Longley-Rice	Maritime Temperate Oversea	8,0	2,1	8,6
Longley-Rice	Maritime Temperate Overland	8,0	2,1	8,6
Longley-Rice	Maritime Tropical	8,0	2,1	8,6
Longley-Rice	Continental Temperate	8,0	2,1	8,6
Longley-Rice	Continental Subtropical	8,0	2,1	8,6
Longley-Rice	Desert	8,0	2,1	8,6
ITUR 526-13	Rounded	8,1	2,2	8,8
ITUR 370-7	Rural	8,1	2,1	8,8
ITUR 370-7	Suburban / Urban	8,1	2,1	8,8
Free Space	---	8,2	2,2	8,8
ITUR G06	Urban	15,1	3,5	16,2
ITUR 1546-5	Urban	15,1	3,5	16,3
Okumura-Hata	Suburban	18,3	4,4	19,7
ITUR G06	Dense Urban	20,7	4,8	22,2
ITUR 1546-5	Dense Urban	21,0	4,8	22,6
Okumura-Hata	Urban	27,0	6,3	29,0

When analyzing each model separately, Table II concludes that the ITUR 1546-3 propagation model, in the rural, open or suburban geographic region option, presents the smallest mean error and is the most reliable to be used in the study of Rio de Janeiro in situations with line of sight in very high HNMT. When analyzing the techniques of propagation models, Table II concludes that the models that use propagation curves, present better efficiency.

Table III compares the values measured in the field with the simulated values by software, only in the line of sight paths, with HNMT below 150 meters.

Table III - Medium error of line of sight and HNMT links below 150 meters compared to field measurement.

Average (dB)				
Propagation Model	Selectable Option	DMA	σ	RMS
CRC-Predict	Continntal / Great Lakes / Maritime Overland / Maritime Oversea	3,9	2,0	5,1
ITUR G06	Rural / Open / Suburban	4,3	2,4	5,7
ITUR 1812-3	Dense Urban	6,4	3,7	8,5
Okumura-Hata	Quasi Open	7,5	4,2	10,0
Okumura-Hata	Open	7,7	4,7	10,4
ITUR 370-7	Rural	9,1	5,0	11,9
ITUR 370-7	Suburban / Urban	9,1	33,9	80,2
Deygout-Assis	Knife Edge	9,6	5,0	12,6
Deygout-Assis	Main Rounded	9,6	5,0	12,6
Deygout-Assis	Rounded	9,6	5,0	12,6
ITUR 526-13	General Method	9,7	5,1	12,7
ITUR 526-13	Rounded	10,4	5,3	13,6
Free Space	---	11,1	5,5	14,4
ITUR 1812-3	Clutter Forest / Urban	11,6	7,0	15,5
Longley-Rice	Continental Subtropical	11,6	5,8	15,1
Longley-Rice	Desert	11,6	5,8	15,1
Longley-Rice	Equatorial	11,6	5,8	15,1
Longley-Rice	Maritime Temperate Overland	11,6	5,8	15,1
Longley-Rice	Maritime Temperate Oversea	11,6	5,8	15,1
Longley-Rice	Maritime Tropical	11,6	5,8	15,1
ITUR 1546-5	Rural / Open	11,8	10,9	17,9
ITUR 1546-5	Suburban	11,9	11,0	18,0
ITUR1 812-3	Clutter Database	13,2	7,2	17,3
ITUR 1812-3	Clutter Suburban	13,2	7,2	17,3
Okumura-Hata	Suburban	13,9	7,9	18,5
Longley-Rice	Continental Temperate	16,7	10,7	22,7
ITUR G06	Urban	17,9	8,9	23,3
ITUR 1546-5	Dense Urban	23,7	11,6	30,7
ITUR G06	Dense Urban	23,7	11,6	30,7
Okumura-Hata	Urban	23,9	12,3	31,2
ITUR 1546-5	Urban	28,6	17,0	38,3

When analyzing each model in isolation, Table III concludes that the CRC-Predict propagation model has the lowest mean error and is the most reliable to be used in the study of Rio de Janeiro in situations with line of sight in lowers HNMT. In analyzing the techniques of propagation models, Table III concludes that the models that use propagation curves and losses in the clutter, present better efficiency.

Table IV compares the values measured in the field with the simulated values by software, only in the links obstructed by a single knife edge obstacle.

Table IV - Medium error of the obstructed paths by a single knife edge obstacle, compared to field measurement.

Average (dB)				
Propagation Model	Selectable Option	DMA	σ	RMS
CRC-Predict	Continntal / Great Lakes / Maritime Overland / Maritime Oversea	4,1	2,1	5,1
ITUR 526-13	General Method	5,4	2,0	6,4
Deygout-Assis	Rounded	5,7	2,1	6,8
Deygout-Assis	Main Rounded	5,7	2,1	6,8
ITUR 1812-3	Forest / Urban	7,2	2,9	8,6
ITUR 1812-3	Suburban	7,4	2,8	8,8
ITUR 1546-5	Urban	7,4	3,3	8,9
ITUR G06	Urban	7,4	3,3	9,0
ITUR1 812-3	Database	7,5	2,9	8,9
ITUR 1812-3	Dense Urban	7,5	3,2	9,0
ITUR 526-13	Rounded	8,2	3,9	10,0
Deygout-Assis	Knife Edge	9,2	3,8	11,0
Longley-Rice	Desert	10,8	4,2	12,8
Longley-Rice	Continental Temperate	10,9	4,2	13,0
Longley-Rice	Continental Subtropical	11,0	4,3	13,1
Longley-Rice	Maritime Temperate Overland	11,0	4,3	13,1
Longley-Rice	Maritime Temperate Oversea	11,0	4,2	13,1
Longley-Rice	Equatorial	11,0	4,3	13,1
Longley-Rice	Maritime Tropical	11,3	4,3	13,5
ITUR 1546-5	Dense Urban	11,7	4,7	14,0
ITUR G06	Dense Urban	11,7	4,7	14,0
ITUR 370-7	Rural	12,0	4,9	14,4

http://www.set.org.br/ijbe/ doi: 10.18580/setijbe.2019.8 Web Link: http://dx.doi.org/10.18580/setijbe.2019.8

ITUR 370-7	Suburban / Urban	12,0	4,9	14,4
Okumura-Hata	Suburban	13,1	5,5	15,7
Okumura-Hata	Quasi Open	13,4	6,1	16,2
ITUR 1546-5	Rural / Open	13,4	5,6	16,1
ITUR 1546-5	Suburban	13,4	5,6	16,1
ITUR G06	Rural / Open / Suburban	13,8	5,8	16,6
Okumura-Hata	Open	16,4	7,3	19,8
Okumura-Hata	Urban	16,4	7,2	19,8
Free Space	---	24,0	9,4	28,6

In analyzing each model in isolation, Table IV concludes that the CRC-Predict propagation model presents the smallest mean error and is the most reliable to be used in the Rio de Janeiro study in situations obstructed by a single knife-edge obstacle. In analyzing the techniques of propagation models, Table IV concludes that the models that use calculations of losses in the path of the electromagnetic wave and losses in the clutter, present better efficiency.

Table V compares the values measured in the field with the simulated values by software, only on paths obstructed by a sequence of knife-edge obstacles.

Table V - Mean error of the paths obstructed by a sequence of knife-edge obstacles, compared to field measurement.

Average (dB)				
Propagation Model	Selectable Option	DMA	σ	RMS
Deygout-Assis	Knife Edge	3,3	2,5	5,5
ITUR 526-13	General Method	5,7	5,2	10,0
Deygout-Assis	Main Rounded	8,1	8,4	14,8
ITUR 1546-5	Dense Urban	10,9	10,9	19,6
ITUR G06	Dense Urban	10,9	11,0	19,7
ITUR 1812-3	Dense Urban	11,2	11,3	20,2
Okumura-Hata	Urban	11,5	11,5	20,8
ITUR 1812-3	Forest / Urban	12,4	11,9	22,0
ITUR 1812-3	Suburban	12,4	11,3	21,8
CRC-Predict	Continntal / Great Lakes / Maritime Overland / Maritime Oversea	12,5	13,3	23,0
ITUR1 812-3	Clutter Database	12,5	11,5	22,0
ITUR 1546-5	Urban	12,8	11,2	22,3
Deygout-Assis	Rounded	12,9	13,6	23,6
ITUR G06	Urban	12,9	11,2	22,3
Okumura-Hata	Suburban	14,6	15,4	26,8
Longley-Rice	Equatorial	18,1	16,1	31,6
Longley-Rice	Maritime Tropical	18,1	16,0	31,6
Longley-Rice	Maritime Temperate Oversea	18,2	16,1	31,7
Longley-Rice	Continental Subtropical	18,3	16,3	31,9
Longley-Rice	Desert	18,3	16,5	32,0
Longley-Rice	Maritime Temperate Overland	18,3	16,3	31,9
Longley-Rice	Continental Temperate	18,3	16,4	32,0
ITUR 526-13	Rounded	18,7	19,0	33,9
ITUR 370-7	Rural	18,9	17,1	33,0
ITUR 370-7	Suburban / Urban	18,9	17,1	33,0
ITUR 1546-5	Rural / Open	21,7	21,4	39,0
ITUR 1546-5	Suburban	21,7	21,4	39,0
ITUR G06	Rural / Open / Suburban	22,0	21,7	39,5
Okumura-Hata	Quasi Open	25,5	24,5	45,4
Okumura-Hata	Open	30,5	28,4	53,8
Free Space	---	39,9	35,9	69,8

When analyzing each model in isolation, Table V concludes that the Deygout-Assis propagation model, with obstacle type selected for knife edge, presents the smallest mean error and is the most reliable to be used in the Rio de Janeiro study in situations obstructed by a sequence of knife-edge obstacles. When analyzing the techniques of propagation models, Table IV concludes that the models that use calculations of losses in the path of the electromagnetic wave and Delta Bullington algorithms, present better efficiency, however, the Deygout-Assis propagation model obtained a great advantage.

Table VI compares the values measured in the field with the simulated values by software, only in the paths with total obstruction in the course of the electromagnetic wave.

Tabela VI - Average error of the paths with total obstruction in the course of the electromagnetic wave, compared to field measurement.

Average (dB)				
Propagation Model	Selectable Option	DMA	σ	RMS
Okumura-Hata	Suburban	2,8	3,3	6,5
Okumura-Hata	Urban	6,2	8,1	14,8
ITUR 1812-3	Suburban	14,0	19,1	33,9
ITUR 526-13	General Method	14,1	19,3	34,3
ITUR1 812-3	Database	14,4	19,7	34,9
ITUR 370-7	Rural	15,7	21,8	38,3
ITUR 370-7	Suburban / Urban	15,7	21,8	38,3
Okumura-Hata	Quasi Open	15,8	21,7	38,3
ITUR 1812-3	Forest / Urban	16,1	22,1	39,1
ITUR 1812-3	Dense Urban	18,1	25,0	44,0
Okumura-Hata	Open	20,8	28,7	50,6
ITUR G06	Rural / Open / Suburban	39,6	55,4	96,6
Free Space	---	41,4	57,9	101,0
Longley-Rice	Maritime Tropical	46,5	65,1	113,6
Longley-Rice	Equatorial	46,7	65,4	114,1
Longley-Rice	Maritime Temperate Oversea	46,8	65,5	114,3
Longley-Rice	Continental Subtropical	47,2	66,1	115,3
Longley-Rice	Maritime Temperate Overland	47,2	66,1	115,3
Longley-Rice	Continental Temperate	47,4	66,4	115,8
Longley-Rice	Desert	47,7	66,8	116,5
Deygout-Assis	Knife Edge	47,9	67,8	117,4
ITUR 1546-5	Rural / Open	52,1	73,0	127,2
ITUR 1546-5	Suburban	53,3	74,7	130,1
ITUR G06	Urban	57,2	80,2	139,7
CRC-Predict	Continntal / Great Lakes / Maritime Overland / Maritime Oversea	58,5	82,0	142,8
ITUR G06	Dense Urban	62,6	87,9	152,9

http://www.set.org.br/ijbe/ doi: 10.18580/setijbe.2019.8 Web Link: http://dx.doi.org/10.18580/setijbe.2019.8

ITUR 1546-5	**Urban**	**70,9**	**99,6**	**173,2**
Deygout-Assis	**Main Rounded**	**75,6**	**106,3**	**184,8**
ITUR 1546-5	**Dense Urban**	**76,3**	**107,2**	**186,5**
ITUR 526-13	**Rounded**	**82,8**	**116,4**	**202,4**
Deygout-Assis	**Rounded**	**105,0**	**149,2**	**257,7**

In analyzing each model in isolation, Table VI concludes that the Okumura-Hata propagation model, in the suburban geographic region option, presents the lowest average error and is the most reliable to be used in the Rio de Janeiro study in situations of total obstruction in the path of the electromagnetic wave. The high errors of the other models of propagation, make it difficult to interpret which model of propagation technique is most efficient in situation of total obstruction.

VII. Conclusion

When comparing field measurements with a prediction of coverage of a massive SFN in the city of Rio de Janeiro, it is concluded that the ITUR P.1812-3 propagation model in the dense urban geographic region option presents the smallest average error and is what more adequate to the characteristics of the Rio de Janeiro terrain. It is also concluded that the models that employ losses in the clutter, present better efficiency.

The SFN added a greater complexity in coverage prediction. The possibility of installing auxiliary retransmitter stations in shaded areas, maximizes the need for prediction of reliable coverage in micro-regions.

For line of sight paths with very high HNMT, the propagation model ITUR 1546-3, in the in the rural, open or suburban geographic region option, presents the smallest average error and the techniques that use propagation curves, present better efficiency in line of sight with very high HNMT.

For line of sight paths with low HNMT, the CRC-Predict propagation model has the smallest average error, and the techniques that employ propagation curves and losses in the clutter have the best efficiency in line of sight with low HNMT.

For links obstructed by a single knife-edge obstacle, the CRC-Predict propagation model presents the smallest average error and the techniques that employ calculations of losses in the path of the electromagnetic wave and losses in the clutter, present better efficiency in a single knife edge obstruction.

For links obstructed by a sequence of knife-edge obstacles, the Deygout-Assis propagation model, with obstacle type selected for knife-edge, presents the smallest mean error. Even though models that use calculations of losses in the path of the electromagnetic wave and Delta Bullington algorithms have presented better efficiency, Deygout-Assis, with type of obstacle selected for knife-edge presented wide advantage of other models in a sequence of knife edge obstructions.

For paths in situations of total obstruction in the course of the electromagnetic wave, the Okumura-Hata propagation model, with suburban geographic region option, presents the smallest average error. The high errors of the other models of propagation, make it difficult to interpret the efficiency of which model of propagation in situation of total obstruction.

The results presented contribute to a better interpretation of which propagation model or propagation model technique may be more efficient in a micro region. This contribution can optimize the planning of an auxiliary station.

References

[1] ARTHUR, R.; IANO, Y; CARVALHO, S.R.M.; LARICO, R.F., Planificación de la expansión del servicio de retransmisión de TV digital en Brasil usando redes SFN, IEEE Latin America Transactions, vol. 5, nº 8, 2007.

[2] ARIB STD-B31, Version 1.6, translated to english, 2005. Online. Available in: http://www.arib.or.jp/english/index.html, access in 28 april 2019.

[3] MINISTÉRIO DAS COMUNICAÇÕES: Portaria nº 925, de 22 de Agosto de 2014, published in D.O.U, 27 august 2014.

[4] BOTELHO, A. L. P.; AKAMINE, C.: Optimization of the propagation model choice by measuring field and artificial intelligence. SET INTERNATIONAL JOURNAL OF BROADCAST ENGINEERING, 2018.

[5] LM TELECOM. 2018. Online. Available in: http://www.lmtelecom.com.br/, access in 28 may 2019.

[6] DONZELLI, V. Polarização Elíptica: Influência no Desempenho de Cobertura da TV Digital; 2011. 83 f. Dissertação (Mestrado em Engenharia Elétrica) - Universidade Presbiteriana Mackenzie, São Paulo, 2011.

[7] BARSOCCHI, P.; Channel Models for Terrestrial Wireless Communications: a Survey, ISTI Institute, 2006.

[8] FÉLIX, M: Visualization Tools for Cellular Planning: Instituto Superior Técnico, Lisboa, Portugal, 2014.

[9] RIBEIRO, J. A. J.: Propagação das Ondas Eletromagnéticas, Princípios e Aplicações, Editora Érica, Primeira Edição, 2004.

[10] MARTINS R. A.: Modelagem e medições de onda de radio para predição de perda de propagação em ambientes urbanos: Tese (Doutorado em Engenharia Elétrica) - Universidade Federal do Rio Grande do Norte, Natal, 2006.

[11] BOTELHO, A. L. P.: Otimização da Escolha de Modelo de Propagação por Medição de Campo e Inteligência Artificial: Tese (Mestrado em Engenharia Elétrica e Computação) - Universidade Presbiteriana Mackenzie, São Paulo, 2019.

[12] RIBEIRO, J. A. J.: Propagação das Ondas Eletromagnéticas, Princípios e Aplicações, Editora Érica, Primeira Edição, 2004.

[13] RICE, P. L.; LONGLEY, A. G.; NORTON, K. A.; BARSIS, A. P.: Transmission Loss for Tropospheric Communications Circuits, U.S. Department of Commerce, National Bureal of Standards, Vol. 1, 1965

[14] DEYGOUT, J.: Multiple Knife-Edge Diffraction of Microwaves: IEEE Transictions on Antennas and Propagation, Volume 14, n 4, 1966.

[15] ITUR P.526-11: Propagation by diffraction, 2013.

[16] ITU-R P.1812-3: A path-specific propagation prediction method for point-to-area terrestrial services in the VHF and UHF bands, 2013.

[17] ITU-R P.1546-5: Recommendation ITU-R P.1546-5, Method for point-to-area predictions for terrestrial services in the frequency range 30 MHz to 3 000 MHz, 2013.

[18] ITUR P.370-7: VHF and UHF Propagation Curves for the Frequency Range from 30 MHz to 1 000 MHz, 1995.

[19] WHITTEKER, J. H.: Physical Optics and Field-Strength Predictions for Wireless Systems: IEEE Journal on Selected Areas in Communications, Vol. 20, number 3, 2002.

[20] HATA, M: Empirical Formula for Propagation Loss in Land Mobile Radio Services: IEEE Transactions on Vehicular Technology, Volume 29, n 3, 1980.

[21] ASSIS, M. S.: A Simplified Solution to the Problem of Multiple Diffraction over Rounded Obstacles: IEEE Transactions on Antennas and Propagation, 1971.

[22] ITUR GE06, 2006: Final Acts of the Regional Radiocommunication Conference for planning of the digital terrestrial broadcasting service in parts of Regions 1 and 3, in the frequency bands 174-230 MHz and 470-862 MHz (RRC-06), 2006.

[23] PROGIRA, SOME OF OUR CLIENTS. 2018. Online. Available in: www.progira.com/aboutus/some-of-our-clients/, access in 28 may 2019.

[24] LUIZ A.V. P.; ASSIS M. S.: A Hybrid Prediction Model for Propagation Over Irregular Terrain in the VHF and UHF Bands, IEEE Latin America Transactions, VOL. 13, NO. 9, 2015.

[25] SILVA, F. S.; MATOS, L. J.; PERES, F. A. C.; SIQUEIRA, G. L.: Coverage prediction models fitted to the signal measurements of digital TV in Brazilian cities, 2013 SBMO/IEEE MTT-S International Microwave & Optoelectronics Conference (IMOC), 2013.

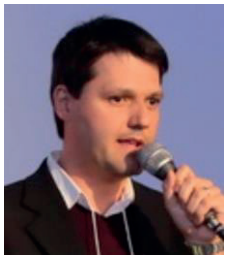

Alberto Leonardo Penteado Botelho was born in São Paulo / SP, in 1979. He received the Master of Science degree in electrical engineering from Universidade Presbiteriana Mackenzie, degree in Electrical Engineering Telecommunications mode by the Universidade Paulista (UNIP), specializations in Engineering of Digital Television Systems by the Instituto Nacional de Telecomunicações (INATEL), Telecommunications Networks Engineering by the National Instituto Nacional de Telecomunicações (INATEL) and MBA in Management of Projects by Fundação Getúlio Vargas (FGV).
He has worked as a broadcast network project engineer since 2002, with project specifications, performance standards and regulation of broadcasting stations. Currently works at LM Telecomunicações (RecordTV group) and studies PHD in electrical engineering from Universidade Presbiteriana Mackenzie.

Received in 2019-05-28 | Approved in 2019-11-25

http://www.set.org.br/ijbe/ doi: 10.18580/setijbe.2019.8 Web Link: http://dx.doi.org/10.18580/setijbe.2019.8

Design of Ultra-wideband Textile Antenna for TV Broadcasting

Euclides Lourenço Chuma
Yuzo Iano
Diego Pajuelo
Gabriel Gomes de Oliveira

CITE THIS ARTICLE

Chuma, Euclides Lourenço, Iano, Yuzo, Pajuelo, Diego, de Oliveira, Gabriel Gomes; 2019. Design of Ultra wideband Textile Antenna for TV Broadcasting. SET INTERNATIONAL JOURNAL OF BROADCAST ENGINEERING. ISSN Print: 2446-9246 ISSN Online: 2446-9432. doi: 10.18580/setijbe.2019.9. Web Link: http://dx.doi.org/10.18580/setijbe.2019.9

Design of Ultra-wideband Textile Antenna for TV Broadcasting

Euclides Lourenço Chuma, Yuzo Iano, Diego Pajuelo, Gabriel Gomes de Oliveira

***Abstract*—Digital television (DTV) has been adopted in many places throughout the world, and it is received in different device types, such as laptops, portable media players, and smartphones. However, the current antennas used in these devices to receive DTV channels have drawbacks, such as low performance and non-practical physical structure in many situations.**

This paper presents a flexible, lightweight, and thin textile antenna for DTV, operating at an ultra-wideband (UWB) of 200 MHz–800 MHz and capable of being embedded in a garment or bag, making it easily transportable when folded. The antenna operation was simulated and measured to verify its performance, and based on the measurement results, the proposed flexible textile antenna was confirmed to have good performance, even in real conditions.

***Index Terms*— antenna, microstrip, TV, textile**

I. Introduction

ANTENNAS are essential parts of television broadcasting systems. Integrating them into portable receivers is very challenging, mainly because of their dimensions and rigid structure. Therefore, a new generation of flexible and lightweight antennas integrated into garments or bags should be developed [1, 2].

This article proposes a flexible, lightweight, and thin textile antenna applied to broadcasting receivers and operating at an ultra-wideband (UWB) of 200 MHz–800 MHz to be embedded into portable devices. The antennas can be easily transported when folded or integrated into the physical structure of a large-format television (i.e., back cover).

The proposed antenna could be used as part of smart clothing [2, 3, 4, 5, 6, 7, 8], which has received so much attention due to the high interest in wearable electronics connected in a large network with other devices through the Internet of Things (IoT) [9, 10, 11, 12].

This paragraph of the first footnote will contain the date on which you submitted your paper for review. It will also contain support information, including sponsor and financial support acknowledgment. For example, "This work was supported in part by the U.S. Department of Commerce under Grant BS123456".

E. L. Chuma, Department of Communications, School of Electrical and Computer Engineering, University of Campinas - UNICAMP, 13083-852, Campinas-SP, Brazil (e-mail: euclides.chuma@ieee.org).

Y. Iano, Department of Communications, School of Electrical and Computer Engineering, University of Campinas - UNICAMP, 13083-852, Campinas-SP, Brazil (e-mail: yuzo@decom.fee.unicamp.br).

D. Pajuelo, Department of Communications, School of Electrical and Computer Engineering, University of Campinas - UNICAMP, 13083-852, Campinas-SP, Brazil (e-mail: diego.pajuelo.castro@gmail.com)

G. Gomes de Oliveira, Department of Communications, School of Electrical and Computer Engineering, University of Campinas - UNICAMP, 13083-852, Campinas-SP, Brazil (e-mail: oliveiragomesgabriel@live.com)

II. Antenna Design

The proposed antenna uses a log-periodic structure, which is a member of structures known as frequency-independent antennas; these antennas have been studied for more than five decades [13, 14, 15, 16, 17] and are still relevant because of their ability to maintain quasi-frequency-independent characteristics over a wide band of frequencies [18, 19, 20].

The log-periodic antennas have a very large bandwidth, with a reasonable gain, making them an excellent candidate for UWB systems. Therefore, because of these features, log-periodic antennas have been used for low-cost applications and a great broadband coverage.

The antenna structure shown in Fig. 1 is a planar log-periodic antenna proposed by DuHamel [13]. In the antenna, R_1 = 331.1 mm, R_2 = 215.2 mm, = 0.65, = 0.81, = 45º, = 45º, and port gap width = 20 mm.

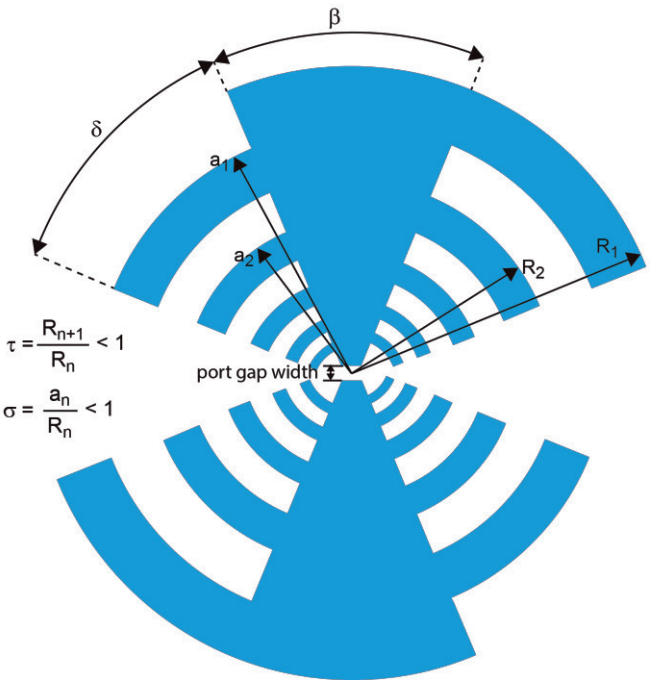

Fig. 1. Geometry structure of planar log-periodic antenna.

The substrate material is a polyester clothing with relative permittivity = 3.2 and thickness of 0.15 mm. The conductor material used in the patch is a conductive fabric composed of 50% polyester and 50% silver-plated woven, as can be seen in Fig. 2.

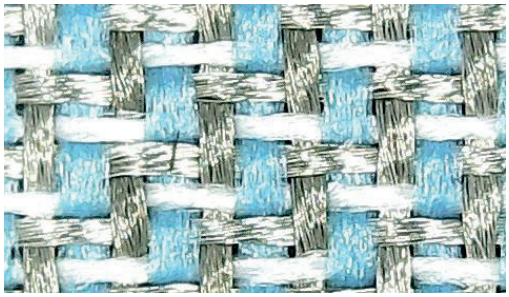

Fig. 2. Close-up image of the conductive textile used in the patch of the microstrip log-periodic antenna.

The structure of the conductive textile directly affects the surface resistivity. If the conductive paths in the woven are better aligned with the current direction, there will be less conductive loss [21, 22]. It is also important to mention that elongation and/or compression of the textile decreases the geometric precision of the antenna shape and changes the antenna features, such as the resonance frequency and directivity gain [23].

The initial dimensions of the microstrip log-periodic antenna were calculated. Then, simulations were performed using the full-wave simulator ANSYS HFSS to obtain the most optimized antenna dimensions for operations between 200 MHz and 800 MHz.

Figure 3 shows the model built in the simulator software and the simulated 3D radiation pattern. The simulation with a perfect electric conductor (PEC) presented an antenna gain of ~5.7 dB.

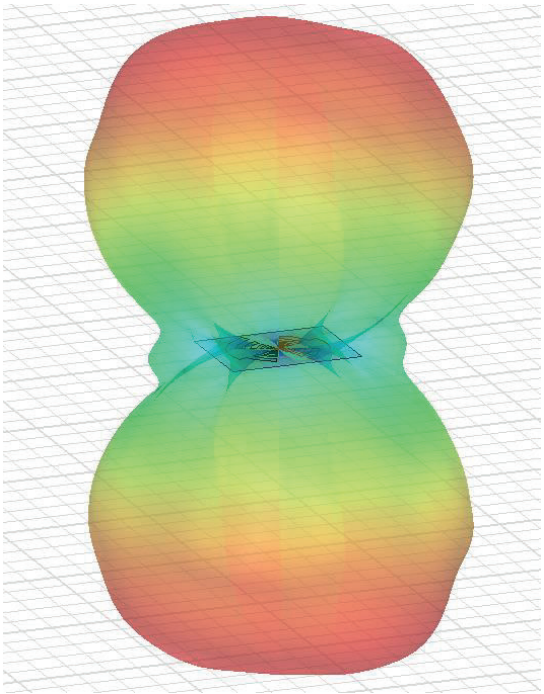

Fig. 3. Simulated 3D radiation pattern.

III. Measurements and Results

A prototype of the antenna was manufactured. The conductive textiles patches were cut and fixed into the polyester clothing substrate by sewing. Figure 4 shows the antenna prototype.

Fig. 4. Fabricated prototype of the antenna.

The performance of the antenna prototype was measured using a vector network analyzer (VNA) in order to obtain the S-parameters, as shown in Fig. 5.

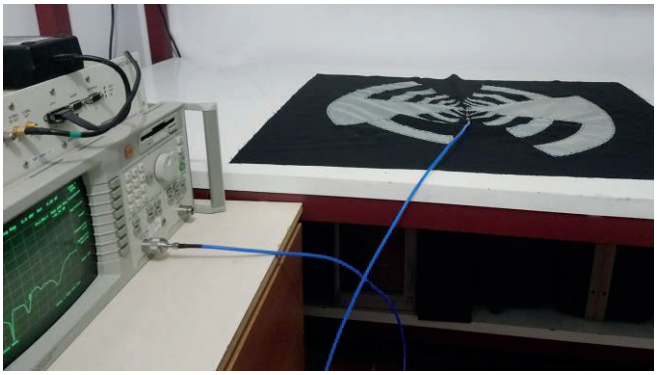

Fig. 5. Antenna measurement with VNA.

Figure 6 shows the antenna scattering parameters (S_{11}) according to the VNA measurement results and the electromagnetic simulation results.

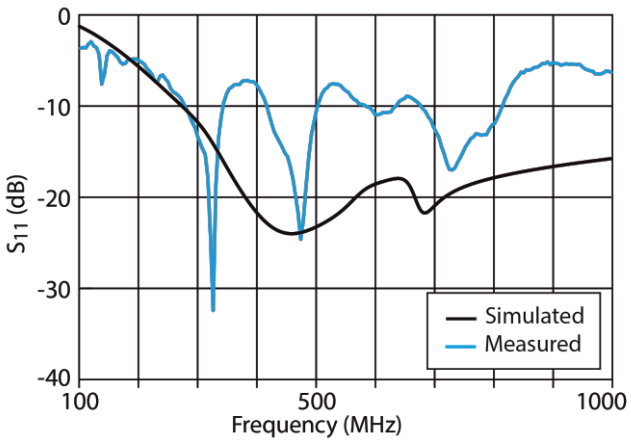

Fig. 6. Comparison of measured and simulated scattering parameters (S_{11}) of antenna.

http://www.set.org.br/ijbe/ doi: 10.18580/setijbe.2019.9 Web Link: http://dx.doi.org/10.18580/setijbe.2019.9

The measurements show an operating band for the antenna between 200 MHz and 800 MHz. Figure 7 shows the reception of channel television. A balun matching transformer is used for practical conditions.

Fig. 7. Proposed antenna working with television.

The proposed antenna can be carried by the user and folded so that it occupies very little space. Figure 8 shows the prototype of the folded antenna.

Fig. 7. Folded antenna.

IV. Conclusions

This work developed and tested a textile UWB microstrip log-periodic antenna to be able to operate over a frequency range of 200 MHZ–800 MHz. The proposed antenna is simple to manufacture and exhibits good flexibility. This paper presents a proven qualitative agreement between the experimental results and the numerical simulations. The differences are because PEC materials were used in the simulation models.

References

[1] S. Lemey, S. Agneessens, H. Rogier, “Wearable Smart Objects: Microwaves Propelling Smart Textiles: A Review of Holistic Designs for Wireless Textile Nodes”, IEEE Microwave Magazine, 2018, v.19, i.6, pp. 83-100

[2] P. J. Soh, B. V. D. Bergh, H. Xu, H. Aliakbarian, et al., “A Smart Wearable Textile Array System for Biomedical Telemetry Applications”, IEEE Transactions on Microwave Theory and Techniques, 2013, v.61, i.5, pp.2253-2261

[3] S. Seneviratne, Y. Hu, T. Nguyen, G. Lan, et al., A Survey of Wearable Devices and Challenges, IEEE Communications Surveys & Tutorials, 2017, v.19, i.4, pp. 2573-2620

[4] J. Foroughi, T. Mitew, P. Ogunbona, R. Raad, F. Safaei, “Smart Fabrics and Networked Clothing: Recent developments in CNT-based fibers and their continual refinement”, IEEE Consumer Electronics Magazine, 2016, v. 5, i. 4, pp. 105-111

[5] M. Chen, Y. Ma, Y. Li, D. Wu, Y. Zhang, C. Youn, “Wearable 2.0: Enabling Human-Cloud Integration in Next Generation Healthcare Systems”, IEEE Communications Magazine, 2017, v. 55, i. 1, pp. 54-61

[6] K. Nesenbergs, “Architecture of smart clothing for standardized wearable sensor systems”, IEEE Instrumentation & Measurement Magazine, 2016, v. 19, i. 5, pp. 36-64

[7] S. Cass, "Anouk Wipprecht: dynamic dresses merge high fashion and technology", IEEE Spectrum, 2016, v. 53, i. 2, pp. 19-20

[8] M. Suh, K. Carroll, N. Cassill, “Critical Review on Smart Clothing Product Development”, Journal of Textile and Apparel Technology and Management, 2010, v. 6, i. 4

[9] S. B. Baker, W. Xiang, I. Atkinson, “Internet of Things for Smart Healthcare: Technologies, Challenges, and Opportunities”, IEEE Access, 2017, v. 5, pp. 26521-26544

[10] M. S. Hossain, G. Muhammad, “Cloud-Assisted Industrial Internet of Things (IIoT)–Enabled Framework for Health Monitoring”, Computer Networks, 2016, v. 101, pp.192-202.

[11] M. Chen et al., “Smart Clothing: Connecting Human with Clouds and Big Data For Sustainable Health Monitoring”, Mobile Networks and Applications, 2016, pp. 1-21.

[12] T. Wu, F. Wu, J. Redouté, M.R. Yuce, “An Autonomous Wireless Body Area Network Implementation Towards IoT Connected Healthcare Applications” IEEE Access, 2017, v. 5, pp. 11413-11422

[13] R. H. DuHamel, D. E. Isbell, “Broadband logarithmically periodic antenna structures,” IRE National Convention Record, 1957, Pt. 1, 119-128

[14] D. E. Isbell, “Nonplanar logarithmically periodic antenna structures,” Tech. Rep. 30, Antenna Lab., University Illinois, Urbana, Illinois, U. S. A., 1958.

[15] R. H. DuHamel, F. R. Ore, “Logarithmically periodic antenna designs,” IRE National Convention Record, Pt. 1, 1958, 139-152

[16] D. E. Isbell, “Log-periodic dipole arrays,” IRE Trans. Antennas Propagat., 1960, v.8, 260-267

[17] R. L. Carrel, “Analysis and design of the log-periodic dipole antenna,” Tech. Rep. 52, Antenna Lab., University Illinois, Urbana, Illinois, U. S. A., 1961.

[18] X. Wei, J. Liu, Y. Long, “Printed Log-Periodic Monopole Array Antenna With a Simple Feeding Structure”, IEEE Antennas and Wireless Propagation Letters, 2018, v.17, i.1

[19] J. Ha, D. S. Filipovic, “Wideband and Efficient Slot Cavity Backing for Unidirectional Log-Periodic Antenna”, IEEE Antennas and Wireless Propagation Letters, 2018, v.17, i.2, pp.299-302

[20] K. Anim, Y. Jung, “Shortened Log-Periodic Dipole Antenna Using Printed Dual-Band Dipole Elements", IEEE Transactions on Antennas and Propagation, 2018, v.66, i. 12, pp.6762-6771

http://www.set.org.br/ijbe/ doi: 10.18580/setijbe.2019.9 Web Link: http://dx.doi.org/10.18580/setijbe.2019.9

[21] Y. Ouyang, W.J. Chappell, "High Frequency Properties of Electrotextiles for Wearable Antenna Applications", IEEE Transactions on Antennas and Propagation, 2008, v. 56, n. 2, pp. 381–389.
[22] I. Locher, M. Klemm, T. Kirstein, G. Tröster, "Design and Characterization of Purely Textile Patch Antennas", IEEE Transactions on Advanced Packaging, 2006, V. 29, n. 4, pp. 777-788.
[23] P. Salonen, Y. Rahmat-Samii, M. Schaffrath, M. Kivikoski, "Effect of textile materials on wearable antenna performance: a case study of GPS antennas", IEEE Antennas and Propagation Society International Symposium, 2004

Euclides Lourenço Chuma earned a degree in Mathematics from UNICAMP (2003), graduate degree in Network and Telecommunications Systems in the INATEL (2015), and MSc in Electrical Engineering at UNICAMP (2017). Currently is PhD Candidate in Electrical Engineering at UNICAMP, SP-Brazil. His research interests are Antennas, Microwave, Millimeter-Wave, Wireless Power Transfer, Software Defined Radio and Cognitive Radio.

Yuzo Iano is Professor in Electrical Engineering at Unicamp and the head and founder of the Laboratory of Visual Communications since 1972. He obtained his B.Sc (1972), M.Sc (1974) and PhD (1986) in Electrical Engineering at University of Campinas, SP-Brazil. Research Interests: Digital Signal Processing (images/audio/video), Digital TV, 4G (LTE) and 5G Cellular Networks, Pattern Recognition, Smart Cities, Smart Grid, Internet of Things.

Diego Pajuelo, Graduate in Electrical Engineering from the Peruvian University of Applied Sciences (UPC), Lima, Peru in 2012. He is currently working towards his Doctoral degree in Sciences and Telecommunications at Unicamp. His research interests are: HDR Video and audio coding, Image processing, Digital television and Satellite communications.

Gabriel Gomes de Oliveira, Graduated in Civil Engineering at UNIP University in 2018, studying for a Master's degree at UNICAMP, FEEC (Faculty of Electrical and Computer Engineering), DECOM (Communications Department), Laboratory of Visual Communication (LCV), currently researches and studies the area Smart City.

Received in 2019-07-07 | Approved in 2019-11-25

http://www.set.org.br/ijbe/ doi: 10.18580/setijbe.2019.9 Web Link: http://dx.doi.org/10.18580/setijbe.2019.9

Video Content Delivery Schemes: Approaches and Directions

Diego Pajuelo
Yuzo Iano
David Minango
Gabriel Gomes de Oliveira
Ana Carolina Borges
Reinaldo Padilha

CITE THIS ARTICLE

Pajuelo, Diego, Iano, Yuzo, Minango, David, de Oliveira, Gabriel Gomes, Borges, Ana Carolina, Padilha, Reinaldo; 2019. Video Content Delivery Schemes: Approaches and Directions. SET INTERNATIONAL JOURNAL OF BROADCAST ENGINEERING. ISSN Print: 2446-9246 ISSN Online: 2446-9432. doi: 10.18580/setijbe.2019.10. Web Link: http://dx.doi.org/10.18580/setijbe.2019.10

Video Content Delivery Schemes: Approaches and Directions

Diego Pajuelo, Yuzo Iano, *Member, IEEE,* David Minango, Gabriel Gomes de Oliveira, Ana Carolina Borges, Reinaldo Padilha

***Abstract*—This paper addresses the main two types of video delivery networks deployed into digital television services throughout the years. Underlying and Overlay networks are described in order to introduce how the physical infrastructure and network architecture impacted on the modeling of the latest video content delivery schemes. The convergence of different video delivery networks, in a technical sense, is a real thing and may disrupt the broadcasting industry in the long-term.**

***Index Terms*—Broadcasting, IPTV, OTT, video delivery network.**

I. Introduction

DURING the last decade, the explosion of access to video-content over the current networks by users all-over-the-world has been remarkable. As more people are experiencing better video-based services, called as *killer-applications*, daily Internet traffic has increased considerably from the ISP (Internet Service Provider) edge, in some cases more than doubled regarding the evolution of five years [1]. As a consequence, new video content delivery networks have been appeared, driven by the erosion of the heterogeneous networks and devices, for instance, adaptive video streaming scheme over wireless networks [2] or global overlay live streaming [3] proposals are crossing the same network domains, seeking to optimize the end-to-end video content delivery and reach the best QoE (Quality-of-Experience) of end-users.

On the other hand, one important factor to consider that really arouses this audiovisual content tsunami over the Internet is the great efficiency that the video encoder has achieved in recent years. It is known that a new technological evolution on video codecs is when compression ratio reaches 50% with respect to its predecessor codec. Benjamin Bross, who is with Germany's Fraunhofer Henrich Herts Institutes, states that: *"the more efficient we are in compressing video, the [easier] and more accessible it is for people to watch HD (High Definition) video at home and so more and more people watch HD video at home"*[4], the so-called 'Jevons Paradox'. This remarkable codec efficiency without precedent in the audiovisual world allows to offer better content and attract a new audience, hungry to see innovator productions of high artistic quality. Telecommunication engineers must be aware of these changes and global trends to be able to propose efficient end-to-end video content delivery schemes, either re-modeling the current layering architecture based on cross-layer design or deploying new physical network.

Video codec efficiency has undoubtedly been achieved in multimedia industry, but the video content is really the thing more meaningful by the users against the transmission technical details. Citing to Matthew Postgate, CTO of the BBC, says *"People interact with TV in search of content that contains interesting stories and engages them"*[5]. By many time, big players in television networks deployed means of communications based on different technologies, as were Cable TV (Television), Satellite TV (Sat-TV) and Over-the-Air TV (OTA), to deliver video content. Something in common was the type of delivery, broadcasting or point-to-multipoint transmission scheme. In recent years, with the emergence of the so-called *Over-the-Top* (OTT) services, delivery of point-to-point transmissions schemes for video content allowed to the arrival of productions with high quality in the mainstream media, paving the way to a revolutionary video streaming service. The notion on which it is supported is that it can reach a global relevance with relative less infrastructure using the Internet as its main technological partner. These services are become a new concept of watching television, it drastically changed the behavior of users and viewing experience, giving greater comfort and more interactivity. This phenomenon did impact the audiovisual industry, leading to the branded TV companies has come into this ecosystem, where the content is the king of the jungle. People are no longer move between channels, instead, people tend to change of content, which is in turn, in a technical sense, going to another physical infrastructure or network architecture.

The domains involved in this audiovisual ecosystem try to decipher the path to follow in a disruptive technological environment. This paper explores both technological and academic approaches, compiling the main video delivery networks deployed in the latest years, the schemes adopted to face with communication channel impairments; and by last, to analyze how those schemes drive the future networks and which are the directions that they are aiming at, where growing diversity of TV content is a consequence of this fast-changing digital era.

The remaining of this paper is organized as follows: Section II presents a technical overview of Video Delivery Networks. Section III discusses about the latest Video Content Delivery Schemes. Finally, Section IV reveals the final remarks and trends.

II. Video Delivery Networks

Since the releasing of Television as a community service, Video Delivery Networks were modeled about the notion of a *point-to-multipoint* transmission scheme over an underlay network, After that, new television services came to light that offered more variety of programs; Cable TV was the pioneer

http://www.set.org.br/ijbe/ doi: 10.18580/setijbe.2019.10 Web Link: http://dx.doi.org/10.18580/setijbe.2019.10

service to distribute television channels over coax, afterwards Satellite TV was inserted in this industry thanks to the rapid development of satellite communications that allow to land up at the households. The *Over-The-Top* services came out in the last years and it seems to be a promissory technology. This whole environment configures the TV entertainment industry just as it is. In this section, two concepts will be discussed, Overlay and Underlay Networks, in order to highlight the importance of their main ideas and how can contribute to the modeling of video delivery networks.

A. Underlay Networks

The Underlay Network is physical infrastructure in telecommunications, concerning all physical elements and interfaces comprehended in a communication system, either simplex, half-duplex or full-duplex; whose main feature is the establishment of a dedicated communication channel between interested parties. In particular, the deployment of infrastructure was mandatory for broadcasters because there were no networks spread across an entire region or worldwide back in the 50s, for instance, the Internet originated in the late 1960s with a world footprint in the mid-90s. Television networks can be classified as: private and public networks. Cable TV and Satellite TV providers make use of walled-garden environments, but Over-the-Air TV uses the shared radio frequency spectrum under the concept of *'free-to-air'* transmission instead.

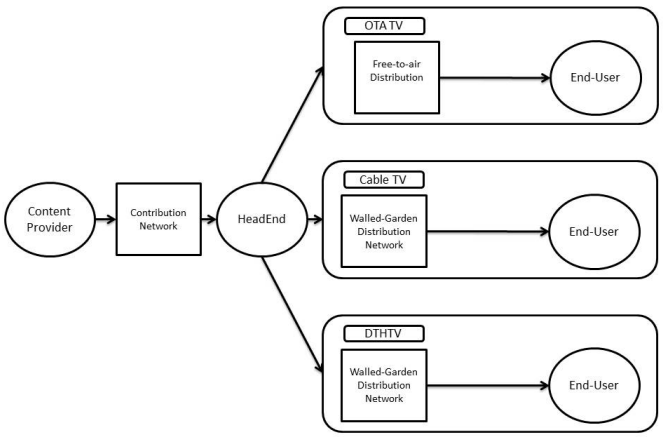

Fig. 1. Broadcast Architecture for TV

As shown in Figure 1, the Contribution Network and Headend are common for these three types of commercial television platforms. The Contribution Network is in charge of delivery video content from different content providers; producing live feeds, transmitting local video sources, gathering Video-On-Demand (VOD) Content or video content from the Internet; to Headend. In the Headend, all television signals are captured, processed and modulated in digital channels before distribution.

About the distribution network, technologies on Cable TV first delivered digital video signals were implemented using HFC (Hybrid-Fiber-Coax) technology and lately that one was surpassed by the FTTh (Fiber-To-The-home) technology. Moreover, Direct-To-Home Television (DTHTV) delivers digital video signals through a direct broadcast satellite provider. To be specific, Eutelsat, one of the word's leading satellite operators, *"reaches over 274 million homes across Europe, Middle East, and Africa at 20 key video neighborhoods"*[6]. The analog-digital transition implied to broadcasters, from a technical perspective, delivering more television channels with diversified programming for end-users over distribution networks, leveraging so, the infrastructure already built by themselves.

Free-to-air distribution or terrestrial broadcasting does not contemplate physical intermediary nodes or network equipment but sends television signals via line-of-sight radio propagation until the end-user. Its main technologies have taken the lead when it comes to innovations in digital processing techniques for communication as opposed to walled-garden distribution technologies because they had to face with time and frequency selective fading channels, whose modeling remains a challenge to this day. These technological advances focused on optimizing physical layer performance by means of supporting a wide range of transmission parameters in order to satisfy the optimal trade-off between robustness and throughput according to broadcasters decisions. In this respect, Table I details the different transmission parameters of the most advanced terrestrial broadcasting standards; ISDB-T/Tb [7], DVB-T2 [8] and ATSC3.0 [9]. It is a fact that OFDM (Orthogonal Frequency Division Multiplexing) modulation is the cornerstone for television waveform generation and is a general consensus. Figure 2 shows the signal processing diagram of the protection-at-the-bit-level stage and the constellation mapper module, which fulfills the function of improving spectral efficiency; ISDB-T/Tb standard named it as the modulation and error protection module and DVB-T2 and ATSC3.0 standards as Bit Interleaved Coding and Modulation (BICM) module, it is important to mention that Outer Encoder evolved from Reed Salomon codes to BCH (Bose, Ray-Chaudhuri and Hocquenghem) codes and Inner encoders evolved from Convolutional codes to LPDC (Low-Density Parity Check) codes, both forms part of the Forward Error Correction (FEC) codes. According to this work [10], the performance of the ATSC 3.0 BICM reaches very closely to the upper bound capacity, in terms of spectral efficiency, proposed by Shannon in AWGN (Additive white Gaussian noise) channel.

Before framing, ATSC 3.0 incorporates a constellation superposition technology unlike DVB-T2 and ISDB-T/Tb standards, known as LDM (Layered Division Multiplexing). It allows to multiplex two data streams; the BICM Core Layer (CL) and the BICM Enhanced Layer (EL); at different power levels [11]. In practical systems, the Core Layer delivers robust mobile broadcasting services, it means that operates with negative CNR (Carrier-to-Noise ratio), and the Enhanced Layer delivers UHDTV (Ultra-High Definition Television) or multiple HDTV (High Definition Television) services. After LDM processing, Time Interleaving (TI) module is designed for coping with long burst errors in the time domain [12]. A

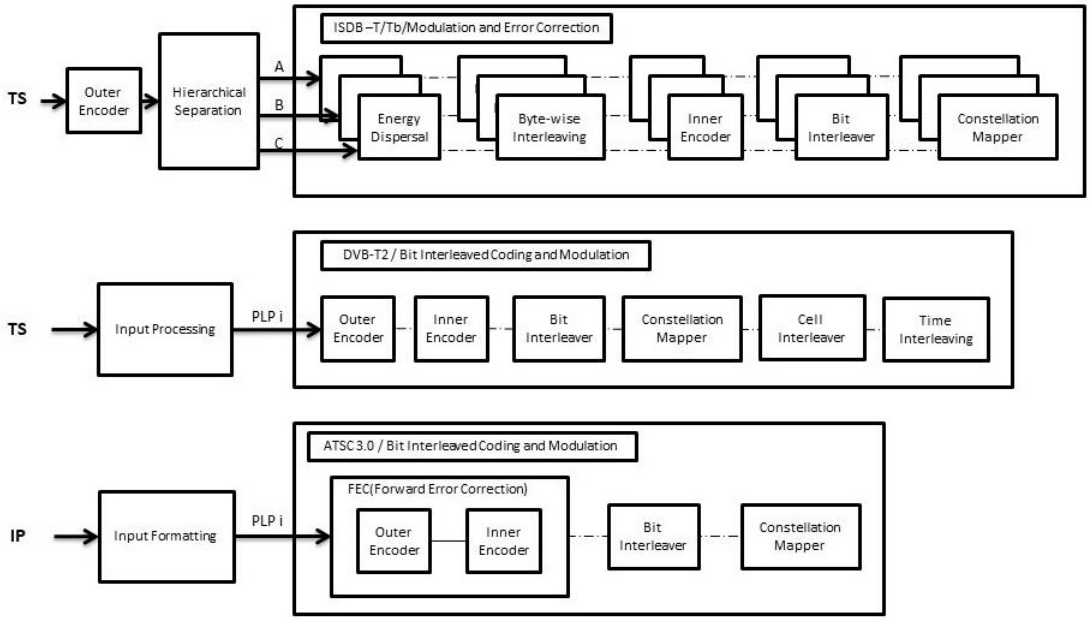

Fig. 2. Protection-at-the-bit-level and Modulation Stage,adapted from [7], [8] and [9]

salient difference is at the moment of the Framing process, ISDB-T/Tb applies Frequency Interleaver (FI) after the TI process, but DVB-T2 and ATSC3.0 wait for Framing process first and after FI is applied. As the same of TI, Frequency Interleaving (TI) module is designed for separating bursts errors in frequency domain. As the last stage, the pilot carriers, that are used for channel estimation, are inserted into the final OFDM symbol and the Guard Interval (GI) is time-aligned with the OFDM symbol in order to mitigate ISI (Inter-Symbol Interference). Figure 3 shows the entire process of the OFDM waveform generation.

One of the contributions that have been maintained over time was the sending of signaling information. ISDB-T/Tb introduced the TMCC (Transmission Multiplexing Configuration Control) signal providing to a broadcaster the option to configure different transmission schemes that are tailored to service-specific robustness levels [7]. Basically, an arrange of carriers of an OFDM segment were set up to deliver the transmission parameters (inner-code, coding rate, modulation scheme, and time interleave) of each layer, up to three hierarchical layers (A, B or C). Also, this scheme was very useful for narrow-band mobile receivers. Following this thread, L1 signaling information, in DVB-T2 and ATSC3.0, carrying information about how Physical Layer Pipes (PLPs) are allocated in the frame and their respective physical parameters, as well as the waveform parameters of the Preamble OFDM symbols [8], [9]. This flexibility at the transmission level was extrapolated to the link layer, ATSC 3.0 encapsulated the binary input streams into ALP (ATSC Link-Layer Protocol) packets for letting generic data streams as a valid input source to the system, for instance, the IP packets or Transport Stream could be part of the same channel [9].

It is clear that the motto driving the terrestrial broadcasting is focused on strengthening the receiver signal for rooftop antenna (fixed) and mobile receivers, however, backward compatibility has been always the main drawback of worldwide television standards. For this reason, some kind of information about incoming signals are mandatory, DVB T2 launched a first proposal inserting the P1 symbols within the T2 frame. This enables synchronization and signaling of the entire frame but does not resolve the problem [8]. Based on these ideas, ATSC 3.0 disclosed the bootstrap symbol signaling the most basic information, such as the version of the ATSC 3.0 standard, the Emergency Alert Service (EAS) wake up bit, the sampling rate of the current frame and the preamble structure [9]. Really, this technology could disrupt the telecommunication industry, enabling cooperative transmission between different network operators [13].

This sub-section summarizes the physical layer architecture of terrestrial broadcasting and the evidence proves that broadcasters invested in improving point-to-multipoint transmission without involving the redesign of network architecture by leveraging all the resources of a dedicated communication channel. However, streaming video services are increasingly popular over the Internet and competing with the mainframe television infrastructure. By not owning one, these services are being born on the concept of an overlay network, that will be detailed in the next sub-section.

B. Overlay Networks

The Overlay Network refers to the approach of adding resources on top of an existing network infrastructure [15].These resources not only cover services such as a local proxy, but services that can be offered anywhere in the world without having a network deployed directly to the client. Internet could be the case study to explain the main ideas about overlay network. Despite its network infrastructure was never designed to be optimal for any particular application [16], in the case

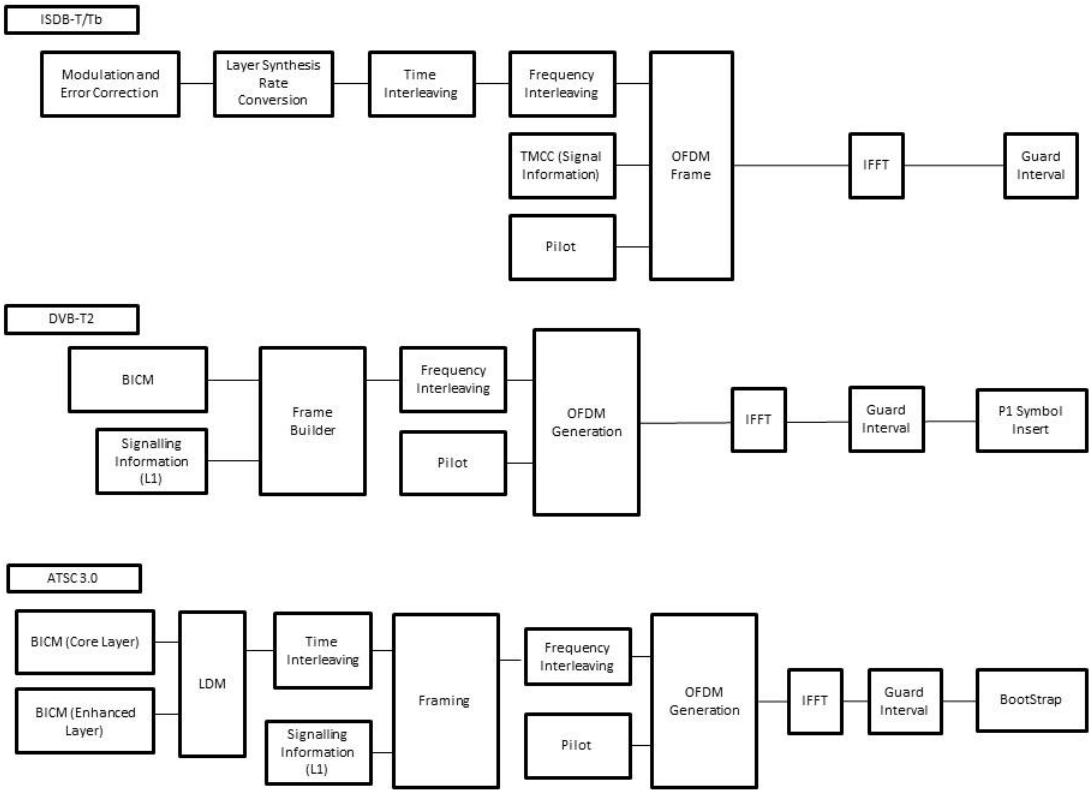

Fig. 3. OFDM Waveform Generation, adapted from [7], [8] and [9]

of the access network or *'last mile'* in Internet Infrastructure, the PSTN (Public Switched Telephone Network) network and the walled-garden TV networks, or others underlay networks, enable the access from end-users to the Internet. The ADSL (Asymmetric Digital Subscriber Line) technology was spread over the PSTN network, the DOCSIS (Data Over Cable Service Interface Specification) 3.0 protocol [17] did the same thing in a HFC network, as well as the GPON (Gigabit-capable Passive Optical Network) [18] in FTTh network. Hence, it was no suprise that local area networks, such as the *IEEE 802.11* Standards Body [19], and the latest cellular generation released in 2011, the *LTE Advanced* [20], made possible the final convergence of all networks over IP-based technologies, known as broadband networks.

The operators in their constant search to improve their services decided to invest on deployment Internet network backhaul within their own core network as a manner of adding new applications over their last-mile connection. The MNOs (Mobile Network Operator) saw this opportunity to build a infra-based overlay network. Hence, experiences such as the EPC (Evolved Packet Core) network serves to the MNOs as, on the one hand, a management system between end-user and MNO, called as Control Plane, and, by the other hand, as a virtual interface at the application level, whether for external connections, or a local mobility anchor for MNO's internal purpose [21]. Figure 4 depicts the EPC arquitecture, the Radio Acces Network (RAN) involves the eNodeB (Enhanced Node B) and the User Equipment (UE) of end-user. The MME (Mobility Management Entity) is in charge of all the control plane functions, e.g. the end-user authentication process works with the Home Subscriber Server (HSS), the management of end-user QoS and the tracking update process. Moreover, the GW (Serving Gateway) receives the incoming packets and routing them to the eNodeB, whose end-user currently stays after the respective displacement in a mobility context. The closest entity to the Internet is the Packet Data Network Gateway (PDN-GW) and its function is similarly as Layer2/3 router in the backbone Internet [21]. In recent years, MNOs operators are pushing the development of IP Multimedia Subsystem (IMS) because can provide the multimedia services over IP in next-generation mobile networks with the intention of surpassing the current OTT services by offering slices of network resources inside its infrastructure in order to guarantee a high QoS for real-time applications [22].

The same problem was experienced in the television industry. As were explained in the previous sub-section, television networks distributed digital video signals in broadcasting mode restricted to the radio frequency bands of the physical transmission medium. In fact, with an ever-improving video codec efficiency, more channel programs were multiplexed over a single RF thanks to MP2T (MPEG-2 Transport Stream) packets [23]. Nevertheless, this increasing programming number of options did little to impact the viewing behaviors[24]. For instance, cable channels rose by more than 45% between

TABLE I
COMPARISON OVERVIEW BETWEEN TERRESTRIAL DIGITAL TELEVISION STANDARDS IN 6MHZ, ADAPTED FROM [9], [14] AND [7]

Parameter	ISDB-T (1997) / ISDB-Tb (2006)	DVB-T2 (2008)	ATSC 3.0 (2016)
Input Formatting	Hierarchical Transmission (A,B,C)	PLP	PLP
Outer Code	Reed-Salomon code	BCH	BCH, CRC, none
Inner Code	Convolutional code (1/2, 2/3, 3/4, 5/6, 7/8)	LPDC code (1/2, 3/5, 2/3, 3/4, 4/5, 5/6)	LDPC code {2, 3, 4, 5, 6, 7, 8, 9, 10, 11, 12, 13}/15
Constellation Mapper	QPSK, 16-QAM, 64-QAM	QPSK, 16-QAM, 64-QAM, 256-QAM	QPSK, 2D-16NUC, 2D-64NUC, 2D-256NUC, 1D-1024NUC, 1D-4098NUC
Multiplexing	FDM	TDM	TDM legacy/TDM-FDM hybrid/LDM
Modulation	Band Segmented Coded OFDM	Coded - OFDM	OFDM
FFT size	2K, 4K and 8K	1K, 2K, 4K, 8K, 16K and 32K	8K, 16K and 32K
GI (Guard Interval)	1/4, 1/8, 1/16, 1/32	1/128, 1/32, 1/16, 19/256, 1/8, 19/128, 1/4	3/512, 3/256, 1/64, 3/128, 1/32, 3/64, 1/16, 19/256, 3/32, ,{57, 512, 3}/16, 1/8, 19/128, 1/4 (symbol and time-aligned frames)
Multiple PLPs per service	-	No (1 commom PLP)	Yes (up to 4)
Link layer	MPEG2-TS	MPEG2-TS	ALP (ATSC Link-Layer Protoco)
Main Transport Protocol	TS	TS	IP
Min-Max Data Rate 6Mhz	3,65 Mbps - 23,23 Mbps	5,6 Mbps - 38 Mbps	1 Mbps - 57 Mbps
Channel Bonding	-	No	Yes (Two RFs)
Video Codec Support	H.264/AVC	H.264/AVC	H.265/HEVC
SNR operating range AWGN	3,2 dB - 19,8 dB	+1 dB, 22 dB	-6,2 dB, +32 dB

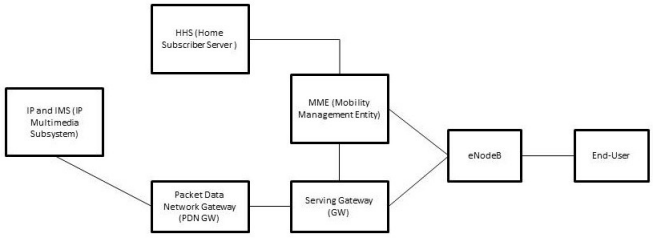

Fig. 4. The Evolved Packet Core Arquitecture, adapted from [21]

2008 and 2013 in the North-American industry reaching a total amount of 180 channels, but users continued to consume from an average of 17 or 18 channels [25]. In that sense, the inefficient use of resources within the broadcasting gave rise to the appearance of new multimedia platforms such as the *media overlay networks*, whose leading technology was the IPTV.

The IPTV (Internet Protocol Television) platform was the first effort to take advantage of the resources of enterprise private networks in order to provide a more personalized service to the user by leveraging the whole IP stack protocols and the full-duplex communication. Hence, additionally to provide live channels and Video on demand (VOD), new types of services were offered to final users, such as Schedule TV services, Content on demand (COD), Personal Video Recorder (PVR), Information service, Communication service, Notification Service and Advertisement service [26], so to improve the audiovisual interactivity and addressability.

Legacy IPTV was deployed into managed operator networks over the traditional broadcasting system for the sake of competing with the conventional cable and satellite TV services in terms of *QoS*, full-HD transmission with above 6 Mbps video rate and a transport delay shorter than 2 seconds [27] by aggregating layer 3 capabilities, by redesigning network topology and by offering to the users web services in order to make more efficient video content delivery and render a more interactive product. By contrast, just a few ISPs were prepared to modernize their underlying networks and be became as IPTV providers, because of the large initial investment and a high operational cost. Hence, only network operators that owned a large metropolitan area infrastructure can be able to commercialize varied IPTV packages until the emergence of OTT service providers.

Broadband networks have been experiencing the gradual growth of data access speeds which caused that the constraint on bandwidth when delivering video content over these networks be lifted, either local or mobile networks. This technological breakthrough opened countless opportunities for content creators and video-service providers. The emergence of *OTT* services over unmanaged networks consolidated an agile and flexible communication system, being modeled to interact with the user giving him the opportunity to have

control of the content he wants to see at anywhere and anytime, which was rarely possible with traditional broadcasting or IPTV systems. For instance, user-generated content applications such as *YouTube* is watched by 5 billion people per day [28] and everything indicates that it is expanding thanks to the proliferation of Content Delivery Networks (CDN) within the large Internet infrastructure [29].

This section summarizes the two kinds of networks deployed in the television industry, highlighting their main innovations and drawbacks. New video delivery schemes are been addressed in the last years driven by technological innovations and new user demands.

III. Latest Video Content Delivery Schemes

So far, the networks that participate in the process of delivering video content to the final user have been discussed above. An efficient end-to-end video content delivery scheme should consider upon which type of network is being deployed, e.g. which network components are reachable and manageable by the provider, since this will define the type of technology to use and the business model to be implemented. For this reason, the latest video content delivery proposals model enhanced video transmission systems based on cutting-edge technologies, leveraging novel mathematical approaches and heuristic methods which seek to find the most optimized video content delivery scheme over resource-constrained networks.

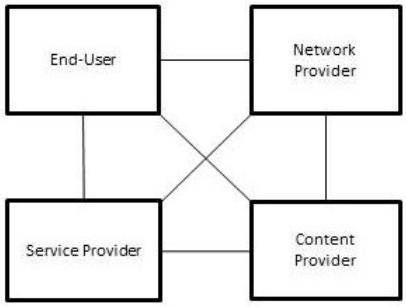

Fig. 5. IPTV domains, adapted from [30]

Fig 5 depicts the four domains of IPTV service provisioning [30]:

1) Content Provider: who owns the content copyright for distribution.
2) Service Provider: Generally is who offers a telecommunication service, but recently CDN's owner performs the same work for content providers.
3) Network Provider: who really reaches and manages the network equipment and is the first hop node form end-user edge.
4) End-User: who enjoys the service.

In contrast to the architecture of Fig 1, The IPTV architecture allows direct interaction of the content provider with the end-user, without having to go necessarily through a service provider. From this moment, new video-service providers emerged and disrupted the television industry in an unexpected way. Netflix's service, the most popular streaming video service, takes advantage of the multiple cloud technologies that exist to offer a value-added video service to end-users. Netflix employs three popular CDNs with footprint worldwide to serve its subscribers through chunked-based delivery, enabling adaptive video streaming to face unstable and unreliable channels [31]. In 2018, Netflix's traffic is responsible for 26.58% of global video streaming traffic share according to [32].

Commonly, the television protocols focus on strengthening the signal-to-noise ratio and increasing the spectral efficiency of the physical transmission medium, but the sudden appearance of streaming services over packet-based networks made the audiovisual industry face new challenges. Two types of schemes are been discussed in the latest years: push-based schemes (server pushes the to client such as broadcasting-based technologies) and pull-based scheme (client pulls video content from the server). Real-Time Streaming Protocol (RTSP)/Real-time Transport Protocol (RTP) fits well in the first scheme and relies on just-in-time data delivery with just-in-time rendering [33] and HyperText Transfer Protocol (HTTP) streaming is a pull-based scheme, very popular for file delivery, that achieves near-live streaming due to the user needs to wait until the buffer is ready to render the first Group of Pictures (GOP) affecting the end-to-end delay. This fact notwithstanding, there is a subclass of HTTP-based streaming, known as *adaptive multimedia streaming schemes*, It is mainly modeled to adapt to the instabilities of the transmission channel such as losses, delay and time-varying bandwidth, typical of wireless transmission and can be classified as: transcoding-based, scalable video coding, multi-layer encoding, multiple description coding and independent bitrate encoding solutions [33]. Hence, hybrid schemes that make use of the best of both proposals have become visible, deploying in favored video-service applications, for instance, Periscope allows users broadcasting over the Internet. To achieve this, the first 100 viewers access to the real-time server for minimizing the end-to-end latency and the rest of them pushes the video content from the adaptive streaming media server for reducing processing overhead [34].

It is worth mentioning that the advent of CDN networks inside the Internet allowed new distribution and transmission schemes in the different layers of the Open Systems Interconnection (OSI) stack. It is an environment where new OTT stakeholders , which involves Content Providers, CDNs and ISPs, want to position on the live TV broadcast market. Akamai, the worlds largest and most trusted cloud delivery platform, *"forecasts that 500 million viewers will soon be watching prime-time live sports online"* [26]. According experimental tests, low-Latency chunked streaming schemes enables ranged from 2.3 to 3 seconds of delay with acceptable *QoE* [35]. Moreover Layer 3 capabilities and beyond were necessary to make viable this type of architectures. IP multicast, Peer-to-peer (P2P) Sharing and Proactive caching [26] are the most promising systems in order to alleviate unicast limitations.

http://www.set.org.br/ijbe/ doi: 10.18580/setijbe.2019.10 Web Link: http://dx.doi.org/10.18580/setijbe.2019.10

IV. Final Remarks and Trends

Future video content delivery networks will be modeled as a media overlay network with global coverage with IP convergence and ubiquitous radio access through distributed array antennas. However, it still too soon to forecast how will be the market model that allows a free-competition scenario and be able to incentive the emergence of new video producers with better content to offer to the end-user.

Acknowledgment

The authors would like to thank the CAPES (*Coordenao de Aperfeioamento de Pessoal de Nvel Superior*) and FAEPEX (*Fundo de Apoio ao Ensino, Pesquisa e Extenso*) programs for the financial support and the academic incentive.

References

[1] M. Trevisan, D. Giordano, I. Drago, M. Mellia, and M. Munafo, "Five years at the edge: Watching internet from the ISP network," *CoNEXT 2018 - Proceedings of the 14th International Conference on Emerging Networking EXperiments and Technologies*, pp. 1–12, 2018.

[2] J. Guo, X. Gong, J. Liang, W. Wang, and X. Que, "An Optimized Hybrid Unicast/Multicast Adaptive Video Streaming Scheme over MBMS-Enabled Wireless Networks," *IEEE Transactions on Broadcasting*, vol. 64, no. 4, pp. 791–802, 2018.

[3] D. Ren, Y. Xu, and S. H. Gary Chan, "Beyond 1Mbps global overlay live streaming: The case of proxy helpers," *ACM Transactions on Multimedia Computing, Communications and Applications*, vol. 11, no. 2, 2014.

[4] J. E. O'Neal, "BMSB Attracts Video/Broadband Experts From Around The World," *IEEE Broadcast Technology*, vol. 3, p. 8, 2018.

[5] D. F. Feitosa, "Transmissão híbrida na TV aberta brasileira: o DTV Play e as suas potencialidades," *Revista da SET*, jan 2019. [Online]. Available: http://www.set.org.br/news-revista-da-set/revista/transmissao-hibrida-na-tv-aberta-brasileira-o-dtv-play-e-as-suas-potencialidades/

[6] Eutelsat, "Eutelsat Home Page," 2019. [Online]. Available: https://www.eutelsat.com/en/satellite-communication-services/broadcasting-solutions.html

[7] M. Takada and M. Saito, "Transmission System for ISDB-T," *Proceedings of the IEEE*, vol. 94, no. 1, pp. 251–256, jan 2006.

[8] I. Eizmendi, M. Velez, D. Gomez-Barquero, J. Morgade, V. Baena-Lecuyer, M. Slimani, and J. Zoellner, "DVB-T2: The second generation of terrestrial digital video broadcasting system," *IEEE Transactions on Broadcasting*, vol. 60, no. 2, pp. 258–271, 2014.

[9] L. Fay, L. Michael, D. Gomez-Barquero, N. Ammar, and M. W. Caldwell, "An Overview of the ATSC 3.0 Physical Layer Specification," *IEEE Transactions on Broadcasting*, vol. 62, no. 1, pp. 159–171, mar 2016.

[10] L. Michael and D. Gómez-Barquero, "Bit-Interleaved Coded Modulation (BICM) for ATSC 3.0," *IEEE Transactions on Broadcasting*, vol. 62, no. 1, pp. 181–188, 2016.

[11] L. Zhang, W. Li, Y. Wu, X. Wang, S. I. Park, H. M. Kim, J. Y. Lee, P. Angueira, and J. Montalban, "Layered-Division-Multiplexing: Theory and Practice," *IEEE Transactions on Broadcasting*, vol. 62, no. 1, pp. 216–232, 2016.

[12] P. Klenner, J. S. Baek, N. S. Loghin, D. Gómez-Barquero, and W. S. Ko, "Physical Layer Time Interleaving for the ATSC 3.0 System," *IEEE Transactions on Broadcasting*, vol. 62, no. 1, pp. 253–262, 2016.

[13] Y. Wang, D. He, L. Ding, W. Zhang, W. Li, Y. Wu, N. Liu, and Y. Wang, "Media Transmission by Cooperation of Cellular Network and Broadcasting Network," *IEEE Transactions on Broadcasting*, vol. 63, no. 3, pp. 571–576, sep 2017.

[14] G. Bedicks, F. Yamada, F. Sukys, C. E. S. Dantas, L. T. M. Raunheitte, and C. Akamine, "Results of the ISDB-T system tests, as part of digital TV study carried out in Brazil," *IEEE Transactions on Broadcasting*, vol. 52, no. 1, pp. 38–44, 2006.

[15] M. Van der Schaar and P. A. Chou, *Multimedia over IP and wireless networks: compression, networking, and systems*. Elsevier, 2011.

[16] M. Handley, "Why the Internet only just works," *BT Technology Journal*, vol. 24, no. 3, pp. 119–129, 2006.

[17] B. Hamzeh, M. Toy, Y. Fu, and J. Martin, "DOCSIS 3.1: Scaling broadband cable to Gigabit speeds," *IEEE Communications Magazine*, vol. 53, no. 3, pp. 108–113, 2015.

[18] I. Cale, A. Salihovic, and M. Ivekovic, "Gigabit passive optical network GPON," *Proceedings of the International Conference on Information Technology Interfaces, ITI*, pp. 679–684, 2007.

[19] B. Bellalta, "IEEE 802.11ax: High-efficiency WLANS," *IEEE Wireless Communications*, vol. 23, no. 1, pp. 38–46, 2016.

[20] A. Ghosh, R. Ratasuk, B. Mondal, N. Mangalvedhe, and T. Thomas, "LTE-advanced: Next-generation wireless broadband technology," *IEEE Wireless Communications*, vol. 17, no. 3, pp. 10–22, 2010.

[21] P. Lescuyer and T. Lucidarme, *Evolved Packet Systems (EPS): THE LTE AND SAE EVOLUTION OF 3G UMTS*. John Wiley & Sons Ltd, 2008.

[22] S. S. A. Gilani and M. H. B. Waheed, "QoENGN : A QoE Framework for Video Streaming over Next Generation Mobile Networks," pp. 109–113, 2019.

[23] L. Beloqui Yuste, F. Boronat, M. Montagud, and H. Melvin, "Understanding timelines within MPEG standards," *IEEE Communications Surveys and Tutorials*, vol. 18, no. 1, pp. 368–400, 2016.

[24] M. L. Wayne, "Netflix, Amazon, and branded television content in subscription video on-demand portals," *Media, Culture and Society*, vol. 40, no. 5, pp. 725–741, 2018.

[25] T. Spangler, "Cord-cutting alert: Americans watch just 9% of TV channels available to them," 2014. [Online]. Available: https://variety.com/2014/tv/news/cord-cutting-alert-americans-watch-just-9-of-tv-channels-available-to-them-1201172883/

[26] S. M. Fati, S. Azad, and A.-S. K. Pathan, *IPTV Delivery Networks: Next Generation Architectures for Live and Video-on-demand Services*. John Wiley & Sons, 2018.

[27] Y. Liu, Z. Liu, X. Wu, J. Wang, and C. C. Y. Yang, "IPTV system design: An ISP's perspective," *Proceedings - 2011 International Conference on Cyber-Enabled Distributed Computing and Knowledge Discovery, CyberC 2011*, pp. 234–240, 2011.

[28] S. Aslam, "YouTube by the Numbers: Stats, Demographics & Fun Facts." [Online]. Available: https://www.omnicoreagency.com/youtube-statistics/

[29] N. Erik, S. Ramesh K., and J. Sun, "The Akamai Network: A Platform for High-Performance Internet Applications," *ACM SIGOPS Operating Systems Review*, 2010.

[30] G. M. Lee, C. S. Lee, W. S. Rhee, and J. K. Choi, "Functional Architecture for NGN-Based Personalized IPTV Services," *IEEE Transactions on Broadcasting*, vol. 55, no. 2, pp. 329–342, 2009.

[31] V. K. Adhikari, Y. Guo, F. Hao, V. Hilt, Z. L. Zhang, M. Varvello, and M. Steiner, "Measurement Study of Netflix, Hulu, and a Tale of Three CDNs," *IEEE/ACM Transactions on Networking*, vol. 23, no. 6, pp. 1984–1997, 2015.

[32] Sandvine, "The Internet Global Phenomena Report, October 2018," Fremont, CA, USA, Tech. Rep., 2018.

[33] K. J. Ma, R. Bartoš, S. Bhatia, and R. Nair, "Mobile video delivery with HTTP," *IEEE Communications Magazine*, vol. 49, no. 4, pp. 166–175, 2011.

[34] B. Wang, X. Zhang, G. Wang, H. Zheng, and B. Y. Zhao, "Anatomy of a Personalized Livestreaming System," *Proceedings of the 2016 ACM on Internet Measurement Conference - IMC '16*, pp. 485–498, 2016.

[35] A. Bentaleb, C. Timmerer, A. C. Begen, and R. Zimmermann, "Bandwidth prediction in low-latency chunked streaming," in *Proceedings of the 29th ACM Workshop on Network and Operating Systems Support for Digital Audio and Video - NOSSDAV '19*. New York, New York, USA: ACM Press, 2019, pp. 7–13.

Diego Pajuelo Graduate in Electrical Engineering from the Peruvian University of Applied Sciences (UPC), Lima, Peru in 2012. He is currently working towards his Doctoral degree in Sciences and Telecommunications at Unicamp. His research interests are: HDR Video and audio coding, Image processing, Digital television and Satellite communications.

Yuzo Iano is the head and founder of the LCV since 1972. He obtained his BSc (1972), MSc (1974) and PhD (1986) in Electrical Engineering at Unicamp, SP-Brazil. Research Interests: Digital Signal Processing (images/audio/video), Digital TV, 4G (LTE) and 5G Cellular Networks, Pattern Recognition, Smart Cities, Smart Grid, Internet of Things.

David Minango Graduated in Electronic Engineering at the University Polytechnic Salesian (UPS). Currently, He is an M.S.c candidate by Department of Communications (DECOM), Faculty of Electrical and Computer Engineering (FEEC) at State University of Campinas (UNICAMP). Professional with engineering experience at Configuration and maintenance of repeater equipment, link antennas, calibration of equipment used in radio frequency in the VHF frequency range for two-way radio equipment. Knowledge in MotoTRB, TCP/IP, WAN Networks. Research Interests: Deep Learning, Machine Learning, Digital Image Processing with Medicals images.

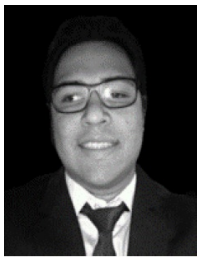

Gabriel Gomes de Oliveira Graduated in Civil Engineering at UNIP University in 2018, studying for a Master's degree at Unicamp, FEEC (Faculty of Electrical and Computer Engineering), DECOM (Communications Department), Laboratory of Visual Communication (LCV) Currently researches and studies the Smart City area.

Ana Carolina Borges Monteiro Graduated in Biomedicine from University Center Amparense - UNIFIA (2015). Currently is a Ph.D. Candidate by Department of Communications (DECOM), Faculty of Electrical and Computer Engineering (FEEC) at State University of Campinas (Unicamp) and a researcher at the Laboratory of Visual Communications (LCV). Also, she is currently the Registration Chair of the Brazilian Symposium on Technology (BTSym). Has expertise in the areas of Clinical Analysis and digital image processing through MATLAB software.

Reinaldo Padilha France Graduated in Computer Engineering (University Regional Center of the Holy Spirit of Pinhal - 2014). Currently is a Ph.D. Candidate by Department of Communications (DECOM), Faculty of Electrical and Computer Engineering (FEEC) at State University of Campinas (Unicamp) and a researcher at the Laboratory of Visual Communications (LCV). Also, He is currently Chair Proceedings of the Brazilian Symposium on Technology (BTSym). Has interest and affinity in the area of technological and scientific research as well as knowledge in programming and development in C / C ++, Java and .NET languages. The main topics of interest are Simulation, Operating Systems, Software Engineering, Wireless and Network, Internet of Things, Broadcasting and Telecommunications Systems.

Received in 2019-07-11 | Approved in 2019-11-25

Broadcast: The historical development of World Broadcasting and its impact reflected in Brazil

Gabriel Gomes de Oliveira
Yuzo Iano
Ana Carolina Borges
Reinaldo Padilha França
Pablo Minango
Diego Pajuelo

CITE THIS ARTICLE

de Oliveira, Gabriel Gomes, Iano, Yuzo, Borges, Ana Carolina, França, Reinaldo Padilha, Minango, Pablo, Pajuelo, Diego; 2019. Broadcast: The historical development of World Broadcasting and its impact reflected in Brazil. SET INTERNATIONAL JOURNAL OF BROADCAST ENGINEERING. ISSN Print: 2446-9246 ISSN Online: 2446-9432. doi: 10.18580/setijbe.2019.11. Web Link: http://dx.doi.org/10.18580/setijbe.2019.11

Broadcast: The historical development of World Broadcasting and its impact reflected in Brazil

Gabriel Gomes de Oliveira, Yuzo Iano, Ana Carolina Borges Monteiro, Reinaldo Padilha França, Pablo Minango and. Diego Pajuelo

Abstract- Broadcasting is a method of message transfer to all receivers simultaneously, its services are those that perform the transmission of sounds and images (television) or just sounds (radios) to the general public. The present study was conducted by analyzing scientific papers present in the Scielo platform and main academic research platforms. These works were selected because they meet the criteria of time (2015-2019) and location (Brazil). The data below illustrates the main findings, creating a link between the first steps of world broadcasting and their respective impacts in Brazil.

Index Terms- Broadcast, Radio, Television, Media, Technology, Information.

I. INTRODUCTION

The broadcast term, is the addition of "broad" meaning wide, or large-scale and "cast" is meant to send, design, and transmit. So, this growing wave towards the theme over the recent past, nowadays commonly associated with radio and television, is understood, however, its concept is much broader, since "broadcasting" is related to the transmission of sound and image of the radio. not get more radio waves thus reaching other types of electronic devices, broadcasting word has become archaic to mention the broadcast term. It is the process by which certain information is transmitted or transmitted to many receivers at the same time, where it is responsible for the transmission of any kind of media, through several ways (radio waves, satellite, cables, optical fibers, telephone lines), and on the internet, broadcasting is broadcasting videos and music, as it is usually [1] [2].

Moreover, with the spread of many different media, it is considered that broadcast is as an act of transmitting something, is a form of data transmission where all receivers receive the same information simultaneously. Where currently the vast majority of the population has desires to share everything they like and want, with the rest of the world, therefore the services they are offering ways to make this feasible are becoming increasingly popular [3].

In addition, it is believed that not only residential users are responsible for the content explosion in the late 1990s and early 2000, but also globalization and digital transformations have brought with it the dissemination of the term broadcast [4][5].

As time went on, the internet has evolved, transforming the way people communicate, as they do today, with 4G technology circulating on mobile devices, and this progress is only just beginning. And along with the development of the 4G system, as well as the improvement behind Internet connection and content sharing services [6].

The very companies from various branches invest their millions in sound transmission solutions, image, and video over the internet and other means.

The development and expansion of digital technology produced an explosive increase in communication platforms in the last twenty years. Because of them, the diversity of opinions, existing ideas, and beliefs in society have greater opportunities to manifest itself in the public sphere. The foregoing, however, did not impede increasing regulatory intensity of the state, to ensure pluralism of information [7].

The last few years have been marked by a gradual and multiple increases of new portable media devices. Laptops, tablets, and mobile reproduce news, movies and shows anywhere, anytime. The traditional media such as radio and newspaper have been losing ground for different ways to communicate and share information, and the idea of a means to reach a unified mass no longer resonates within a technological configuration that presents [8].

The digital TV to replace the analog television broadcasts because it has the advantage of including interactive applications, such as research, programming and their schedules, emergency signs among others, as well as different types of high-definition signal quality (HD) and standard definition (SD) [7] [9].

With this briefly explained views, this paper aims to develop a review of the subject, on the various academic perspectives in tune with the subject in academia.

G. G. Oliveira is currently studying for a Master's degree at the State University of Campinas
Y. Iano is a teacher at the State University of Campinas
A. C. B. Monteiro is currently studying for a Ph.D.'s degree at the State University of Campinas
R. Padilha is currently studying for a Ph.D.'s degree at the State University of Campinas
D. Minango is currently studying for a Master's degree at the State University of Campinas
D. Pajuelo is currently studying for a Ph.D.'s degree at the State University of Campinas

http://www.set.org.br/ijbe/ doi: 10.18580/setijbe.2019.11 Web Link: http://dx.doi.org/10.18580/setijbe.2019.11

II. Methodology

This study was conducted by analyzing scientific platform present in Scielo and main academic research platforms, being selected because they meet the criteria of time (2015-2019) and location (Brazil). The following data illustrate the main findings and trends related to the topic of the broadcast.

III. HISTORICAL REVIEW

Given the analysis of the selected articles note that the major peculiarities of the classical media Broadcasting, known as broadcasting have been classified by the radio stations.

Reginald Fessenden in 1900, pointing an alternator in which allowed the launch through the continuous wave, transmitting sound through waves. In 1906, Lee de Forest invented the triode, which in the future would be a device for the detection and amplification of radio signals, being at that time a vacuum tube containing three valves. This eventually served in the World War I, where it served as a mode of communication point to similar extent telephony and wireless networks, represented a significant slowdown in public broadcasting radio [3] [10].

Some academics believe that radio wave sound technology has its beginnings in the late nineteenth century, by the Italian Guglielmo Marconi, but should give merit to the creation of radio for Nikola Tesla, since Marconi used Tesla's patented technologies. The form of historically important as the radio model was performed approximately in 1920 in the United States [11 - 15].

Being in Europe, particularly in England, the first model evolved differently in the dimension in which, on September 1929, a landmark for world television, where British naturalized Scottish John Baird was allowed to air an experimental television service with the BBC of London. However, the US model was imposed to other countries, primarily from the radio, then television, while during 1960-1970, the use of the electromagnetic spectrum turned out to be available in most Western countries [13 - 19].

In the period of war, the transmission of electromagnetic waves was under the control of the governments of the countries in the conflict, which led to a delay in the deployment of broadcasting to the general public, being offset by the advances made in the period, which facilitate the growth of radio stations in the world postwar [12 - 15].

Under the supervision of the Navy, companies started to mass-produce and mass devices with standardized parts that were based on vacuum tube technology as a base. In the post-war, joining multiple alternators, created transmitters large transmission power on one hand, and receiving relatively inexpensive devices in their production, it became increasingly marked the difference between the complex technological devices [14 - 18].

Thus, the radio began to take its modern form when it came to sound signal amplification and emission technology technologically, since broadcasting has spread all over the world, and has become very complex and economically expensive, because of the use of vacuum tube, alternators, and when almost simultaneously developed one based on the receiving device technology (sets) simple and increasingly inexpensive. In possession of this technology, which could no longer be drained for military purposes, manufacturers have embarked on the creation of a mass-market to absorb the mass production of these simple devices and cheap [11 - 19].

Already alluded to the fact that the technological device's radio sending and receiving all have been patented. In addition to the technological and economic aspects, regulation indirectly exercised by the legal system of patents was another determining factor in the emergence of broadcasting, where these three aspects are retroactive all together [11 - 19].

In the next period of the beginning of the war, companies founded Fessenden and Lee of Forest disappeared or had been bought. In particular, they have been its main as-purchased sets, patents. These purchases generated some of the great companies of the time. Lee from Forest to sell in 1913 its most valuable patent (the triode), resulting in AT&T, the company that started then voice transmissions over long distances. In 1912, Edwin Armstrong understood the true triode's potential when he developed a feedback circuit that not only quite amplified the signal to allow the vacuum tube to generate radio waves [11 - 19].

The Navy led to the creation of the RCA (Radio Corporation of America) in 1919, which now holds the basic patents of GE (General Electric), AT & T and American Marconi, where continued to face the radio science as an environment topic communication topic to be known commercially in line with this frame [11 - 19].

In turn, Westinghouse, left out of RCA, the company founded in 1920 that will eventually have been the first radio broadcast, the KDKA, where the broadcast was born as an environment for sale equipment [11 - 19].

The interests of the various RCA member companies were not convergent, since GE and Westinghouse were especially intellectual characteristic of the receivers and had been effectively specialized in the production and sale of such devices. This was a much more lucrative market than the market transmitters in which AT&T had specialized [11 - 20].

Then the broadcasting Internet monopolist of the US telephone network sold its stake in RCA and created their stations broadcasting in 1922. Unlike other companies, the aim of AT & T was not to sell receivers, but antecedently rent air time to potential bidders; however, this did not mean that the company should aim the broadcasting itself, as its business model was considered as a decal telephone usage time of sale for the transmission of voice, the peculiarity of AT&T. In any case, the business model at the time aroused little interest, the result was a patent war, where AT&T finally abandoned the broadcasting [14 - 21].

Patents are a way to indirectly regulate the use and economic exploitation of technological communication devices. The direct regulation operates especially for the right to emit. The need to regulate the use of the electromagnetic spectrum was historical originality with which the governments have faced in the first decades of the 20th century.

In the English case, the interests of various equipment manufacturers led to the creation of the British Broadcasting marketing year, after which, was transformed into a fully public company, the British Broadcasting Corporation (BBC) [15 - 22].

In the United States, the path was more complicated and are referred to herein only the essentials, the first law that regu-

lated the use of the spectrum, the essential idea of the law was to enjoy access spectrum as a privilege, not a right automatically possessed by someone, the government granted four types of privileges: a bandwidth intended to be used by management; two other types of bandwidth intended for commercial use and, finally, a band consisting of only a single frequency intended to amateur operator's radio [16 - 23].

In order already mentioned, the battle involved spectrum integral control by the Navy through the adjustment need only to get turned after the explosion of the number of transmitters occurs during the years 20 [11 - 18].

A set of series of lectures organized by the United States Secretary of Commerce, through the years 1922-24, would perhaps decide the radio regulator in the authenticity, the conference would decide the general characteristics of the radio and television regulation that nowadays eventually change dominant in most Western countries [16 - 24].

Following the 1912 law, the basic idea remained that the electromagnetic spectrum is very restricted use of which is a privilege granted by the political authority in the form of licenses. The management would give two (first three) types spectrum usage licenses, the licenses A and B. The type B license allowed by emission power 500 watts and 1000 included in the frequency chez 750. The type of licenses emitted less than 500 watts (some are limited to 5 watts), and the frequencies were allocated between 1360 and 1500 chez. Gender licenses B favored stations rehearsing the sample broadcasting and could finance transmitters each more powerful and more expensive condition. On the contrary, amateurs, university, and religious associations are moved to a type of licenses, category A, with short distance and operating at frequencies subject to multiple interferences and tuning difficulties [12 - 20].

The solution turned regulation, consequently, for providing the broadcasting standard based on powerful, expensive transmitters and receivers humble and cheap, rather than the amateur copy of that in many cases were individuals who emitted either as received. Repeats that he was inseparable from growth thanks have just to companies like GE or Westinghouse, a market based on a simple receiving device becoming cheaper and intended to happen marketed in bulk.

Then this new market required the creation of stations of broadcasting sending richly appealing content, in 1998, held in the evolution of radio [16 - 24].

The intersection between economic costs, technology, a market economy, and regulations led to conduct a communication standard in broadcasting, in which equal a complete asymmetry between two options: the 'emission' and 'reception'. Positions characterized the technological level by devices, in which a position receives signal and the other issues.

IV. BROADCAST IN BRAZIL

The media are practical examples of broadcast distribution, and one or more transmission antennas refer to a television signal, or known as radio diffuser, through electromagnetic waves through TV or radio, that captures the signal [1 - 16].

The radio in Brazil was first held in 1922, soon after, in 1923, the Henry Moirize masters and founded Roquette Pinto held the first Brazilian broadcaster, known as the Radio Society of Rio de Janeiro. It is extremely important to point out that in 1893, in Brazil; Roberto Mandelli de Moura also sought similar effects in experiments, he made the first broad-casts in the world, Mediatrix and the Santa Teresa hill [1 - 16].

The broadcast was started in Brazil when Assis Chateaubriand, started a makeshift way, broadcasts of TV Tupi station in Sao Paulo, where the first transmission was with a musical performance, the famous taskmaster cinema of the time, Frei José Mojica [2 - 19].

The first content transmitted were adaptations of radio programs and plays, being everything done live because the only way to record sound and images at the time was in motion picture film. In 1980, he started internet in the Brazilian territory, with limited access to a scientific level, and academic, and in 1991 the Internet began to be used by local, state and federal agencies, finally after 15 years in 1995 internet obtained public access [13 - 19].

It took place in 1999 in Latin America, the first transmission of video/audio via the internet, where in the 2000s they were marked by the success of social networks. In 2002, one of the most popular social networks in Brazil, Orkut was created, two years later, in 2004, Mark Zuckerberg founded Facebook, which was to become the largest social network in the world [3 - 19].

The popularization of the broadcast concept came through the evolution of the Internet, with the beginning of YouTube, in 2005, and over the years, the internet has evolved, becoming increasingly popular and radically changing the way people to communicate. Giving a balance of 10 years, in 2015, the 4G (Fourth Generation mobile) arrives in Brazil, where this band is characterized by better signal penetration, allowing better coverage indoors [3 - 19].

With the release to the 4G network, the quality of streaming media content increases exponentially, where undoubtedly, the image quality is far superior to the analog signal. However, this is not the only or the main factor for change, all this reshuffling is going for the 700 MHz bands currently used by analog TVs [2 - 19].

Currently, the mobile network uses a frequency of 2600 MHz, having a length in the upper wave, thus facing greater difficulty in the period through various obstacles, usually walls. By owning a larger spread, the range of 700 MHz has reached larger numbers of users, thus facilitating the purchase of equipment abroad, since hiding the compatibility issue, since these devices also use 4G frequency [11 - 24].

For the qualification of the internet service, and the development of 4G, it takes to explore the scope of technology Live broadcast live streaming and it's already popularized by social networks today and the development of sharing and communication videos [11 - 24].

V. TRENDS

The new evolution, or technological revolution, has begun in telecommunications devices, impacting networks, and the companies providing these services, is in its initial stages, but is already overwhelming. The world of telecommunications is advancing over broadcasting services, it would no longer be legal regulation, pseudo-structure like a dam to contain and maintain separation. Since telecommunications

http://www.set.org.br/ijbe/ doi: 10.18580/setijbe.2019.11 Web Link: http://dx.doi.org/10.18580/setijbe.2019.11

networks demand differentiated content, the preparation of which is historically in the hands of broadcasting.

In addition to simply improving sound and reception quality, it is necessary to enable broadcasters to achieve equitable quality on the technology platform, so that they can differentiate themselves into their unique production, broadcasting, content and coverage area capabilities.

The convergence of TV with the internet, as technology advances, we now have TVs that offer internet access, with various apps available, and other features. People are abandoning pay-TV and have migrated to the Internet to watch videos, shows, shows, and movies, meaning that pay-TV service will have to change to maintain its customer base in the country.

For radio, again podcast appears with a growing trend. Like TV, radio and the newspaper, a podcast is an information medium, but the origin of podcast media is very recent and still in its infancy. growth process, especially in Brazil, where it reaches few people.

The podcast is like a radio show, but its primary difference and advantage is content on demand. You can be listened to whatever you want, anytime you want.

Images remain on the rise since the vertical video format is doubling year after year. Yet even more concern about privacy has increased considerably in the last three years. The lack of curated online content and the use of social networking algorithms has heightened polarization and extremist views.

The importance of sound broadcasting is acknowledged, it is natural that policies for scientific, technological and industrial development sustain a broadcast capable of meeting the challenges of the new millennium, since this is the future. It is essential to identify and understand the new requirements, adopting any technical solution without considering the ongoing transformations, resulting in the gradual improvement of Brazilian broadcasting.

VI. CONCLUSION

Based on the broad applicability of this method is extremely important to develop studies that bring to light the history and evolution of techniques as comprehensive and notorious as the broadcasting. Thus, this paper aims to conduct a literature review on the history and the applicability of such technology this global trend. After all research, work should be well-founded based on methodology and strong literature.

Given the analysis of the analyzed papers realizes the broadcasting technique is an ancient methodology and that has accompanied man since the year 1920, undergoing changes and developments to monitor trends and needs over time. Where is clear the impact that the first steps from its patent dispute in the United States impacted the first content transmission made in Brazil reaching the current 4G scenarios.

Currently, note a strong link between the Internet and broadcasting as long as it is expected that with the advancement of 5G technologies allow greater synergy between both technologies employing higher speed and reliability in data transmission. Therefore, the broadcasting has shown great potential applicability not only in the areas of telecommunications, but currently in the transmission of data education, health, science, finance, and smart cities.

References

[1] SALVADORI, MARIA ANGELA BORGES. LETTERS IN and rhythms: SCHOOL views, education and work Samba Brazilian (1930-1950).Educ. rev. [online]. 2018, vol.34.

[2] BECKER, Beatriz; MACHADO, Hector Leal; WALTZ, Igor and TASSINARI, Joana. The centrality of television news in the converging media environment: rethinking how the interactions between production and reception give directions to Rio 2016 Games Intercom, Rev. Bras. Ciênc.Common. [Online]. 2018, vol.41, n.3.

[3] MARTINS, Geraldo Vicente and. BULHOES, Ricardo Magalhães. Literature and religious spectacle on a short story of Marcelino Freire.Honor student. Lit. Bras. Contemp. [Online]. 2017 n.52.

[4] VILELA, IVAN. Hillbilly: culture, withstands INSTANCE and rooting. Honor student. av. [Online]. 2017, vol.31, n.9 0.
ALMEIDA, Heloisa Buarque de. body education: the Women series and the promotion of medical and educational messages.Rev. Estud. Fem. [Online]. 2017, vol.25, n.1.

[5] CARVALHO, Vanessa Brazil and of Massarani, Luísa. Men and women scientists: gender issues in the two main television broadcasters Brasil.Intercom, Rev. Bras.Ciênc. Common. [Online]. 2017, vol.40, n.1 .

[6] Haussein Painis Fagundes. Brazilian communication journals record the research on the radio (2002-2012). Intercom, Rev. Bras. Ciênc. Common. [Online]. 2016, vol.39, n.3.

[7] CADIMA, Rui Francisco. European public TV to the "alienation" of Europa. Intercom Idea, Rev. Bras. Ciênc. Comun. [Online]. 2016, vol.39, n.2.

[8] DORNELAS, Rodrigo; GIANNINI, Susana Pimentel Pinto and FERREIRA, Leslie Piccolotto. World Voice Day news: analysis of reports on the Voice Campaign in Brazil. Codas [online]. 2015, vol.27, n.5.

[9] COSTA, Patrícia Coelho and. the PAULILO, André Luiz. HERALDS THE UNLIKELY, PIONEERS AND FILM radio EDUCATION IN BRAZIL (1920-1930).Educ. rev. [Online]. 2015, vol.31, n.2

[10] ANDRADE, Dilma Maria and to BARBOSA-WHITE, Anadergh. Synovitis and tenosynovitis in Brazil: an analysis of sickness benefits.Rev. bras. Epidemiol. [online]. 2015, vol.18, n.1.

[11] Mendonca, Veridiana Zocoler et al. The straw NUTRIENT RELEASE DE FORAGE intercropped with CORN WITH SOYBEANS AND SUCCESSION. Rev. Bras. Ciênc. Solo [online]. 2015, vol.39, n.1.

[12] NICHILE, Maria Cecilia F. De. The end of television, an end or a fresh start? Galaxy (Sao Paulo), Sao Paulo, n. 29, p. 290-292, June 2015.

[13] ONATE, Luis; GOMEZ, José and LAPO, Holger. ISDB-T ANALYSIS AND COMPARISON USING OFDM AND CC-OFDCM.Ingenius MODULATIONS [online]. 2019, no. 21, pp. 71-77. ISSN 1390-860X. http://dx.doi.org/10.17163/ings.n21.2019.07.

[14] CHARNEY-BERDICHEWKY, John. Freedom of expression and informative pluralism: compatibilities and tensions in the context of television. Rev. Derecho Estado [online]. 2019, no.42, pp.117-148. ISSN 0122-9893. http://dx.doi.org/10.18601/01229893.n42.05.

[15] McElroy, Ruth, Christina Papagiannouli, and Hywel Wiliam. "Broadcasting after devolution: policy and critique in the Welsh media landscape 2008–2015." International Journal of Cultural Policy 25.3 (2019): 377-391.

[16] Ahn, C. H. "Status of Development of Broadcasting Technology for the Disabled." Electronics and Telecommunications Trends 34.3 (2019): 1-12.

[17] Frischmann, Brett. "The British Broadcasting Corporation case study." Routledge Handbook of the Study of the Commons (2019): 256.

[18] Arcos, Juan Manuel Velazquez, et al. "Optimum Efficiency on Broadcasting Communications." Telecommunication Systems. IntechOpen, 2019.

[19] Khosa, Risimati Maurice, and Miyelani Khosa. "Policy, regulation and implementation of advertiser-funded programming in South Africa: A case of the South African Broadcasting Corporation (SABC)." Journal of African Media Studies 11.1 (2019): 81-101.

[20] Irfan, Asmara, et al. "The Influence of Social Media on Public Value: A Systematic Review of Past Decade." Journal of Public Value and Administration Insights 2.1 (2019): 1-6.

[21] Pilar, Puertas-Molero, et al. "Impact of sports mass media on the behavior and health of society. A systematic review." International journal of environmental research and public health 16.3 (2019): 486.

[22] Suh, Young Ik, Taewook Chung, and Jong Min Kim. "The Relationship between Motivation of Social Viewing Experiences, Satisfaction, and Loyalty in Sports Broadcasting." International Journal of Computer Science in Sport 18.1 (2019): 148-159.

[23] Nande, Sushmita, Rucha Chitnis, and Simran Bose. "A Review Based Study of Gender Equality in Media." Available at SSRN 3396114 (2019).

[24] Priyam, A., et al. "Time Transfer based on the satellite digital TV broadcasting system." 2019 URSI Asia-Pacific Radio Science Conference (AP-RASC). IEEE, 2019.

Gabriel Gomes de Oliveira. Graduated in Civil Engineering at UNIP University in 2018, studying for a Master's degree at Unicamp, FEEC (Faculty of Electrical and Computer Engineering), DECOM (Communications Department), Laboratory of Visual Communication (LCV) Currently researches and studies the Smart City area.

Yuzo Iano. B.Sc. (1972), M.Sc. (1974) and Ph.D. degrees (1986) in Electrical Eng. At Campinas, Brazil. Then he Has Been working in the technological production field, with one granted patent, patent applications filed 8 and 36 projects completed with research and development agencies. He has supervised 29 doctoral theses master's dissertations 49, 74 and 48 undergraduate initiation scientific works. He has participated in master's examination boards 100, doctoral 50 degrees, author of two books and more than 250 articles published. He is currently a teacher at Campinas, Editor-in-Chief of the SET International Journal of Broadcast Engineering and General Chair of the Brazilian Symposium on Technology (BTSym). He has experience in Electrical Engineering, with knowledge in Telecommunications, Electronics and Information Technology, Mainly in the field of audio-visual and multimedia communications.

Ana Carolina Borges Monteiro. Graduated in Biomedicine from University Center Amparense - UNIFIA (2015). Currently is a Ph.D. Candidate by Department of Communications (DECOM), Faculty of Electrical and Computer Engineering (FEEC) at State University of Campinas (Unicamp) and a researcher at the Laboratory of Visual Communications (LCV). Also, she is currently the Registration Chair of the Brazilian Symposium on Technology (BTSym). Has expertise in the areas of Clinical Analysis and digital image processing through MATLAB software. This knowledge was acquired through the realization of research projects and internship in a municipal hospital, the experience Also in the revision of scientific works by acting as a reviewer in congresses

Reinaldo Padilha France. Graduated in Computer Engineering (University Regional Center of the Holy Spirit of Pinhal - 2014). Currently is a Ph.D. Candidate by Department of Communications (DECOM), Faculty of Electrical and Computer Engineering (FEEC) at State University of Campinas (Unicamp) and a researcher at the Laboratory of Visual Communications (LCV). Also, He is currently Chair Proceedings of the Brazilian Symposium on Technology (BTSym). Has interest and affinity in the area of technological and scientific research as well as knowledge in programming and development in C / C ++, Java and .NET languages. The main topics of interest are Simulation, Operating Systems, Software Engineering, Wireless and Network, Internet of Things, Broadcasting and Telecommunications Systems.

Pablo Mango. Graduated in Electronic Engineering at the Polytechnic University Salesian (UPS), Quito, Ecuador in 2017. Currently, He is a M.Sc. candidate by Department of Communications, Faculty of Electrical and Computer Engineering at State University of Campinas - Unicamp. Have research Interests in Deep Learning, Machine Learning, Digital Image Processing with Medical's images.

Diego Pajuelo, in Graduate Electrical Engineering from the Peruvian University of Applied Sciences (UPC), Lima, Peru in 2012. He is currently working towards his doctoral degree in Sciences and Telecommunications at Unicamp. His research interests are HDR Video and audio coding, Image processing, digital television and Satellite communications

Received in 2019-09-21 | Approved in 2019-11-25

http://www.set.org.br/ijbe/ doi: 10.18580/setijbe.2019.11 Web Link: http://dx.doi.org/10.18580/setijbe.2019.11

Vibration and Position Monitoring in Civil Structures using WI-FI Systems

Wander P. Jesus
Evandro J. G. Lima
Joyce R. Silva
Rafael G. Alvares
Zelia M. A. Peixoto

CITE THIS ARTICLE

Jesus, Wander P., Lima, Evando J. G., Silva, Joyce R., Alvares, Rafael G. and Peixoto, Zelia M. A.; 2019. Vibration and Position Monitoring in Civil Structures using WI-FI Systems. SET INTERNATIONAL JOURNAL OF BROADCAST ENGINEERING. ISSN Print: 2446-9246 ISSN Online: 2446-9432. doi: 10.18580/setijbe.2019.12. Web Link: http://dx.doi.org/10.18580/setijbe.2019.12

Vibration and Position Monitoring in Civil Structures using WI-FI Systems

Wander P. Jesus, Evandro J. G. Lima, Joyce R. Silva, Rafael G. Alvares
and Zelia M. A. Peixoto, Member, IEEE

***Abstract* — This study presents the design, development and experimental implementation of a system for monitoring and signaling of vibration and position in civil structures, aiming to provide tools to perform predictive maintenance. Basically, the proposed system consists of an Espressif 32-bit microcontroller from the ESP32 chip series and a gyroscope and accelerometer module for vibration and position measurements. The system communicates via Wi-Fi with Android-based smartphones, using the Blynk app, which is specially designed for IoT applications. It also has its own electric power generation unit from a solar panel, what makes it autonomous and flexible. Test results confirm a good prototype performance, adaptability for different civil structures and indicates promising possibilities for future applications.**

***Index Terms*— Accelerometer, Gyroscope, IoT, Predictive Maintenance, SHM, Structural Health Monitoring, Vibration.**

I. Introduction

Civil structures are fundamental in the current world's scenario due to its importance in urban traffic or cities connections through bridges and viaducts, housing and business, large reservoirs used for tailings and hydrographic dams in industries and energy generation, among others. A commonality in the mentioned structures is the need of safety for users and actions that can prevent upheavals or serious accidents, which makes it mandatory that any changes in these structures must be monitored [1].

In this context, this work consists of design, development, experimental implementation and testing of a monitoring system that makes measurements related to the occurrence of vibrations and displacements in civil structures based on a pre-established standard, considered as a reference for the project. Upon changes in this pattern, the user will receive a signal and thus will be able to intervene in advance to meet safety standards, reducing costs and preventing structural collapses.

W. A. Jesus (wander.pjesus@gmail.com), E. J. G. Lima (evandrojgr@gmail.com), J. R. Silva (joyce.eng07@gmail.com) and R. G. Alvares (rafalvares@gmail.com) are currently studying for a Bachelor's degree in Electronic and Telecommunication Engineering at Pontifical Catholic University of Minas Gerais (PUC Minas), Belo Horizonte, 30535-901 Brazil).

W. A. Jesus is with Federal University of Minas Gerais (UFMG), Brazil.

E. J. G. Lima is with Serviço Nacional de Aprendizagem Industrial (SENAI), Brazil.

Z. M. A. Peixoto is with Electronic and Telecommunication Department and Graduate Program in Electrical Engineering of Pontifical Catholic University of Minas Gerais (PUC Minas), Belo Horizonte, 30535-901 Brazil (assiszmp@pucminas.br).

II. Vibrations in Civil Structures

Vibrations are usual occurrences in civil structures, since these structures are constantly subject to mechanical efforts and have a limited level of rigidity. Despite being robust to these types of effects, several problems can emerge when the vibration intensity exceeds the maximum tolerance [2] [3].

In a system, the change rate in its dynamic forces generated from external influences is a quantity named vibration, that is, vibration is any repetitive motion that occurs in structures when these are subjected to external stimulation. The structure can vibrate at ever greater amplitudes causing the resonance effect, when the excitation frequency levels match the structure natural frequency, which will move with sufficient intensity to cause its collapse.

Mathematically, this motion can be represented by root mean square value (RMS) of acceleration, speed or displacement, which is an electrical quantity that effectively indicates the energy consumed in time-varying circuits and can measure the work performed, for instance the light generated, heat, etc. [4]. Thus, the RMS acceleration value in structures can provide the vibration energy measurement.

Considering the average power in a direct current (DC) circuit $P_{av}(dc)$ equal to the average power of an equivalent alternating current (AC) circuit $P_{av}(ac)$, it leads to:

$$P_{av}(dc) = P_{av}(ac) \tag{1}$$

$$P_{av}(dc) = \frac{v^2}{R} \tag{2}$$

$$P_{av}(ac) = \frac{1}{T}\int_0^T \frac{v(t)^2}{R} dt \tag{3}$$

$$v(t) = A\sin(\omega t + \theta) \tag{4}$$

where $v(t)$ is the applied voltage, T is the signal period, R is the equivalent load resistance, $\omega = 2\pi f$ is angular velocity, A is the maximum voltage value and θ is the initial phase angle. Therefore, from equations (2) and (3), it is possible to calculate the applied voltage as (5):

$$v(t) = \sqrt{\frac{1}{T}\int_0^T A\sin(\omega t + \theta)^2 dt} \tag{5}$$

http://www.set.org.br/ijbe/ doi: 10.18580/setijbe.2019.12 Web Link: http://dx.doi.org/10.18580/setijbe.2019.12

Equations (1) to (5) will be used so that the measured voltage values can indicate whether vibration and displacement are within the specified value range.

III. System Description and Operation

The system is powered by a lithium battery that can be charged by an electronic module connected to a micro USB cable or a photovoltaic panel. This power supply system allows the sensor to be used for a long time in remote areas far from urban centers, provided there is sunlight.

A module containing a gyro sensor and an accelerometer is used to measure vibration and position. In this project, only the accelerometer is used to indicate the system status, defined by calculating the vibration signal RMS values. The system has three Light-Emitting Diodes (LED) for status display, in a way that the green LED indicates acceptable levels of vibration and position, the yellow LED indicates alert and the red LED indicates critical situation. It is worth noting that the red alert may indicate an imminent sign of structural collapse, which can be life-threatening and cause property damage.

The vibration and position measuring device also includes a feature for displaying graphs generated from the gauged signals. An application was created on the Blynk platform for viewing, which is the interface between devices applied in Internet of Things (IoT) such as ESP 32, used for the project control. The sensor detects the signals and a microcontroller receives and forwards them to a smartphone. A key and significant point in the project is the possibility of viewing and controlling graphics anywhere in the world, if provided that Internet connection is available. What makes this possible is the use of the Blynk server, where the vibration and position values are stored and sent to a pre-defined cell phone.

Fig. 1 presents a prototype block diagram highlighting the power system, vibration and position signals, the proposed system main steps, the Blynk server and the cell phone for reception. These subsystems will be explained in more detail in Section V.

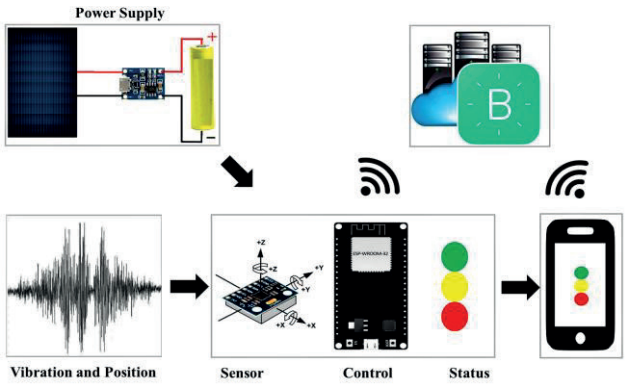

Fig. 1. Block diagram of the proposed system.

IV. Prototype Development

The prototype was developed by using a computer-aided designing (CAD) software [5] and built on a LPKF ProtoMat S63 prototype machine.

Fig. 2 and Fig. 3 show the electronic modules schematics, which were integrated into a single Printed Circuit Board (PCB).

Fig. 2 shows the power supply module U1, a capacitor bank responsible for filtering the power ripple and high frequency noise, and a push-bottom that allows the user to choose the network to which the device will connect or if the connection should remain on the previously configured device.

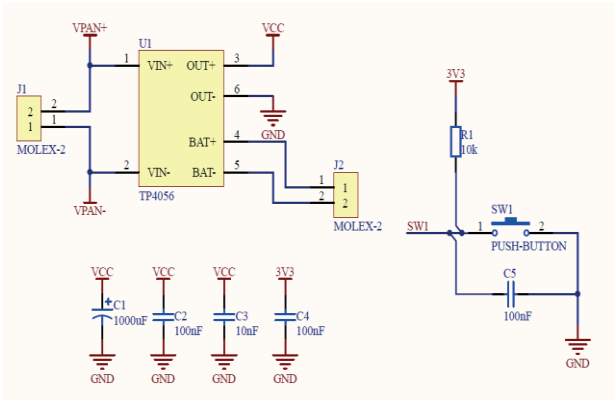

Fig. 2. Charger module, capacitive filter and push button.

According to the electronic schematic shown in Fig. 3, module U2 is responsible for system control through the ESP32 microcontroller and MOD1 (GY-521) is responsible for receiving and processing vibration measurement signals. It also shows a set of 3 LEDs used for signaling monitoring status.

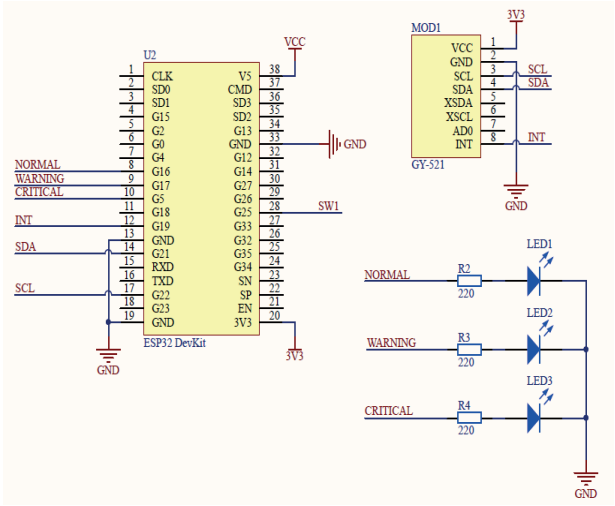

Fig. 3. Vibration and Position sensors, Control Unit and indicator LEDs.

Fig. 4 and Fig. 5 show a 3D-version prototype and the version implemented after the board manufacturing, respectively.

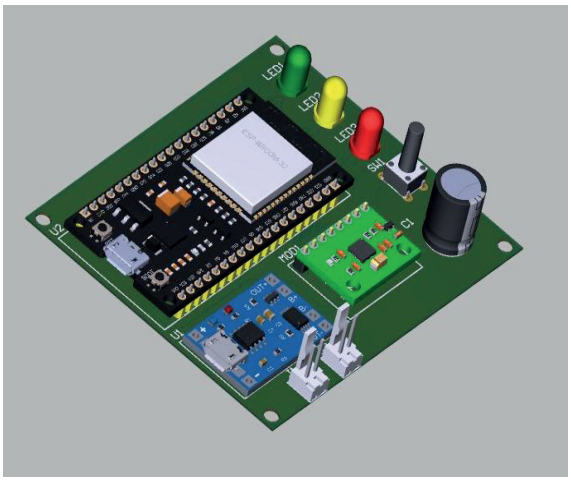

Fig. 4. PCB in 3D version.

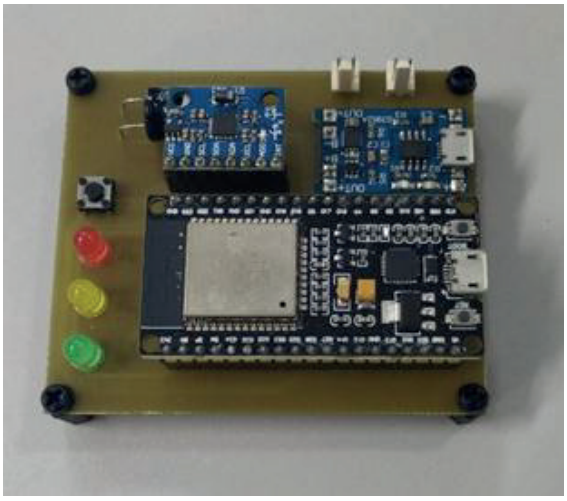

Fig. 5. The proposed system implemented in PCB.

V. Electronic Devices

A. ESP32 Module

ESP32-Wroom-32 [6] is a module that contains a high performance ESP32 microcontroller for low power, wireless communication applications. The board contains the ESP32 chip with built-in antenna, a serial USB interface and a 3.3V voltage regulator. It is possible to program it in LUA or using Arduino Integrated Development Environment (IDE) by a micro USB cable. With a 4MB flash memory, ESP32 permits creating a variety of applications for IoT projects, remote access, webservers and dataloggers, among others.

Table I shows the specifications and Fig. 6 and Table II show the ESP32 module pin identification.

TABLE I
ESP32 Technical Description

Items	Specifications
CPU	Xtensa® Dual-Core 32-bit LX6
ROM	448 Kbytes
RAM	520 Kbytes
Flash	4 Mbytes
On-board clock	240 MHz
Bluetooth Protocol	BLE 4.2
GPIO	11
GPIO Functions	PWM, I2C, SPI, etc.
Operating voltage	4,5V ~ 9V
Transfer Rate	110-460800 bps

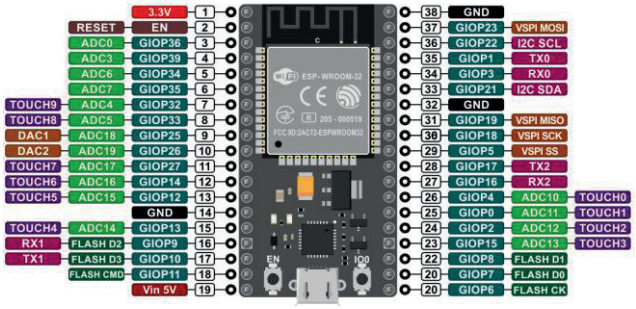

Fig. 6. ESP32 Pin Layout

TABLE II
ESP32 Module Pin Identification

Pin Layout	Pin Description	Color Code
3.3V	power supply	
GND	ground	
ADC	analog-to-digital converter	
SP	serial interface	
GPIO	general purpose input/output	
DAC	digital-to-analog converter	
TOUCH	capacitive touch sensor	
Vin	Input power	

B. MPU6050 Module (Accelerometer and Gyroscope)

The MPU-6050 sensor module [7] contains an accelerometer and a Micro Electro Mechanical Systems (MEMS) gyroscope on a single chip. There are 3 axes for the accelerometer and 3 axes for the gyroscope, making it 6 Degrees of Freedom (6DOF).

This module is responsible for measuring vibrations in the system board, which represents slight variations in position. This project uses both functions, which enables the reading of vibrations in the x, y and z axis.

The vibration sensor data is read through the SLC and DAS pins via an I2C communication aimed at connecting peripherals through two lines, serial data and serial clock, respectively. Fig. 7 and Table II show the MPU6050 module and its especifications, respectively.

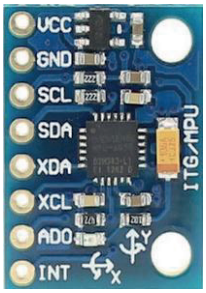

Fig. 7. MPU6050 Module

C. TP4056 Battery Charger Module

The TP4056 module [8] is a device used to charge batteries, especially lithium ones. It has a green LED to indicate that the charging process has been completed and a red LED to signal an ongoing charging process. It has a mini USB cable, which makes connecting easy, allowing batteries to be recharged without the need to remove them from the circuit.

http://www.set.org.br/ijbe/ doi: 10.18580/setijbe.2019.12 Web Link: http://dx.doi.org/10.18580/setijbe.2019.12

The TP4056 battery charger module is suitable for use in robots, drones and micro-controlled equipment, among others, and it makes recharging in the device itself possible. In the presented project, a mini photovoltaic panel was used to provide more autonomy and efficiency. Table III presents the TP4056 device specifications.

TABELA III
TP4056 SPECIFICATIONS

Features	Especifications
Operation Voltage	5 V
Maximum current	1 A (ajustable)
Output cut-off voltage	4.2V +/- 1%
Overcurrent protection	-
Mini USB conection	-
Indicator LED	-
Operating temperature	-10ºC à 85ºC0
Size	26 x 17 x 5mm

D. *Mini Solar Panel*

The mini solar panel is used for sustainable energy generation using sunlight, in which solar cells are responsible for capturing sunlight and electricity production. It is a device used in electronic project development to obtain electricity from renewable sources and it allows system operation in areas isolated from utility company power grids.

The mini solar panel makes it possible to connect to other panels in series or in parallel to generate higher voltages or currents. It will depend on the arrangement of how they will be assembled and electrically connected. In this project, the panel provides the electrical power required for the charger module, offering more autonomy and efficiency for the device. Table IV presents the mini solar panel specifications, whose structure is shown together with the battery charger module in Fig. 8.

TABELA IV
MINI SOLAR PANEL SPECIFICATIONS

Recurso	Especificação
Operation Voltage	5 V
Power	1 W
Maximum current	200mA
Size	100x69x3mm
Weight	22g

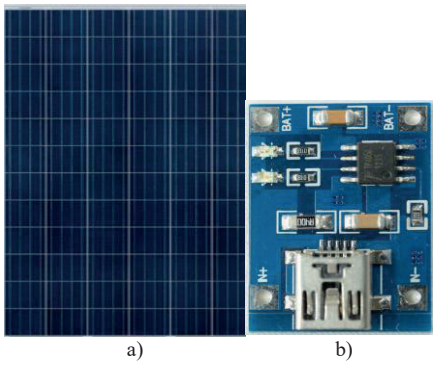

a) b)

Fig. 8. a) Solar Panel b) Battery Charger

E. *Blynk Plataform*

The Blynk [9] is a platform for building IoT interface applications. It supports over 400 hardware modules, which includes Arduino, ESP32, Node MCU, raspberry and more. Internet connection is possible via WI-FI, bluetooth, ethernet, mobile, serial communication and USB. Blynk permits controlling hardware remotely, viewing and storing sensor data.

Basically, the Blynk plataform is made up of three parts consisting of Blynk App, Blynk Server and Blynk Library, as illustrated in Fig. 9.

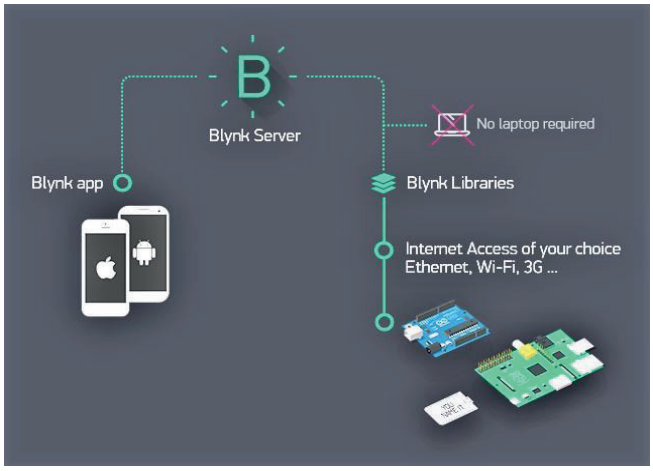

Fig. 9. Blynk Environment: Blynk App, Server and Libraries

Blynk App is available for Android and iOS operating systems and it allows the user to create applications that interact with the hardware. Through its own environment for each project, the user can insert widgets that implement control functions such as buttons, sliders, switches, and hardware data reading and notification, which are presented on displays, graphs and maps.

All communication between the application and user hardware is accomplished through the Blynk cloud. The server is responsible for transmitting data to the hardware, storing application and hardware status, and storing sensor data read by the hardware even when the application is not running.

It is noteworthy that the data stored on the Blynk server can be accessed externally through an HTTP API, which makes it possible to use Blynk to store periodically generated data such as temperature sensor data, among others.

Finally, on the hardware side there are the Blynk libraries for various development platforms. These libraries manage all hardware connection to the Blynk server, requests for input and output data and commands. Although it is easier and faster to use the library as Arduino, it is possible to obtain its versions for Linux, raspberry, python, LUA, among others. The Tests and Results section shows how the Blynk application was implemented.

VI. TESTS AND RESULTS

Fig. 10 shows the interface developed for the proposed monitoring system. The three screens show the vibration and

position signal variation graphs and provide the 3 vibration status indicators, which simulate the real LEDs signaling.

Another key point in this project is the possibility of presetting the values to desired levels of vibration and position, which makes the system implementable in any type of civil structure.

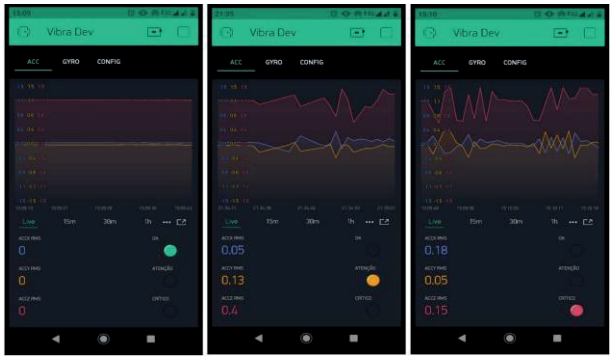

Fig. 10. Screen Interface of the MPU Module

VII. Conclusion

This study presented the development and implementation of a prototype to analyze vibration and position signals. The proposed system based on the ESP32 and GY521 microcontroller was able to monitor civil structure status through acquisition and processing of measurement signals performed by a module composed by an accelerometer, a gyroscope and adjustable reference values.

The results were presented in a graphical interface with WI-FI communication using the Blynk platform for IoT interfaces.

Therefore, as it is a prototype, the system usage responded satisfactorily to the vibration levels adopted in the experiments within the scope of tests already performed

For future work, it is advisable to examine more effective and broader measurements that could generalize the application of such monitoring system to different civil structures.

References

[1] Chalouhi, “Vibration Based SHM of Railway Bridges Using Machine Learning: The Influence of Temperature on the Health Prediction”, Springer International Publishing Ag, 2018. p. 200-211.

[2] F. Leonhardt, “Construções de concreto – Vol. VI – Princípios Básicos da Construção de Pontes de Concreto”, Ed. Interiencia, 6ª ed, 2013.

[3] F. Hauksson, “Dynamic Behaviour of Footbridges Subjected to Pedestrian-Induced Vibration”, Master´s Dissertation, Lund University, Lund, Scania, Sweden, 2005. pp 29

[4] R. L. Boylestad, “Sinusoidal Alternating Waveforms,” in Introductory Circuit Analysis, 12th ed. Pearson Education Limited, Ed. New Jersey: Upper Saddle River, 1913, pp. 572–578.

[5] Altium Designer software, www.altium.com/altium-designer/

[6] ESP 32. Site Espressif, 2019. Available: https://www.espressif.com/en/products/hardware/esp32/overview TDK InvenSense, 2019. Available: https://www.invensense.com/products/motion-tracking/6-axis/mpu-6050/

[7] TP 4056. Site D&B Hoovers, 2019. Available: https://dlnmh9ip6v2uc.cloudfront.net/datasheets/Prototyping/TP4056.pdf/

[9] Blyink, 2019. Available: https://blynk.io/

Wander P. de Jesus was born in Belo Horizonte city, Brazil, in 1980. He is electronic technician and undergraduate of Electronic and Telecommunication Engineering in Pontifical Catholic University of Minas Gerais (PUC Minas). Currently, he works at Federal University of Minas Gerais (UFMG) where searches on nanomaterials, as graphene and carbon nanotubes.

Evandro J. G. Lima was born in Belo Horizonte city, Brazil, in 1995. He is electronic technician and undergraduate of Electronic and Telecommunication Engineering in Pontifical Catholic University of Minas Gerais (PUC Minas). Currently, he is technology assistant in electronic innovation project development at SENAI - CETEL, Belo Horizonte.

Joyce R. Silva was born in Belo Horizonte city, Brazil, in 1989. She is automation and control technician and undergraduate of Electronic and Telecommunication Engineering in Pontifical Catholic University of Minas Gerais (PUC Minas). At present, she is working as a trainee in electronic development at CBTU, Belo Horizonte.

Rafael G. Alvares was born in Belo Horizonte city, Brazil, in 1996. He is electronic technician and undergraduate of Electronic and Telecommunication Engineering in Pontifical Catholic University of Minas Gerais (PUC Minas). At present, he is working as a trainee at MaisSI – FIEMG LAB4.0 Project.

Zelia M. A. Peixoto received the Bachelor degree in Electronic and Telecommunication Engineering from the Pontifical Catholic University of Minas Gerais (PUC Minas) and Master and Ph.D. degrees in Electrical Engineering from the Federal University of Minas Gerais, in 1995 and 2001, respectively. She is an Associate Professor at the Graduate Program in Electrical Engineering and the Department of Electronics and Telecommunication Engineering at PUC Minas, Belo Horizonte, Brazil.

Received in 2019-07-11 | Approved in 2019-11-25

Applied Medical Informatics in the Detection and Counting of Erythrocytes and Leukocytes Using the Image Segmentation Algorithm

Ana Carolina Borges Monteiro
Yuzo Iano
Reinaldo Padilha França
Rangel Arthur

CITE THIS ARTICLE

Monteiro, Ana Carolina Borges; Iano, Yuzo; França, Reinaldo Padilha and Arthur, Rangel; 2019. Applied Medical Informatics in the Detection and Counting of Erythrocytes and Leukocytes through an Image Segmentation Algorithm. SET INTERNATIONAL JOURNAL OF BROADCAST ENGINEERING. ISSN Print: 2446-9246 ISSN Online: 2446-9432. doi: 10.18580/setijbe.2019.13. Web Link: http://dx.doi.org/10.18580/setijbe.2019.13

Applied Medical Informatics in the Detection and Counting of Erythrocytes and Leukocytes through an Image Segmentation Algorithm

Ana Carolina Borges Monteiro, Yuzo Iano, Reinaldo Padilha França and Rangel Arthur

***Abstract*— More than half of the medical decisions rely on laboratory tests, which are essential to complete diagnosis or to refer the patient to more specific tests. In this context, the blood count is the most requested laboratory test. Even though there is a wide variety of CBC equipment, many are similar in cost. The automated methodologies present high speed and high accuracy. However, the high cost is often incompatible with the cost of living of people living in less-favored countries. In this way, it is essential to develop methodologies that reduce the cost of the blood count. The present study builds on the development of a laboratory medical algorithm for the detection and counting of erythrocytes and leukocytes in digital blood smear images. The algorithm employs the Hough Transform and the detection of objects by coloration. The deployment and performance analysis of the algorithm were performed in the virtual environment of Matlab software. The experiments were conducted through 10 digital images from open-access platforms with later analysis of sample execution times through the "tic toc" function. The results of the quantifications were expressed separately. The methodology developed showed high accuracy (90%) as well as low time to execute each of the images analyzed, with the average execution time being less than 2 seconds. Therefore, this study can be considered the first step in the accomplishment of hemograms with low cost, greater accessibility, and speed without the loss of reliability of the method.**

***Index Terms*— Hematology; Blood cells; Erythrocyte indices; Biomedical engineering; Medical informatics; Cytology; Hough transform.**

I. Introduction

The hemogram is a highly requested laboratory test in the medical routine because it directly provides the diagnosis of pathologies and pinpoints several diseases. This test consists of the erythrogram, leukogram, and platelet, which quantitatively and qualitatively evaluate erythrocytes, leukocytes, and platelets, respectively [1].

The hemograms' automation (HA) expedites exams and their reports. However, they are more expensive than manual exams. HA began in the 1950s when Coulter Eletronic, Inc. introduced the impedance principle for cell counts. Later, in the 1960s the conductivity technique based on the high-frequency electromagnetic current provided information about cell volume, nucleus size and cytoplasmic content of granulations [4].

Then, in 1970, laser beam scattering and hydrodynamic focus techniques were introduced. Both techniques preserve nuclei and granulocytes of leukocytes, retracting only the cytoplasmic membrane. These techniques exploit the principles of diffraction, refraction, and reflection of the light emitted. However, in these techniques, the red blood cells are undetectable. In order to solve this problem, the red cells started to be counted utilizing flow cytometry and hydrodynamic focus, where these cells are counted one by one through an extremely fine capillary [4].

Currently, there are a large number of multiparameter devices, which use the impedance, conductivity, and dispersion techniques of emitted light. However, before acquiring a hematological device it is necessary to consider the following parameters: automation device x type of patient attended; the number of hemograms day x samples/hour of the apparatus; cost of each blood count; quality control; technical assistance; and staff training [3] [4].

However, even with the acquisition of hematological equipment, the manual hemogram is not a dispensed practice and is recommended for the confirmation of hematologic reports of pediatric patients, patients over 75 years of age, cancer patients, patients with suspected leukemia or polycythemia, patients with leukocytosis and patients in severe condition [4].

In recent years, techniques developed in the engineering field have demonstrated the potential to solve problems and/or innovations in the medical areas in order to benefit both medical professionals and patients.

In the year 1970, was created Matlab software. While other computational languages work mainly as numbers one at a time, Matlab can operate on all matrices and commands. All the variables of this tool are multidirectional commands, regardless of data type [5] [6]. Matlab applicability in digital image processing [16] result from an extensive set of multidimensional arrangement processing functions

A. C. B. Monteiro pursues a D.Sc. degree in Electrical Engineering (EE) at Laboratory of Visual Communications (LCV) from the State University of Campinas (UNICAMP) (monteiro@decom.fee.unicamp.br).
Y. Iano is a professor and coordinator of the LCV at UNICAMP (yuzo@decom.fee.unicamp.br).
R. Padilha is currently pursuing a D.Sc. degree in EE, LCV at UNICAMP (padilha@decom.fee.unicamp.br).
R. Arthur is a professor of the Faculty of Technology (FT) of Unicamp, lecturer, and advisor to the Innovation Agency (INOVA) of UNICAMP (rangel@ft.unicamp.br).

http://www.set.org.br/ijbe/ doi: 10.18580/setijbe.2019.13 Web Link: http://dx.doi.org/10.18580/setijbe.2019.13

of image arrays. The Matlab IDE eases image-processing operations in a compact and clear way being ideal for solving image processing problems [7] [8].

Ji Y. Xie, introduced the Random Hough Transform (HT) in the detection of red blood cells to improve the detection curve of precision and robustness, as well as computational efficiency [9]. Subsequently, Smereka modified the HT, proposing improvement in the detection of low-contrast circular objects [10]. Already, Arivu and colleagues performed the counts of red cells and leukocytes by differentiating the distinct morphological characteristics that these cells present with each other [11]. Humaimi carried out research whose objective was to develop a computer vision system capable of detecting and estimating the number of red blood cells and leukocytes in an image [12]. Recently, Sahastrabuddhe et al. carried out a study with 5 patients, where digital images of red cells and leukocytes were present in blood smears, and the segmentation of the image was performed through the Hough Circular Transform [13].

Thus, in this context, it is well known that the HT is robust, valuable, and used in many fields of science, in the same way, that it is a fine-grained segmentation of radio or TV broadcasts [20 - 28]. The use of digital images has shown explosive growth in the last decades, where it is considered impossible to list so many modern applications that involve digital images, mentioning among them areas of special relevance as broadcasting [20 - 28].

Techniques for medical diagnostic imaging are an increasingly present trend fueled by the daily routine of medical activity, which is marked by a constant search for an increasingly accurate diagnosis [34 - 41].

With this focus on this horizon, this paper aims to develop an image segmentation algorithm that is capable of detecting and counting erythrocytes and leukocytes present in digital images of blood smear fields stained, with the purpose of developing a low-cost methodology, without the need of specific equipment and that is accessible disadvantaged populations.

II. Methodology

The research was developed at the Faculty of Electrical Engineering and Computing (FEEC) of the State University of Campinas - UNICAMP, Campinas, Brazil. The experiments were conducted through the Matlab software, where an algorithm was developed based on the union of the HT methodologies and the detection of objects by coloration. Thus, the algorithm was named HT-DC, an acronym that originated "Hough Transform and Detection Color".

The HT was introduced by P.V.C. Hough in 1962, in order to detect the lines and arcs in the photographs obtained in chambers of clouds. The HT is classified in the middle range of the image processing hierarchy. This methodology assigns a logical label to an object that existed only as a collection of pixels. Therefore, it can be classified as a segmentation procedure [14] [15].

The idea behind the method is simple: parametric shapes in an image are detected through points accumulated in the parameter space. As a result, if a particular shape is present in the image, the mapping of all its points in the parameter space must be grouped around the parameter values that correspond to that shape. This approach maps distributed and disjoint elements of the image to a localized accumulation point [14] [15]. The logic of the creation of the HT-DC algorithm and the stages of the detection and counting process of red blood cells and leukocytes are presented in Figure 1:

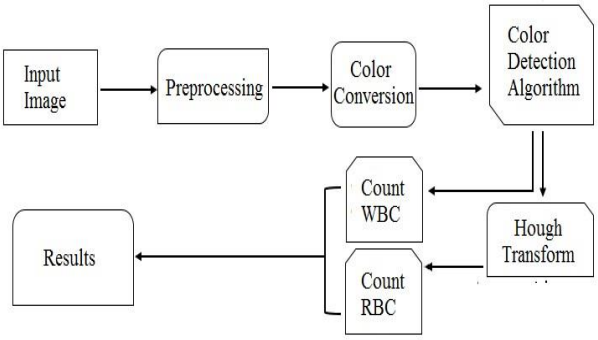

Figure 1 - Logic of the Hough Transform and Detection Color (HT-DC) algorithm for the detection and counting of erythrocytes and leukocytes present in digital blood smear images.

The HT-DC methodology is dependent on digital images, which is defined as a two-dimensional function $f(x, y)$, where x and y are spatial coordinates, and the amplitude f for any pair of coordinates is called image intensity. The term grayscale is often used to refer to the intensity of monochrome images. The intensity of the level of each pixel is essential information about the image. Pixel intensity values are also used to perform operations such as segmentation or filtering. In addition, one can use the intensity to extract information, such as the number of cells in an image [5] [17]. In this context, colored images are formed by combining individual images. In the RGB (Red, Green, and Blue) color system a color image consists of 3 individual monochrome images referred to as primary images or red, green, and blue components [7] [18].

The experiments were conducted through images obtained through hematology database open access: https://imagebank.hematology.org/. These images of microscopic fields have images of erythrocytes and leukocytes in the non-pathological state. These images were acquired in digital format 'png', 'jpg' or 'jpeg' and were later transferred to Matlab software. Subsequently, the image is subjected to the pre-processing and color conversion phase in order to correct problems that may arise during the capture of the images under an optical microscope, such as brightness, contrast, and sharpness. The image is then subjected to the color detection algorithm. This tool aims at detecting and counting leukocytes, which are detected and counted through their azurophilic staining. Finally, the results of erythrocyte and leukocyte counts are released separately.

Detection by staining avoids erroneous counts of blood cells since erythrocytes and leukocytes are circular and can easily be counted without distinction by the HT. Thus, the blue staining of the leukocyte nuclei can be easily separated from the image by means of the RGB staining separation process, preventing leukocytes from being counted as erythrocytes.

http://www.set.org.br/ijbe/ doi: 10.18580/setijbe.2019.13 Web Link: http://dx.doi.org/10.18580/setijbe.2019.13

As discussed earlier, a digital image is defined through the *x*, *y* coordinates. In this way, the detection algorithm by coloring marks the leukocytes as the "+" sign, which indicates the center of each detected form. The detection of objects by staining can be done through the Matlab Image Processing Toolbox.

Due to the morphological characteristic of the red cells having a biconcave disk format, the HT is applied in order to detect circular objects in the images. The HT is responsible for detecting erythrocytes present in the digital image. For this, the green color component was extracted from the image by the HT-DC algorithm, since it contains the maximum value necessary for this type of segmentation. It is possible to develop logics from the HT, how to draw circles around the detected cells. The HT-DC algorithm detects the edge points in each circle and draws the best possible circle around each cell. This developed methodology also uses a 3-D matrix, the first two dimensions being responsible for representing the coordinates of the matrix, which increases each time the circle is drawn around the rays on each edge point. An accumulator is responsible for maintaining proper counting [31, 32, 33].

Subsequently, the HT-DC algorithm was evaluated for its accuracy and execution time. The accuracy was determined by the values obtained in the manual counts performed by a biomedical professional with a comparison with the values found in the counts of red cells and leukocytes emitted by the HT-DC algorithm. This process uses 10 images of optical microscopy fields stained from free open-access platforms were used to avoid the need for submission and approval of the project by the Research Ethics Committee (CEP).

For the analysis of the execution time of the HT-DC algorithm, the "tic toc" function was used via the command line at the Matlab software prompt, and it was responsible for measuring the execution time of each of the analyzed samples, that is, this function quantifies the time that the image needs to perform a simulation [6] [7]. The "tic" function starts a timer to measure performance, recording the internal time of the "tic" command execution - and displaying the elapsed time with the "toc" function [6] [7].

In addition to detecting and counting erythrocytes and leukocytes, the HT-DC algorithm has a function capable of determining the erythrocyte indices. For this, the algorithm is based on the mathematical formulas previously determined by the literature. The determination of the Mean Corpuscular Volume (MCV) and Mean Corpuscular Hemoglobin (HCM) and Mean Corpuscular Hemoglobin Concentration (CHCM) are dependent on hemoglobin, hematocrit, and total erythrocyte counts, as presented in Equations 1, 2 and 3 [1] [2] [3] [4].

$$CVM = \frac{Hematocrit\ x\ 10}{Erythrocytes\ Count} \quad (1)$$

$$CHM = \frac{Hemoglobin\ x\ 10}{Erythrocytes\ Count} \quad (2)$$

$$CMCH = \frac{Hemoglobi\ 100}{Hematocrit} \quad (3)$$

III. RESULTS

The detection and counting of erythrocytes occur by inserting a circle around each of the red cells present in the image of the blood smear field, while the leukocytes are marked by a "+" at its center and are accompanied by your description of coordinates in the image. The way the HT-DC algorithm detects and counts red blood cells and leukocytes is shown in Figure 2.

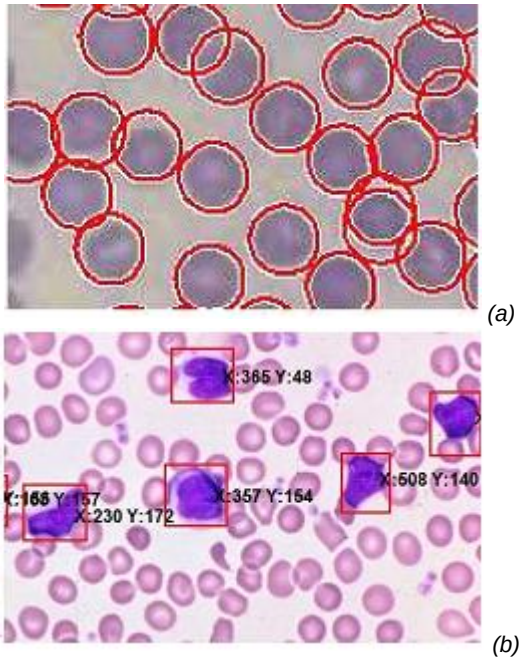

(a)

(b)

Figure 2 - Hough Transform used in the detection of red cells (a) with detection of leukocytes by staining (b)

Microscopy fields' images with erythrocytes and leukocytes underwent manual counts by a biomedical professional. Afterward, these images were transferred to the HT-DC image segmentation algorithm, where red blood cells and leukocytes were detected and counted with the values released separately.

Then, the erythrocyte and leukocyte values obtained by means of the manual counts and the counts by the HT-DC algorithm were compared to each other, as shown in Figures 3 and 4. Through the values shown, it is possible to note that the accuracy of the erythrocyte and leukocyte counts is 90%.

http://www.set.org.br/ijbe/ doi: 10.18580/setijbe.2019.13 Web Link: http://dx.doi.org/10.18580/setijbe.2019.13

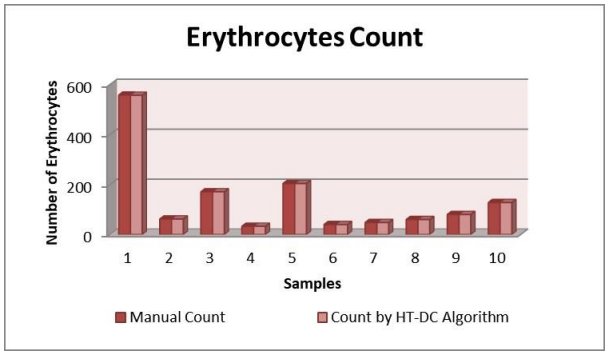

Figure 3 - Comparison of erythrocyte counts by manual methodology and HT-DC algorithm

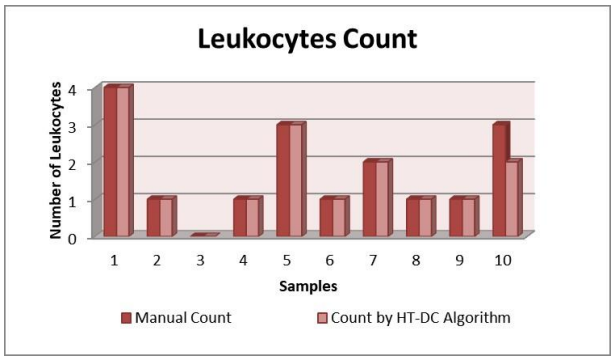

Figure 4 - Comparison of leukocytes counts by manual methodology and HT-DC algorithm

The detection and counts of erythrocytes and leukocytes by the HT-DC algorithm were performed in computers with different configurations: (1) Intel Core i3 processor, with 4GB RAM and (2) Intel Core i5 processor with 8 GB RAM. The run-time results of the samples are shown in Figure 5 and 6:

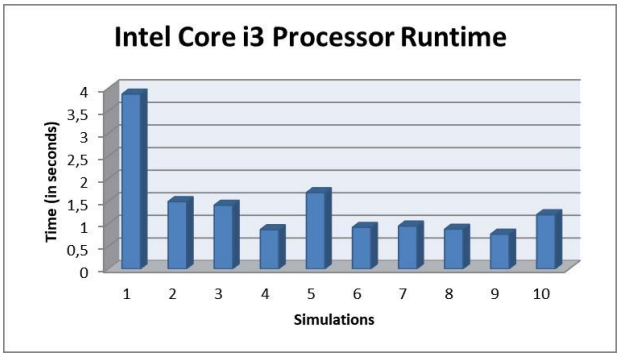

Figure 5: Time of execution of the samples submitted to the Hough Transform and Detection Color (HT-DC) algorithm on an Intel Core i3 processor

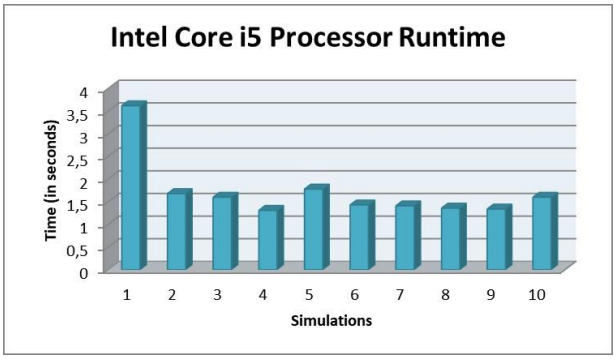

Figure 6: Time of execution of the samples submitted to the Hough Transform and Detection Color (HT-DC) algorithm on an Intel Core i5 processor

The average execution time of the images submitted to the HT-DC algorithm in computers with Intel Core i3 and Intel Core i5, corresponds to 1.4 and 1.7 seconds, respectively. The values of the hematimetric indexes VCM, HCM and CHCM obtained by the hematological equipment, common in laboratories of clinical analysis, were used as a parameter of comparison with the results obtained by the algorithm. Thus, it was possible to verify that the three functions implemented CVM, CHM, and CMCH presented 100% accuracy.

IV. Discussion

A high accuracy (90%) was obtained in the detection and counting of erythrocytes and leukocytes via the values obtained between the comparisons of the manual counts and the counts performed using the HT-DC algorithm. The same can be noticed through high accuracy (100%) presented by the function of the determination of hematimetric indexes. In this context, it is necessary to consider that the process of manually counting cells in blood smears, when performed repeatedly, becomes tiring and can lead to errors in counts. Such erroneous counts lead to an erroneous result, which can trigger an incorrect treatment for the patient.

In this way, the use of the HT-DC methodology can be seen as an important tool for both the health professional and the patient. In addition, larger laboratories with a higher demand for daily examinations that justify the acquisition of high-cost automated hematology equipment can use the HT-DC methodology as a confirmatory method for more altered exams released by the equipment conventional, thus conferring greater reliability to the medical reports issued.

One of the disadvantages of the automated methodology currently available is the need for specific equipment to perform the exams. These devices often present high acquisition cost, interface, maintenance, and require specific reagents for their operation, restricting the user to a specific company [4]. Therefore, in order to reduce equipment acquisition costs and consequently decrease the price of the final product, the HT-DC algorithm is able to provide a cheaper alternative than the current methodologies present in the market. In this way, with the reduction of the final price, it is possible to reach more widely the populations of developed and developing countries.

http://www.set.org.br/ijbe/ doi: 10.18580/setijbe.2019.13 Web Link: http://dx.doi.org/10.18580/setijbe.2019.13

Moreover, when using the HT-DC methodology, the healthcare professional has low cost, as this exempts the need for an hematocitometer and specific reagents for its operation: a mobile device, computer or notebook does the task.

From the patient's point of view, there is also a reduction in the final cost of service, since much of the burden of the exam is related to the type of methodology used. Another critical benefit to patients is the greater reliability and speed conferred to the hemograms, as these can be performed by a methodology that avoids counting and calculations failures. In addition, the rapidity of hematological examination is essential for the detection and indication of the most appropriate treatment of the individual [4]. Thus, runtime averages less than 4 seconds, prove that the HT-DC algorithm can be seen as an effective tool for laboratories and hospitals with a high demand for tests per day.

Considering the need for accessibility to health for all people, the process of counting blood cells by the HT-DC algorithm was performed on computers with different configurations. These devices were chosen because they are the most widely used today and provide more options for users who choose to perform blood cell counts through imaging methods. Considering the results of the simulations, it is noted that the accomplishment of hematological examinations can be carried out in the future in simple computers, complementing or even dispensing with the use of high-cost hematological equipment.

To verify the applicability of the HT-DC algorithm in different scenarios, the execution time of each of the digital blood smear images was analyzed. According to the work of Shoby et al. [19], the average execution time of each of the images was 4 seconds. Thus, the values presented in this research demonstrate an improvement of 35% on average in execution time on Intel Core i3 computers and 42.5% on Intel Core i5 machines, concerning works in the literature.

In addition, it is essential to consider that hematimetric indices are an important part of the erythrogram [2] [3]. Thus, the use of functions for its determination through a computer, provides more reliability to medical reports, because CVM, CHM, and CMCH are essential allies that indicate and/or detect the presence of anemia and leukemia.

In turn, the fact that the developed CVM, CHM, and CMCH functions receive a command that assists students and health professionals in the erythrocyte indices. By means of the "help" command, it is possible to display the name of each hematimetric index as well as its function in the blood count and its respective reference value. Thus, this methodology can be seen as a scientific-academic tool, which may also aid in the learning of medical students.

V. Conclusion

The confirmation of the diagnosis or even the accomplishment of laboratory tests through algorithms provides greater reliability of the results to both health professionals and patients because the algorithms reduce the chances of human failures. The good performance of the proposal on different hardware platforms concludes that the algorithm is feasible for the different realities of the laboratories.

The health area is a broad field directly linked to medical diagnoses through images, so the proposal of this study also predicts that the results suggestive of more serious pathologies can be stored in digital files for future consultations, dispensing with the creation of physical space, in this case for hospitals.

The function developed in this research to obtain the hematimetric indexes, as well as its immediate applicability can inform the students of the medical areas of the reference values and the applicability of each index.

In this way, the complete automation of the laboratory tests is a reality still distant for some laboratories of underdeveloped and developing countries. However, the creation of new methodologies, such as the one presented in this study, using image segmentation algorithms, results in a considerable reduction in equipment costs without loss in the quality and accuracy of hematological diagnoses.

Acknowledgment

The authors thank the National Council for Scientific and Technological Development (CNPq) for financial support and the State University of Campinas for the structure provided for the development of this study.

References

[1] F. Bernadette, G.A Rodak, K.D. Fristma, “Hematology – Clinical Principles and Applications,” New York: Elsevier, 2015.
[2] B. Ciesla, “Hematology in Practice,” 2nd ed., Davis Company, 2012
[3] M.L Turgeon, “Clinical Hematology Theory and Procedures,” 4th ed. Philadelphia: Lippincott Williams and Wilkins, 2004.
[4] R. Failace, F. Fernandes, “Hemograma, Manual de Interpretação,” 5th ed., Porto Alegre: Artemed, 2009.
[5] C. C. Reyes-Aldosoro, “Biomedical Image Analysis Recipes in Matlab: for Life and Engineers,” London: Wiley Blackwell, 2015.
[6] B. Hahn, D.T. Valentine, “Essential Matlab for Engineers and Scientists,” 3rd ed. Elsevier: Boston, 2007.
[7] R. C. Gonzalez, R.E. Woods, S.L. Eddins, “Digital Image Using Matlab,” 2nd ed., Gatesmark, 2009.
[8] R. C. Gonzalez, R.E. Woods, “Digital Image Processing,” 3rd ed. United States: Pearson: Prentice-Hall,2008.
[9] Y. Ji, E. Xi, “Randomised Hough transform with error propagation for line and circle detection,” In Springer-Verlag London, 2003.
[10] M. Smereka, I. Duleba. “Circular object detection using a modified Hough transform,” Int. J. Appl. Math. Comput. Sci., 2008, Vol. 18, No. 1, 85–91, DOI: 10.2478/v10006-008-0008-9, 2008.
[11] S. K. Arivu, M. Sathiya, “Analyzing blood cell images to differentiate WBC and counting of linear & non-linear overlapping RBC based on morphological features,” Elixir Comp. Sc. & Eng. 48, 2012 94109413.
[12] N. H. Mahmood, A.M. Muhammad, “Red blood cells estimation using Hough transform technique,” SIPIJ, Vol.3, No.2, 2012.
[13] A. P. Sahastrabuddhe, S.D. Ajij, “Blood group detection and RBC, WBC counting: An image processing approach,” Int’l J. Eng. and Computer Science, Vol. 5, 10, 2016, 18635-18639, ISSN: 2319-7242.
[14] A. Danko, “Review of the Hough Transform Method, with an Implementation of the Fast Hough Variant for Line Detection,” School of Informatics, Comp. and Eng., Indiana University Bloomington, 2008
[15] F. A Nava. “The intersective Hough transform for geophysical application,” Geofísica Internacional, 53-3: 321-332, 2014.
[16] A.C.B. Monteiro, Y. Iano, R.P. França, R. Arthur, “Toxoplasmosis Gondii: From discovery to advances in image processing,” in Proc. 4th Brazilian Technology Symp. (BTSym) 2018, Vol 140. Springer, 2019. DOI: 10.1007/978-3-030-16053-1_9
[17] J. D. Bronzino, “Medical Devices and Systems: The Biomedical Engineering Handbook,” 3th ed, United States: Taylor & Francis, 2006.
[18] T. Morris, “Image Processing with Matlab,” 2005.

[19] N. M. Sobhy, and M.A. Dosoki, "Comparative study of white blood cells segmentation using Otsu threshold and watershed transformation," J. Biomed. Eng. and Med. Im., Soc. Sc. and Educ., UK, Vol. 3, 3, 2016.
[20] H. Denman, Niall Rea, and A. Kokaram, "Content-based analysis for video from snooker broadcasts," Computer Vision and Image Understanding, 92, 2-3, 176-195, 2003.
[21] R. Dahyot, et al. "Joint audio-visual retrieval for tennis broadcasts," in Proc. 2003 IEEE Int'l Conf. Acoustics, Speech, and Signal Processing (ICASSP'03), Vol. 3. IEEE, 2003.
[22] K. Wan, J. Lim, C. Xu, and X. Yu. "Real-time camera field-view tracking in soccer video," in 2003 ICASSP Proc., VIII, 185-188, 2003.
[23] X. Yu, C. Xu, H. W. Leong, Q. Tian, Q. Tang and K. W. Wan. "Trajectory-based ball detection and tracking with applications to semantic analysis of broadcast soccer video," in Proc. 2003 ACM MM, Nov. 2-8, 2003, Berkley, CA, USA, 11-20
[24] X. Yu, H.W. Leong, C. Xu, Q. Tian, "A robust Hough-based algorithm for partial ellipse detection in broadcast soccer video," in Proc. 2004 IEEE Int'l Conference on Multimedia and Expo (ICME), 2004.
[25] A. Yao, J. Gall, and L. Van Gool, "A Hough transform-based voting framework for action recognition," in Proc. 2010 IEEE Comp. Society Conf. Comp. Vision and Pat. Recognition, IEEE, 2010.
[26] L.-H. Chen, H.-W. Chang, and H.-A. Hsiao. "Player trajectory reconstruction from broadcast basketball video," in Proc. 2nd Int'l Conf. Biomedical Signal and Image Processing, ACM, 2017.
[27] C.-C. Chang, and T.-L. Lee, "Fencing tactics analysis in broadcast video: A point-by-point analytical system," IEEE Trans. Circuits and Systems for Video Technology, 2018.
[28] K. Abhishek, and A. Yogi, "Summarization and visualization of large volumes of broadcast video data," arXiv preprint:1901.03842, 2019.
[29] A.C.B. Monteiro, Y. Iano, R.P. França, and R. Arthur, "A comparative study between methodologies based on the Hough Transform and watershed transform on the blood cell count," in Proc. BTSym'18, Vol 140. Springer, 2019. DOI: 10.1007/978-3-030-16053-1_7
[30] A.C.B. Monteiro, Y. Iano, and R.P. França, "Detecting and counting of blood cells using watershed transform: an improved methodology," in Proc. 3rd BTSym, 1st ed., vol. 1, 301–310, Springer, 2018.
[31] A.C.B. Monteiro, Y. Iano, and R.P. França, "An improved and fast methodology for automatic detecting and counting of red and white blood cells using watershed transform," in Proc. VIII Simpósio de Instrumentação e Imagens Médicas (SIIM)/ VII Simpósio de Processamento de Sinais da UNICAMP, 2017, vol. 1, 2017.
[32] B.P. Marsh, N. Chada, R.R. Gari, K. P. Sigdel, and G.M. King, "The Hessian blob algorithm: Precise particle detection in atomic force microscopy imagery," Scientific Reports, 2018.
[33] T. Kanade, Z. Yin, R. Bise, S. Huh, S. Eom, M.F. Sandbothe, and M. Chen, "Cell image analysis: Algorithms, system and applications," in Proc. 2011 IEEE Works. Applications of Computer Vision (WACV), 374-381, 2011.
[34] Lundervold, Alexander Selvikvåg, and Arvid Lundervold. "An overview of deep learning in medical imaging focusing on MRI." Zeitschrift für Medizinische Physik 29.2 (2019): 102-127.
[35] Fryback, Dennis G., and John R. Thornbury. "The efficacy of diagnostic imaging." Medical decision making 11.2 (1991): 88-94.
[36] Smith-Bindman, Rebecca, Diana L. Miglioretti, and Eric B. Larson. "Rising use of diagnostic medical imaging in a large integrated health system." Health affairs 27.6 (2008): 1491-1502.
[37] Doi, Kunio. "Diagnostic imaging over the last 50 years: research and development in medical imaging science and technology." Physics in Medicine & Biology 51.13 (2006): R5.
[38] Seibert, J. Anthony. "One hundred years of medical diagnostic imaging technology." Health physics 69.5 (1995): 695-720.
[39] Nakata, Norio. "Recent technical development of artificial intelligence for diagnostic medical imaging." Japanese journal of radiology 37.2 (2019): 103-108.
[40] Pesapane, Filippo, Marina Codari, and Francesco Sardanelli. "Artificial intelligence in medical imaging: threat or opportunity? Radiologists again at the forefront of innovation in medicine." European radiology experimental 2.1 (2018): 35.
[41] Morris, Michael A., et al. "Reinventing radiology: big data and the future of medical imaging." Journal of thoracic imaging 33.1 (2018): 4-16.

Ana Carolina Borges Monteiro. B.Sc. in Biomedicine from Centro Universitário Amparense (UNIFIA), 2015. D.Sc. candidate by the Department of Comm. (DECOM), Faculty of Electrical and Computer Engineering (FEEC) at State University of Campinas (UNICAMP), Brazil, and a researcher at the Laboratory of Visual Communications (LCV). Current Registration Chair of the Brazilian Technology Symp. (BTSym) with expertise in clinical analysis and image processing. She had internships in municipal hospitals and is as an experienced reviewer.

Yuzo Iano. B.Sc. (1972), M.Sc. (1974) and D.Sc. degrees (1986) in Electrical Eng. (EE) at UNICAMP. Works in the technological production field, with 1 patent granted, 8 filed patent applications and 36 projects completed with research and development agencies. He supervised 29 D.Sc. theses, 49 M.Sc. dissertations, 74 undergraduate and 48 scientific initiation works. He participated in 100 M.Sc. and 50 D.Sc. examination boards, authored 2 books and more than 250 articles. Currently a professor at UNICAMP, Editor-in-Chief of the SET Int'l Journal of Broadcast Eng., and General Chair of the BTSym. He has experience in EE, with knowledge in Telecommunications, Electronics and Information Technology, mainly in the field of audio-visual communications and multimedia.

Reinaldo Padilha França. B.Sc. in Computer Engineering (University Regional Center of Espírito Santo de Pinhal, 2014). Ph.D. candidate by DECOM, FEEC at UNICAMP, and a researcher at the LCV. Currently, the Proceedings Chair of the BTSym. Interested in the research, programming, and development in C / C ++, Java and .NET languages. Main interests: simulation, operating systems, software engineering, wireless networks, internet of things, broadcasting, and telecommunications systems.

Rangel Arthur He has a B.Sc. from the Paulista State University Júlio de Mesquita Filho (1999), an M.Sc. in EE (2002), and a D.Sc. all in EE (2007) from UNICAMP. From 2011 to 2014, he was Coordinator and Associate Coordinator of Technology Courses in Telecommunication Systems and Telecommunication Engineering of FT, which created in his management. Associate Director of the Technology (FT) of UNICAMP

from 2015 to 2016. Currently, he is a lecturer and advisor to the Innovation Agency (INOVA) of UNICAMP with EE experience (Telecommunications Systems), working mainly on computer vision, embedded systems and control systems.

Received in 2019-05-28 | Approved in 2019-11-25

http://www.set.org.br/ijbe/ doi: 10.18580/setijbe.2019.13 Web Link: http://dx.doi.org/10.18580/setijbe.2019.13

Classification of Automatic Skin Lesions from Dermoscopic Images Utilizing Deep Learning

Pablo Minango
Yuzo Iano
Ana Carolina Borges Monteiro
Reinaldo Padilha França
Gabriel Gomes de Oliveira

CITE THIS ARTICLE

Minango, Pablo; Iano, Yuzo; Monteiro, Ana Carolina Borges; França, Reinaldo Padilha and de Oliveira, Gabriel Gomes; 2019. Classification of Automatic Skin Lesions from Dermoscopic Images Utilizing Deep Learning. SET INTERNATIONAL JOURNAL OF BROADCAST ENGINEERING. ISSN Print: 2446-9246 ISSN Online: 2446-9432. doi: 10.18580/setijbe.2019.14. Web Link: http://dx.doi.org/10.18580/setijbe.2019.14

Classification of Automatic Skin Lesions from Dermoscopic Images Utilizing Deep Learning

Pablo Minango, Yuzo Iano, Ana Carolina Borges Monteiro, Reinaldo Padilha França and Gabriel Gomes de Oliveira

***Abstract*—Skin cancers are the most incidental in Brazil. Thousands of Brazilians are diagnosed annually with the disease, which occurs due to the abnormal growth of the cells that make up the skin and, therefore, can give rise to several types of skin cancer, being divided into two types melanoma and non-melanoma. Skin cancer, which represents respectively 25% of the malignant tumors and about 30% of the cases of cancer in Brazil, being the majority due to the excessive exposure to the sun's ultraviolet rays. Skin tumors are usually perceived more efficiently, and when diagnosed early, they are more likely to heal. The present study is relies on the development of an algorithm based on Deep Learning for the recognition of tumors in skin images. The AlexNet, which is a Deep Learning architecture is modified to attending our classification problem. The experiments are conducted through 1400 and 2400 images, after twice training with different optimizer, SGD is the better optimizer with 99.79% of accuracy and 0.0120% of loss in training, for the scenery of 2400 images.**

***Index Terms*—Deep Learning, Python, Biomedical Image Processing, Skin, Melanoma.**

I. Introduction

THE melanoma skin cancer originates in melanocytes (melanin-producing cells, a substance that determines skin color), which is more common in white adults, appearing anywhere on the body, on the skin or mucous membranes, in the form of spots or signs. On the other hand, black-skinned individuals, it is more common in clear areas such as the palms of the hands and soles of the feet. This type of disease is especially dangerous because it can spread to other tissues of the body, i.e., if not detected early, it generates metastases that make the patient's clinical picture more serious [1][2].

Although skin cancer is the most frequent in Brazil and accounts for about 30% of all registered malignancies. Melanoma represents only 3% of malignant neoplasms of the organ, being the most serious type, due to its high possibility of provoking metastasis (spread of cancer to other organs).

Among the symptoms, there are spots on the skin, wounds that do not heal, and spots that change their appearance, and melanomas can appear on healthy skin or existing skin nevi. It may also form brown, irregular, flat or protruding skin plaques with different color spots, or hard black or gray lumps. Melanomas may vary in relation to their appearance, where some are brownish, flat, irregular plaques and contain small black spots, and others are tall brownish-brown colored plaques with red, white, black or blue dots, where for sometimes melanoma appears as a hard tumor of a red, black or gray color [1][3][4].

The prognosis of this type of cancer can be considered good if it is detected in its initial phase, and in recent years, there has been a great improvement in the survival of patients with melanoma, mainly due to the early detection of the tumor and the introduction of new immunotherapeutic drugs. Still, in consideration, the most common type, non-melanoma skin cancer, has low lethality. However, their numbers are very high. This disease is caused by the abnormal and uncontrolled growth of the cells that make up the skin, where the cells are arranged forming layers, and according to those that are affected, the different types of cancer are defined. The most common types are basal cell and squamous cell carcinomas, where the rarer and lethal than carcinomas, melanoma is the most aggressive type of skin cancer [2][4].

Brazil has an estimated 6260 new cases each year, of which 2920 are men, and 3340 are women (2018 – INCA (National Cancer Institute)), and unfortunately there are 1794 deaths, where 1012 men and 782 women (2015 – SIM (Mortality Information System). Early detection of cancer is a strategy to find a tumor at an early stage and thus enable a greater chance of treatment. This detection can be done through the investigation with clinical, laboratory or radiological examinations, of people with signs and symptoms suggestive of the disease (early diagnosis), or with the use of periodic examinations in people without signs or symptoms (tracing) but belonging to groups with a greater possibility of having such a disease.

Among the main factors, sun exposure ends up being the main means of obtaining the disease, through ultraviolet (UV) rays is a significant risk factor for most melanomas, where they damage the DNA of skin cells and thus affect the control of their cell growth [4].

People who have taken too much sun through their lifetime without adequate protection (sunscreen and/or sunblock) are at increased risk for melanoma, where sunburns, especially in childhood or adolescence, increase the risk of developing skin cancer. Still taking into consideration that geographically, living near the equator or at higher altitude also increases the risk, once the sun's rays are more direct. This people living at high altitudes are more exposed to UV radiation [1][4].

In recent years, we are experiencing a revolution in the area of Artificial Intelligence (AI) [5] – [8] and the main driver of this revolution are technologies based on Deep Learning (DL),

P. Minango is pursuing an M.Sc. degree in Electrical Eng. (EE), at the Lab. of Vis. Comm. (LCV) at the State Univ. of Campinas (UNICAMP), pablodavid218@gmail.com

Dr. Y. Iano is the LCV-UNICAMP head yuzo@decom.fee.unicamp.br

A.C.B. Monteiro is currently pursuing an Ph.D. degree in EE at LCV-UNICAMP, monteiro@decom.fee.unicamp.br

R. Padilha is currently pursuing an Ph.D. degree in EE at LCV-UNICAMP, padilha@decom.fee.unicamp.br

G. G. Oliveira is currently pursuing an M.Sc. degree in EE at LCV-UNICAMP, oliveiragomesgabriel@ieee.org

http://www.set.org.br/ijbe/ doi: 10.18580/setijbe.2019.14 Web Link: http://dx.doi.org/10.18580/setijbe.2019.14

and taking into account the recent advances in computational power have enabled the possibility of developing algorithms based on Computer Vision and related to DL [5] – [9]. This method, in simple terms, is the part of Machine Learning (ML) that, through high-level algorithms, mimics the neural network of the human brain, generally using deep neural networks and depending on many data for training [10] – [12].

In order to reach the more advanced DL level, the artificial neural networks principle has been developed to support discrete layers, connections and data propagation directions, and such data is subjected to several non-linear processing layers that simulate the way of thinking of neurons [10][13][14][15][16].

In a simplified and generic way, DL is complex algorithms built from a stack of layers of digital ”neurons”, fed by an immense volume of data, capable of recognizing images and speech, processing them, and learning to perform extremely tasks without human interference, in this scenario having classification and recognition tasks, especially for image recognition [16]–[19].

Python is a language that was created for production and development in an easy, practical and fast way, being an agile, easy and objective language, democratizing its teaching, making it increasingly sought after. Being an object-oriented language, its simplicity is its main characteristic. It is also open and non-profit language.

Pyhton is ideal for scientific applications as DL where it is an expressive language, where it is easy to translate the reasoning into an algorithm, and still taking into account that it allows the work and development with data science and ML [18], [20]–[25].

Thus, in this paper, an algorithm based on DL was developed, which aims to the recognition of skin melanomas patterns, with the use of 1200 and 2400 images for training, wherewith show the accuracy and the loos for each training.

The present paper is organized as follows: Section 2 discusses DL algorithms. Section 3 presents the proposed algorithm methodology. Section 4 presents the results and, finally, in Section 5, the conclusions are discussed.

II. Deep Learning

DL is one of the technological trends of the moment, which is ML. ML refers to the fact that computers and devices perform their functions without seeming programmed and as soon as they learn as they are used. DL can be considered as type of ML for the purpose of training computers to perform tasks as humans, i.e., speech recognition, image identification and prediction types, through configurations and standardization, into the set of data that will be worked [18] – [25].

In this way, DL learns alone and is fed by the multiple data generated at all times, through multiple analyzes in the sealed dataset, being able to decipher for example natural language and to relate terms, generating a corresponding meaning, as well as used in image processing and computer vision. Such approaches allow a complex and abstract representation of the data forming an orderly classification, through the use of algorithms that do not require a pre-processing of the data and automatically generate optimal results through the hierarchical layers of representation consisting of the technique, where such layers are non-linear data [16], [18] – [27].

Nowadays, the importance of DL can be seen by a direct connection to neural networks, which provided, for example, the automatic learning used for the creation of autonomous cars as well as the significant improvement of the searches on the web. Further, Deep Learning techniques have been enhancing computers' ability to classify, recognize, detect, and describe them over time in order to understand [18], [20]–[28]. DL and ML are concepts that go hand in hand are closely linked with Artificial Intelligence (AI). They are not synonyms, and DL evolved from machine learning. Since AI is a rather broad term, a branch of computer science, in which research is developed to find solutions that simulate the human capacity for reasoning. ML is already using concepts of AI, through algorithms, making the machines able to organize data and identify patterns without necessarily a pre-programming, making in simple terms. AI is similar to the process of human reasoning, related to this process of learning by inputs, and thus finding patterns. Moreover, finally, there is DL, where it can be considered, to be at a deeper level, with high-level algorithms, where machines begin to act similarly to the neural network of the human brain. Thus, the data are submitted to several layers (in the same way as a network of neurons), in order to recognize images and/or speech. For example, without human intervention in the sequence [22] – [29].

So, essentially, DL is an emerging technological within the field of AI, which is considered a subcategory of ML. DL uses neural networks to improve speech recognition, computer vision, image processing, and natural language processing [23] – [27].

Due to the iterative nature of DL, much computational power is needed to solve problems where its complexity grows as the number of layers employed and consequently, the necessary data volumes are getting large enough to improve the network training. The dynamic nature of DL presents the opportunity to introduce dynamic behaviors to analytics related to the dataset, that is, due to the capacity for continuous improvement and adaptation to changes in the pattern of underlying information [22] – [26].

Technologically speaking, DL performs the ”training” of a computational model so that it can decipher and recognize the pattern in the data set where this model relates terms and characteristics, thus resulting in the inference of meaning as it feeds with a large amount of data. DL has many practical applications already in use by companies around the globe, among the many existing techniques we can relate speech recognition and image, image classification, object detection, content description, natural language processing, recommendation systems popularized by Amazon and Netflix, for example where they hit with certain precision the users' interest after taking action on their platform, just as from previous behaviors, systems such as Siri and Cortana are partially fed by DL, is also the base technology for tools like Google Translate, among others [23] – [29].

In short, with an enormous amount of computing power, today's machines have the possibility and ability to recognize

http://www.set.org.br/ijbe/ doi: 10.18580/setijbe.2019.14 Web Link: http://dx.doi.org/10.18580/setijbe.2019.14

objects and translate voice in real-time, among many other complex activities of human life, finally making the AI applicable [15] – [26].

III. Methodology

Nowadays, pattern recognition and medical images classification using Deep Learning are possible to computational advances and large datasets [30].

Convolutional Neural Networks (CNN), is an architecture of Deep Learning inspired by the human visual cortex. CNN is utilized in several medical application as skins lesion classification problems [31], pancreas segmentation [32], extraction of vessels in fundus images [33], and brain tumor segmentation [34] [35].

In this work, we employ the architecture of AlexNet [36], where has five convolutional layers and three fully connected layers. This architecture is used to obtain the binary classification between benign and malign cancer.

A. Dataset Description

The International Skin Imaging Collaboration (ISIC) [37] dataset of open access was utilized for training AlexNet architecture. ISIC is an organization that impulses Melanoma Project by providing the access of their images, for academics and industries, with the purpose of decrease mortality rate occasioned for the skin cancer known as Melanoma, because if skin cancer is early recognized in its initial stages, the probability of cure is better.

ISIC is a collector dataset with almost 23906 images of many different skin lesions with their own histopathological diagnostic. Our principal focus is the classification of images with benign and malignant cancer, which represents binary classification.

In this work, AlexNet architecture is trained twice with different quantities of images. This procedure is described below.

B. Architecture Description

We use the idea of AlexNet [36], which was used and applied to recognize the ImageNet Large Scale Visual Recognition Challenge. Fig 1 depicts the detailed configuration. The structure of AlexNet consists of five convolutional layers, which include the concept of MaxPooling [38] and BatchNormalization [39] in each one of their layers.

The original AlexNet architecture was modified for adapting our problem. The first part of this architecture is the block of input images, determined by the batch size hyperparameter. The output of the first block (IN) passes through five convolutional blocks to obtain the better accuracy during the training classification, where each one of these convolutional blocks are composed for small convolutional filters also named kernels. The size of these kernels are matrices of (11 × 11) for C1, (5 × 5) for C2 and (3 × 3) for C3, C4 and C5 (see Fig 1). Each one of these blocks is equipped with Rectified Linear Unit (ReLU) as the activation function of each layer.

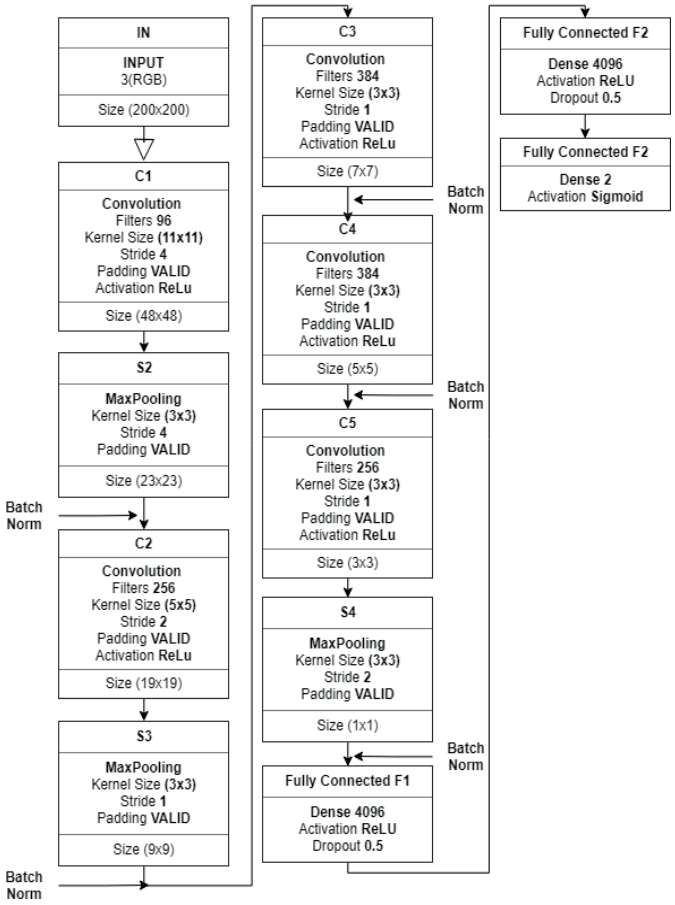

Fig. 1. AlexNet architecture adapted to our problem.

In Fig 1, the last three layers are known as dense layers. During the training step, in each one of the dense layers, every neuron has a probability p of being temporally off. It means that it is deactivated, but probably it will be activated during the next steps. This process is known as Dropout [40].

After each batch size of images are filtered, the results pass to the dense layer stage, which is composed of three dense layers. This work modifies the last one-layer output in order to perform a binary classification between benign and malignant, as well as their activation function was modified from a Softmax to a Sigmoid[1], which is very used for binary classifications problems.

With the use of AlexNet architecture modified and previously described, the weights of the output are sent to an optimizer during each one epoch, with the purpose of to measure accuracy and loss. The results of these optimizers are tested in each one epoch until attaining their convergence. To attain this premise, we use three different types of optimizer, which are Stochastic Gradient Descent (SGD), RMSprop, and Adam [41]. We consider an initial learning rate of 0.001 for the three optimizers with a Binary cross-entropy loss function [42]. Furthermore, an early stopping criterion was implemented to interrupt the training process after the training accuracy "AUC" does not improve on 10 epochs.

[1]When applied a Sigmoid activation function in the last layer. The architecture only learns to predict values between 0 and 1. For this reason is one of the most used in binary classification.

http://www.set.org.br/ijbe/ doi: 10.18580/setijbe.2019.14 Web Link: http://dx.doi.org/10.18580/setijbe.2019.14

IV. Results and Discussion

We employed the Keras package [43] in order to build and train the model. For data and results visualization, we used the Matplotlib package [44]. All codes were implemented in the Kaggle environment, which provides a free programming environment with the following specifications described in Table I.

TABLE I
KAGGLE ENVIRONMENT SPECIFICATIONS

Specifications	CPU	GPU
Cores	4	2
Gigabytes of RAM	16	13

AlexNet architecture was trained twice times with different quantity of dataset images. During the first training, we choose 1400 images for each class, which is 700 images for benign and 700 images for malignant. All images are resized in 200 × 200 pixels RGB and normalized (subtract from the mean and divide by the standard deviation).

For the second training, we considered 2400 images, which are divided into 1200 images of benign and 1200 images of cancer. The same conditions described above were taking in this training.

The evaluation of our methodology was performed using the following metrics in the training dataset:

- *Accuracy*, which represents the correct predictions in each one class divided by the total number of predictions.
- *Loss*, which corresponds to the number of images wrong classify, considering the true label.

Fig 2. shows the accuracy and the loss of our methodology for the first training. The SGD optimizer outperforms the Adam and RMS optimizer due to SGD achieves a percentage of 97.66% and 0.0567% in learning and loss, respectively.

Table II, shows the comparison performance of the three optimizers.

TABLE II
ACCURACY AND LOSS COMPARISONS OF THE DIFFERENT TYPES OF OPTIMIZERS.

	Adam	Epochs	RMSprop	Epochs	SGD	Epochs
Acc	96.66	19	87.64	46	**97.66**	34
Loss	0.0817	19	0.3141	46	**0.0567**	34

For the second training, we can appreciate the performance of the model in Fig 3. Again, in this case, SGD is better over the others optimizers achieved a 99.79% of learning and 0.0120% of loss.

Table III shows the performance of the three optimizers, where we appreciate that SGD has better accuracy and loss results.

Concerning the epochs of each one optimizer, Adam and RMSprop were stopped with the criterion of early stopping because they attain an accuracy convergence, and do not improve more if we continued with more epochs of training.

V. Conclusion

We have proposed a binary classification to detect the early stages of melanoma. The solution used was AlexNet

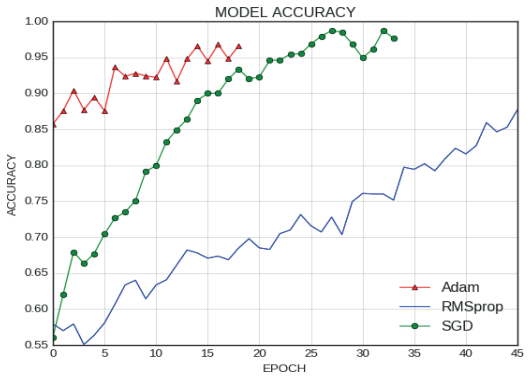

(a)

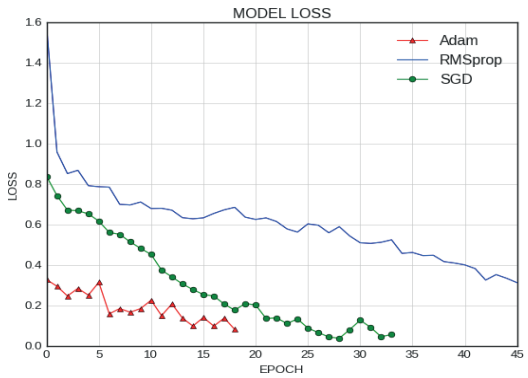

(b)

Fig. 2. Performance of the model with 1400 training images. (a) Accuracy, (b) Loss

TABLE III
ACCURACY AND LOSS COMPARISONS OF THE DIFFERENT TYPES OF OPTIMIZERS.

	Adam	Epochs	RMSprop	Epochs	SGD	Epochs
Acc	97.85	24	89.72	27	**99.79**	35
Loss	0.0591	24	0.2434	27	**0.0120**	35

which is an architecture of learning. We have tested it with different quantities of images for three types of optimizers, where we have observed that SGD is the better optimizer with an accuracy of 99.79% for 2400 images of training. In this context, we have appreciated the improvement of learning with the increasing of the quantity of images. In our adaptation of AlexNet, the number of epochs does not have a difference when analyzed SGD optimizer since for 1400 images SGD needs 34 epochs for obtaining its maximum accuracy which was 97.66% and for 2400 images it needs 35 epochs, for obtaining an accuracy of 99.79%.

Acknowledgment

We thank the State University of Campinas (UNICAMP), Brazil for providing all the necessary infrastructure for the development of this study.

References

[1] "Análise de dados das campanhas de prevenção ao câncer da pele promovidas pela Sociedade Brasileira

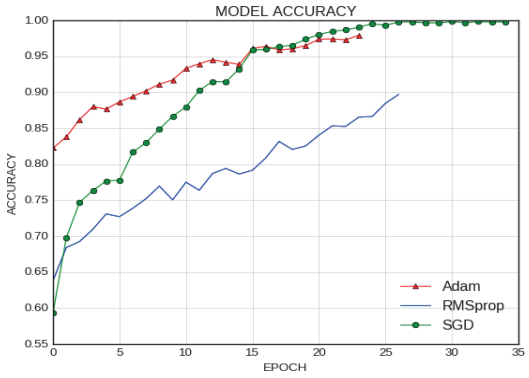

(a)

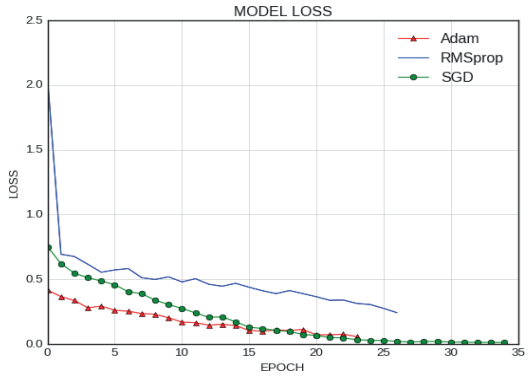

(b)

Fig. 3. Performance of the model with 2400 images of training. (a). Accuracy, (b). Loss

de Dermatologia de 1999 a 2005," pt, *Anais Brasileiros de Dermatologia*, vol. 81, pp. 533–539, Dec. 2006, ISSN: 0365-0596. [Online]. Available: http: / / www. scielo.br / scielo.php? script= sci_arttext& pid= S0365 - 05962006000600004&nrm=iso.

[2] C. M. Balch, "Cutaneous melanoma.," *Annals of Surgical Oncology*, 1992.

[3] W. Clark, L. From, E. Bernardino, and M. Mihm, "The histogenesis and biologic behavior of primary human malignant melanomas of the skin," *Cancer Research*, vol. 29, no. 3, pp. 705–727, Mar. 1969, ISSN: 0008-5472. [Online]. Available: http://europepmc.org/abstract/MED/5773814.

[4] J. Scotto and T. R. Fears, "The association of solar ultraviolet and skin melanoma incidence among caucasians in the united states," *Cancer Investigation*, vol. 5, no. 4, pp. 275–283, 1987, PMID: 3664331. DOI: 10.1080/07357908709170100. eprint: https://doi.org/10.1080/07357908709170100. [Online]. Available: https://doi.org/10.1080/07357908709170100.

[5] N. Razmjooy, V. V. Estrela, H. J. Loschi, and W. Farfan, "A comprehensive survey of new meta-heuristic algorithms," *Recent Advances in Hybrid Metaheuristics for Data Clustering*, 2019.

[6] N. Razmjooy, M. Ashourian, V. V. Estrela, and H. J. Loschi, "Entropy-based breast cancer detection in digital mammograms using world cup optimization algorithm," *International Journal of Swarm Intelligence Research (IJSIR)*, 2019, ISSN: 1947-9263.

[7] N. Razmjooy, M. Ashourian, V. V. Estrela, H. J. Loschi, R. P. França, and M. Vishnevski, "Computer-aided diagnosis of skin cancer: A review," *Current Medical Imaging Reviews*, 2019, ISSN: 1573-4056 (Print).

[8] N. Razmjooy and V. V. Estrela, "Applications of image processing and soft computing systems in agriculture," 2019. DOI: 10.4018/978-1-5225-8027-0.

[9] D. J. Hemanth and V. V. Estrela, *Deep Learning for Image Processing Applications*, ser. Advances in Parallel Computing. IOS Press, 2017, ISBN: 9781614998228. [Online]. Available: https://books.google.com.br/books?id=vsFVDwAAQBAJ.

[10] I. Goodfellow, Y. Bengio, and A. Courville, *Deep Learning*. MIT Press, 2016, http://www.deeplearningbook.org.

[11] L. Deng and D. Yu, "Deep learning: Methods and applications," *Found. Trends Signal Process.*, vol. 7, no. 3–4, pp. 197–387, Jun. 2014, ISSN: 1932-8346. DOI: 10.1561/2000000039. [Online]. Available: http://dx.doi.org/10.1561/2000000039.

[12] C. Dong, C. C. Loy, K. He, and X. Tang, "Learning a deep convolutional network for image super-resolution," in *Computer Vision – ECCV 2014*, D. Fleet, T. Pajdla, B. Schiele, and T. Tuytelaars, Eds., Cham: Springer International Publishing, 2014, pp. 184–199, ISBN: 978- 3-319-10593-2.

[13] M. A. Nielsen, *Neural networks and deep learning*, misc, 2018. [Online]. Available: http://neuralnetworksanddeeplearning.com/.

[14] G. J. S. Litjens, T. Kooi, B. E. Bejnordi, A. A. A. Setio, F. Ciompi, M. Ghafoorian, J. A. W. M. van der Laak, B. van Ginneken, and C. I. Sánchez, "A survey on deep learning in medical image analysis.," *Medical Image Analysis*, vol. 42, pp. 60–88, 2017. [Online]. Available: http://dblp.uni- trier.de/db/journals/mia/mia42.html#LitjensKBSCGLGS17.

[15] Y. Lv, Y. Duan, W. Kang, Z. Li, and F.-Y. Wang, "Traffic flow prediction with big data: A deep learning approach," *IEEE Transactions on Intelligent Transportation Systems*, vol. 16, pp. 865–873, 2015.

[16] Y. Chen, Z. Lin, X. Zhao, G. Wang, and Y. Gu, "Deep learning-based classification of hyperspectral data," *IEEE J. Sel. Topics in Applied Earth Observations and Remote Sensing*, vol. 7, no. 6, pp. 2094–2107, Jun. 2014, ISSN: 1939-1404. DOI: 10.1109/JSTARS.2014. 2329330.

[17] N. Papernot, P. McDaniel, S. Jha, M. Fredrikson, Z. B. Celik, and A. Swami, "The limitations of deep learning in adversarial settings," in *2016 IEEE European Symp. on Sec. and Priv. (EuroS P)*, Mar. 2016, pp. 372–387. DOI: 10.1109/EuroSP.2016.36.

[18] I. Arel, D. Rose, and T. Karnowski, "Deep machine learning - a new frontier in artificial intelligence research [research frontier].," *IEEE Comp. Int. Mag.*, vol. 5, pp. 13–18, Jan. 2010.

[19] D. Shen, G. Wu, and H.-I. Suk, "Deep learning in medical image analysis," *Annual Review of Biomedical Engineering*, vol. 19, Mar. 2017. DOI: 10.1146/annurev- bioeng-071516-044442.

[20] Y. Bengio, "Learning deep architectures for ai," *Found. Trends Mach. Learn.*, vol. 2, no. 1, pp. 1–127, Jan. 2009, ISSN: 1935-8237. DOI: 10.1561/2200000006. [Online]. Available: http://dx.doi.org/10.1561/2200000006.

[21] V. Mnih, K. Kavukcuoglu, D. Silver, A. A. Rusu, J. Veness, M. G. Bellemare, A. Graves, M. Riedmiller, A. K. Fidjeland, G. Ostrovski, S. Petersen, C. Beattie, A. Sadik, I. Antonoglou, H. King, D. Kumaran, D. Wierstra, S. Legg, and D. Hassabis, "Human-level control through deep reinforcement learning," *Nature*, vol. 518, no. 7540, pp. 529–533, Feb. 2015, ISSN: 00280836. [Online]. Available: http://dx.doi.org/10.1038/nature14236.

[22] W. Samek, T. Wiegand, and K. Müller, "Explain- able artificial intelligence: Understanding, visualizing and interpreting deep learning models," *CoRR*, vol. abs/1708.08296, 2017. arXiv: 1708.08296. [On- line]. Available: http://arxiv.org/abs/1708.08296.

[23] F. Pedregosa, G. Varoquaux, A. Gramfort, V. Michel, B. Thirion, O. Grisel, M. Blondel, P. Prettenhofer, R. Weiss, V. Dubourg, J. Vanderplas, A. Passos, D. Cournapeau, M. Brucher, M. Perrot, and É. Duchesnay, "Scikit-learn: Machine learning in python," *J. Mach. Learn. Res.*, vol. 12, pp. 2825–2830, Nov. 2011, ISSN: 1532-4435. [Online]. Available: http://dl.acm.org/citation.cfm?id=1953048.2078195.

[24] T. E. Oliphant, "Python for scientific computing," *Computing in Science Engineering*, vol. 9, no. 3, pp. 10–20, May 2007, ISSN: 1521-9615. DOI: 10.1109/MCSE.2007.58.

[25] M. F. Sanner, "Python: A programming language for software integration and development.," *Journal of Molecular Graphics Modelling*, vol. 17 1, pp. 57–61, 1999.

[26] F. Sebastiani, "Machine learning in automated text categorization," *ACM Comput. Surv.*, vol. 34, no. 1, pp. 1–47, Mar. 2002, ISSN: 0360-0300. DOI: 10.1145/505282.505283. [Online]. Available: http://doi.acm.org/10.1145/505282.505283.

[27] I. H. Witten and E. Frank, *Data Mining: Practical Machine Learning Tools and Techniques*, 2nd, ser. Morgan Kaufmann Series in Data Management Systems. Morgan Kaufmann, 2005.

[28] M. Abadi, P. Barham, J. Chen, Z. Chen, A. Davis, J. Dean, M. Devin, S. Ghemawat, G. Irving, M. Isard, M. Kudlur, J. Levenberg, R. Monga, S. Moore, D. G. Murray, B. Steiner, P. Tucker, V. Vasudevan, P. Warden, M. Wicke, Y. Yu, and X. Zheng, "Tensorflow: A system for large-scale machine learning," in *12th USENIX Symp. on Op. Systems Des. and Implem. (OSDI 16)*, 2016, pp. 265–283. [Online]. Available: https://www.usenix.org/system/files/conference/osdi16/osdi16-abadi.pdf.

[29] E. Alpaydin, *Introduction to Machine Learning*, 2nd. The MIT Press, 2010, ISBN: 026201243X, 9780262012430.

[30] J. Deng, W. Dong, R. Socher, L. Li, Kai Li, and Li Fei-Fei, "Imagenet: A large-scale hierarchical image database," in *2009 IEEE Conference on Computer Vision and Pattern Recognition*, Jun. 2009, pp. 248–255. DOI: 10.1109/CVPR.2009.5206848.

[31] C. N. Vasconcelos and B. N. Vasconcelos, "Increasing deep learning melanoma classification by classical and expert knowledge based image transforms," *CoRR*, vol. abs/1702.07025, 2017. arXiv: 1702.07025. [On- line]. Available: http://arxiv.org/abs/1702.07025.

[32] H. Roth, A. Farag, L. Lu, E. B. Turkbey, and R. M. Summers, "Deep convolutional networks for pancreas segmentation in CT imaging," *CoRR*, vol. abs/1504.03967, 2015. arXiv: 1504.03967. [On- line]. Available: http://arxiv.org/abs/1504.03967.

[33] M. Melinscak, P. Prentasic, and S. Loncaric, "Retinal vessel segmentation using deep neural networks," *VISAPP 2015 - 10th International Conference on Computer Vision Theory and Applications; VISIGRAPP, Proceedings*, vol. 1, pp. 577–582, Jan. 2015. DOI: 10.5220/0005313005770582.

[34] M. Havaei, A. Davy, D. Warde-Farley, A. Biard, A. C. Courville, Y. Bengio, C. Pal, P. Jodoin, and H. Larochelle, "Brain tumor segmentation with deep neural networks," *CoRR*, vol. abs/1505.03540, 2015. arXiv: 1505.03540. [Online]. Available: http://arxiv.org/abs/1505.03540.

[35] S. Pereira, A. Pinto, V. Alves, and C. Silva, "Deep convolutional neural networks for the segmentation of gliomas in multi-sequence mri," vol. 9556, Jan. 2016, pp. 131–143, ISBN: 978-3-319-30857-9. DOI: 10.1007/ 978-3-319-30858-6 12.

[36] A. Krizhevsky, I. Sutskever, and G. E. Hinton, "Imagenet classification with deep convolutional neural networks," *Neural Information Processing Systems*, vol. 25, Jan. 2012. DOI: 10.1145/3065386.

[37] I. porject, *Public skin lesion image archive*, https://www.isic-archive.com/#!/topWithHeader/onlyHeaderTop/gallery, 2018.

[38] H. Wu and X. Gu, "Max-pooling dropout for regularization of convolutional neural networks," *CoRR*, vol. abs/1512.01400, 2015. arXiv: 1512.01400. [Online]. Available: http://arxiv.org/abs/1512.01400.

[39] S. Ioffe and C. Szegedy, "Batch normalization: Accelerating deep network training by reducing internal covariate shift," *CoRR*, vol. abs/1502.03167, 2015. arXiv: 1502.03167. [Online]. Available: http://arxiv.org/abs/1502.03167.

[40] A. Gron, *Hands-On Machine Learning with Scikit-Learn and TensorFlow: Concepts, Tools, and Techniques to Build Intelligent Systems*, 1st. O'Reilly Media, Inc., 2017, ISBN: 1491962291, 9781491962299.

[41] S. Ruder, "An overview of gradient descent optimization algorithms," *CoRR*, vol. abs/1609.04747, 2016.

arXiv: 1609.04747. [Online]. Available: http://arxiv.org/abs/1609.04747.

[42] K. Janocha and W. M. Czarnecki, "On loss functions for deep neural networks in classification," *CoRR*, vol. abs/1702.05659, 2017. arXiv: 1702.05659. [On- line]. Available: http://arxiv.org/abs/1702.05659.

[43] F. Chollet *et al.*, *Keras*, https://keras.io, 2015.

[44] J. D. Hunter, "Matplotlib: A 2d graphics environment," *Computing in Science & Engineering*, vol. 9, no.3, pp. 90–95, 2007. DOI: 10.1109/MCSE.2007.55.

Pablo Minango. B.Sc. in Electronic Engineering from the Universidad Politécnica Salesiana (UPS), Quito, Ecuador, in 2017. Currently, he is an M.Sc. candidate by Department of Communications, Faculty of Electrical and Computer Engineering (FEEC) at State University of Campinas – UNICAMP. His research interests include Deep Learning, Machine Learning, Digital Image Processing with Medicals images.

Yuzo Iano. B.Sc. (1972), M.Sc. (1974) and Ph.D. degrees (1986) in Electrical Eng. at UNICAMP, Brazil. He has been working in the technological production field, with 1 patent granted, 8 filed patent applications and 36 projects completed with research and development agencies. He has supervised 29 doctoral theses, 49 master's dissertations, 74 under-graduate and 48 scientific initiation works. He has participated in more than 100 master's examination boards, 50 doctoral degrees, author of 2 books and more than 250 published articles. He is currently Professor at UNICAMP, Editor-in-Chief of the SET International Journal of Broadcast Engineering and General Chair of the Brazilian Symposium on Technology (BTSym). He has experience in Electrical Engineering, with knowledge in Telecommunications, Electronics and Information Technology, mainly in the field of audio-visual communications and multimedia.

Ana Carolina Borges Monteiro. Graduated in Biomedicine from Centro Universitário Amparense-UNIFIA (2015). Currently, she pursues a Ph.D. Candidate by Department of Communications (DE-COM), Faculty of Electrical and Computer Engineering (FEEC) at State University of Campinas (UNICAMP), and a researcher at the Laboratory of Visual Communications (LCV). She is also the Registration Chair of the Brazilian Symposium on Technology (BTSym) and has expertise in the areas of Clinical Analysis and digital image processing through MATLAB software. She has performed work, research experiments/projects, and internship in municipal hospital, and works as a reviewer.

Reinaldo Padilha França. B.Sc. in Computer Engineering from University Regional Center of Espírito Santo de Pinhal - 2014. Presently, he is a Ph.D. Candidate by Department of Communications (DECOM), Faculty of Electrical and Computer Engineering (FEEC) at State University of Campinas (UNICAMP), and a researcher at the Laboratory of Visual Communications (LCV). He is also the Proceedings Chair of the Brazilian Symposium on Technology (BTSym). His interest includes programming and development in (C / C ++, Java and .NET languages). Simulation, Operating Systems, Software Engineering, Wireless and Network, Internet of Things, Broadcasting, Image Processing, Multimedia, and Telecommunications Systems.

Gabriel Gomes de Oliveira. B.Sc. in Civil Engineering from the UNIP University in 2018. He is pursuing a master's degree at UNICAMP, Faculty of Electrical and Computer Engineering (FEEC), Communications Department (DECOM), Laboratory of Visual Communication (LCV). Currently, he researches and studies the area Smart Cities, Internet of Things, environmental engineering and cyber- physical systems.

Received in 2019-07-10 | Approved in 2019-11-25